

AMERICAN UNIVERSITY OF BEIRUT

VIRALLY-INDUCED HEMATOLOGICAL MALIGNANCIES
WITH DISMAL PROGNOSIS:
IMPACT OF EPIGENETICS AND POTENTIAL
THERAPEUTICS

By
SARA HISHAM MOODAD

A thesis
submitted in partial fulfillment of the requirements
for the degree of Doctor of Philosophy in Biomedical Sciences
to the Department of Internal Medicine
of the Faculty of Medicine
at the American University of Beirut

Beirut, Lebanon
December, 2020

AMERICAN UNIVERSITY OF BEIRUT

**VIRALLY-INDUCED HEMATOLOGICAL MALIGNANCIES WITH
DISMAL PROGNOSIS: IMPACT OF EPIGENETICS AND
POTENTIAL THERAPEUTICS**

by
SARA HISHAM MOODAD

Approved by:



[Dr. Ali Bazarbachi MD, Professor]
[Department of Internal Medicine,
Department of Anatomy, Cell biology, and Physiological Sciences, AUB]

Advisor



[Dr. Hiba El Hajj, Associate Professor]
[Department of Experimental Pathology, Immunology, and Microbiology]

Co-Advisor

[Signature]



[Dr. Nadine Darwiche, Professor]
[Department of Biochemistry and Molecular Genetics, AUB]

Chair of Committee



[Dr. Marwan El Sabban, Professor]
[Department of Anatomy, Cell biology, and Physiological Sciences, AUB]

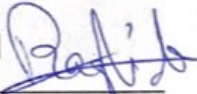
Member of Committee

[Signature]

[Dr. Chloe Journo, Associate professor]
[Centre International de Recherche en Infectiologie, Université Claude Bernard Lyon 1]



Member of Committee

[Signature] 
Member of Committee

[Dr. Raghida Abu Merhi, Professor]
[Department of Biology, Lebanese university]

Date of thesis/dissertation defense: [December 15, 2020]

AMERICAN UNIVERSITY OF BEIRUT

DISSERTATION RELEASE FORM

Student Name: Moodad Sara Hisham
Last First Middle

I authorize the American University of Beirut, to: (a) reproduce hard or electronic copies of my dissertation; (b) include such copies in the archives and digital repositories of the University; and (c) make freely available such copies to third parties for research or educational purposes:

- As of the date of submission
- One year from the date of submission of my dissertation.
- Two years from the date of submission of my dissertation.
- Three years from the date of submission of my dissertation.



Signature

8/Feb/2021

Date

ACKNOWLEDGMENTS

I would like to thank my advisors Dr. Ali Bazarbachi and Dr. Hiba El Hajj for their guidance and support throughout my PhD journey. Dr. Hiba, thank you for being not only an invaluable genuine mentor, but also a role model that we all look up to. Thank you for your infinite support in all aspects, you are indeed a blessing and I was lucky to be among your team.

I would also like to thank the thesis committee members for accepting to read and judge my work.

A big thank you for Rana El Hajj and Rania Najm for your support and precious friendship. You were next to me in all the ups and downs of this journey. Rana without you I wouldn't have accomplished the PEL this easily. We made it!

I would also like to thank all HEH and AB team members.

Finally, a big thank you goes to my family who believed in me, tolerated and supported me all the way and thank you for my other half, Kifah, for your love and support throughout these years and cheers for new beginnings.

ABSTRACT OF THE THESIS OF

Sara Hisham Moodad for PhD in Biomedical Sciences
Major: Cell biology of Cancer

Title: Virally-Induced Hematological Malignancies with Dismal Prognosis: Impact of Epigenetics and Potential Therapeutics

Blood malignancies are a heterogeneous group of cancer affecting blood cells or their hematopoiesis, and are the leading cause of increased mortality rates worldwide. The molecular mechanisms dictating oncogenesis and the currently used therapeutic approaches still present many gaps and require further understanding, to increase the overall survival of patients and alleviate the burden of these malignancies. In this manuscript, we tackled two virally driven hematological malignancies having a dismal prognosis and associated with chemo-resistance and high relapse rates.

Primary effusion lymphoma (PEL) is a rare aggressive subset of non-Hodgkin B cell lymphoma. PEL is secondary to Kaposi sarcoma herpes virus (KSHV) and predominantly develops in serous cavities. Current treatment modalities depend on aggressive chemotherapy, yet fail to achieve long lasting remission or to improve overall survival in PEL patients. Lenalidomide (Lena) is an immune-modulatory drug, which exhibits anti-proliferative effects on PEL cell lines. Arsenic trioxide (ATO) proved efficient when used as a combination therapy to treat multiple blood malignancies, including PEL. We demonstrated that ATO/Lena enhanced survival of PEL mice, decreased peritoneal ascites volume, and suppressed tumor organ infiltration. In *ex vivo* ascites-derived PEL cells, ATO/Lena inhibited cell growth, downregulated latent viral proteins, and decreased NF- κ B activation. This was associated with decreased cytokine production and lytic reactivation leading to apoptosis. Our results elucidate the mechanism of action of ATO/Lena and present it as a promising targeted therapeutic modality in PEL management, which warrants further clinical investigation.

Adult T cell leukemia (ATL) is an aggressive T-cell malignancy associated with the human T-cell leukemia virus type 1 (HTLV-1). ATL associates with dismal prognosis and develops after a long latency period, following accumulation of multiple genetic and epigenetic alterations. Two viral proteins, Tax and HBZ, play central roles in ATL leukemogenesis. Tax oncoprotein transforms T cells *in vitro*, induces ATL-like disease in mice, and a rough eye phenotype in *Drosophila melanogaster*, indicative of transformation. Among multiple functions, Tax modulates the expression of the enhancer

of zeste homolog 2 (EZH2), a methyltransferase of the Polycomb Repressive Complex 2 (PRC2), leading to H3K27me3-dependent reprogramming of around half of cellular genes. HBZ is a negative regulator of Tax-mediated viral transcription. HBZ effects on epigenetic signatures are underexplored. In this work, we established an *hbz* transgenic fly model, and demonstrated that, unlike Tax, which induces NF- κ B activation and enhances PRC2 activity creating an activation loop, HBZ neither induces transformation nor NF- κ B activation *in vivo*. However, overexpression of Tax or HBZ increases the PRC2 activity. Moreover, we report a novel interaction between HBZ and polycomb core components EZH2 and SUZ12 resulting in upregulation of H3K27me3, a repressive transcription hallmark. Importantly, overexpression of HBZ in *tax* transgenic flies prevents Tax-induced NF- κ B or PRC2 activation and totally rescues Tax-induced transformation and senescence. Our results establish the *in vivo* antagonistic effect of HBZ on Tax-induced transformation and cellular effects, and opens perspectives for new therapeutic strategies targeting the epigenetic machinery in ATL. Overall, our work proposed a promising therapeutic approach for PEL and offered a better molecular understanding on viral transformation in ATL.

CONTENTS

ACKNOWLEDGEMENTS.....	1
ABSTRACT.....	2
ILLUSTRATIONS.....	8
TABLES.....	13
ABBREVIATIONS.....	14
INTRODUCTION.....	16
A. Primary effusion lymphoma.....	16
1. Epidemiology.....	17
2. Clinical presentation.....	17
3. Prognosis.....	18
4. Diagnosis.....	20
5. Cytological features of PEL.....	21
B. Kaposi Sarcoma Herpesvirus KSHV.....	21
1. Discovery Of Kaposi Sarcoma Herpesvirus.....	21
2. KSHV Epidemiology And Transmission.....	24
3. KSHV Virion Structure And Genome.....	26
4. KSHV life cycle.....	28
a) Invasion and primary infection.....	28
b) Viral latency.....	31

c) Lytic reactivation	38
d) KSHV inter play between latent and lytic cycles.....	39
C. PEL angiogenic factors and growth factors.....	41
D. PEL treatment.....	42
1. Frontline therapy.....	42
a) Chemotherapy.....	42
b) Antiretroviral therapy.....	44
2. Relapsed or refractory therapy.....	44
a) Radiation.....	45
b) Stem cell transplant.....	45
c) Antiviral therapies.....	46
d) Targeted therapies.....	46
3. Preclinical studies.....	47
E. Arsenic trioxide	48
F. Lenalidomide.....	50
G. Adult T-Cell leukemia.....	51
1. Clinical manifestations of Adult T-cell leukemia.....	51
H. Treatment of adult T-cell leukemia.....	54
1. Chemotherapy.....	54
2. Antiviral Regimens.....	55
3. Alternative approaches for ATL management.....	55
4. Epigenetic regimens targeting ATL.....	55
I. Human T-cell lymphotropic virus 1 (HTLV-1).....	57
1. Tax protein.....	59
a) Tax: a powerful oncogene.....	61
b) Tax activate NF-KB pathway.....	62
c) Tax inhibits apoptosis and promotes cell survival	65
2. HTLV-I basic leucine zipper protein.....	67

a) The biological functions of HBZ.....	70
b) HBZZ mRNA: a distinct role.....	77
J. Epigenetic alterations in adult T-cell leukemia.....	78
1. Introduction to Polycomb Repressive Complex PRC2.....	78
2. Epigenetic landscape in ATL.....	80
AIMS AND SIGNIFICANCE OF THE STUDY.....	83
A. Aims	83
B. Significance.....	84
MATERIALS AND METHODS	86
A. PEL project.....	86
1. Cells and drugs.....	86
2. Xenograft mice and treatments.....	86
3. Histopathology.....	88
4. Ex-vivo cell culture and treatment.....	88
5. Cell viability.....	88
6. Real Time quantitative PCR.....	89
7. Immune-florescence assay.....	90
8. Immunoblot assay.....	91
9. Angiogenesis assay.....	92
10. CD45 staining.....	92
11. Statistical analysis.....	93
B. ATL project.....	93
1. Fly stocks.....	93
2. HBZ transgenic flies.....	93

3. Scanning electron microscopy.....	94
4. Scoring of eye phenotypes.....	94
5. Hemocyte count.....	95
6. B-galactosidase assay.....	95
7. Cell culture.....	96
8. Transfections and transduction.....	96
9. Quantitative Real time PCR.....	97
10. Immunoblot assay.....	98
11. Immunoprecipitation.....	98
12. Chromatin immunoprecipitation.....	99
13. Immunofluorescence assay.....	101
14. In situ proximity ligation assays (Duolink).....	101
15. Statistical analysis.....	102
RESULTS.....	103
A. PEL part.....	103
B. ATL part.....	129
DISCUSSION.....	164
GENERAL CONCLUSION.....	178
REFERENCES.....	181

ILLUSTRATIONS

Figure

1. Geographical seroprevalence of KSHV.....	25
2. KSHV virion structure and structural proteins.....	26
3. The invasion, entry, latent and lytic phases of KSHV.....	30
4. KSHV-mediated dysregulation of NF-KB and Notch pathway.....	36
5. Interplay between KSHV latency and lytic reactivation.....	40
6. An Illustrative model for transformation of HTLV-1 infected cells and progression towards ATL.....	57
7. Schematic representation of the HTLV-1 provirus genome and regulatory proteins.....	58
8. Schematic representation of Tax1 domains.....	60
9. Schematic representation summarizing altered pathways and multiple functions mediated by Tax.....	61
10. Schematic representation of Tax-mediated activation of canonical and non-canonical pathways of NF-B.....	63
11. Schemative representation of HBZ domains and their functions.....	69
12. Illustrative representation of cellular proteins that interact with HBZ.....	73
13. Schematic representation of the antagonistic effects of Tax and HBZ on NF-κB... ..	75
14. Schematic representation of PRC2 complex subunits and its interactions with chromatin.....	79
15. Epigenetic landscape in ATL cells.....	80
16. Accumulation of H3K27m3 contributes to ATL cell phenotype.....	82
17. ATO/Lena enhanced the survival of NOD/SCID PEL mice.....	102
18. ATO/Lena reduces malignant effusions in PEL mice.....	104
19. ATO/Lena decreased peritoneal volume in PEL mice.....	105
20. ATO/Lena inhibit cell proliferation in ascites-derived PEL cells.....	106
21. ATO/Lena decreases Latent gene expression in ascites-mediated PEL cells.....	107

22. Confocal microscopy analysis of LANA-1 nuclear expression in ascites-derived BC-3 and BCBL-1 cells.....	108
23. RTq-PCR analysis of KSHV latent v-FLIP and v-Cyclin in ascites-derived BC-3 and BCBL-1 cells.....	109
24. ATO/Lena decreases I κ B α phosphorylation in ascites-mediated PEL cells.....	110
25. Confocal microscopy analysis of P65 translocation in BC-3 and BCBL-1 ascites derived cells 48 h post treatment with ATO/Lena.....	111
26. RTq-PCR analysis of human IL-6 and IL-10 in BC-3 ascites derived cells 48 h post treatment with ATO and/ or Lena.....	112
27. RTq-PCR analysis of human IL-6 and IL-10 in BC-3 and BCBL-1 ascites derived cells 48 h post treatment with ATO and/ or Lena.....	113
28. RTq-PCR analysis of RTA and ORFK8 expression in BC-3 and BCBL-1 ascites derived cells 48 h post treatment with ATO and/ or Lena.....	115
29. RTq-PCR analysis of K8.1 expression in BC-3 and BCBL-1 ascites derived cells 48h post treatment with ATO and/ or Lena.....	116
30. Immunoblot analysis procaspase-3, cleaved caspase-3, and and PARP expression in BC-3 and BCBL-1 ascites derived cells 48 h post treatment with ATO/Lena.....	117
31. Confocal microscopy analysis of ascites-derived BC3 or BCBL-1 cells stained with Diamidine-2'-phenylindole dihydrochloride (Dapi) following 48h treatment with ATO/Lena.....	118
32. Mice peritoneum vascularization before and after one-week treatment of BC-3 PEL mice with ATO/Lena.....	119
33. Light microscopy images of capillary-like tube formations in HAEC cells.....	120
34. The capillary-tube formation analysis method used.....	121
35. ATO/Lena decreased organ infiltration in PEL mice.....	122
36. Immunephenotype analysis of CD45 expression in peritoneal ascites of BC3 PEL mice.....	123
37. ATO/Lena decreased latent protein expression in BC-3 PEL mice.....	124
38. Immunephenotype analysis of CD45 expression in peritoneal ascites of BCBL-1 PEL mice.....	125

39. ATO/Lena decreased latent protein expression in BCBL-1 PEL mice.....	126
40. RTq-PCR analysis of cytokine expression in PEL treated mice.....	127
41. Tax but not HBZ induce eye roughness in transgenic flies.....	128
42. RTq-PCR and Immunoblot analysis of expression of Tax and HBZ in Tax transgenic (Tax Tg) and HBZ transgenic (HBZ Tg) fly heads.....	129
43. Real-time quantitative PCR analysis of D-jun expression in hbz transgenic fly heads.....	130
44. RTq-PCR and Immunoblot analysis of the expression of Tax and HBZ in Tax (Tax Tg) and HBZ (HBZ Tg) transgenic hemocytes.....	131
45. Tax increases the number of circulating hemocytes in transgenic flies.....	132
46. Immunoblot analysis of the expression of E(z), SUZ12, H3K27me3, and H3K4me3 in fly heads from control , Tax-Tg and HBZ Tg flies.....	133
47. RTq-PCR analysis of the expression of Relish, E(z), and SUZ12 in heads of Tax Tg crossed with Relish-RNAi, E(z) RNAi, and Sua12 RNAi respectively.....	135
48. Scanning electron microscopy images of adult fly eyes pertaining to control (GMR-Gal4) or tax transgenic flies (GMR-Gal4; UAS-Tax) crossed with Relish- RNAi, E(z) RNAi, and Sua12 RNAi respectively.....	136
49. RTq-PCR expression of Relish and Dipterucin in fly heads from control, Tax Tg, or HBZ Tg flies.....	137
50. RTq-PCR analysis of the expression of Relish or Dipterucin in fly heads from control or Tax Tg, or HBZ Tg flies.....	138
51. RTq-PCR analysis of the expression of NF- κ B or PRC2 components in fly heads from control or Tax Tg flies with knocked down Relish, E(z), or SUZ12.....	140
52. Representative immunoblot of the expression of H3k27me3.....	141
53. Immunoblot analysis of the expression of Tax and HBZ in fly heads of control, tax, hbz, or tax/hbz transgenic flies.....	142
54. HBZ co-expression in Tg flies rescues Tax-mediated eye roughness.....	143
55. HBZ prevent Tax-mediated increase in hemocyte count in Tax Tg flies.....	144
56. RTq-PCR analysis of the expression of Relish and Dipterucin in control, Tax Tg, HBZ Tg, and Tax/HBZ fly heads.....	145

57. Expression of PRC2 components in control, Tax Tg, HBZ, and Tax/HBX Tg flies..	146
58. SA- β -gal expression eye imaginal discs of third instar larvae of control, Tax Tg, HBZ Tg, or Tax/HBZ Tg	147
59. RT-qPCR analysis of the expression of Dacapo in fly heads from control, Tax Tg, or HBZ Tg fly heads.....	148
60. RTq-PCR analysis of the expression of Tax and HBZ in circulating hemocytes.....	148
61. SA- β -gal activity in circulating hemocytes derived from control (HML Δ -Gal4>w1118), Tax Tg (HML Δ -Gal4>UAS-Tax), HBZ Tg (HML Δ -Gal4>UAS-HBZ), or Tax/HBZ transgenic (HML Δ -Gal4>UAS-Tax:HBZ) third instar larvae.....	149
62. SA- β -gal expression in circulating hemocytes from flies with silenced Relish, E(z), and Suz12 expression.....	151
63. Immunoblot analysis of EZH2, SUZ12, H3K27me3, Tax, and HBZ in HEK293T cells transfected for 48 h with increasing concentrations of His-Tax plasmid.....	152
64. Immunoblot analysis of the expression of EZH2, Suz12, H3K27me3, Tax, and HBZ in HEK293T cells transfected for 48 h with increasing concentrations of HBZ in presence of exogenous Tax.....	153
65. Immunoblot analysis of the expression of EZH2, Suz12, H3K27me3, Tax, and HBZ in Jurkat cells transfected with empty vector, His-Tax, Myc-HBZ, or His-Tax/Myc-HBZ vectors together.....	154
66. ChIP- RTqPCR analysis of H3K27me3 enrichment at target genes in empty vector, His-Tax, Myc-HBZ, or Tax/HBZ transfected HEK293T cells for 48 h.....	156
67. Real time quantitative PCR analysis of CDKN1A, NDRG2, and BIM expression in cells transfected with Tax and/or HBZ.....	156
68. Representative immunoblot of the expression of EZH2, SUZ12, and H3K27me3 in ATL-derived MT-1 cells transduced with scrambled or shHBZ vector.....	157
69. Representative Immunoprecipitation blot revealing the interaction between Tax and EZH2 in Tax and/or HBZ transfected HEK293T cells.....	158
70. Representative immunoblots of the expression of EZH2, SUZ12, H3K27me3, and HBZ in HEK293T cells transfected for 48 h with increasing concentrations of HBZ.....	159

71. Representative immunoblot of the immunoprecipitation assay for the interaction between EZH2 AND SUZ12 with HBZ in Myc-HBZ-transfected 293T following 48 h of transfection.....	159
72. Representative Confocal microscopy images of interactions between endogenous EZH2 or SUZ12 with HBZ using Duolink ® proximity ligation essay in HBZ-transfected Hela cells or ATL-derived MT-1 cells with endogenous HBZ.....	160
73. Representative confocal microscopy images of the co-localization of HBZ and EZH2 or SUZ12 in Hela cells transfected with Myc-HBZ vector.....	161
74. Illustrative model summarizing the suggested mechanism of action of ATO/Lena in primary effusion lymphoma.....	167
75. Proposed model for the interplay between Tax and HBZ for modulating NF-κB and PRC2.....	171

TABLES

Table

1. Human herpes viruses' classification, characteristics, and resultant diseases.....	23
2. Examples on preclinical studies targeting dysregulated pathways in PEL	48
3. Shimoyama classification of clinical subtypes of ATL.....	52
4. Examples of NF- κ B target genes whose expression is altered by Tax.....	64
5. Comparative table depicting major characteristics and functions of Tax vs. HBZ.....	69
6. List of primers used for Real time quantitative PCR.....	89
7. List of ATL primers used for Real time quantitative PCR.....	97
8. List of primers used for CHIP RT-qPCR.....	100

ABBREVIATIONS

AD	Activation domain	GFP	Green florescent protein
ADCC	antibody-dependent cell cytotoxicity	HAART	Highly active antiretroviral therapy
AIDS	Acquired immunodeficiency syndrome	HAEC	Human Aortic Endothelial Cells
AlloSCT	allogeneic stem cell transplantation	HAM/TSP	HTLV-1 associated myelopathy/tropical spastic paraparesis
AML	Acute myeloid leukemia	HBZ	HTLV-I basic leucine zipper protein
AP1	Activator protein 1	HHV8	human herpesvirus type 8
APL	Acute promyelocytic leukemia	HIV	Human immunodeficiency virus
ART	Antiretroviral therapy	HSCT	hematopoietic stem cell transplantation
ASCT	Allogenic stem cell transplantation	HSV	Herpes simplex virus
ATF	Activating transcription factor	hTERT	Human telomerase reverse transcriptase
ATL	Adult T-cell leukemia	HTLV-1	Human T cell leukemia virus type 1
ATO	Arsenic trioxide	IL-6	Interleukin 6
AZT	Zidovudine	IL-10	Interleukin 10
BDNF	brain-derived neurotropic factor	IFN- α	Interferon- α
BER	Base excision repair	IKK γ	inhibitor of kB-kinase γ
BET	bromodomain and extra terminal	KS	Kaposi Sarcoma
bZIP	basic leucine zipper protein	KSHV	Kaposi sarcoma herpesvirus
c-ART	Combined anti-retroviral therapy	LANA1	Latency-associated nuclear antigen
c-Cbl	Casitas B-lineage Lymphoma	LBS	LANA binding sites
CCR4	C-C chemokine receptor 4	LDH	Lactate dehydrogenase
CD	Central domain	Lena	Lenalidomide
CDK	Cyclin dependent kinase	LIC	Leukemia initiating cells
CDKN2A	Cyclin dependent kinase inhibitor	LUR	Long unique region
CHIP	Chromatin Immunoprecipitation	MCD	Multicentric Castleman's disease
CHOP	cyclophosphamide, doxorubicin, vincristine, and prednisone	MMR	Mismatch repair
CHVP	Cyclophosphamide, Hydroxydaunorubicin Vumon and prednisone	miRNA	Micro RNA
CK1 α	Casein kinase 1 α	NER	Nucleotide excision repair
CMV	Cytomegalovirus	NHL	Non-Hodgkin lymphoma

CR	Complete remission	NLS	Nuclear localization signal
CREB	cAMP response element-binding protein	ORF	Open reading frame
DA-EPOCH	Dose adjusted EPOCH: etoposide, prednisolone, vincristine, cyclophosphamide, doxorubicin	Ori-P	Origin of replication
DDR	DNA damage response	OS	Overall survival
DNZep	3-Deazaneplanocin A	PBMC	Peripheral blood mononuclear cells
DSB	Double strand break	PCR	Polymerase chain reaction
EBV	Epstein bar virus	PE	Phycoerythrin
EED	Embryonic ectoderm development	PEL	primary Effusion lymphoma
EZH2	Enhancer of zeste homolog	PFS	Progression free survival
FADD	Fas-associated death domain	PRC2	Polycomb repressive complex 2
GAPDH	Glyceraldehyde-3-Phosphate dehydrogenase	RA	Retinoic acid
Rb	Retinoblastoma protein	T reg	Regulatory T cells
REF	Rat embryonic fibroblasts	usHBZ	Un-spliced HBZ
ROS	Reactive oxygen species	vCRE	viral CREB responsive element
Rp49	Ribosomal protein 49	v-cyclin	Viral cyclin
SCR	scrambled	VEGF	Vascular endothelial growth factor
sHBZ	Spliced HBZ	v-FLIP	viral FLICE inhibitory protein
Sp1	Specificity protein 1	VHL	Von hippel-lindau
SUZ12	Suppressor of zeste 12	v-IRF3	interferon regulatory factor-3(LANA-2)
TR	Terminal repeats	WIP1	wild-type p53-induced phosphatase 1
TRE	Tax responsive elements	XIAP	X-linked inhibitor of apoptosis

CHAPTER I

INTRODUCTION

A. Primary Effusion Lymphoma

Primary Effusion Lymphoma (PEL) is a rare, aggressive, non-Hodgkin B-cell lymphoma secondary to infection with the Kaposi sarcoma herpesvirus (KSHV), also known as human herpesvirus type 8 (HHV8)^{1, 2}. PEL is associated with dismal prognosis and high mortality rates³. It develops in immunocompromised patients including those undergoing organ transplantation and more commonly in HIV-infected patients⁴⁻⁶.

In 1989, PEL was first described as a distinct uncommon AIDS-related neoplasm of B-cell origin⁷. This new non-Hodgkin lymphoma (NHL) was unique in its morphologic, immunophenotypic, and molecular genetic characteristics^{8, 9}, and infected patients developed weakness and cachexia with profound malignant pleural effusions⁷. Later in 1995, Cesarman et al. identified the presence of KSHV genome in lymphoma cells derived from malignant effusions of AIDS-related body-cavity lymphoma¹⁰. This distinct KSHV-associated lymphoma with body cavity effusions was designated as PEL in 1996⁸ and in 2001, the world health organization (WHO) classified PEL as a unique neoplasm of large B-cell lymphoma¹¹.

1. Epidemiology

PEL is a rare lymphoma that is mostly, but not exclusively, observed in HIV patients with decreased CD4 counts^{6, 12}. It accounts for around 4% of HIV-related NHL and 1% of non-HIV related NHL^{6, 12}. PEL manifests also in immunocompromised patients including organ transplant patients^{4, 13}, patients with liver cirrhosis¹⁴, or KSHV/HHV8 seropositive elderly patients¹⁵. PEL development is associated with multiple risk factors, the most important of which are male homosexuality and drug abuse¹¹. PEL mostly presents in young to middle aged men with a median age of 41-57 years at diagnosis^{16, 17}. It is predominant in men with a 6:1 ratio as compared to women¹⁶. In the Mediterranean region, KSHV seroprevalence ranges between 20 and 30%¹⁸. Co-infection with Epstein Bar virus (EBV) is quite common in PEL whereby 70-90% of these patients test positive for EBV^{10, 11, 19}. Yet, the role of EBV in PEL pathogenesis is still unclear. EBV-negative PEL is commonly detected in HIV-negative elderly from endemic HHV-8 areas such as central Africa and Mediterranean regions^{11, 19, 20}.

2. Clinical presentation

Clinically, classical PEL presents as lymphomatous malignant effusions in body cavities, with absence of a visible tumor mass^{2, 8}, hence, the former name “body cavity lymphoma”. PEL serous effusions occupy various body cavities including the pleural space which is the most common site, peritoneal and pericardial cavities^{2, 9, 21}. Other spaces

such as meningeal and joint spaces can be rarely affected⁹. Typically, a single cavity is involved, yet patients with the involvement of multiple cavities were also reported²².

Symptoms associated with PEL largely depend on the location of the disease and the respective involved cavities^{9, 23}. Enlarged abdominal girth, increased abdominal pressure from ascites accumulation, and edema in lower extremities often accompany peritoneal accumulation of malignant effusions^{9, 23}. When PEL involves pleural or pericardial effusions, symptoms such as cough, dyspnea, chest heaviness, cardiac tamponade with dizziness, decreased blood pressure, and electrocardiogram abnormalities may be encountered^{9, 21}. Patients may also complain of typical B-lymphoma symptoms characterized by fever, night sweats, and weight loss²¹.

Occasionally, extra-cavitary PEL with solid tumor formation may develop^{24, 25}. This subtype of PEL develops in regional lymph nodes (which represent the most common location accounting for 58% of extra-cavitary PEL), or extra-nodal sites including the bone marrow, lungs, mesenteric and gastrointestinal tract, central nervous system, and skin^{24, 26-28}.

3. Prognosis

PEL is associated with a dismal prognosis and low survival rates^{2, 16, 29}. Aside from lymphoma progression, the most common causes of death are immunosuppression or HIV-related complications, such as opportunistic infections^{3, 21, 29}.

Due to rarity of the disease, large randomized clinical trials are lacking, which hindered the improvement of PEL management^{2,3}. An optimal regimen for PEL is still unachieved and treatment is mostly guided by small longitudinal observational studies and case reports¹⁹. In untreated patients, the median survival for PEL after diagnosis is limited to 2-3 months^{12,19}. A multicenter retrospective study on 28 PEL patients demonstrated that chemotherapy improved the median survival to approximately 6.2 months, and a one-year survival rate in 39% of patients³⁰.

Multiple potential prognostic factors for patients with PEL were identified. Poor performance and lack of combined anti-retroviral therapy (c-ART) prior to PEL diagnosis were identified as negative prognostic factors contributing to a lower overall survival in HIV-positive PEL patients³⁰. The location and the number of affected cavities play also a role in the prognosis of PEL. In a retrospective study of 104 PEL patients, patients with only one involved cavity had a better overall survival (18 months) as compared to patients with more than one affected cavity (Overall survival 4 months)¹⁶. In addition, the location of the affected cavity affects disease prognosis. Indeed, patients with pericardial cavity involvement had better overall survival than those with pleural or peritoneal cavity involvement (40 months compared 27 and 5 months respectively)¹⁶. This might be due to the volume and size of the body cavity which reflects the tumor burden. High lactate dehydrogenase (LDH) levels and decreased CD4 cells counts may also contribute to dismal outcomes⁵. Recently, Lurain et al. established that EBV status and inflammatory cytokines (Interleukin-10 (IL-10) and (IL-6)) are among the strongest prognostic factors for PEL³¹. EBV positivity in PEL was identified as a positive prognostic factor associated

with better prognosis while inflammatory cytokines were linked to inferior prognosis³¹. Finally, when compared to classic PEL, extra-cavitary PEL was associated with a better prognosis³².

4. Diagnosis

PEL diagnosis can be guided by an array of clinical manifestations and imaging. However, lymphomatous effusion examination is essential for definitive diagnosis^{3, 21, 29}. In PEL, effusions are commonly bloody and exudative. Cytological preparation (cytospin) allow the identification of malignant PEL cells, which exhibit a predilection to grow in the liquid effusions^{3, 21}. Assessment of cell morphology, immunophenotype unique characteristics, and viral components detection contribute to PEL diagnosis^{29, 33}. Morphologically, PEL cells are pleomorphic large cells with intense abundant basophilic cytoplasm and occasional vacuolated cells^{33, 34}. Nuclei are large and round with an irregular shape and prominent nucleoli^{33, 35}. Large anaplastic cells with poor differentiation resembling Reed Sternberg cells may be occasionally present. For extra-cavitary PEL, the histological features of cells in sections/biopsies resemble those in effusions^{11, 35}.

Detection of KSHV/HHV8 infection in PEL cells is a must for confirmation of PEL diagnosis^{10, 36, 37}. Immunohistochemistry assay for Latency-associated nuclear antigen (LANA-1), a KSHV/HHV8 viral protein, is currently the gold standard method for definitive diagnosis^{38, 39}. Amplification of HHV8 constructs by Polymerase chain reaction

(PCR) is another alternative⁸. Verification of HHV8 infection is crucial for the differential diagnosis of PEL from other lymphomas with similar morphological characteristics and clinical presentation such as plasmablastic lymphoma^{8, 10, 37}. It is worth noting that, any PEL patient presenting with effusions at diagnosis belongs to stage IV of the disease, following Lugano classification criteria for NHL.

5. Cytological features of PEL

PEL cells express the common leukocyte antigen marker CD45 but lack B-lymphocyte markers including CD19, CD20, and CD79a as well as surface and cytoplasmic immunoglobulins^{2, 33, 34, 37}. In addition, PEL cells express lymphocyte activation markers such as CD30 and CD38, and typically express post-germinal B-cell antigens/plasma cell-associated markers (CD138, VS38c, and MUM-1/IRF4) implying that malignant cells are commonly in a late B-cell differentiation stage^{33, 34, 40-42}. Moreover, malignant cells usually lack NK cell markers and T-lymphocyte markers (CD2, CD3, CD4, CD5, CD7, and CD8), although atypical T-cell antigen expression have been reported particularly in extra-cavitary PEL^{33, 42}.

B. Kaposi's Sarcoma Herpesvirus/Human Herpesvirus-8

1. Discovery of Kaposi's Sarcoma Herpesvirus/Human Herpesvirus-8

KSHV belongs to the *rhadinovirus* genus in the γ 2-herpesvirus subfamily of mammalian herpesviruses in the Herpesviridae family^{19, 43, 44}. Members of this family are

classified into α , β , and γ -herpesviruses and are well known for establishment of life-long infection and latency in infected hosts^{45, 46}. Mostly, these viruses result in mild to asymptomatic illness with severe disease developing in immunocompromised settings only^{45, 47}. Eight human herpesviruses have been identified (Summarized in table 1). Human α -Herpesviruses such as Human Simplex Viruses 1 and 2 (HSV-1 and HSV-2, also known as HHV-1 and HHV-2) and Varicella zoster virus (HHV-3) establish latency in neuronal cells of infected people^{46, 47}. β -herpesviruses include Cytomegalovirus (CMV, also known as HHV-5) as well as Human Herpes Viruses 6 and 7 (designated HHV-6 and HHV-7 respectively)⁴⁶. These establish their latency in peripheral blood mononuclear cells (PBMC) excluding B-lymphocytes. As for γ -herpesviruses, these include EBV (HHV-4) and KSHV (HHV-8) whose main, but not exclusive, target for latency is B-lymphocytes⁴⁸. In fact, KSHV may also infect endothelial cells lining blood or lymph vessels^{46, 47, 49, 50}.

Table 1. Human herpes viruses' classification, characteristics, and resultant diseases.

Viral Subfamily	Taxonomic name	Common Name	Primary Target Cells	Major Related Disease
α-herpesvirinae	Human Herpes Virus-1 (HHV-1)	Human simplex virus 1 (HSV-1)	Muco-epithelial cells	Oral herpes Encephalitis
	Human Herpes Virus-2 (HHV-2)	Human simplex virus 2 (HSV-2)	Muco-epithelial cells	Genital herpes
	Human Herpes Virus-3 (HHV-3)	Varicella Zoster Virus (VSV)	Muco-epithelial cells	Chickenpox Shingles
β-herpesvirinae	Human Herpes Virus-5 (HHV-5)	Human Cytomegalovirus (HCMV)	Monocyte Lymphocytes Epithelial cells	Mononucleosis
	Human Herpes Virus-6 (HHV-6)	HHV-6 variant A or B	T-Lymphocytes	Roseola Infantum
	Human Herpes Virus-7 (HHV-7)	HHV-7	T-Lymphocytes	Roseola Infantum
γ-herpesvirinae	Human Herpes Virus-4 (HHV-4)	Epstein Bar Virus (EBV)	B-Lymphocytes Epithelial cells	Mononucleosis Lympho-proliferative diseases
	Human Herpes Virus-8 (HHV-8)	Kaposi Sarcoma Human Virus (KSHV)	B-Lymphocytes Endothelial cells Epithelial cells	KS PEL MCD

CCID: Congenital cytomegalic inclusion disease, KS: Kaposi Sarcoma, PEL: primary effusion lymphoma, MCD: multi-centric disease.

KSHV was first discovered by Chang and Moore et al. in 1994⁴³. Since 1980, studies on Kaposi Sarcoma (KS), an AIDS-defining tumor, linked the disease to an unknown sexually-transmitted infectious agent^{51,52}. It was until 1994 that Chang, Moore, and their colleagues used representational difference analysis on KS and normal

counterpart tissue and identified unique DNA sequences that were solely present in the AIDS-KS patients⁴³. The two identified fragments of 330 bp and 631 bp were present in 90% of KS patients⁴³. DNA sequences of these fragments were homologous, but not identical, to genes encoding capsid and tegument proteins of γ -herpesviruses capable of cellular transformation^{43, 53, 54}. Since then, KS was linked to a newly identified herpesvirus designated as HHV -8 or KSHV. KSHV entire genome was then cloned and its complete DNA sequence was later identified⁵³. Soon after, KSHV was linked to the rare deadly lymphoma PEL^{8, 10}, among other malignancies including KS, Multicentric Castleman's disease (MCD), KSHV inflammatory cytokine syndrome (KICS)^{10, 43, 55-58}.

2. KSHV epidemiology and Transmission

KSHV is highly endemic in areas such as sub-Saharan Africa and south America (the Amerindian population) (Figure 1)^{12, 18, 19}. The two regions present a similar pattern of prevalence, where 70% of children, aged 4-9, are seropositive and the prevalence increases with age to reach >90% at age 40 suggesting an early childhood KSHV infection. In the Mediterranean region (Spain, Italy, Sardinia, and Sicily)^{59, 60}, KSHV seroprevalence is around 20-30%. Low seroprevalence rates (<10%) is reported in the United States⁶¹⁻⁶³, Asia⁶⁴, and Northern Europe. The geographical variation of KSHV seroprevalence is still not understood. Some studies suggested that sociological or environmental factors including co-infection with parasites, such as malaria, may increase KSHV seroprevalence^{12, 65}.

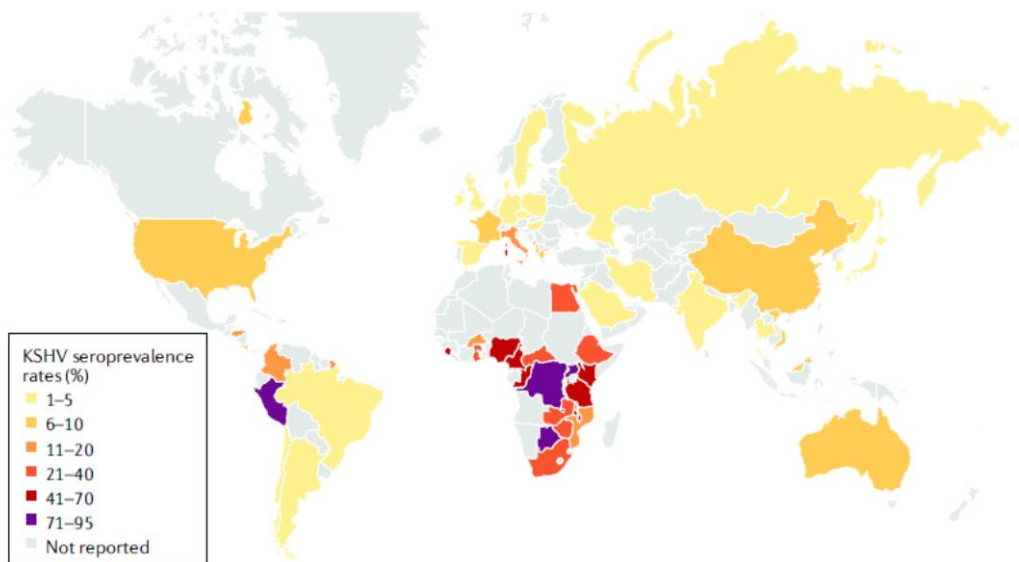


Figure 1. Geographical sero-prevalence of KSHV. KSHV is endemic in sub-saharan Africa (>40%), less prevalent in Mediterranean (Italy, Spain, Sicily, Sardinia) with 10-30%, and slightly detected in Asia, USA, and northern Europe (<10%)^{66, 67}.

Primary KSHV infection may occur at any age during childhood or adulthood and the virus may be transmitted through sexual or asexual routes^{12, 19, 68}. KSHV is present in PBMC and can be shed in saliva and oropharyngeal mucosa⁶⁹. It can be also found in other body secretions such as vaginal secretions, semen, and in prostate glands⁶⁸. KSHV modes of transmission depend on the endemicity of the region¹². In non-endemic areas, such as United states, sexual transmission especially among homosexual men, may be the most probable route of transmission^{12, 63, 68}. In endemic areas, the major route of transmission is through saliva^{12, 69}.

3. KSHV Virion Structure and Genome

KSHV share the characteristic architecture of herpesviruses^{47, 70}. In electron micrographs of KSHV-infected PEL cell lines and KS biopsies, KSHV appears as particles of 100-150 nm in diameter with an electron dense core and an outer lipid envelope⁷¹. KSHV comprises a double stranded linear DNA genome of approximately 165-170 kb encapsulated within a thick-walled icosahedral nucleocapsid^{44, 53, 70, 72}. The capsid is surrounded by an amorphous protein tegument layer and an outer envelope layer. KSHV envelope is a lipid bilayer derived from host cells and covered with viral glycoproteins^{44, 45, 73} (Figure 2).

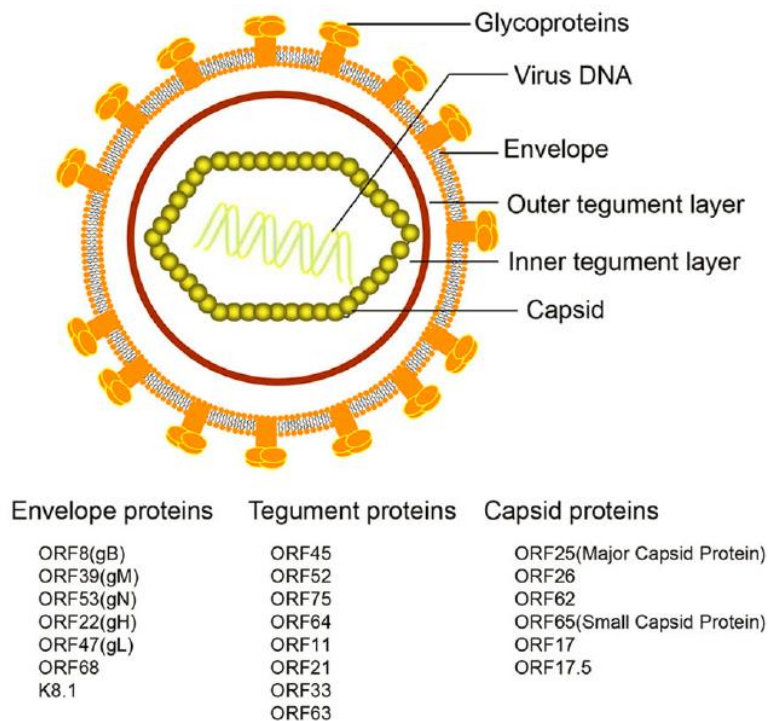


Figure 2. KSHV virion structure and structural proteins⁷⁴.

KSHV genome encompasses a central long unique region (LUR) of approximately 140.5 kb with low GC content (53.3%) accommodating all coding sequences^{53, 70, 72}. This coding region is flanked on both sides by multiple terminal repeats (TR), of 801 bp each, with rich GC content (84%)^{53, 54, 72}. KSHV isolates comprise different numbers of TRs varying between 16-75 TR which explains the difference in genome size among isolates. LUR encodes for highly conserved genes designated with the prefix “ORF” (open Reading frame) numbered consecutively across the genome from left to right as ORF4 to ORF75^{53, 54, 74}. Many ORF have homologs in other herpesvirus members and encode for proteins involved in viral replication or structural proteins⁵⁴. In addition, KSHV genome encodes for unique genes that interspace the LUR and are assigned with prefix “K” (K1 to K15). Originally, these genes were thought to be distinctive of KSHV^{53, 54, 74, 75}. However, K3, K5, K7 and K13 and others were later found to have homologues and additional new unique genes were identified⁷⁶. These unique genes control various functions including virus-associated diseases and viral replication⁷⁶. KSHV also encodes for multiple viral microRNAs (miRNA) and long non-coding RNAs^{53, 54, 74}.

Among various KSHV encoded proteins are structural proteins; these include the icosahedral capsid proteins; ORF62, ORF26, ORF65 and ORF25^{74, 77}. The Tegument layer proteins such as ORF11, ORF21, ORF33, ORF45, ORF52, PORF63 and ORF75 contribute to genome entry following primary infection and early replication events^{76, 78, 79}. Virally encoded envelope glycoproteins are seven; ORF8 (also called glycoproteinB, gB), K8.1, ORF22 (gH), ORF47 (gL), ORF39 (gM), ORF53 (gN), and ORF68^{74, 80-82}. These are

crucial for viral recognition, binding, and invasion of target cells during primary infection^{80, 81, 83}.

Interestingly, some KSHV genes are thought to be up taken by the virus from previous hosts as part of the viral evolution process^{84, 85}. As such, KSHV encodes for viral homologs of cellular genes such as viral interleukin 6 (v-IL-6), viral cyclin D (v-cyclin), viral bcl-2 (v-bcl2), viral c-FLIP (v-FLIP), and viral IL-8R (v-IL-8R)^{76, 84}. Studies suggest that these homologous genes allow for direct manipulation of host cell machinery by the virus⁸⁴. Additional cellular proteins including actin, HSC70, HSP90, and translational repressor EF-2b were also detected in virions⁷⁶.

4. KSHV Life Cycle

a) Invasion and primary infection

KSHV infects an array of cells including B-lymphocytes, endothelial cells, keratinocytes, monocytes, and epithelial cells^{74, 86}. The virus identifies and infects target cells through glycoproteins including gB, gH, K8.1, and gL embedded/studded in its outer envelop⁸⁷. Glycoproteins bind multiple host cell receptors including heparin sulfate, ephrin receptor tyrosine kinase (EphA2), integrins, cysteine transporter xCT, and dendritic cell specific intercellular adhesion molecule 3-grabbing nonintegrin (DC-SIGN)^{81, 83, 87-90}. Binding of glycoproteins to host cell receptors provide the first point of contact and result in membrane fusion between the virus and host cells^{81, 86, 87}.

Following initial binding, viral endocytosis is facilitated by a cellular E3 ligase protein referred to as Casitas B-lineage Lymphoma (c-Cbl), which transfers the KSHV-host cell receptor complex onto lipid rafts⁹¹⁻⁹³ (Figure 3). This enables the association of integrins with ephrin receptors resulting in a complex formation composed of c-Cbl, integrins, and myosin^{91,94}. Formation of such complex induce endocytic blebs through which KSHV virus gain access to the cell⁹⁴. In addition, binding of KSHV to integrin receptors also result in auto-phosphorylation of cytoplasmic focal adhesion kinase (FAK)^{95,96}. Once phosphorylated, FAK interacts with downstream effectors such as Src, c-Cbl, and phosphatidylinositol-3-kinase (PI3-K) to aid in viral entry and endocytosis^{93, 95-97}. In the cytoplasm, KSHV loses its envelope and traffics in its capsid form. Phosphorylated FAK also facilitates the transport of the viral capsid across the cytosol and its delivery to the nucleus through association with RhoA and cytoskeletal proteins, in specific Dynein and microtubules^{74, 92, 93, 96, 97}. Once the viral capsid reaches the nucleus, viral DNA is released into the nucleus through nuclear pores⁹². Inside, viral genome circularizes forming an episome^{74, 92, 98}. Afterwards, viral genome expresses an array of viral genes involved in host cell reprogramming such as activation of anti-apoptotic machinery, deregulation of cell cycle, host cell immune evasion, and deregulation of key signaling pathways including Notch, NF- κ B, and MAPK^{44, 92}.

The outcome of KSHV primary infection and expression of viral genes vary according to the targeted cell whether a B lymphocyte, an endothelial cell, or a keratinocyte^{44, 74}. Similar to other human herpesviruses, KSHV life cycle has two major phases; a transient short lytic replication phase and a persistent latent replication phase^{19, 74}.

⁹⁹. Both phases have complex, yet distinct, gene expression patterns. Life-long latency is considered as the default life cycle for KSHV virus following primary host infection^{38, 99}. Occasionally, throughout its life cycle, the virus may undergo sporadic episodes of lytic reactivation⁹⁹ (Figure 3).

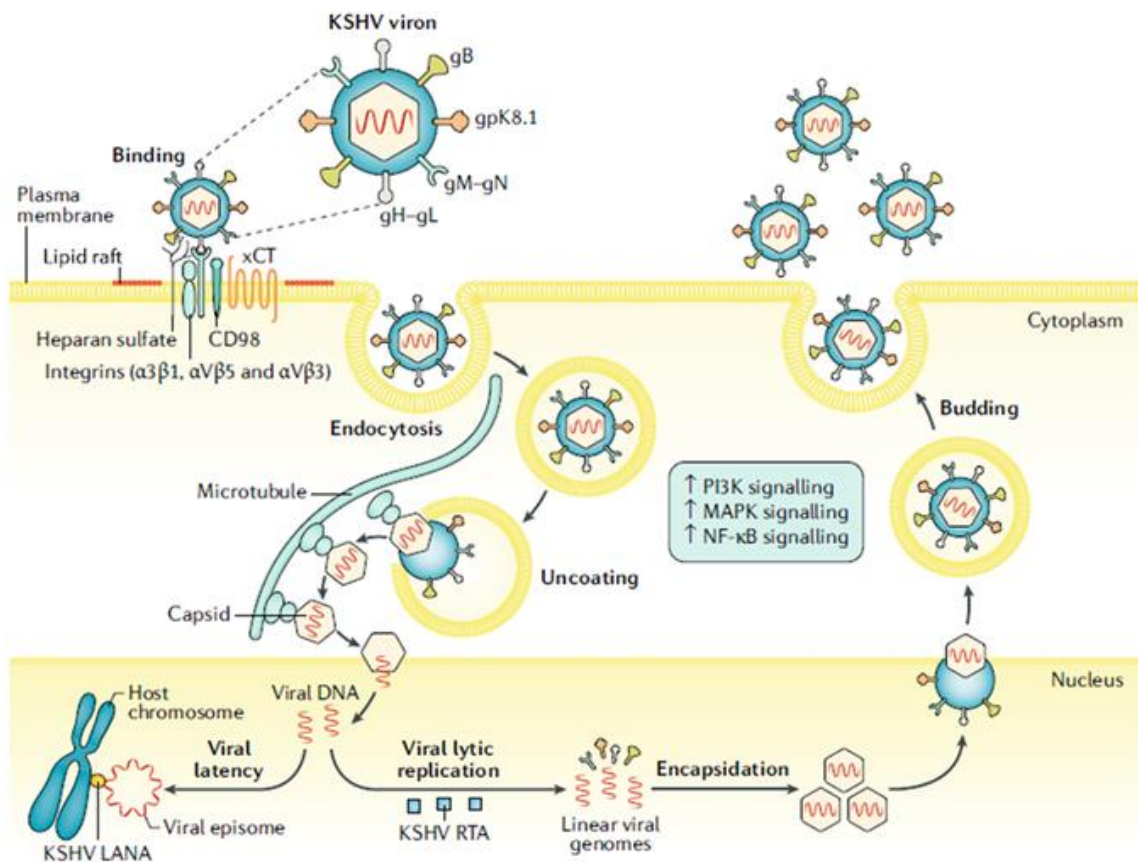


Figure 3. Illustrative figure depicting the invasion, entry, latent and lytic phases of KSHV⁶⁷. Surface viral glycoproteins mediate cell fusion and entry by binding cellular receptors including integrin receptors, heparin sulfate. The viral-host interaction triggers an intracellular signaling cascade which recruits microtubule proteins (blue lines). This results in viral transport throughout the cytoplasm to the nucleus where viral expression allows for either establishment of latency via LANA or initiation of virion production via RTA-mediated lytic replication. Once inside, KSHV manipulates several key pathways including PI3K, MAPK, NF-κB.

b) Viral Latency

KSHV latency is mainly established in B lymphocytes and endothelial cells of infected hosts^{74, 100, 101}. To enter the latent phase, viral genome circularizes and is maintained as episomes in the nucleus of host cell; Episomes tightly control gene expression in an off-on latent specific form^{102, 103}. Latency is maintained through the simultaneous replication of the viral genome along with the host cellular DNA^{38, 103}. KSHV replicated genome is passed in highly precise and even manner to the host daughter cells and is maintained as limited 10-150 genome copies in each infected cell^{38, 104}. During latency, daughter virion progenies are not produced^{34, 38}. Rather, the virus maintains a limited viral expression confined for latent genes crucial for latency maintenance^{34, 105, 106}. These involve the major latency locus genes which includes ORF73 (encoding for LANA-1)^{38, 98, 106, 107}, ORF71 (encoding for viral FLICE inhibitory protein (v-FLIP))^{108, 109}, ORF72 (encoding for v-Cyclin (ORF72))^{106, 110}, ORFK12 (encoding for kaposins)^{76, 111}, and 12 miRNAs (also called K-miRNA)¹¹². Latent genes also involve ORFK10.5 (encoding for viral interferon regulatory factor-3 (v-IRF3), also called LANA-2)¹¹³.

In PEL, KSHV is maintained in latent replicative state^{98, 104}, whereby latency-associated proteins are always expressed and their expression is paramount for the survival of latent-infected PEL cells^{74, 104}. KSHV latent infection promotes oncogenesis and presents a barrier against the elimination of malignant cells mainly through alteration of host cell survival machinery and immune response^{105, 114}. Indeed, expression of viral latency locus latent genes in B cells increased predisposition to lymphoma and hyperplasia in mice¹¹⁴. KSHV latency is maintained through multiple mechanisms including

suppression of lytic replication and evasion of immune system^{38, 115}. Latency is a reversible state; it can be disrupted by multiple physiological and/or environmental stimuli including inflammatory cytokines, hypoxia, and oxidative stress^{116, 117}. Such stimuli may induce the resting viral genome/hidden virus to switch into the lytic replicative phase^{116, 117}. In the below section, an overview on latent proteins and their known functions will be provided.

i. LANA-1: the major regulator of latency

LANA-1 also called ORF73, is a multifunctional protein and the master regulator of latent infection that drives KSHV-induced malignancies³⁸. Among latent proteins, LANA-1 is detected in almost all KSHV-infected cells with a dot-like nuclear pattern by immunohistochemistry and immunofluorescence assays^{38, 39}. Detection of LANA-1 in PEL ascites/tissues became the gold standard for definitive diagnosis of PEL³⁷⁻³⁹.

LANA-1 establishes and maintains KSHV latency and viral genome stability by tethering the episome to the host genome^{38, 98}. In brief, LANA-1 directly binds to the LANA-binding sites (LBS) in the TR repeats of the viral genome *via* its C-terminal DNA-binding domain, while binding to the host chromatin-associated proteins *via* its N-terminal histone-binding regions thereby securing KSHV genome on the host genome^{118, 119}. This allows for episomal replication, prevents viral genome loss during host cell mitosis, ensures even distribution of replicated viral DNA copies to daughter cells, and thus maintains latency^{118, 120}. In addition, viral replication in latent cells is totally dependent on the host cellular replication machinery^{118, 120}. LANA recruits host DNA replication machinery to the viral origin of replication (ori-P) to allow KSHV replication and ensures strictly controlled replication of one viral replication cycle per host cell cycle¹¹⁸.

LANA-1 plays also a pivotal role in maintenance of viral latency through inhibition of lytic gene expression^{38, 121}. Indeed, LANA-1 acts as negative regulator of lytic reactivation via direct binding to the promoters of lytic genes thereby hurdling their gene expression¹²¹. Alternatively, it recruits DNA methyl transferases to the promoters of lytic genes preventing their transactivation¹²². The most important silenced lytic gene is RTA, which is the major transcriptional activator of lytic gene expression also called the lytic switch protein¹²². LANA-1 also prevents transactivation by RTA through both direct binding with RTA and competitive interaction with RBP-J κ , a cellular component in the RTA transactivation complex^{123, 124}. This direct interaction between LANA-1 and RBP-J κ represses RTA expression and prevents uncontrolled viral reactivation^{121, 123, 124}. Moreover, transfection of a KSHV mutant where LANA-1 was deleted, results in prompt early lytic gene expression highlighting the critical role of LANA-1 in controlling lytic gene expression¹²⁵.

In addition to its importance in latency maintenance, LANA-1 contributes to the survival and growth of infected cells by interacting with multiple cellular proteins^{38, 74}. Indeed, LANA-1 binds and inhibits tumor suppressor genes such as p53, and retinoblastoma protein (pRb) among others, resulting in apoptosis inhibition and increased proliferation^{126, 127}. In fact, LANA inhibits both p53 transcriptional activity and p53-mediated apoptosis¹²⁸. It also upregulates the levels of Aurora A, Ser/thr oncogenic centrosome-associated kinase, which promotes p53 ubiquitylation and subsequent degradation resulting in cell survival¹²⁹. On the other hand, interaction of LANA with pRb results in the activation E2F-responsive gene, which enhances cell cycle progression^{127, 130}.

Co-expression of LANA-1 and H-ras led to the transformation of primary rat embryonic fibroblasts (REF)¹²⁷. In transgenic mice, expression of LANA-1 in B cells resulted in enhanced germinal center formation, follicular hyperplasia, and lymphomas presenting LANA-1 as a potential oncogene with key role in KSHV-associated lymphomas¹³¹. Expression of LANA1 in lymphoid cells stimulated S-phase entry and overcame cyclin-dependent kinase inhibitor, CDKN2A, and induced G1 cell-cycle arrest suggesting that LANA-1 promotes cell cycle progression¹³⁰.

LANA-1 undermines cellular immune response *via* attenuation of STAT-1-dependent IFN- γ -inducible gene expression by competing with STAT1 from binding the promoter region¹³². In addition, LANA-1 modulates multiple signaling pathways such as NOTCH and Wnt pathways^{92, 133}. LANA-1 deregulation of Wnt pathway results in β -catenin stabilization and activation of c-Myc oncogene^{133, 134}.

ii. LANA-2

LANA-2 is expressed in most but not all KSHV-infected cells¹³⁵. LANA-2 is exclusively detected in PEL and MCD patients but not detected in KS tissues¹³⁵. In PEL, LANA-2 is crucial for the survival and proliferation of infected PEL cells¹¹³. Indeed, knocking down LANA-2 in PEL cells *in vitro* resulted in reduced cell proliferation and enhanced caspase-3 and caspase-7 activity enhancing cell death¹¹³. LANA-2 is also involved in development of chemotherapy resistance to anti-mitotic drugs by reducing the stability of polymerized microtubules¹³⁶. In addition, LANA-2 plays a role in impairment of apoptosis through inhibition of p53-mediated cell death¹³⁵. It also averts p53 SUMOylation resulting in cell senescence¹³⁷. Recently, Manzano et al. nicely

demonstrated that LANA-2 cooperates with cellular interferon (IFN) regulatory factor 4 (IRF4) and basic leucine zipper ATF-like TF (BATF) as oncogenic transcription factors to activate a super-enhancer mediated oncogenic transcription program in PEL which enhances survival and proliferation of malignant cells¹³⁸.

iii. Viral FLICE inhibitory protein

Viral FLICE inhibitory protein, v-FLIP or K13, is the viral homologue of the cellular FLICE inhibitory protein (Fas-associated death domain (FADD)-like interleukin-1 beta-converting enzyme)^{76, 139}. V-FLIP is an oncogene crucial for PEL progression and survival of PEL cells¹⁰⁸. It blocks death-receptor Fas and inhibits TNF-mediated caspase activation resulting in apoptosis inhibition and cell survival¹³⁹.

More importantly, v-FLIP binds to the inhibitor of κ B-kinase γ (IKK γ) resulting in activation NF- κ B pathway^{140, 141}. NF- κ B is a key cellular pathway for KSHV tumorigenesis (Figure 4) and latent-infected PEL cells proliferation and survival^{140, 142-144}. NF- κ B inhibits lytic reactivation and maintains latency in KSHV-infected PEL cells^{145, 146}, making this pathway a potential druggable target in PEL^{143, 144}.

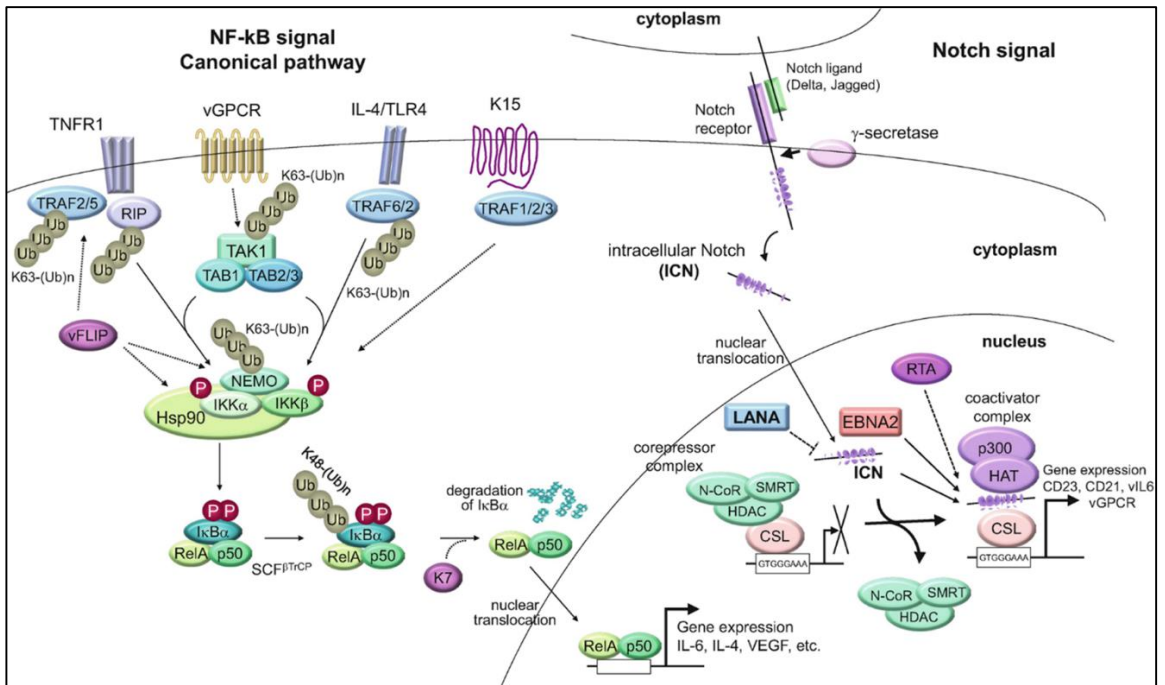


Figure 4. KSHV-mediated dysregulation of NF-κB and Notch pathway⁴⁵. KSHV alters various cellular pathways that contribute to malignant transformation, immune evasion, and modulation of key cell functions such as survival and proliferation. Among these pathways, KSHV constitutively activates NF-κB mainly through its latent protein v-FLIP which binds IKK. Activation of NF-κB activates gene expression of cytokines and angiogenic factors such as IL-6, VEGF. KSHV also modulate the NOTCH pathway. During latency, LANA-1 suppresses NOTCH pathway to inhibit RTA transcription and thereby maintain latency.

Recently, Ye et al., elucidated that activation of NF-κB by v-FLIP inhibits AP-1 pathway, which leads to inhibition of viral lytic reactivation and maintenance of latency¹⁴⁷. The oncogenic potential of v-FLIP was mainly elucidated in transgenic mice. Indeed, v-FLIP transgenic mice exhibited B-cell differentiation and developed a progressive lymphoma associated with activation of NF-κB reminiscent to what is seen in PEL patients¹⁴⁸. Furthermore, knocking down v-FLIP resulted in decreased NF-κB activation

and apoptosis induction suggesting that v-FLIP is essential for the survival of latent-infected PEL cells¹⁰⁸.

iv. v-Cyclin

v-Cyclin is the viral homologue of the cellular cyclin D2¹⁰⁶. It promotes cell cycle progression and cellular proliferation *via* constitutive activation of cyclin-dependent kinase 6 (CDK6) and pRb inactivation promoting G1/S transition^{110, 149, 150}. In addition, vCyclin-CDK6 complex promoted shorter G1/S phase transition through phosphorylation of other substrates including p21 and p27¹⁴⁹. In PEL cells, vCyclin-CDK6 complex may control latent infection through the phosphorylation of nucleophosmin protein¹⁵¹.

Deletion of v-Cyclin decreased cell proliferation and delayed cell cycle progression¹⁵². v-Cyclin mutant cells exhibited contact inhibition and were arrested at G1 phase suggesting that v-Cyclin contributes to oncogenesis by promoting cell proliferation and overriding contact inhibition in lymphoid tissue¹⁵². NF-κB constitutive activation induced by v-FLIP may result in p21/p27 mediated G1 cell cycle arrest and senescence¹⁵³. Zhi et al., demonstrated that v-Cyclin, encoded from the same bicistronic mRNA of v-FLIP, counteracted or mitigated the G1 arrest/senescence inflicted by v-FLIP *via* phosphorylation and degradation of p21 and p27 thereby allowing cells to escape senescence and resume proliferation¹⁵³.

c) Lytic reactivation

The latent phase of KSHV infection is reversible and can be disrupted by multiple stimuli including physiological and environmental stimuli^{99, 116, 117}. Once disrupted, the resting/dormant genome is activated and the virus enters a new short phase of its life referred to as “lytic reactivation”, characterized by sequential massive expression of most viral genes, ultimately resulting in infectious virion production¹⁵⁴.

During viral reactivation, lytic gene expression follows a temporal and sequential transcriptional cascade that starts with “immediately early genes (IE)” such as *rta*¹⁵⁵⁻¹⁵⁸. These genes initiate lytic reactivation by encoding regulators and transcription factors^{155, 159}. This is followed by the transcription of “early genes” such as *orfk8* and *orf59* whose main function is to prepare the cells for viral genome replication and viral protein synthesis^{74, 156, 158, 160}. The last transcribed genes are the “late genes” including those encoding for glycoproteins such as *k8.I*, whose expression follows the onset of replication and encodes for viral structural proteins^{74, 158, 161}. Once all lytic genes are expressed, the assembly of new virion particles is initiated in the nucleus^{159, 162}. Briefly, replicated viral DNA is incorporated in icosahedral capsids, surrounded by a tegument before budding through the cell membrane thereby gaining its envelope¹⁶³. A clear boundary between latent and lytic states is not present⁹⁹. Indeed, during lytic reactivation, infected cells simultaneously express both lytic and latent viral proteins^{99, 154}. Among the most important lytic proteins in KSHV, RTA (also referred to as ORF50) is a major lytic transactivator referred to as “lytic switch protein”^{164, 165}. RTA is a nuclear transcription factor, transcribed as immediate-early gene that can be detected as early as 4h post primary infection^{158, 166}. It

is also detected in TPA-induced PEL cells such as BCBL-1. Lukac et al. demonstrated that RTA expression itself is sufficient for KSHV reactivation¹⁶⁷. Indeed, mutant KSHV with a deletion in RTA failed to express lytic viral genes or to produce daughter virions. Multiple studies demonstrated that RTA transactivates lytic gene promoters including early genes (such as *orf 57*, *orf59*, *v-il6*, *k8*, *k9*), and late genes (such as the gene encoding for assembly protein, glycoprotein gB (ORF8.1))¹⁶⁷⁻¹⁶⁹. In addition, RTA auto-activates its own promoter¹⁷⁰, and exhibits a ubiquitin E3 ligase activity, which results in degradation of host and viral proteins. Target proteins include the MyD88, an important player in innate immunity¹⁷¹, and whose degradation by RTA allows for immune evasion during lytic reactivation¹⁷¹.

d) KSHV interplay between latent and lytic cycles

The relationship and expression patterns of latent and lytic KSHV proteins are quite complex⁷⁴ (Figure 5). Indeed, RTA plays a key role in initiating lytic early replication and activates LANA promoter¹⁷². Once LANA is expressed, it inhibits RTA activity and transcription thereby maintaining a persistent latency¹⁷² (Figure 5). Moreover, during latency, v-FLIP binds RTA and activates NF- κ B which by itself can also contribute to RTA inhibition¹⁴⁷. Conversely, upon lytic reactivation, RTA is expressed to induce expression of lytic genes¹⁶⁹. Once expressed, RTA further inhibits NF- κ B by targeting v-FLIP for proteasomal degradation¹⁷³.

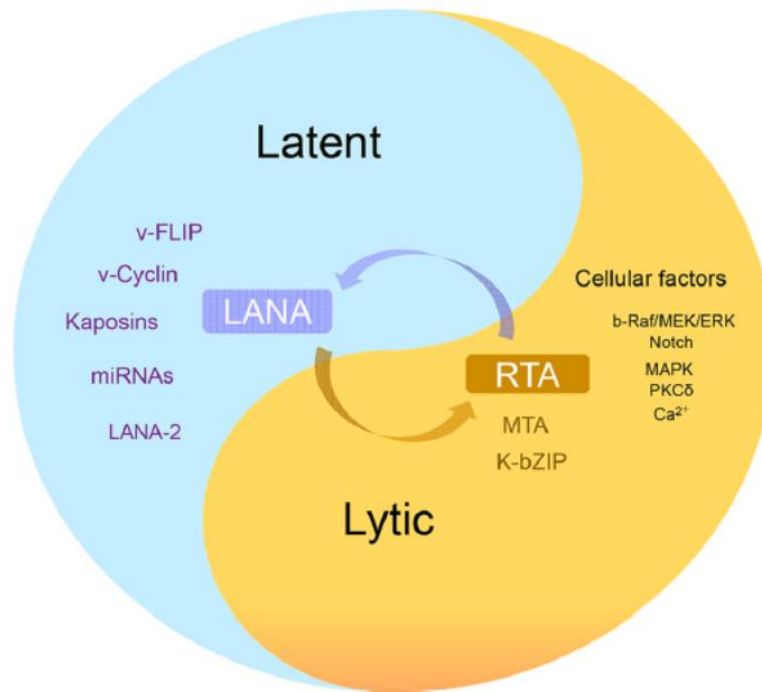


Figure 5. Interplay between KSHV latency and lytic reactivation. Blue section represents latent proteins among which LANA is a major player of latency. Yellow section represents lytic proteins among which RTA is a key lytic player. Black font represents key cellular factors or signaling pathways implicated in viral lytic cycle⁷⁴.

Recent studies presented viral switch from latency to lytic reactivation as a promising therapeutic approach for herpesviruses-associated neoplasia^{174, 175}. In PEL, Li et al., demonstrated that inhibition of NF- κ B survival pathway may increase oxidative stress, which mediates KSHV lytic reactivation resulting in massive cell death¹¹⁷. A similar study by Zhou et al. introduced oncolytic reactivation of endogenous KSHV as a rational therapeutic approach for PEL management¹⁷⁴. In more details, a combination of bromodomain and extra terminal (BET) protein inhibitor and ingenol-3-angelate (PEP005) induced lytic reactivation, inhibited IL-6 production by malignant PEL cells, and resulted

in apoptosis¹⁷⁴. This approach exploited the concept of inducing oncolysis *via* viral replication while simultaneously inducing an immune response to lytic antigens thereby clearing the virus^{174, 175}.

C. PEL angiogenic factors and growth factors

PEL cells secrete high levels of human interleukin-6 (IL-6) and IL10 cytokines. These two cytokines act as autocrine growth factors, which promote PEL growth and proliferation^{37,38,39}. Preclinical studies assessed the importance of IL-6 in PEL progression¹⁷⁶. Anti-IL-6 receptor antibody, Tocilizumab, decreased or delayed ascites formation in murine PEL model resulting in prolonged survival of these mice¹⁷⁶. Recently, elevated IL-6 levels were considered as negative prognostic factors in PEL patients, as patients with elevated IL-6 serum levels exhibited an inferior survival³¹. *Il-6* is a downstream gene of NF- κ B¹⁷⁷. Indeed, ν -FLIP latent protein was shown to activate the IL-6 promoter *via* activation of NF- κ B¹⁷⁷.

IL-10 is another crucial growth factor for PEL progression¹⁷⁸. Jones et al., demonstrated that interleukin 10 is involved in the spontaneous growth of PEL cells¹⁷⁸, and inhibition of IL-10 by anti-IL-10 antibodies or soluble IL-10 receptors delayed the proliferation of PEL cell lines (BCBL-1 and BC-1)¹⁷⁸.

In addition to cytokines, PEL cells produce high levels of angiogenic factors such as Vascular endothelial growth factor (VEGF)¹⁷⁹. High levels of VEGF were detected in PEL ascites *in vivo* and strongly correlate with PEL progression¹⁷⁹. In murine PEL model,

anti-VEGF antibody, bevacizumab, impeded ascites formation and enhanced survival of PEL mice¹⁷⁶.

D. PEL treatment

Given the rarity of the disease, large-scale longitudinal randomized studies are lacking^{2, 21}. As a result, Treatment and management decisions are guided by and restricted to some available preclinical data, small retrospective studies, and individual case reports^{2, 21}.

1. Frontline therapy

a) Chemotherapy

Conventional chemotherapy remained the mainstay of treatment of PEL patients presenting with no comorbidities and a good performance status^{21, 180}. Yet, an optimal regimen was not achieved. Since a universally-accepted standard regimen effective as first line therapy is lacking, an aggressive lymphoma chemotherapy is typically opted. Examples of adopted chemotherapy include CHOP (cyclophosphamide, doxorubicin, vincristine, and prednisone) or DA-EPOCH (dose-adjusted EPOCH: etoposide, prednisolone, vincristine, cyclophosphamide, doxorubicin)^{2, 21, 180}.

In a study conducted by the national cancer institute, the effect of DA-EPOCH in thirty-nine newly diagnosed patients with AIDS-associated B-cell lymphoma was investigated¹⁸¹. This treatment resulted in an 87% overall response rate, of which 74%

were complete remissions (CR)¹⁸¹. In addition, 52 months post treatment initiation, the overall survival was 60%¹⁸¹. Several case reports recommended the use of DA-EPOCH in combination with antiretroviral drugs (ART) for PEL patients infected with HIV¹⁸². In one report, an HIV patient presenting with extra-cavitary PEL affecting the colon was treated with four cycles of EPOCH, in addition to highly active retroviral therapy (HAART) and achieved a complete remission that lasted for 14 months after treatment¹⁸².

The efficacy of CHOP-like regimens was also evaluated in PEL. In a retrospective study, the potency of CHOP-like regimen in eight patients was assessed. Prednisone was omitted to prevent KS emergence⁶. 42% of patients achieved CR. However, the median survival was still limited to 6 months. In a multi-regimen retrospective study, CHVP (Cyclophosphamide, Hydroxydaunorubicin (Doxorubicin), Vumon, Prednisone) plus methotrexate were evaluated on seven AIDS patients with PEL¹⁸³. Three patients achieved CR which lasted for 18-78 months. However, these patients suffered from hematological toxicity attributed to methotrexate¹⁸³. As such, the combination was not recommended for patients with effusions due to the delay in methotrexate clearance.

In rare cases, PEL cells can express CD20. For CD20-positive PEL, a chemo-immunotherapy consisting of CHOP and rituximab (R-CHOP) which is a monoclonal anti-CD20 antibody, was investigated^{184, 185}. Two case reports on one patient each, showed that R-CHOP induced a durable CR which lasted for 22 and 30 months¹⁸⁴. Moreover, in HIV patients with CD20 positive PEL, R-EPOCH resulted in CR that lasted for one year¹⁸⁵. collectively, and despite multiple case reports and retrospective studies, management of PEL by chemotherapy remains poor.

b) Anti-retroviral therapy

For PEL patients diagnosed in the setting of HIV, ART/chemotherapy combination is a reasonable first-line approach²¹. Indeed, in a retrospective study conducted on HIV-infected patients with concurrent PEL, a shorter OS was reported in patients with poor performance and who were untreated with ART prior to PEL diagnosis³⁰. In a similar study, Simonelli et al. elucidated that patients treated with CHOP-like therapy without ART also exhibited a shorter OS limited to 3 months and failed to achieve CR⁶. Conversely, it was reported that ART alone resulted in CR in one HIV-positive PEL patient, and this CR lasted for 14 months¹⁸⁶. As a result, addition of ART to chemotherapy is the usual norm for treating HIV-positive patients with PEL.

Based on preclinical reports, some retroviral agents like Azidothymidine resulted in growth inhibition of PEL cell-lines¹⁸⁷. Similarly, Lopinavir, a proteasome inhibitor, induced apoptosis of PEL cells through inhibition of NF-kB pathway¹⁸⁸.

2. Relapsed and refractory PEL

Following frontline therapy, most PEL patients relapse within 6-8 months requiring further management^{2, 21}. In this setting, therapeutic options depend on comorbidities, and performance status, which are highly dependent on individuals^{21, 180}. Treatment options include radiation, stem cell transplant, antiviral drugs, and targeted therapies such as bortezomib¹⁸⁰.

a) Radiation

In PEL, radiation is an option in patients with a refractory/relapsed disease and whose tumor is causing physical pain^{21, 180}. By itself, radiation is not sufficient to achieve CR, but is useful for decreasing PEL burden²¹. Indeed, radiation can be considered for cases with solid PEL mass confined to one radiation field. In that sense, in a case report of a patient with pleural-based PEL mass, localized radiation resulted in sustained remission for 1 year¹⁸⁹.

b) Stem cell transplant

Autologous stem cell transplant (ASCT) was implemented in PEL²¹. An HIV-negative PEL patient who received ASCT following CR with chemotherapy (Ifosfamide, carboplatin, and etoposide) had a sustained CR for 12 months post ASCT¹⁹⁰.

As most PEL patients present with coinciding HIV infection, concerns pertaining to the use of ASCT in that population were reported²¹. Nevertheless, in one case report, an HIV-positive patient, was treated with reduced intensity regimen followed ASCT resulting in CR that was sustained for 31 months post transplantation¹⁹¹. Yet, with the lack of sufficient reports that support the use of ASCT in PEL, the benefit of this approach remains questionable.

c) Antiviral therapies

Several case reports supported the use of antivirals in PEL management. In three HIV-negative patients with PEL, intracavitary injection of cidofovir into the affected cavity resulted in promising response¹⁹². Indeed, in two patients, intrapleural injection resulted in 10 and 15 months of CR. In the third patient, intraperitoneal injection of cidofovir resulted in 5 months of CR¹⁹². However, this regimen was limited to patients with one cavity and no data exist on intracavitary cidofovir administration into multiple cavities. In another report, an HIV patient refractory to chemotherapy achieved a CR exceeding 13 months when treated with valganciclovir while receiving ART¹⁹³.

d) Targeted therapies

i. Proteasome inhibitors

Proteasomal activity is essential for viral replication of KSHV-infected cells and survival of PEL cells^{144, 194, 195}. Indeed, the ubiquitin/proteasome system was shown to mediate entry and endosomal trafficking of KSHV into target cells¹⁹⁶. Moreover, KSHV was reported to hijack the 26S proteasome in order to manipulate proteasome-dependent pathways involved in cell regulation, apoptosis, and cell proliferation including NF- κ B and Notch pathways¹⁹⁴. Bortezomib, a proteasome inhibitor, is approved for treatment of multiple myeloma and mantle cell lymphoma¹⁹⁷. Clinically, bortezomib combined with rituximab and PEGylated liposomal doxorubicin resulted in sustained CR of two years in CD20-positive HIV-negative PEL patient¹⁹⁸.

3. *Preclinical studies*

Preclinical studies provided insights into potential targeted therapies for PEL (Table.2). Among multiple pathways, the phosphatidylinositol-3-kinase/Akt/mammalian (PI3/AKT/mTOR) pathway is frequently activated in PEL. Rapamycin, targeting this pathway, induced apoptosis and decreased proliferation of PEL cell lines *in vitro*, and inhibited PEL tumor growth in a xenograft murine PEL model¹⁹⁹. NF- κ B is another fundamental constitutively activated pathway in PEL^{140, 141}. Dual inhibition of NF- κ B and PI3/AKT pathways, by Bay11-7085 and LY294002 respectively, resulted in synergistic apoptosis of PEL cells¹⁴³. Preclinical studies also investigated VEGF and IL-6 as potential targets for therapy. As discussed before, VEGF- specific antibody and anti-IL-6 antibody delayed PEL ascites development *in vivo* and improved survival of PEL mice¹⁷⁶.

Since PEL cells are infected with the KSHV virus, attempts to target malignant cells with antiviral drugs were conducted^{21, 180}. However, since the virus exist in its latent state in malignant cells, it was resistant to most antiviral regimens. One proposed regimen depended on induction of viral reactivation followed by treatment with anti-viral drug resulting in apoptosis of KSHV-infected cells²⁰⁰. Indeed, cells with lytic replication were found to be sensitive to foscarnet, ganciclovir, and cidofovir^{200, 201}.

Preclinical studies also investigated the anti-tumor effects of proteasome inhibitors *in vitro*. Indeed, proteasome inhibition resulted in decreased cell proliferation and inflicted apoptosis in PEL cell lines²⁰². Combined with vorinostat, a histone deacetylase inhibitor, the proteasome inhibitor, Bortezomib resulted in KSHV reactivation, cell death, and enhanced survival in PEL murine model²⁰³.

Table 2. Examples on preclinical studies targeting dysregulated pathways in PEL

Drug	Molecular Target	Key findings	Ref
Berberine	NF-kB inhibition	Induction of apoptosis and Suppression of NF-kB activity via inhibition of IKK phosphorylation	204
Bortezomib (PS-341)	NF-kB inhibition Proteasome inhibition	Induction of apoptosis and inhibition of proliferation	195
Bortezomib Vorinostat	Proteasome inhibition HDAC inhibition	Inhibited proliferation, induced apoptosis and KSHV reactivation in PEL murine model	203
ATO/ IFN- α	NF-kB inhibition Latent gene transcripts	Inhibition of proliferation, induction apoptosis, decreased latent transcription and NF-Kb Enhanced survival <i>in vivo</i>	205 206
Bay11-7085/ LY294002	NF-kB and PI3 kinase/ Akt inhibition	Synergistic apoptosis of PEL cells	143
PF-04691502 & AKTi ½	PI3K/AKT/mTOR inhibition	Dual inhibition of PI3K/AKT/ mTOR and glycolytic pathway enhanced cytotoxicity in PEL cells	207
PEP005/ JQ1	BET inhibition and NF-kB inhibition	Induction of HHV8/KSHV lytic replication, inhibition of IL6, production and proliferation, and induction of apoptosis Delay tumor growth <i>in vivo</i>	174
Everolimus	mTOR inhibition	downregulation of KSHV latent gene expression, Induction of caspase-mediated apoptosis	208
Thioridazine	MALT1 inhibition	MALT1 inhibition switched into the lytic phase and reduced cell growth and survival	209
PX-478	HIF-1 α inhibition	dose-dependent reduction in HIF-1 α mRNA and cell proliferation	
PF-2341066	c-MET inhibition	G2/M cell cycle arrest, induction of DNA damage and apoptosis of PEL cells <i>in vitro</i> . Delay PEL <i>in vivo</i>	210
Metformin	intracellular ROS inhibition mTOR inhibition	Downregulation of v-FLIP, decreased intracellular ROS, inhibition of mTOR, and the dephosphorylation of STAT3 leading to apoptosis.	211
Lenalidomide Pomalidomide	immunomodulation	Inhibit KSHV-mediated downregulation of MHC-1 surface expression	212
Lenalidomide Pomalidomide	immunomodulation	Inhibit proliferation, induce apoptosis and cell cycle arrest due to IRF4 inhibition and degradation of IKZF1	213

E. Arsenic trioxide

Arsenic trioxide (ATO) is used as a combination therapy for multiple hematological neoplasms^{214, 215}. It exerts versatile mechanisms of action which include

inhibition of proliferation and angiogenesis, induction of differentiation, apoptosis, and deregulation of cellular redox state²¹⁵⁻²¹⁸. Currently, ATO is a first line therapy for relapsed acute promyelocytic (APL) and has been recently suggested as an effective consolidation for patients with adult T cell leukemia (ATL) following induction therapy²¹⁹⁻²²². Indeed, in APL, ATO triggers the degradation of PML-RAR α oncoprotein resulting in APL remission^{219, 220, 223}. Similarly, ATO combined with all trans retinoic acid (RA), was suggested as a promising therapeutic option for acute myeloid leukemia (AML)²²⁴. *In vitro*, ATO/RA results in selective apoptosis of AML cells with mutant nucleophosmin-1 protein *via* degradation of the mutant protein resulting in apoptosis^{217, 224}. In ATL, ATO synergizes with Interferon α (IFN α) resulting in cell death *in vitro* with selective elimination of leukemia initiating cells in *tax*-transgenic murine model^{216, 225, 226}. In phase II clinical trial, ATO, combined with IFN α and zidovudine, resulted in 100% response rate and 70% remission in chronic ATL patients²²⁷. Recently, ATO was proposed as a consolidation therapy following induction therapy for ATL patients who are not eligible for ASCT²²⁰. In Multiple Myeloma, ATO and Lena exhibited independent effects *in vitro*²²⁸, where ATO exhibited a potent cytotoxic effect while Lena showed an immunomodulatory effect²²⁸. In more details, ATO sensitized myeloma cells to Lena and the combination ATO/Lena decreased MDM2 expression levels without affecting p53²²⁸. ATO-induced sensitization to Lena occurred via upregulation of cereblon expression levels²²⁹.

In PEL, ATO/ IFN α inhibited NF- κ B activation, decreased cell growth, and induced caspase-dependent apoptosis in HHV8⁺ PEL cell lines²⁰⁶. This combination

synergistically prolonged the survival of PEL mice by decreasing the peritoneal ascites volume, downregulating KSHV latent gene transcripts, and inducing cell death²⁰⁵. Despite these promising results, ATO/IFN α combination failed to achieve the *in vivo* cure²⁰⁵.

F. Lenalidomide

Lenalidomide belongs to the immunomodulatory class of drugs^{230, 231}. It is a thalidomide analog approved for the treatment of multiple myeloma^{232, 233}. Lena exhibits antiangiogenic, antineoplastic, and immune activating properties^{231, 234}. Thus, it was presented as a potential drug for treatment of blood malignancies including mantle cell lymphoma, chronic Lymphocytic leukemia, and Diffuse Large B-cell lymphoma^{231, 235, 236}.

The potential effects of Lena on PEL therapy were previously investigated. Indeed, Lena inhibited PEL cell proliferation and induced cell cycle arrest by targeting IKZF1-IRF4-MYC axis in a cereblon-dependent manner²¹³. Lena's anti-proliferative effects were due to degradation of Casein kinase 1 α (CK1 α) and downregulation of IRF4²³⁷. However, overexpression of CK1 α and IRF4 expression in treated cells failed to overcome Lena toxicity strongly suggesting that other pathways are also involved²³⁷. Lena restored the immune surface molecules downregulated by KSHV to subvert immunity in PEL cell lines²¹².

Clinically, Lena resulted in complete remission in a 77 years old HIV-negative patient²³⁸. Interestingly, after 18 months of therapy, complete remission was sustained²³⁸.

Lena is currently in phase I/II clinical trials along with DA-EPOCH and rituximab for treatment of PEL patients (NCT02911142).

G. Adult T-Cell leukemia

Adult T-cell leukemia (ATL) is an aggressive T-cell neoplasm secondary to infection with the human T-cell lymphotropic virus type 1 (HTLV-1)^{239, 240}. ATL was first discovered by Takatsuki et al. in Japan in 1976²⁴¹. Later in 1980, the retroviral origin of this leukemia was identified and assigned as HTLV-1²⁴².

HTLV-1 infects around 10-20 million people worldwide²⁴³⁻²⁴⁵. Among infected personnel, 1-5% develop ATL after a long latency period that may reach 50 years^{240, 243, 246}. HTLV-1 is endemic in multiple countries including the Caribbean islands, southern Japan, Romania, Central and Latin America, intertropical Africa, Central Australia, areas in the Middle East (mainly Iran), and Melanesia²⁴³⁻²⁴⁵. Recently, an alarmingly rising prevalence of ATL was discovered in non-endemic area including north of Japan and the United States^{247, 248}.

1. Clinical manifestations of Adult T-cell leukemia

ATL development arises following clonal expansion of mature T lymphocytes with characteristic CD3⁺CD4⁺CD5⁺CD7⁻CD8⁻CD25⁺ expression pattern²⁴⁹⁻²⁵¹. At the clinical level, ATL patients present with different forms of the disease. These can range from an

indolent slowly progressive disease to an aggressive and life-threatening disease. Based on the heterogeneity of the disease, the Shimoyama classification encompasses four major subtypes: smoldering, chronic, lymphoma, and acute (summarized in table 3), that differ in clinical features, therapeutic management, and prognosis ²⁵².

Table 3. Shimoyama classification of clinical subtypes of ATL²⁵².

	Smoldering	Chronic	Lymphoma	Acute
Lymphocyte count ($\times 10^3/L$)	<4	≥ 4	<4	High
Flower cells (%)	<5	≥ 5	≤ 1	High
LDH level	≤ 1.5 times ULN	<2.5 times ULN	High	High
Ca ²⁺ level	Normal	Normal	High	High
Skin and/or lung involvement	+/-	+/-	+/-	+/-
Lymph node involvement	No	+/-	Yes	+/-
Spleen/liver involvement	No	+/-	+/-	+/-
Central nervous system/bone/pleural/ascites	No	No	+-	+/-

All forms of ATL are characterized by a dismal long-term prognosis and a low median survival rate, ranging between 6 months for the acute subtype and 24 months for the chronic subtype. Moreover, their clinical manifestations of ATL are quite heterogeneous and may include generalized lymph node swelling, skin rash, hepatosplenomegaly, hypercalcemia, leukocytosis, and secondary opportunistic infections^{239, 253}.

Acute ATL, the most aggressive subtype accounting for 55-60% of total ATL cases^{254, 255}, is identified for profound lymphocytosis with “flower cells” and “cloverleaf” cells, characteristic pathognomonic features of ATL^{252, 256, 257}. Acute ATL patients also exhibit hepatosplenomegaly, lymphadenopathy, elevated lactate dehydrogenase (LDH), hypercalcemia²⁵⁸ along with neuropsychiatric disturbances or renal dysfunction^{239, 252, 256}.

^{259, 260}. In addition, patients endure frequent opportunistic infections secondary to profound immunosuppression including parasitic infections such as disseminated cryptosporidiosis, toxoplasmosis and strongyloidiasis, fungal infections such as *Pneumocystis carinii*-induced pneumonia, viral infections including cytomegalovirus activation, as well as bacterial infections causing frequent abscesses and sepsis^{257, 259-261}. In addition, skin and visceral lesion in the lungs, gastrointestinal tract, and bone were also reported^{259, 260}.

The lymphoma subtype accounts for 20-25% of patients^{252, 254, 255}. Lymphoma ATL is characterized by symptoms similar to those of acute ATL but with the absence of lymphocytosis^{252, 254, 255}. Indeed, ATL cells are barely detected in peripheral blood (<1% of ATL cells).

The chronic subtype is less frequent affecting 10-20% of total ATL cases. It is associated with hepatosplenomegaly, lymphadenopathy, and leukocytosis. However, hypercalcemia and visceral infiltration are absent and LDH levels are normal to slightly elevated^{239, 252, 254, 255}. According to the prognosis, chronic ATL can be further subdivided into favorable and unfavorable subtypes with the unfavorable presenting elevated LDH, elevated serum urea, increased Ki-67 antigen expression, or low serum albumin concentration²³⁹.

Finally, the smoldering subtype is the least frequent subtype and accounts for 5-10% of patients. In this subtype, a normal lymphocyte count is reported but with 1-5% of cells exhibiting the characteristic “flower cell” phenotype. In addition, the smoldering subtype, which is normally of slow progression, presents with organ infiltration limited to the skin and lungs^{252, 262}. Of note, ATL is sometimes classified into aggressive and indolent

ATL; where the “aggressive ATL” refers to the acute, lymphoma, and unfavorable chronic ATL while the “indolent ATL” includes smoldering and “favorable” chronic subtypes^{239, 253}.

H. Treatment of adult T-cell leukemia

Treatment of ATL is quite challenging^{253, 263-265}. Aggressive ATL is associated with a dismal prognosis mainly due to chemoresistance and profuse immunosuppression^{253, 263, 266}. ATL management largely depends on the subtype of the disease and the patient profile. Currently, watchful waiting, chemotherapy and antiviral regimens, such as interferon and zidovudine (AZT), are the first lines of therapy for ATL^{253, 263, 264, 266}.

1. Chemotherapy

Different chemotherapy regimens have been implemented for ATL management. These include modified EPOCH, CHOP, hyper-CVAD^{239, 253, 266}. In the United States, a recent meta-analysis study included ATL patients treated, between 2000 and 2016, with modern chemotherapies²⁴⁸. The study revealed unsatisfactory four-year OS results²⁴⁸ suggesting that current ATL regimens are unsatisfactory with poor impact on long term prognosis.

2. Antiviral regimens

The antiviral regimen, AZT/IFN- α , resulted in high response rates and became a standard regimen for treatment of ATL^{248, 267-270}. The efficacy of AZT/IFN- α combination was confirmed in a worldwide meta-analysis and multiple clinical trials²⁷¹⁻²⁷⁴. It enhanced survival of chronic, smoldering, and lymphoma subtypes as well as the acute subtype harboring a wild-type p53^{253, 263, 275}. Despite encouraging results, high relapse rate was observed upon discontinuation of AZT/IFN- α indicating that per se the combination is not curative.

3. Alternative approaches for ATL management

Alternative approaches to conventional chemotherapy include allogeneic stem cell transplantation (alloSCT)^{276, 277}. Unfortunately, a small percentage of ATL patients are fit candidates for alloSCT. In addition, targeted monoclonal antibodies are currently investigated²⁷⁸. These include anti-CCR4 (C-C chemokine receptor 4) antibody (Mogamulizumab)^{239, 253}. In Japan, Mogamulizumab is approved for treatment of patients with various T-cell neoplasia including refractory CCR4⁺ ATL²⁷⁹.

4. Epigenetic regimens targeting ATL

Epigenetic alterations have been identified as key players contributing to ATL progression and development^{240, 280, 281}. In addition, a deregulated epigenetic landscape characterized by H3K27me3 accumulation at almost half of the genes was reported in

primary ATL cells²⁸¹ (See section D below). Furthermore, microarray gene expression analysis studies revealed an increased expression of histone tri-methylation enzyme, Enhancer of Zeste homolog 2, EZH2 in ATL primary cells²⁸⁰. EZH2 is the major enzyme of the Polycomb Repressive complex PRC2. It mediates the trimethylation of histone 3 at the lysine residue 27 (H3K27me3)^{281, 282}. 3-deazaneplanocin A, a global inhibitor of histone methyl-transferases including EZH2, inhibited the proliferation of ATL cell lines²⁸⁰. In another study, GSK126, a specific EZH2 inhibitor, resulted in selective apoptosis of HTLV-1 infected and ATL derived cell lines *in vitro*²⁸¹. Therefore, EZH2 was identified as potential target for epigenetic regimens in ATL. Consequently, EZH2 inhibitors were investigated in clinical trials for treatment of ATL. Valemetostat (DS-3201) is a dual inhibitor of EZH1 and EZH2 with anti-tumor potential against lymphomas including ATL²⁸³. A phase 1 multicenter dose escalation study in Japan assessed the safety, recommended dose, and pharmacokinetic properties of Valemetostat in Japanese patients exhibiting relapsed/refractory non-Hodgkin lymphoma including ATL. Given the promising results of phase 1 trial, a phase II clinical trial (NCT02732275), is currently ongoing to investigate the efficacy of DS-3201 following Mogamulizumab in patients with aggressive relapsed/refractory ATL.

Histone deacetylases (HDAC) are other epigenetic modifiers of interest in ATL. These enzymes remove the acetyl group from lysine amino acid residues of histones resulting in a tightly wrapped DNA and decreased gene expression²⁸⁴. HDAC inhibitors (HDACi) yielded promising results in multiple T-cell lymphomas²⁸⁵. For instance, HDACi AR42 exhibited cytotoxic properties with inhibition of proliferation, induction of

apoptosis, and hyperacetylation of H3 proteins in ATL cell lines²⁸⁶. Importantly, AR42 prolonged the survival of NOD/SCID ATL xenograft mice²⁸⁶. A phase II clinical trial is currently ongoing to investigate the potential efficacy of HDAC inhibitor Belinostat as consolidation therapy with AZT for aggressive leukemic ATL subtypes (NCT 02737046).

I. Human T-cell lymphotropic virus 1 (HTLV-1)

Early 1980's, HTLV-1 was the first tumorigenic retrovirus to be discovered²⁴². It is the causative agent of malignant ATL leukemia and a chronic neurological disease called HTLV-1 associated myelopathy/tropical spastic paraparesis (HAM/TSP)^{245, 246}. A summary of HTLV-1 transformation and ATL progression is presented in Figure 6. In addition, HTLV-1 induces an array of inflammatory diseases including uveitis, dermatitis, arthritis, and bronchiectasis^{245, 248}.

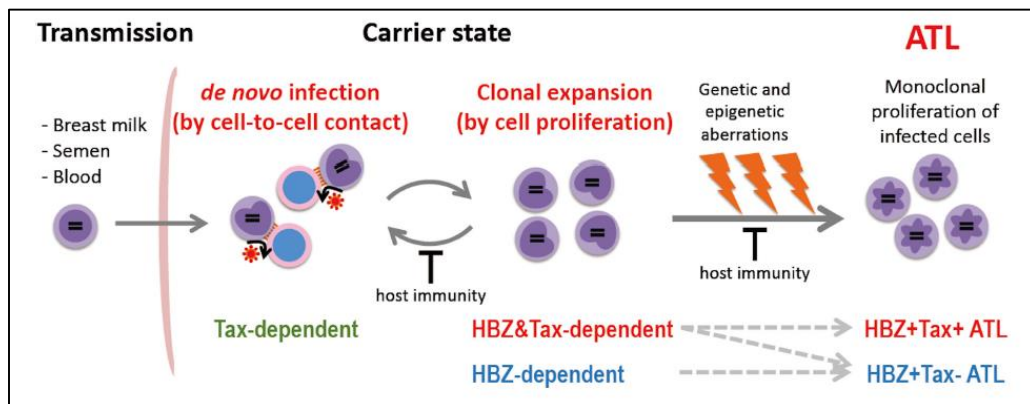


Figure 6. An Illustrative model for transformation of HTLV-1 infected cells and progression towards ATL. HTLV-1 is transmitted via sexual intercourse, blood transfusion, or breast milk. It establishes primary infection and transmission via cell-to-cell

contact. HTLV-1 then spreads in vivo via de novo infection (Tax dependent) and clonal expansion (Tax and HBZ dependent). Host immunity modulate infected cell count and clonality. Due to long latency period, genetic and epigenetic alterations accumulate resulting in a malignant clone which gives rise to ATL²⁸⁷.

HTLV-1 can be transmitted by vertical and horizontal routes; these include mainly breastfeeding, blood transfusion, or sexual intercourse^{243, 244}. HTLV-1 genome encodes for several accessory and regulatory proteins that contribute to the pathogenesis of the virus. Regulatory proteins involve Tax, Rex, p12, p13, p21 and p30, all of which are encoded by the ORF located in the pX region at the 3' end of HTLV-1 genome^{288, 289} (Figure 7). Conversely, HTLV-1 basic leucine zipper protein (HBZ) regulatory protein is transcribed from antisense strand of HTLV²⁸⁹. Among regulatory proteins, Tax and HBZ were mainly linked to HTLV-1 induced pathogenesis^{290, 291}.

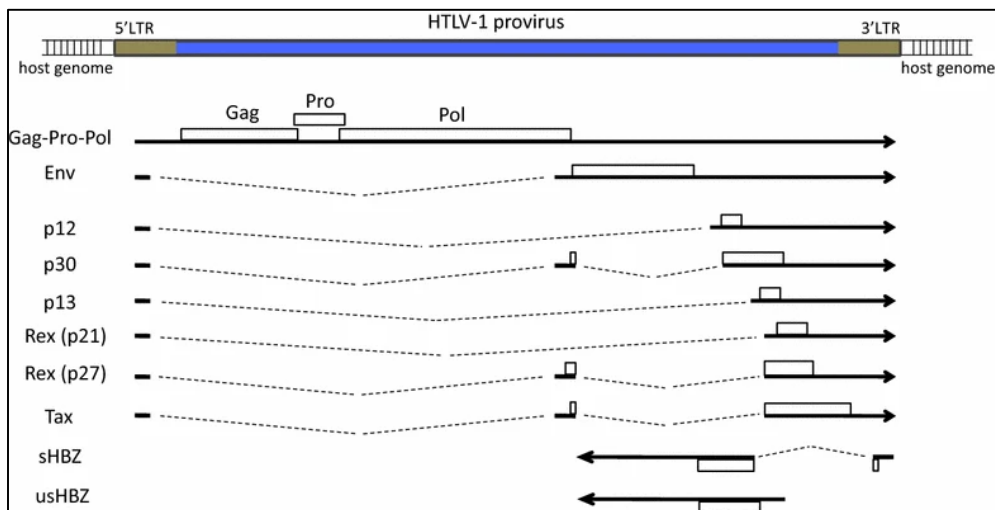


Figure 7. Schematic representation of the HTLV-1 provirus genome and regulatory proteins. HTLV-1 genome encodes for multiple regulatory proteins; Tax, Rex, p12, p13, p21 and p30, all of which are encoded by the ORF located in the pX region at the

3' end of HTLV-1 genome. The antisense strand encodes for regulatory protein HBZ present as two variants: a spliced sHBZ and unspliced usHBZ protein. In addition, the genome encodes for structural retroviral proteins such as gag-pro-pol and Env²⁹².

1. Tax protein

HTLV-1 trans-activator protein Tax is a multifaceted protein comprised of 355 amino acids and transcribed from the 5'LTR as a double spliced mRNA. Tax plays a critical role in transformation and ATL progression. Indeed, Tax expression induces oligoclonal expansion of HTLV-1 infected cells²⁹³ and acts as HTLV-1 transcriptional activator where it initiates transcription of HTLV-1 proteins from the 5'LTR promoter through its Tax responsive elements (TRE)²⁹⁴. Tax also activates the transcription of key cellular pathways, such as NF- κ B, AP-1, and cAMP response element-binding protein/Activating transcription factor (CREB/ATF)²⁹⁴⁻²⁹⁷. Recently, Tax was shown to alter epigenetic modulator complexes such as PRC2²⁸¹. Indeed, Tax-immortalized PBMC cells exhibited an increased PRC2 activity with a global alteration of H3K27me3 profile strikingly similar to that seen in primary ATL cells²⁸¹.

Tax protein contains multiple domains that allow for binding and activation of a plethora of cellular regulators in different compartments of the cell²⁹⁵ (Figure 8). These domains allow for the shuttling of Tax between different cellular compartments to alter various cellular pathways^{239, 294}. Furthermore, these domains are subjected to multiple post-translational modifications that contribute to the capacity of Tax to induce cellular transformation. Tax known post translational modifications include ubiquitination, SUMOylation, Urmylation, phosphorylation, and acetylation^{239, 298-300}.

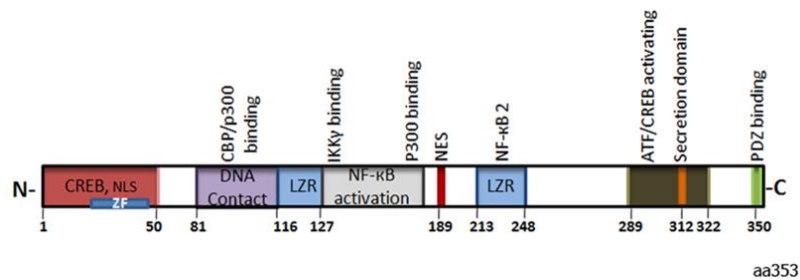


Figure 8. Schematic representation of Tax domains. Tax protein comprise multiple structural and functional domains. These allow Tax to interact with a wide array of cellular proteins, adapters, and transcription factors to modulate host and viral functions and key pathways. In addition, Tax exhibits nuclear localization signal (NLS) that allow it to shuttle between different compartments²⁹⁵.

Post translationally modified Tax activates multiple critical cellular pathways involved in regulation of gene expression, DNA damage, genomic instability, survival machinery, cell cycle progression, epigenetic expression, resulting in transformation and immortalization of T cells^{294, 297} (Figure 9). In addition, Tax regulates the microenvironment and enhances the extravasation and invasion of ATL cells^{301, 302}.

Tax protein is not detected in ATL cells due to multiple mutations in Tax gene and multiple DNA methylations at its 5'LTR promoter²⁹⁷. Despite being undetectable, ATL cells are addicted to Tax continuous expression of Tax³⁰³. Indeed, silencing Tax in HTLV-1-infected and ATL derived cells resulted in cell death.³⁰³ Moreover, ATL-derived cells exhibit sporadic bursts of Tax in around 3% of the whole cell population³⁰⁴. This is a critical event for the maintenance of the whole population³⁰⁴.

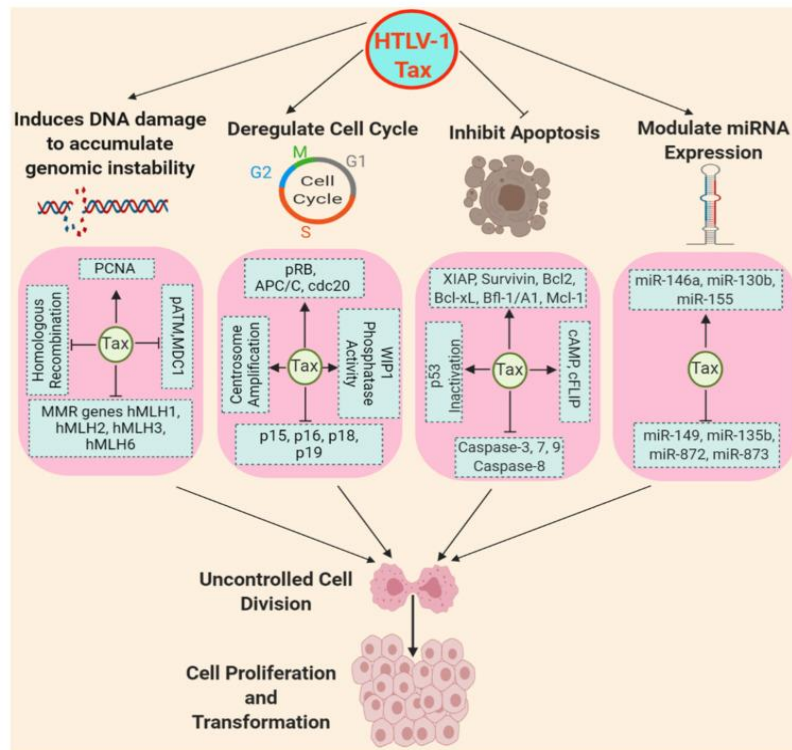


Figure 9. Schematic representation summarizing altered pathways and multiple functions mediated by Tax. Tax alters multiple critical pathways and key players in ATL development. Tax induces DNA damage resulting in genomic instability. It modulates cell cycle proteins promoting cell cycle progression. Tax inhibits apoptosis and alters miRNA expression. Altogether, Tax results in uncontrolled cell division and malignant transformation²⁹⁷.

a) Tax: a powerful oncogene

Prior research established Tax as a potent oncogene driving ATL progression²⁹⁷. *In vitro*, Tax expression in rat fibroblasts resulted in uncontrolled cell growth that led to cellular transformation³⁰⁵. In addition, Tax immortalized CD4⁺ and CD8⁺ T lymphocytes³⁰⁶. Moreover, Tax immortalized PBMC exhibited genetic and epigenetic profiles similar to those of HTLV-1 infected and ATL cells^{281, 307}. The oncogenic potential

of Tax was mainly highlighted *in vivo*³⁰⁸. Hasegawa et al. induced Tax under the *lck* proximal promoter which restricted Tax expression to mature T cells³⁰⁹. *Tax* transgenic mice developed leukemia and multiple ATL-like features including: leukocytosis with characteristic “flower cells”, hepatosplenomegaly, elevated calcium and constitutive activation of NF- κ B³⁰⁹. This NF- κ B activation is similar to what is reported in ATL patients²²⁵. Expression of *tax* in a *Drosophila* model also resulted in constitutive activation of NF- κ B and in rough eye phenotype, indicative of cell transformation³¹⁰. In more details, our Laboratory established a *tax* transgenic *Drosophila* model, where the expression of Tax can be directed into specific compartments allowing for direct assessment of its oncogenic properties. Using the GMR-Gal4 driver, expression of Tax was directed exclusively to the ommatidial structures resulting in eye roughness³¹⁰. Tax expression in hemocytes induced a significantly increased hemocytes count mimicking the elevated blood count seen in ATL³¹⁰. Importantly, Tax expression resulted in increased expression of Relish, the homolog of human NF- κ B and Diptericin, downstream Relish. Inhibition of Relish expression in *tax* transgenic flies by Relish-RNAi resulted in abrogation of Tax-mediated eye roughness elucidating the importance of NF- κ B in Tax-induced cellular transformation³¹⁰.

b) Tax activates NF- κ B pathway

At early stages of HTLV-1 infection, Tax-mediated constitutive activation of NF- κ B is a critical step for cell proliferation and survival of infected T cells^{311, 312} (Figure 10).

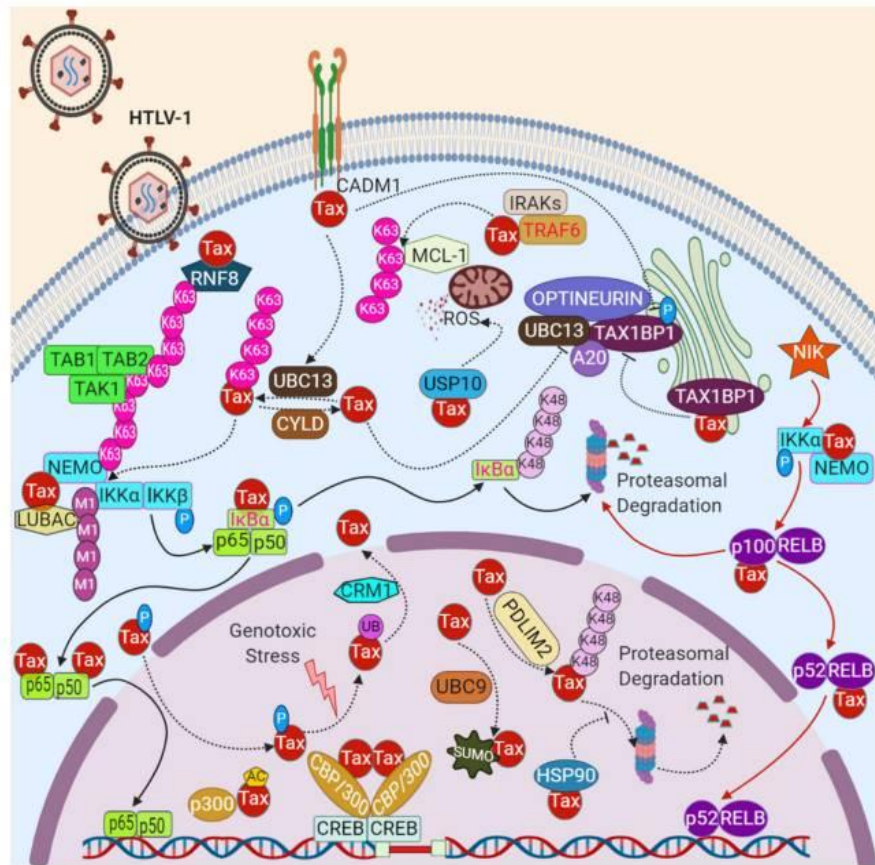


Figure 10. Schematic representation of Tax-mediated activation of classical and non-classical pathways of NF- κ B²⁹⁷. Tax activates the classical and non-classical pathways resulting in constitutive activation of NF- κ B. In the classical pathway, Tax binds to NEMO/IKK γ subunit and connect it to Tax-activated upstream receptor kinases resulting in phosphorylation of IKK α and IKK β leading to IKK complex activation. This activation results in phosphorylation, ubiquitination and subsequent proteasomal degradation of I κ B- α . Tax may directly bind and activate the kinase activity of IKK α and IKK β independent from upstream kinases. In addition, tax may directly bind I κ B- α and mediate its proteasomal degradation resulting in pathway activation. Upon degradation of I κ B- α , the p65 (RelA)/p50 dimer then translocate to the nucleus resulting in modulation of gene expression. In the non-classical pathway, Tax directly binds to p100 NF- κ B subunit resulting in its proteasomal degradation. Afterwards, RelB/p52 subunit translocate to the nucleus.

NF- κ B pathway modulates the expression of more than a hundred genes involved in inflammation, proliferation, immunity, and cancer progression³¹³. Tax activates both the

canonical and non-canonical pathways of NF- κ B (Figure 10), altering the expression of an array of NF- κ B target genes (summarized in Table 4)^{296, 297, 314}.

Table 4. Examples of NF- κ B target genes altered by Tax²⁹⁶

Gene	Gene Description	Effect
Cytokines / chemokines		
IL-6	Interleukin -6	Upregulation
IL-1 α	Interleukin 1 alpha	Upregulation
IL-12 β	Interleukin 12 beta	Upregulation
TNF- α	Tumor necrosis factor alpha	Upregulation
MCP1	Monocyte chemoattractant protein 1	Upregulation
CSF2	Granulocyte-monocyte colony stimulating factor	Upregulation
CSF3	Granulocyte colony stimulating factor	Upregulation
Cell cycle regulators		
CCND1	Cyclin D1	Upregulation resulting in IL-2 independent growth of mouse T-cells
CCND2	Cyclin D2	
Apoptosis inhibition		
Bcl2	Bcl-2 apoptosis regulator	Upregulation
Bcl2 L1	Bcl-2 like long	Upregulation
Bcl2A2	BCL2 related protein A1	Upregulation
ICAM1	Intercellular adhesion molecule 1	Upregulation

VCAM1	Vascular cell adhesion molecule 1	Upregulation
MMP9	Matrix metalloproteinase 9	Upregulation
NF- κ B negative regulators		
I κ BK β	Inhibitor of NF- κ B kinase beta	Downregulation via degradation

c) Tax inhibits apoptosis and promotes cell survival

Tax promotes cell proliferation and survival by creating an imbalance between pro-apoptotic and anti-apoptotic genes²⁹⁷. Tax inhibits p53, a major tumor suppressor protein, via activation of CREB or NF- κ B resulting in immortalization of HTLV-1-infected cells^{297, 315}. In addition, Tax constitutively phosphorylate p53 at serine residues, ser15 and ser392, rendering p53 a functionally inactive protein³¹⁶. Tax also inhibits p53-mediated trans-activation of downstream apoptotic mediators via sequestration of CBP/p300 preventing it from binding p53 promoter^{317, 318}. In fact, in most ATL patients p53 is non-functional and not mutated except for around 30% of patients who harbor p53 mutations³¹⁹. Tax also targets caspases which known to mediate apoptosis. Indeed, through NF- κ B activation, Tax increases the expression of X-linked inhibitor of apoptosis (XIAP) which inactivates caspases-3, -7 and -9^{320, 321}.

On contrary, Tax enhances the expression of anti-apoptotic proteins such as Bcl-xL and BCL2 through its activation of NF- κ B, c-Jun and JunD³²². Moreover, Tax induce the expression of Ras family member proteins which protect HTLV-1 infected and ATL cells from apoptosis³²³.

Through activation of NF- κ B, Tax dysregulates the expression of multiple cytokines which contributes to enhanced survival and proliferation of ATL cells³²⁴. Tax also promotes the expression of IL-6/IL6R, IL-2/IL2R, IL-9 and IL-13 which induce proliferation and inhibit apoptosis of HTLV-1 infected cells^{324, 325}.

d) Tax deregulates cell cycle progression and induces genomic instability

Cell cycle regulation and DNA repair machinery are tightly regulated mechanisms that ensure an errorless inheritance of genetic material. Interestingly, Tax inhibits cell cycle checkpoints resulting in uncontrolled proliferation and tumor progression³²⁶. Indeed, Tax interacts with cyclin-dependent kinase 4 (CDK4) resulting in hyper-phosphorylation of Rb, a tumor suppressor protein, which leads to continuous progression towards the G1 phase of the cell cycle³²⁷. In parallel, Tax also binds the transcription factor E2F and induces transcription of E2F-dependent S phase genes which promotes entry into the S phase³²⁸.

P53 is also known to modulate G1 to S phase transition via its downstream protein P21^{waf1/cip1} which inactivates cyclin E/CDK2 resulting in cell cycle arrest. Tax inactivates P53 and sequesters P21^{waf1/cip1} produced via p53-independent mechanisms which facilitates the progression across the G1/S checkpoint³²⁹. Importantly, Tax suppresses DNA damage response (DDR) and bypasses G1/S checkpoint in cells with DNA lesions via upregulation of the phosphatase activity of WIP1 (wild-type p53-induced phosphatase 1)³³⁰.

DNA replication, or S phase, is highly regulated via cyclin A/CDK2 checkpoint which restricts DNA replication to a single round. Interestingly, Tax-mediated activation

of CREB/ATF inhibits cyclin A promoter resulting in aberrant DNA replication and subsequent accumulation of DNA double-strand breaks (DSBs) which result in genomic instability³³¹.

Tax disrupts mechanisms involved in DNA damage repair and mismatch repair. Base excision repair (BER) normally corrects minor base lesions that constantly occur during the cell cycle. In HTLV-1- infected cells, Tax was shown to inhibit BER activated by oxidative damage³³². Tax also inhibits nucleotide excision repair (NER) which increases mutation frequency and results in genomic instability³³³. Altogether, this disruption of DNA repair and correction mechanisms by Tax results in increased proliferation and accumulation of mutations due to profound genomic instability.

2. HTLV-I basic leucine zipper protein

HTLV-I basic leucine zipper protein, HBZ, is a nuclear protein encoded by the negative antisense strand of HTLV-I provirus^{292, 334}. In 1989, Larocca et al. first identified an HTLV-I transcript encoded by the negative strand of the provirus³³⁵. Thereafter, in 2002, this transcript was reported to encode for HBZ: a bZIP nuclear factor that down regulates HTLV-I transcription through binding and inhibiting CREB-2 mediated viral transactivation³³⁶.

HBZ transcription is initiated from the U5 and R regions of the 3'LTR promoter³³⁷. HBZ gene transcripts exist in two forms; spliced sHBZ and unspliced usHBZ transcripts^{292, 336, 337}. The 3'LTR serves as a TATA-less promoter for sHBZ³³⁸. In this

regard, specificity protein 1 (sp1) and viral CREB responsive element (vCRE) are essential for 3'LTR promoter activity and therefore for HBZ transcription³³⁸. HBZ transcripts are translated into usHBZ (209 amino acids) and sHBZ (206 amino acids) proteins with similar sequences, but which differ only in the first few amino acids (MVNFVSA for usHBZ while MAAS for sHBZ)³³⁹. Consequently, both proteins have similar functions^{338, 339}. However, the two forms of the protein differ in their expression level where the expression of sHBZ is four times higher than that of unHBZ in both HTLV-I infected and ATL cell. Of note, Usui et al. failed to detect the usHBZ protein form in ATL cells³³⁹. In fact, sHBZ gene is more predominant and the half-life of sHBZ protein is longer than that of the unspliced³³⁸. As a result, current research mostly focuses on sHBZ.

HBZ protein contains three major domains: a C-terminus basic leucine zipper (bZIP) domain, a central domain (CD), and an N-terminus activation domain (AD)³³⁶. Due to the presence of Nuclear localization signals (NLS) in its CD and bZIP domains, HBZ is confined to the nucleus where it exists in a speckled pattern³⁴⁰ (Figure 11).

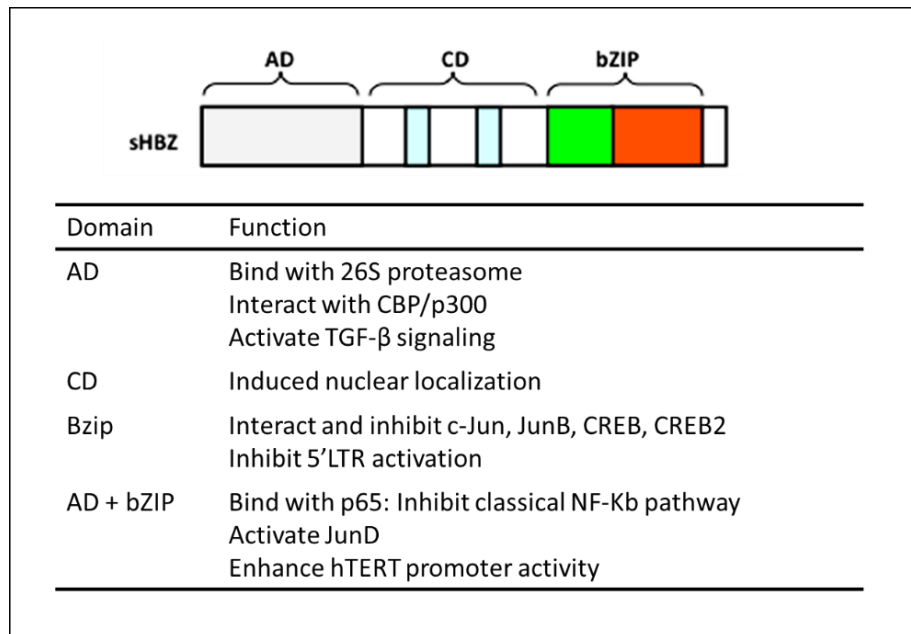


Figure 11. Schematic representation of HBZ domains and their functions³⁴¹. HBZ has three functional domains: Activation domain (AD), central domain (CD), and basic ZIP domain (bZIP). The functions of each domain are listed.

Unlike Tax whose expression is often undetected in ATL patients, HBZ is constitutively expressed in all HTLV-I infected carriers and ATL patients²⁸⁹. This can be due to the fact that the 3' LTR promoter is often intact with no DNA methylation and the *hbz* gene fosters no abortive mutations^{339, 342}. Therefore, HBZ was recently suggested as a potential candidate for vaccine.

Table 5. Comparative table of major characteristics and functions of Tax vs. HBZ³⁴¹.

	Tax	HBZ
Expression in ATL cells	undetectable	100%
Contain genetic changes	Yes	No
Function as mRNA	ND	Yes
Immortalize T cells	Yes	No
Target by CTL	Yes	No
HTLV-1 5' LTR transcription	Activate	Inhibit
Classical NF- κ B pathway	Activate	Inhibit
Alternative NF- κ B pathway	Activate	No
AP-1 activity	Activate	Inhibit
Jun-D transcription	Activate	Activate
T-cell proliferation	Activate	Activate
TGF- β signaling	Inhibit	Activate
Host immune response	Enhance	Suppress

a) The biological functions of HBZ

i. Inhibition of Tax-mediated transactivation

In 2002, Gaudry et al. identified HBZ as a CREB-2 binding protein with a potential for inhibition of HTLV-1 transcription mediated by the 5'LTR³³⁶. HBZ bZIP domain was later found to be responsible for the interaction with CREB/CREB-2³⁴³. This prevents CREB/CREB-2 from binding to Tax-responsive element (TRE) and the cyclic AMP-response element (CRE) present in the 5'LTR and cellular promoters respectively, resulting in inhibition of Tax-mediated HTLV-I transcription from 5'LTR^{336, 343}. Similarly, HBZ binds to KIX domain of CBP/p300 *via* two LXXLL motifs present in its N-terminal

AD domain. This abolishes the recruitment of CBP/p300 to the 5'LTR promoter resulting in inhibition of 5'LTR viral transcription by Tax³⁴⁴ (Figure 12).

ii. Promotion of cell proliferation and inhibition of apoptosis

HBZ was suggested to promote proliferation of ATL cells *in vitro* where knocking down HBZ by siRNA suppressed the proliferation of ATL cell lines including MT-1 and TL-Om1³³⁷. Nevertheless, HBZ modulates cell proliferation through interaction with activator protein 1 (AP1) superfamily proteins including JunD and ATF3 whose expression was elevated in ATL^{345, 346}. In ATL, ATF3 promotes cell proliferation³⁴⁵, by exhibiting a bimodal role in oncogenesis and acting as a tumor suppressor protein that activates P53 signaling on one hand while promoting malignant cells' proliferation on the other hand. Upon binding with ATF3, HBZ impedes ATF3-mediated p53 activation which is detrimental for ATL development while maintaining ATF3 growth-promoting mechanisms which include upregulation of Cyclin E2³⁴⁵. Similarly, HBZ binds JunD forming a heterodimer that results in increased JunD transcription³⁴⁷ and HTLV-1 antisense transcriptional activity³⁴⁸. Interestingly, knocking down JunD abolished HBZ-mediated cell proliferation suggesting that HBZ indirectly promotes cell growth via JunD. Moreover, HBZ/JunD heterodimer enhance the transcription of telomerase reverse transcriptase (hTERT)³⁴⁷. Activation of telomerase activity by HBZ may not only promote cell proliferation but may also contributes to the oncogenesis of ATL. In a different study, Arnold et al. demonstrated that HBZ silencing impedes cell proliferation without affecting apoptosis suggesting that HBZ promotes cell proliferation³⁴⁹.

In addition to the aforementioned mechanisms, HBZ may employ autocrine/paracrine routes to promote cell proliferation in ATL. In brief, HBZ inhibits the canonical Wnt pathway, deleterious for ATL development, while upregulating the transcription of Wnt5a, a non-canonical Wnt ligand involved in the migration and proliferation of ATL cells³⁵⁰. In a similar study, HBZ was shown to increase the promoter activity of brain-derived neurotropic factor (BDNF) resulting in upregulation of BDNF expression which further enhances ATL proliferation³⁵¹.

HBZ inhibits apoptosis by affecting various key players in the cellular apoptosis machinery. In addition to its role in inhibiting ATF3-mediated p53 activation, HBZ also repress p53 activation *via* inhibition of acetyltransferase activity of p300/CBP and HBO1³⁵². Given the importance of p53 inactivation in ATL development and the continuous expression of HBZ in ATL cells. These data may suggest an explanation for the constitutive p53 inactivation in the absence of Tax expression. Furthermore, HBZ suppress the expression of pro-apoptotic genes such as Bim whose basal expression is low in HTLV-I infected cell lines³⁵³. Interestingly, silencing HBZ resulted in increased Bim expression promoting apoptosis³⁵³. In fact, HBZ regulates Bim expression by deregulating the transcription factor that controls Bim transcription called FoxO3a³⁵³. Of note, FoxO3a plays a major role in regulating apoptosis in ATL (Figure 12). Collectively, these results show that HBZ inhibits apoptosis *via* multiple pathways.

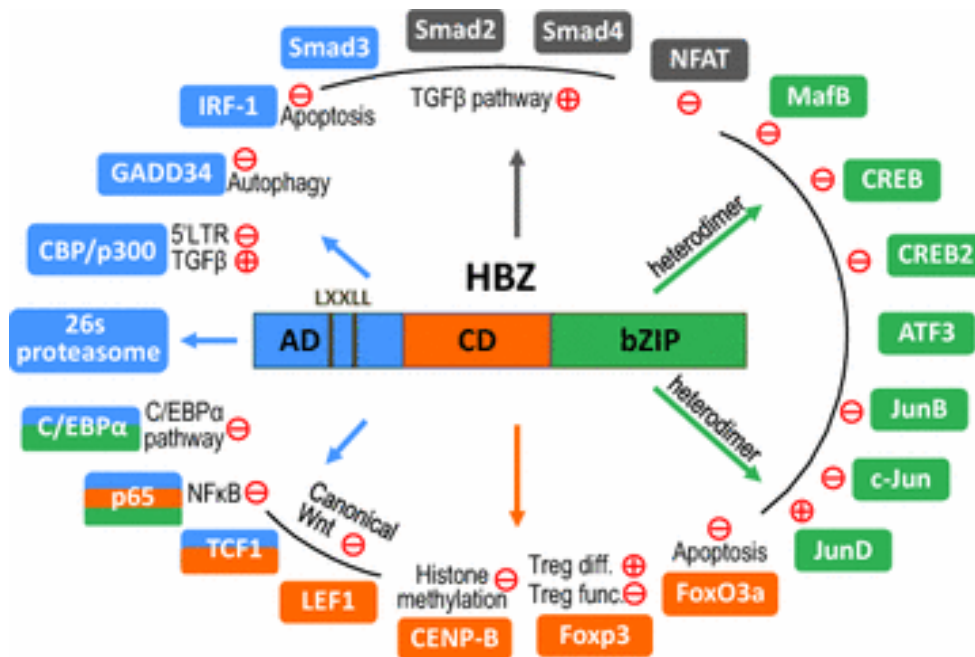


Figure 12. Illustrative representation of cellular proteins that interact with HBZ²⁹². Each domain of HBZ bind to a set of cellular proteins. Cellular proteins with colors corresponding to that of the domain they bind to. Proteins that bind to multiple domains are colored in multiple colors. Proteins in grey lack information about specific domain they bind to. The + or – correspond to the impact of HBZ on these proteins and corresponding pathways. For Foxp3, HBZ exhibits dual effect; It increases transcription from Foxp3 promoter thus promote Treg differentiation (diff) while it inhibits Foxp3 function (Treg func).

iii. Induction of inflammation and impairment of adaptive immunity

In contrary to Tax whose expression resulted in leukemia or tumor formation *in vivo*, HBZ expression in *hbz* transgenic (HBZ Tg) mice failed to induce tumor formation. In HBZ-transgenic model where HBZ was exclusively directed to CD4⁺ T cells, mice mainly developed spontaneous systemic inflammatory disease with dermatitis and lesions on the skin and lungs³⁵⁴. Only few mice developed lymphomas after a long latency period³⁵⁴. HBZ increased the percentage of CD4⁺ cells by promoting thymocyte

proliferation in transgenic mice³⁵⁵. Interestingly, HBZ also increased the number of Foxp3⁺CD4⁺ T cells also referred to as Treg³⁵⁵ known to decrease immunity and subvert effector T cells. HBZ also converts T cells into becoming Treg cells by stimulating the TGF- β /Smad pathway resulting in the upregulation of Foxp3 expression, the major transcription factor of Treg³⁵⁶. HBZ also promoted the secretion of IFN- γ in *hbz* transgenic mice which serves as a key player in HBZ-mediated inflammation³⁵⁷.

In addition to its role in inflammation, HBZ impaired cell-mediated immune response in *hbz* transgenic mice. Indeed, when challenged with herpes simplex virus or *Listeria monocytogenes*, *hbz* transgenic mice failed to mount an optimal Th1 immune response where the production of Th1 cytokines was greatly reduced compared to wild type mice³⁵⁸. This impairment of Th1 immunity is attributed to the HBZ-mediated inhibition of AP-1 and NFAT. It might also correlate with the observation that th1 response is impaired in ATL patients with some patients suffering from opportunistic infections implying a role for HBZ in immunity impairment of ATL patients. Among all HTLV-I proteins, HBZ exhibits the lowest immunogenicity given that anti-HBZ antibodies were rarely detected in infected patients.

iv. Suppression of NF- κ B: maintenance of latent infection

The constitutive activation of NF- κ B is well established as a key driver of ATL development^{311, 314}. While Tax is known for activating NF- κ B, HBZ works in an opposite fashion to halt NF- κ B activation (Figure 13)^{291, 312, 359}.

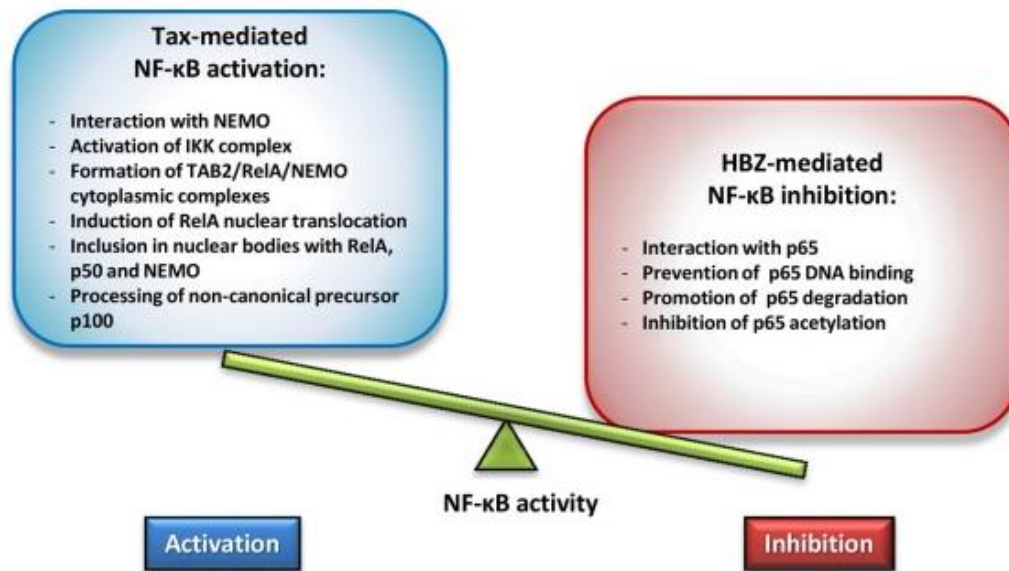


Figure 13. Schematic representation of the antagonistic effects of Tax and HBZ on NF- κ B³¹². Tax and HBZ exerts opposite effects in regulating NF- κ B. Tax activates IKK, induces nuclear translocation of RelA (classical pathway) and cleavage of p100 (non-classical NF- κ B pathway). In contrast, HBZ interacts with P65 (RelA) and prevents it from binding DNA and altering NF- κ B target gene expression. HBZ degrades P65 and inhibits its acetylation all of which results in inhibition of classical NF- κ B pathway by HBZ.

HBZ curbs the transcription of several NF- κ B target genes such as IL-8, IL-2RA, VEGF, CCND1, VCAM-1, and IRF4^{291, 312}. Multiple studies have investigated the molecular mechanisms by which HBZ inhibits NF- κ B activation. HBZ was shown to selectively attenuate the canonical NF- κ B pathway via (i) reduction of p65 (RelA) acetylation, (ii) interaction with p65 and reduction of its DNA binding ability, and (iii) degradation of p65 via increased expression of PDLIM2, a ubiquitin E3 ligase, that targets p65 for proteasomal degradation^{352, 360, 361}. HBZ does not interfere with the non-canonical NF- κ B pathway.

The significance of HBZ-mediated NF- κ B inhibition was obscure until the discovery that Tax-induced constitutive hyperactivation of NF- κ B drives HeLa cells into senescence³⁵⁹. This senescence was relieved by HBZ due to its ability to subvert canonical NF- κ B activation. Interestingly, HBZ totally abrogated canonical NF- κ B activation mediated by Tax without interfering with its activation of the 5'LTR promoter, which enabled cells to escape senescence and proliferate continuously³⁵⁹. This suggests that HBZ may contribute to the persistence of viral latent infection. Indeed, both proteins, Tax and HBZ, are critical for ATL development, where Tax is essential for cellular transformation in the early steps of leukemogenesis, HBZ is needed to allow HTLV-1 infected cells to bypass immune surveillance²⁹⁶. Moreover, Tax-mediated constitutive activation of NF- κ B constitutes a critical step in ATL development, however, if left unattended, this activation can be detrimental to the cells. The virus might express HBZ to balance this activation allowing HTLV-1 infected cells or ATL cells to keep proliferating³⁵⁹.

v. Is HBZ oncogenic?

While Tax is already established as a powerful oncogene driving HTLV-I leukemogenesis, the oncogenic capacity of HBZ remains controversial. As mentioned previously, *hbz* transgenic mice with HBZ expressed under the CD4 promoter resulted in a systemic inflammatory disease rather than leukemia³⁵⁴. Besides, this model failed to emulate the increased NF- κ B activity, a hallmark of ATL³⁵⁴. In another model, HBZ was expressed under the Granzyme B promoter (Gzmb-HBZ) which drives HBZ expression solely to NK cells and T cells³⁶². Only 40% of the Gzmb-HBZ mice developed delayed lymphoproliferative palpable tumors after 18 months³⁶². In a recent study, HBZ was found

to be dispensable for tumor development *in vivo*. Indeed, the infection of a humanized mouse model with HTLV-1 cells harboring a nonfunctional HBZ resulted in a lymphoproliferative disease similar to that in wild type HTLV-1 with no survival difference³⁶³. These data with consistent with previous *in vitro* data by Arnold et al. who demonstrated that in HBZ-mutant viruses, HBZ is not essential for the immortalization of primary T cells^{349, 363}. Collectively, these studies suggested that alone HBZ may not exhibit a powerful oncogenic potential to initiate malignancy as that seen in case of Tax.

b) HBZ mRNA: a distinct role

Among HTLV-I genes, HBZ is unique for being the only gene transcribed from the negative strand of HTLV-I genome³³⁶. Aside from encoding the HBZ protein, HBZ RNA carry important functions including growth promotion and suppression of apoptosis³³⁷. In fact, direct effects of HBZ on T-cell proliferation were attributed to its mRNA form. Indeed, upon stable HBZ expression in T cell line, HBZ mRNA supported the growth of kit255 cells *in vitro*³³⁷. Mutational analysis of HBZ gene demonstrated that the mRNA forms secondary stem-loop structures which promote cell proliferation. HBZ mRNA upregulated the expression of transcription factor E2F1 and its downstream target gene resulting in increased proliferation and cell cycle progression (increased G1/S transition)³³⁷. Recently, HBZ RNA was shown to suppress apoptosis in murine CD4+ T cells³⁶⁴. The mechanism likely involved enhanced transcription of survivin, an anti-apoptotic gene, by HBZ RNA resulting in apoptosis inhibition. These two functional roles

of HBZ mRNA, being anti-apoptotic and proliferation-promoting, likely suggest that HBZ contributes to ATL oncogenesis *via* its mRNA as well.

J. Epigenetic alterations in adult T-cell leukemia

1. Introduction to Polycomb Repressive Complex PRC2

Epigenetic mechanisms are reversible and heritable alterations in gene expression that affect the accessibility to DNA and alter chromatin structure resulting in transcriptional regulation^{365, 366}. Epigenetic mechanisms regulate gene expression *via* histone modifications such as acetylation and methylation, DNA methylation, as well as nucleosome positioning^{365, 366}. Polycomb Repressor Complexes 1 and 2 (PRC1 and PRC2) are epigenetic complexes playing several roles. PRC2 is an evolutionary conserved complex that induces chromatin-based gene silencing³⁶⁷. PRC2 regulates multiple physiological and developmental processes including stem cell maintenance, homeostasis, DNA repair, cell fate, as well as epithelial to mesenchymal transition^{282, 368, 369}. Activation of PRC2 results in transcriptional repression *via* covalent post-translational modifications in specific trimethylation of histone 3 (H3) at lysine 27 (H3k27me3)^{282, 370}. The major subunits of PRC2 complex include Suppressor of Zeste 12 (SUZ12)³⁷¹, Embryonic Ectoderm Development (EED), and Enhancer of zeste homolog 1 and 2 (EZH1/2)^{282, 372, 373} (Figure 14). EZH2 is the catalytic methyl-transferase subunit responsible for H3K27 trimethylation, a marker of transcriptional repression^{282, 372}. SUZ12 activates methyltransferases³⁷⁴ while EED recruits PRC2 complex to chromatin³⁷⁵.

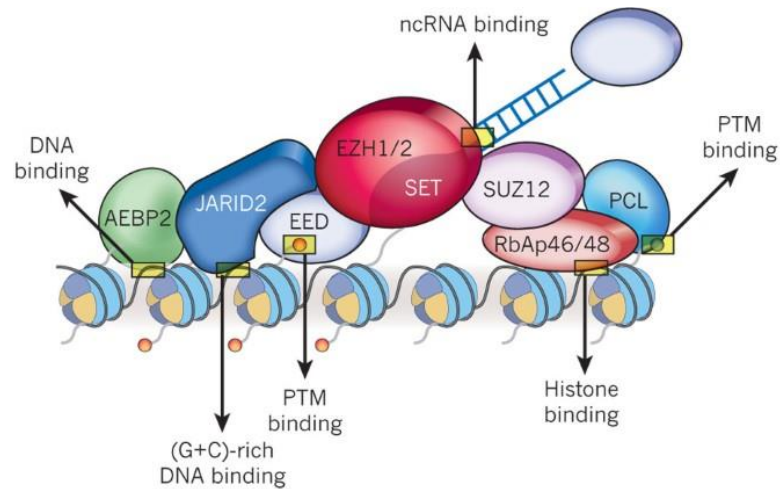


Figure 14. Schematic representation of PRC2 complex subunits and its interactions with chromatin³⁷⁶. Among different subunits, SUZ12, EZH2, and EED are the core PRC2 components. EZH2 is the major methyltransferase enzyme responsible for histone trimethylation and the consequent activation of PRC2. Putative interactions of PRC2 subunits with chromatin are also indicated.

Alterations in EZH2 expression, such as mutations or overexpression, correlate with development of various neoplasms including breast cancer, glioblastoma, prostate cancer, B cell lymphoma, and acute myeloid leukemia³⁷⁷⁻³⁷⁹. In mammalian cells, EZH1 is a homolog for EZH2, and functions as a histone methyltransferase subunit in the non-canonical PRC2 complex. Recent data suggests that EZH1 and EZH2 may collaborate and in case of loss of EZH2, and EZH1 may compensate for its role in trimethylation of H3k27³⁸⁰.

2. Epigenetic landscape in ATL

Alterations in the epigenetic landscape of ATL were recently reported and are summarized in Figure 15. Comparative microarray studies on primary ATL patient samples demonstrated a significantly elevated level of EZH2 transcripts in CD4⁺ cells from ATL patients as compared to CD4⁺ T cells of healthy controls²⁸⁰. Primary ATL cells were sensitive to treatment with 3-Deazaneplanocin A (DZNep), an EZH2 inhibitor, presenting EZH2 as a potential target for epigenetic therapy in ATL²⁸⁰. miR-31 negatively regulates the non-canonical NF- κ B. In ATL cells, transcription of miR-31 is epigenetically silenced due to the aberrant overexpression of EZH2³⁸¹. Indeed, EZH2 downregulates miR-31 expression resulting in NF- κ B activation and resistance to apoptosis³⁸¹.

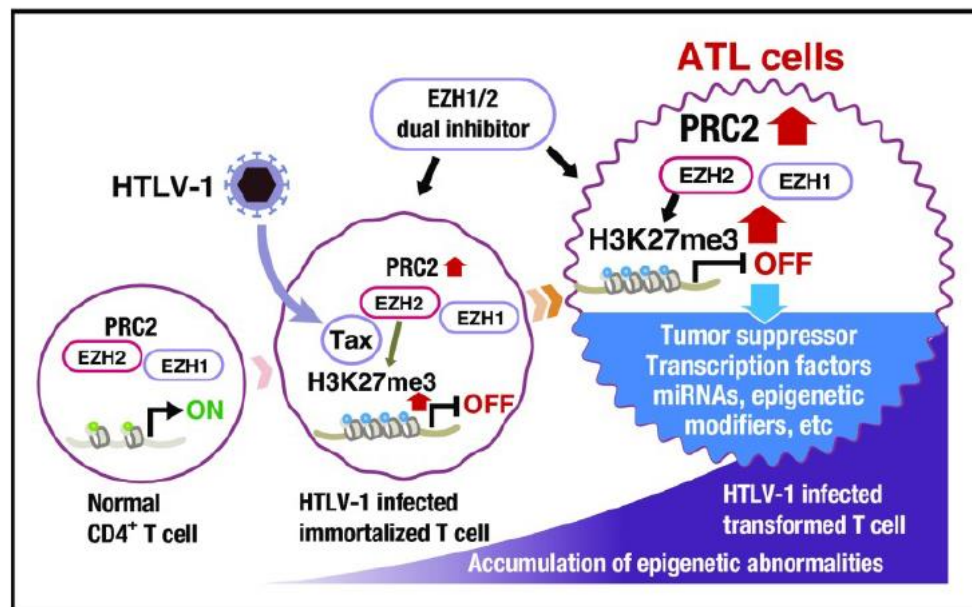


Figure 15. Epigenetic landscape in ATL cells²⁴⁰.

Recently, Fujikawa et al. demonstrated that ATL cells comprise a global alteration in H3k27me3 pattern in almost half of the genes²⁸¹. More importantly, Tax-immortalized PBMC exhibited an H3k27me3 pattern that was strikingly similar to that of primary ATL cells and EZH-2 expression was upregulated by Tax²⁸¹. In addition, pharmacological inhibition of EZH2 by a specific inhibitor, GSK126, reversed epigenetic aberrations and resulted in apoptosis of HTLV-1 infected and ATL cell lines²⁸¹. Collectively, these data presented epigenetic regimens as promising therapeutic options for ATL.

A summary of the effects of deregulation PRC2 complex and accumulation of H3k27me3 on gene expression in ATL is summarized in Figure 16. Briefly, Aberrant PRC2 activity inhibits key tumor suppressors which promoting cell survival. It inhibits miRNA expression and function, alters other epigenetic modifiers, and modulates the expression of certain transcription factors. Consequently, PRC2 deregulation alters the gene expression profile in ATL cells which contribute to the clinical and cellular characteristics of ATL (Figure 16).

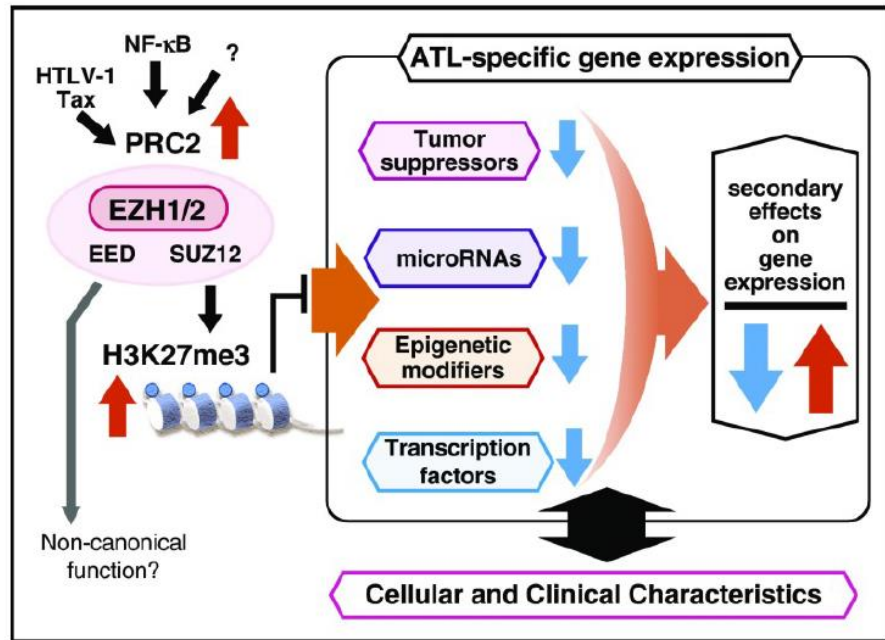


Figure 16. Accumulation of H3K27m3 contributes to ATL cell phenotype. Activation of PRC2 in ATL cells result in accumulation of H3K27me3 which in turn suppresses the expression of tumor suppressors, epigenetic modifiers, miRNAs, and transcription factors, resulting in deregulation of downstream genes crucial for ATL cell's survival²⁴⁰.

CHAPTER II

AIMS AND SIGNIFICANCE OF THE STUDY

A. Aims

An optimal regimen for PEL is still lacking. Current therapeutic approaches rely on chemotherapy yielding good response rates. Yet, high relapse rates and chemoresistance are highly encountered which necessitates the search for alternative targeted therapeutic approaches. ATO and Lenalidomide showed promising effect against PEL, as single agents. In this study, our major aim was to investigate the anti-tumor potential of ATO/Lena combination on PEL. In more details, we 1) investigated the effect of the ATO/Lena combination on the survival of preclinical PEL mice, 2) assessed the effect of the combination on PEL progression *in vivo* in preclinical murine PEL model specifically in terms of peritoneal ascites accumulation and organ infiltration, 3) deciphered the molecular mechanisms underlying the effect of ATO/Lena on *ex-vivo* treated ascites derived PEL cells such as induction of apoptosis, expression of latent and lytic KSHV proteins, cytokine expression, 4) validated the observed mechanism of action *in vivo* in murine PEL model, and finally, 5) elucidated the potential critical pathways involved in the anti-tumor effect of ATO/Lena such as NF- κ B.

Tax and HBZ are crucial HTLV-1 viral proteins for development of ATL. while Tax is established as an oncoprotein that drives transformation and immortalization of ATL cells, murine *tax* transgenics, and *tax* fly transgenics³¹⁰, the oncogenic potential of

HBZ is still controversial. Tax activates NF- κ B and PRC2 pathways. HBZ effect on NF- κ B was documented but its effect on PRC2 was not reported. In our study, our major aim was to compare the effects of Tax and HBZ on PRC2 and NF- κ B and the interplay between the two oncoproteins in modulating these key pathways. We 1) established and validated an *hbz* transgenic fly model, 2) investigated the transformative capacity of HBZ *in vivo*, 3) compared the effects of Tax and HBZ on the PRC2 and NF- κ B activity in *tax* transgenic³¹⁰ and *hbz* transgenic flies respectively, 4) investigated the interplay between HBZ and Tax in double transgenic *tax/hbz* flies *in vivo*, 5) and finally validated this interplay in mammalian cells, CD4⁺ T-cells, and ATL derived cells.

B. Significance

PEL is a rare yet aggressive lymphoma associated with extremely dismal prognosis. Although different chemotherapy regimen (CHOP, DA-EPOCH, ...) are clinically used for the management of PEL yielding good response rates, the median survival for PEL is only six months. This is due to the high relapse rate and rapid emergence of resistance to chemotherapy. This stresses the need for alternative therapeutic options to improve patient's survival and overcome the high relapse rates.

In our study, we used two clinically safe and available drugs, ATO and Lena and demonstrated that the combination of ATO/Lena resulted in prolonged survival and more importantly cured 25% and 75% of BC3 and BCBL-1 mice respectively. We also elucidated the mechanism of action by which this combination exerts its anti-PEL effects.

Our study provides a strong base and warrants further clinical investigation on the use of ATO/Lena in PEL management.

HBZ is known to antagonize multiple functions of Tax. In our study, we reported a novel competition mechanism between HBZ and Tax for binding EZH2 and activating the PRC2 complex. More importantly, we have presented a model that allows for *in vivo* assessment of HBZ-Tax interplay. Interestingly, we showed that only Tax resulted in transformation *in vivo* and HBZ alleviated the detrimental effects of Tax-induced NF- κ B hyper-activation. Our study dissected the mechanism by which HBZ counteracts Tax-induced activation of PRC2. This allows for better understanding of how the two major regulatory proteins interact and provide insight for better understanding of cell transformation, viral persistence and ATL development.

CHAPTER III

MATERIALS AND METHODS

A. PEL project

1. *Cells and drugs*

BC-3 and BCBL-1 are KSHV+/EBV- PEL cell lines derived from PEL patients²²⁹. Cells were obtained from Dr. A. Gessain (Pasteur Institute, France) and maintained in RPMI-1640 medium (Lonza, Belgium) supplemented with 10% heat inactivated fetal bovine serum (FBS, Sigma Aldrich) and 1% penicillin- streptomycin (Biowest, L0018-100).

ATO (Sigma Aldrich, A1010) was dissolved in 1M NAOH as a stock of 100 mM ref. Lena (Celgene Corporation Research Alliance) was prepared in DMSO as a final stock of 38.5 mM check any ref. Working solutions of both agents were freshly prepared in RPMI-1640 or sterile PBS for *ex vivo* or *in vivo* treatments respectively.

2. *Xenograft mice and treatments*

NOD-SCID PEL model was previously described^{217, 230}. Six to eight-week old NOD/SCID immune-compromised mice were used (Charles River, France). Protocols

were first approved by the institutional animal care and utilization committee (IACAC) of the American University of Beirut and mice were maintained in a pathogen-free facility.

For survival experiments, 2 million BC-3 or BCBL-1 cells were intra-peritoneally injected into six to eight-week old NOD/SCID mice (5 mice per group) ref. 4 days' post PEL inoculation, Treatment was initiated with intra-peritoneal inoculation of either ATO (5 μ g/g/day), Lena (5 μ g/g/day), or ATO/Lena combination for a total of 35 days. Drug toxicity was dismissed as none of the single agents nor their combination was toxic in normal NOD/SCID mice treated for 21 days (100% survival was observed > 3 months with no observed toxicity, Data not shown). Survival curves were presented using Kaplan-Meier method. GraphPad prism® software 7.0 was used for statistical analysis where a P value of 0.05 was considered significant.

For short-term treatment, NOD/SCID mice were inoculated with BC-3 or BCBL-1 cells and allowed to develop PEL for six weeks. Mice were then intra-peritoneally treated with 5 μ g/g/day ATO and/or Lena over a period of one week. Ascites development was assessed whereby PEL NOD/SCID mice (n=8) were visually inspected and peritoneal diameter (d) was measured. Peritoneal volume, a measure of lymphomatous effusions, was calculated following the formula: $v=4/3\pi (d/2)^{217, 231}$. For statistical analysis, GraphPad prism software 7.0 with one-way Anova was used; a P value of 0.05 was considered significant.

3. *Histopathology*

Lungs and livers from treated or untreated mice were fixed in 4% Paraformaldehyde (Sigma), embedded in paraffin, and sectioned. Sections were stained with hematoxylin and eosin (H&E) and visualized utilizing light microscopy.

4. *Ex- vivo cell culture and Treatments*

For *ex vivo* experiments, BC-3 and BCBL-1 cells were collected from peritoneal lymphomatous ascites of PEL mice, six weeks following inoculation with PEL cells. Cells were cultured in RPMI-1640 medium supplemented with 10% FBS and 1% pen-strep. Treatment was conducted with 1 μ M ATO, 0.5 μ M Lena, or a combination of ATO/Lena for 24, 48, 72, or 96 h.

5. *Cell viability*

Ascites-derived BC3 or BCBL-1 cells were seeded at a concentration of 2×10^5 cells/ml. Cells were Treated with 1 μ M ATO/and or 0.5 μ M Lena for 24, 48, 72, or 96 hours. Cell viability was assessed using Trypan blue exclusion dye assay. Triplicate wells were counted, and experiments was repeated 3 times.

6. Real time quantitative PCR

Total RNA from lungs of treated or untreated PEL mice, or from *ex-vivo* treated PEL cells was extracted using Trizol (Qiagen, Cat# 79306). cDNA synthesis was performed using a Revert Aid First cDNA synthesis Kit (Thermo Scientific). Syber green qRT PCR was performed using the BIORAD CFX96 machine and primers for qRT-PCR are listed in Table 2. In qRT-PCR, individual reactions were prepared with 0.25 μ M of each primer, 150 ng of cDNA and SYBR Green PCR Master Mix to a final volume of 10 μ l. PCR reactions consisted of a DNA denaturation step at 95°C for 3 min, followed by 39 cycles of (denaturation at 95°C for 15 sec, annealing at 57°C for 60 sec, extension at 72°C for 30 sec). For each experiment, reactions were performed in duplicates and expression of individual genes was normalized to the housekeeping gene Glyceraldehyde-3-Phosphate dehydrogenase (GAPDH). The transcript expression level was calculated according to the Livak method²³².

Table 6. List of primers used for Real time quantitative PCR.

Primer	Sequence 5'-3'	References
K8.1	Forward: 5'-TTCCACACAGATTCGCACAGA-3' Reverse: 5'-GGCACGCCACCAGACAA-3'	233
ORF59	Forward: 5'-CGTCGGTAGCGGCTTCA-3' Reverse: 5'-GGCTATGCCAGCGTCGAGTA-3'	233
ORFK8	Forward: 5'-CAAGAGGCGACTACATAGAAA-3' Reverse: 5'-GATCACATACTTCGGCCTTAAC-3'	234
RTA	Forward: 5'-CGCAATGCGTTACGTTGTTG-3' Reverse: 5'-GCCCGGACTGTTGAATCG-3'	217
V-FLIP	Forward: 5'-GTGTTTCATACCTCAACCCACAC-3' Reverse: 5'-CACACAGCTCCCCGTCTAC-3'	217
V-Cyclin	Forward: 5'-TCAGTTTGCCAGGAATACAACCTAG-3' Reverse: 5'-AAGAAGGAAGTTACGTCCGTCG-3'	217

GAPDH	Forward: 5'-CATGGCCTTCCGTGTTTCCTA-3' Reverse: 5'-CCTGCTTACCACCTTCTTGAT-3'	235
IL-6	Forward: 5'-AACCTGAACCTTCCAAAGATGG-3' Reverse: 5'-TCTGGCTTGTTCCTCACTACT-3'	236
IL-10	Forward: 5'-TCTCCGAGATGCCTTCAGCAGA-3' Reverse: 5'-TCAGACAAGGCTTGGCAACCCA-3'	237

7. *Immune-florescence assay*

PEL cells were *ex-vivo* treated for 48hrs with ATO, Lena, or ATO/Lena. For *in vivo* experiments, ascites from treated or untreated mice were promptly collected. Cells were washed twice with 1xPBS, fixed with ice-cold methanol for 20 minutes, and cytospun onto glass slides. Following permeabilization with 0.1% PBS-Triton, blocking was performed with 0.1% BSA in PBS-Tween for 30 minutes at room temperature. Immunostaining was carried out overnight *via* incubation with primary rabbit monoclonal P65 antibody (Cell Signaling, Cat #) and rat monoclonal LANA-1 antibody (Abcam, cat#). The following day, cells were washed twice with 1x PBS before incubation with Alexa Fluor 488- or Fluor 594- labeled secondary antibodies (Abcam, cat #). Nuclei were stained with 1µg/ml Hoechst (Invitrogen, Cat#) before mounting using prolong antifade (Invitrogen, cat#). Images were acquired by confocal microscopy using a Zeiss LSM710 confocal microscope (Zeiss, Oberkochen, Germany) with a Plan Apochromat 63/1.4 numeric aperture oil-immersion objective, using Zen 2009 (Carl Zeiss). Experiments were repeated for three times.

Zeiss LSM710 confocal microscope (Zeiss, Oberkochen, Germany) with a Plan Apochromat 63/1.4 numeric aperture oil-immersion objective and Zen 2009 (Carl Zeiss) were used for image acquisition.

8. Immunoblot assay

Ascites cells from treated or untreated mice, or 48hr *ex-vivo* treated PEL cells were washed twice with ice-cold 1X PBS. Cells were solubilized in lysis buffer (0.125M Tris-HCl (PH6.8), 2% SDS, 5% β -mercaptoethanol, and 10% glycerol). One hundred μ g of protein lysates were loaded onto 8%, 10%, or 12% SDS-polyacrylamide gels. Following electrophoresis, proteins were transferred onto nitrocellulose membranes and Blocked in 5% fat-free milk dissolved in 0.1% TBS-Tween for 45min. Immunoblotting was performed by overnight incubation with specific primary antibodies; LANA-1(mouse monoclonal, NBP1-30176, Novus), LANA-2 (mouse monoclonal, NB200-167H, Novus), Caspase 3 (rabbit polyclonal, sc-7148, Santa Cruz), PARP (rabbit polyclonal, sc-7150, Santa Cruz), p-IkBa (mouse monoclonal, MA5-15087, Invitrogen), and HRP-conjugated GAPDH (MAB5476, Abnova). The following day, blots were washed with TBS-Tween and incubated with appropriate HRP-conjugated secondary antibodies (m-IgGK BP-HRP sc-516102, mouse anti-rabbit IgG-HRP sc-2357, Santa Cruz). Protein bands were visualized using ECL chemiluminescence (Clarity max, Biorad) and Chemidoc® machine image lab software. Image analysis and densitometry were performed using ImageJ®. Densitometry histograms were reported as average of three independent experiments with standard deviation and statistics.

9. Angiogenesis assay

24-well plates were pre-coated with 200 μ L of gelled growth factor-reduced Matrigel (Becton Dickinson, San Jose, CA, USA)²³⁸. Human Aortic Endothelial Cells (HAEC) were seeded at the density of 8×10^4 cells for 18h. PEL cells were *ex-vivo* treated with ATO and/or Lena for 48hrs, pelleted, and cultured for 24 hours in serum-free media. The resulting supernatants from treated or untreated PEL cells were concentrated and added over HAEC cells for 48h. VEGF was used as a positive control and Bivacizumab, anti-VEGF antibody, as a negative control²³⁸. Plates were photographed using a Zeiss light microscope and analyzed using Zen 2009 software. For quantification, nodes (defined as joint points of 3 or more branches) were counted and results were reported as percentage of untreated cells²³⁹. Data is presented as average of three independent experiments.

10. CD45 staining

Ascites cells from untreated or treated mice were promptly collected and washed twice with PBS. Cells were stained by incubation with anti-human CD45 phycoerythrin (PE) conjugated antibody (bdbioscience, 555483) for 20minutes in the dark. Cells were then washed and analyzed on Guava flow cytometer. Cell sorting was performed using a BD FACSAria SORB.

11. Statistical analysis

For survival experiments, Statistical analysis was performed using GraphPad prism software 7.0; and data was reported as Kaplan-Meier curves. Other statistical analysis was performed using GraphPad prism software 7.0, and one way Anova. A P value of 0.05 was considered significant.

B. ATL project

1. Fly stocks

Oregon-R w1118 (also referred to as wild type), UAS-myc-*Tax*³³⁰, *Relish*-RNAi (VDRC#49414), *E(z)*-RNAi (BDSC#33659), *SUZ12*-RNAi (BDSC#33402), eye-disk specific driver GMR GAL4 (BDSC #1104), and hemocyte-specific driver Hemolectin-GAL4 delta (BDSC#30139) *Drosophila* lines were used. All *Drosophila* stocks were grown on standard cornmeal-yeast-molasses medium at 25°C. For expression of RNAi, flies were shifted to 29°C. Fly work was carried out abiding with the institutional guide for the use of laboratory animals.

2. hbz transgenic flies

hbz transgenic flies were established; in brief, the Phi C31 integrase system was used. For UAS-Gal4 expression, insertion was done on the 2nd chromosome. *hbz-myc-His* plasmid was inserted into the pUAST attB *Drosophila* expression vector. Afterwards, the

resultant pUAST- attB-myc-His-*hbz* was then injected into y1 w67c23; P{CaryP ABLattP2 (8622 BDSC) embryos to generate *hbz* transgenic flies (BestGene Inc, Chino Hills, CA).

3. Scanning electron microscopy (SEM)

Scanning electron microscopy analysis was conducted on the eyes of adult flies as described previously^{330, 383}. Briefly, adult flies were fixed in a solution consisting of 2% glutaraldehyde and 2% formaldehyde in PBS. Afterwards, flies were dehydrated via successive washes of increased ethanol concentrations, before drying with a critical point dryer (k850, Quorum Technologies). Flies are then covered with standard aluminum heads before final coating on gold layer. SEM images were acquired using the Tescan, Mira III LMU, Field Emission Gun (FEG) SEM that uses a secondary Electron detector.

4. Scoring of eye phenotypes

Drosophila eye phenotype scoring method had been previously established by our group^{330, 383}. This scoring method depends on the ommatidial fusions, degree of bristle organization or disruption, and privation of ommatidia. Acquired SEM images were coded and analyzed by two independent researchers. Histograms represent the analyzed data from three independent experiments. In each experiment, 15-20 flies were scored and resultant SEM images were classified into four phenotypic classes.

5. *Hemocyte count*

To drive the expression of target genes to hemocytes, *wild type*, *tax*, and *hbz* flies were crossed with *Hemolectin-Gal4 delta (HMLA-Gal4)*. Resultant third instar larvae were bled into PBS and hemocytes were counted as described previously³³⁰. For each genotype, thirty larvae, from three independent experiments, were bled and hemocytes were counted. Statistical analysis was carried using student's t-test where a p value ($p < 0.05$) was considered significant.

6. *β -galactosidase assay*

For assessing senescence in eye disks, third instar larvae were dissected and fixed with 0.2% glutaraldehyde with 2% formaldehyde in PBS for 5 minutes at room temperature. Dissected larvae were then washed for three times with PBS. Staining was performed overnight at 37°C by incubation with a staining solution (1mM MgCl₂, 4mM potassium ferricyanide, 1% Triton, 2.7mg/ml X Gal in PBS). After two wash cycles with PBS, eye imaginal disks were dissected before mounting on charged slides using Prolong Anti-fade solution (Invitrogen, P36930). Images were acquired using Olympus CX41 light microscope.

For assessing senescence in hemocytes, third instar larvae were bled into PBS and derived hemocytes were cytopun onto slides before being fixed, washed, and stained overnight as above. Following overnight incubation, two wash cycles with PBS were

performed before mounting. For analysis, positively stained cells were counted from 10 random fields for a total of 100 counted hemocytes.

7. Cell culture

Hela and HEK293T cells were maintained in Dulbecco's Modified Eagle's Medium (DMEM, sigma), complemented with 10% FBS (Sigma), sodium pyruvate, and antibiotics. ATL-derived MT-1 cells [a generous gift from K. Ishitsuka] were maintained in RPMI (Sigma) supplemented 10% FBS, 2 mM L-glutamine (Sigma) and antibiotics.

8. Transfections and transduction

Plasmids for Tax (pcDNA3.1-*Tax*-His)³⁸⁴ and HBZ (pcDNA3.1-*hbz*-Myc-His)³⁸⁵ were generous gift provided by R. Mahieux. Transient plasmid transfections were conducted in Hela or HEK293T cells using Lipofectamine 2000 (Gibco, Invitrogen) according to manufacturer's instructions. For lentiviral production, transient transfections were carried in HEK-293T cells using calcium phosphate method. Afterwards, MT-1 cells were transduced using green fluorescent protein (GFP)-lentiviral vectors which encoded a scrambled (SCR) shRNA or an shRNA against HBZ³⁵⁵ (kindly provided by M. Matsuoka). Transduction of target cells by lentiviral particles was performed by spinoculation for three hours at 32°C and at 1500rpm.

9. Quantitative Real time PCR

Total RNA was extracted using TRIzol reagent (Qiagen) according to the manufacturer's instructions. Following DNase-treatment (Turbo DNA-free AM1907, Ambion), one µg of total RNA was reverse transcribed utilizing iScript III (Biorad). Real time PCR was conducted using Syber green and CFX96 machine from Biorad as described above. Primers used are listed in Table 6. Expression of target genes was normalized to *GAPDH* for human cells and ribosomal *protein 49 (Rp49)* for *Drosophila* extracts. Transcript levels were calculated according to Livak method²³². Data reported are from three independent crosses.

Table 7. List of ATL primers used for Real time quantitative PCR.

Primer	Sequence 5'-3'
Relish	Forward: 5'-CCACCAATATGCCATTGTGTGCCA-3' Reverse : 5'-TTCCTCGACACAATTACGCTCCGT-3'
Diptericin	Forward: 5'-ACTGCAAAGCCAAAACCATC-3' Reverse : 5'-CCGCAGTACCCACTCAATCT-3'
Tax	Forward: 5'-CGGATACCCAGTCTACGTGT-3' Reverse : 5'-GAGCCGATAACGCGTCCATCG-3'
HBZ	Forward: 5'-TAAACTTACCTAGACGGCGG-3' Reverse : 5'- CTGCCGATCACGATGCGTTT-3'
Dacapo	Forward: 5'-GCCCTTTAGCTGAAAATCACCC-3' Reverse : 5'-GAGCCAAAGTTCTCCCGTTCT-3'
D-Jun	Forward: 5'-GCTAATTCCGCCGCAATAA-3' Reverse : 5'-CAATGGGATTAACGGTGGGC-3'
GAPDH	Forward: 5'-GTGGACCTGACCTGCCGTCT-3' Reverse : 5'-GGAGGAGTGGGTGTTCGCTGT -3'
Rp49	Forward: 5'- CCGCTTCAAGGGACAGTATCTG-3' Reverse : 5'- ATCTCGCCGACAGTAAACGC-3'

10. Immunoblot assay

Cells, third instar larvae, or adult fly heads were homogenized in lysis buffer as explained previously. Of note, for flies and larvae, lysates were sonicated and one hundred and fifty μ g of protein lysates pertaining to twenty-three fly/larvae were loaded and immunoblot was conducted as explained previously. For immunoblotting, the following primary antibodies were used : mouse anti-c-Myc (ThermoFisher, 9E10), mouse anti-His (Santa Cruz, sc-57598), rabbit anti-EZH2 (Invitrogen, 36-6300), rabbit anti-SUZ12 (Cell signaling, D39F6), rabbit anti-H3k27me3 (Active motif ,39155), rabbit anti-H3k4me3 (EMD Millipore, 07-473), rabbit anti- β actin (Abcam, ab8227), rabbit anti-Histone H3 (Abcam, ab1791), mouse anti-Tax (cat#168-A51 from the National Institutes of Health AIDS Research and Reference Reagent Program), mouse anti- HBZ (a gift from J.M. Péloponèse), rabbit anti-E(z), rabbit anti-SUZ12 (a kind gift from J. Müller), mouse anti-Relish (DSHB, C21F3) and anti-GAPDH (Abnova , B2534M-HRP).

11. Immunoprecipitation

For immunoprecipitation essays, two million HEK293T cells were seeded in 100mm culture dishes.48 h following transfection with different plasmids, nuclear extracts were lysed on ice for 10 min with lysis buffer I (10 mM Hepes, 10 mM KCl, 5mM MgCl₂, 0.5 mM DTT, and EDTA-free protease inhibitor cocktail (Roche cat#11836145001). Lysates were then sonicated and centrifuged at 2100 rpm for 5 min at 4°C. Lysates were

resuspended in lysis buffer II (10 mM Hepes, 150 mM NaCl, 5 mM MgCl₂, and 0.1% NP40 (Sigma, I8896) supplemented with EDTA-free protease inhibitor cocktail. Afterwards, DNase treatment was performed, 0.1 µg/µl DNaseI (Roche), for 20 min at room temperature. Equal amount of total proteins was immunoprecipitated overnight at 4°C using the following primary antibodies: mouse anti-c-myc-tag (9E10) (3µg/ml, abcam; ab32) or rabbit anti-EZH2 (5µg/ml; Merck Millipore, 07-689). Immunoprecipitated complexes were then incubated with magnetic Protein G Dynabeads (LifeTechnologies) for 4h at 4°C. After sequential washes with TBS, 0.5% Tween-20, proteins were eluted using 2x Laemmli buffer and analyzed along with their corresponding lysate controls by immunoblot.

12. Chromatin Immunoprecipitation (ChIP)

3x 10⁶ HEK 293T cells were transfected with 18µg of DNA plasmid (9µg pcDNA3.1-Tax-1-His alone or together with 9µg PcDNA3.1-HBZ-Myc-His. For equal DNA, an empty vector was used to compensate) using calcium phosphate transfection. 48 h post transfection, cells were harvested for CHIP assay.

Briefly, cells were cross-linked via 1% formaldehyde for 15min at room temperature. 125mM glycine was added to terminate cross linking. Nuclear fraction was isolated via incubation with ice-cold lysis buffer I (50 mM Tris-HCl (Biorad), pH 8.0, 20 mM Na-butyrate (Sigma, B5887), 10 mM EDTA, 1% SDS (Biorad), EDTA-free protease inhibitor cocktail (Roche,11836145001). Sonication was then performed on lysed sample using Bioruptor (Diagenode) leading to DNA sheering into fragments that ranges between

100-400 base pairs. Afterwards, immunoprecipitation was conducted with 5 µg of anti-H3K27me3 antibody (Millipore) overnight at 4°C. After successive washes with RIPA buffer (10 mM Tris-HCl, pH 7.5, 1 mM EDTA, 140 mM NaCl, , 1% Triton X-100, 0.5 mM EGTA, 0.1% Na-deoxycholate (Sigma , D6750), 0.1% SDS), followed by washes with TE buffer (10 mM Tris-HCl, pH 8.0, 10 mM EDTA), H3K27me3-bound chromatin complexes were eluted using an elution buffer (20 mM Tris-HCl, pH 7.5 with 50 mM NaCl, 5 mM EDTA, 1% SDS, 20 mM Na-butyrate, and 50 µg/ml proteinase K (NEB, P8107S) for 2 hours at 68°C. Eluted DNA was then washed, purified, and subjected to RT-qPCR using SYBR Green. Primers' sequences used are listed in Table 7. For data analysis, in each condition, enrichment of H3K27me3 in target DNA fragments was normalized to the DNA percentage in the corresponding input sample.

Table 8. List of primers used for CHIP RT-qPCR.

Primer	Sequence 5'-3'
CDKN1A	Forward: 5'-GGG GCG GTT GTA TAT CAG G-3' Reverse : 5'-CTC TCT CAC CTC CTC TGA GTG C-3
NDRG2	Forward: 5'-CAA AGG GCC CTA GAA TCT GTA TGT-3' Reverse : 5'-GTT TCC CAC CCT TCT CAA GTG G-3'
HEG1	Forward: 5'-TGT CCT CGC GGT GAC ATC TC-3' Reverse : 5'-ACG CCC TCT CAA GCT TGG AT-3'
GAPDH	Forward: 5'-AAC TTT CCC GCC TCT CAG C-3' Reverse : 5'-CAG GAG GAC TTT GGG AAC GA-3'
A-S	Forward: 5'-CTG CAC TAC CTG AAG AGG AC Reverse : 5'-GAT GGT TCA ACA CTC TTA CA-3'

13. Immunofluorescence assay

HeLa cells transfected with HBZ-myc plasmid for 48 h were cultured on coverslips and fixed using 4% paraformaldehyde for 10 min. For MT-1 immunofluorescent assay, cells were fixed in methanol and cytospun on slides as explained previously. Post fixation, HeLa and MT-1 Cells were permeabilized with 0.5% PBS-Triton X-100 for 30 min at room temperature and blocked with 1% BSA/10% goat serum for 1 h at room temperature. Cells were incubated with primary antibodies against c-Myc, EZH2, or anti-SUZ12 for 2 hours at room temperature. Primary antibodies were detected by Alexa Fluor-488 or 594 secondary antibodies (Abcam). Nuclei staining was performed by Hoescht before mounting with prolong anti-fade solution. Images or z-stacks were acquired using confocal microscope (Zeiss LSM70), as described before.

14. In situ proximity ligation assays (Duolink)

To assess interactions of protein within close proximity, MT-1 cells and HeLa cells transfected with HBZ were fixed and stained using the Duolink *in situ* proximity ligation assay following manufacturer's instructions³⁸⁶. Antibodies against HBZ, EZH2, SUZ-12, His, and c-Myc were used. Z stack images were acquired using the confocal microscope ZEISS LSM710.

15. Statistical analysis

Data were presented as mean±SEM of three experiments and One-way ANOVA with Bonferroni post-hoc test was implemented to compare means (GraphPad Prism). Results were considered significant when the p-value $p < 0.05$.

CHAPTER IV

RESULTS

A. PEL Part

1. *ATO/Lena promotes Survival and decreases malignant Effusions in PEL Mice*

To investigate the anti-tumor potential of ATO/Lena *in vivo*, NOD/SCID mice were injected with HHV8+ PEL cell lines (BC-3 or BCBL-1) for tumor engraftment. Four days post-inoculation of malignant cells, treatment was initiated with ATO, Lena, or their combination for a total period of one month. Afterwards, mice were monitored for survival (timeline described in Figure 7). Our results demonstrated that in BC-3 PEL mice, median survival was significantly extended from 63 days in untreated mice to 163 days ($p = 0.012$) or 85 days ($p < 0.005$) in mice treated with single agents ATO or Lena respectively. Surprisingly, upon treatment with the ATO/Lena combination, median survival exhibited a striking increase to 272 days ($p = 0.018$) with 25% of treated mice totally cured, and no peritoneal effusions observed, for more than 1-year post-inoculation of PEL cells (Figure 7).

Similarly, in BCBL-1 PEL mice, median overall survival significantly increased from 78 days in untreated mice to 163 days ($p = 0.014$) ATO-treated mice and 263 days ($p = 0.016$) in Lena-treated mice. In BCBL-1 PEL mice, single agent Lena cured 25% of treated mice. More importantly, ATO/Lena treated mice, this median survival was remarkably extended to reach 360 days ($p = 0.016$) with 75% of mice cured after more than one year following

malignant BCBL-1 injection (Figure 7) . Collectively, these results highlighted not only survival promoting effects of ATO/Lena but also presented the strong curative potential of ATO/Lena combination.

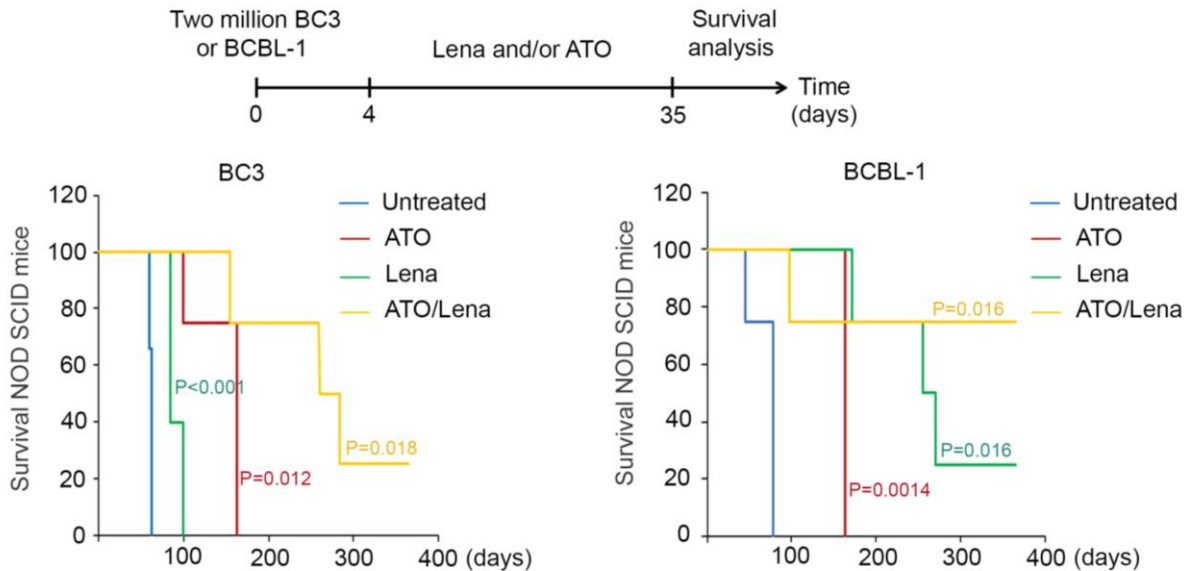


Figure 17. ATO/Lena enhanced the survival of NOD/SCID PEL mice. Kaplan–Meier graphs representing the overall survival curves of BC-3 (left) and BCBL-1 (right) NOD/SCID PEL mice.

2. *ATO/Lena impedes lymphomatous progression in PEL mice*

We then investigated the effect of ATO/Lena on PEL progression following development of malignant effusions in PEL mice. In brief, NOD/SCID mice were injected with either BC-3 or BCBL-1 cells and monitored for tumor development for six weeks (the published time sufficient for PEL malignant effusion development). Afterwards, treatment of PEL mice was conducted daily for one week and mice were monitored for peritoneal volume and ascites development (Timeline explained Figure 8). In both BC-3 and BCBL-1

injected PEL mice, a modest to no effect on peritoneal and ascites volume was observed following treatment with single agents. In contrast, within two days of treatment, a striking difference was observed in peritoneal volume of mice treated with the combination therapy.

This promising result prompted us to investigate the detailed mechanism underlying this finding. As a result, mice were sacrificed after one week of treatment and observed for pathophysiological changes including ascites and peritoneal volumes (Figure 8 and 9). Surprisingly, ATO/Lena treatment was found to significantly decrease both the peritoneal and ascites volumes of PEL mice (Figure 8 and 9). In fact, in mice inoculated with BC-3 cells, combination therapy significantly decreased the mean volume of peritoneal ascites from 4 mL in untreated mice, to 2 mL in mice treated with ATO/Lena ($p < 0.01$) (Figure. 8). Moreover, the mean peritoneal volume or abdominal girth was also decreased to around 40% in combination therapy- treated mice (Figure 9) ($p < 0.001$).

Similarly, in mice injected with BCBL-1 cells, the mean volume of peritoneal ascites declined from 7ml in the untreated mice to 1.4ml in the combination treated mice ($p < 0.001$) (Figure 8) The mean peritoneal volume was also reduced to 28% in mice treated with ATO/Lena ($p < 0.001$) (Figure 9). Altogether, these data suggest that that ATO/Lena combination decreases malignant effusion and promote survival of PEL mice.

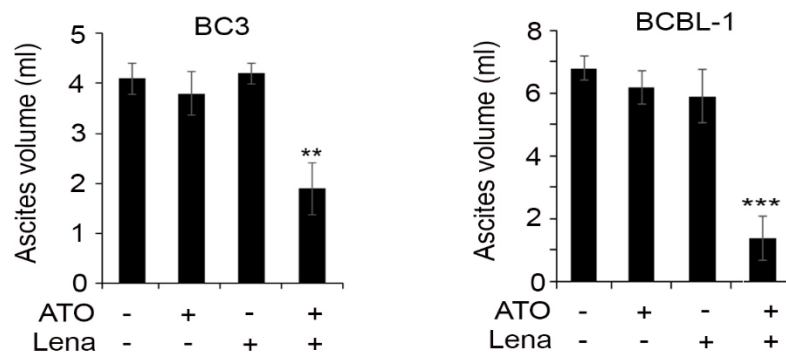
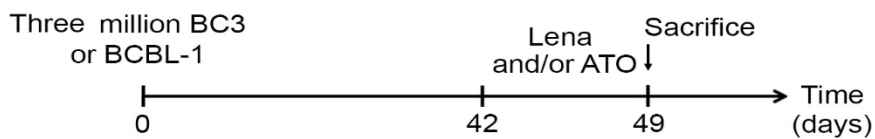


Figure 18. ATO/Lena reduces malignant effusions in PEL mice. Timeline of the treatment with ATO, Lena or their combination. Histograms represent the ascites volume from BC-3 (left) or BCBL-1 (right). PEL mice were allowed to develop ascites for 6 weeks then were treated daily with ATO, Lena, or their combination for one week before sacrifice. (**) indicates $p < 0.01$; and (***) indicates $p < 0.001$.

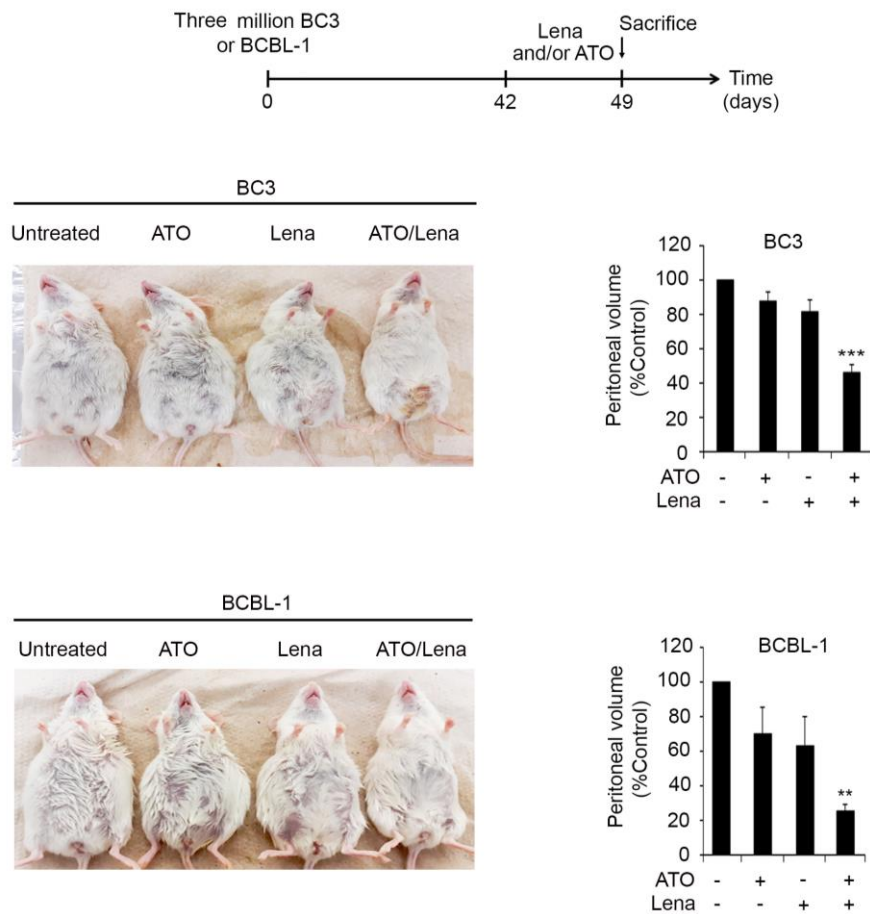


Figure 19. ATO/Lena decreased peritoneal volume in PEL mice. Timeline of the PEL mice treatment with ATO and/or Lena. Mice phenotype (abdominal distention) and histogram plots of peritoneal volume of BC-3 (upper panel) or BCBL-1 (lower panel) mice before and after one-week treatment. (**) indicates $p < 0.01$; and (***) indicates $p < 0.001$.

3. *ATO/Lena suppresses cell growth and Downregulates HHV8 Latent Proteins in Ascites-derived PEL cells Ex Vivo*

BC-3 and BCBL-1 ascites cells derived from lymphomatous peritoneal ascites in PEL mice were treated *ex vivo* with ATO, Lena, or their combination. In both ascites-derived PEL cells, single agents ATO or Lena resulted in a moderate yet significant anti-proliferative effect starting 48 h post *ex vivo* treatment ($p < 0.05$) (Figure 10). Intriguingly,

treatment with a combination of ATO/Lena induced a more profound and significant inhibition of cell proliferation in both BC-3 ($p < 0.01$) and BCBL-1 ($p < 0.001$) at both time points 48 h and 72 h post-treatment (Figure 10). Interestingly, consistent with the *in vivo* data from BCBL-1 PEL mice which exhibited higher percentage of cure with ATO/Lena therapy, BCBL-1 ascites-derived cells exhibited an increased sensitivity to ATO/Lena treatment compared to BC-3 cells (Figure 10).

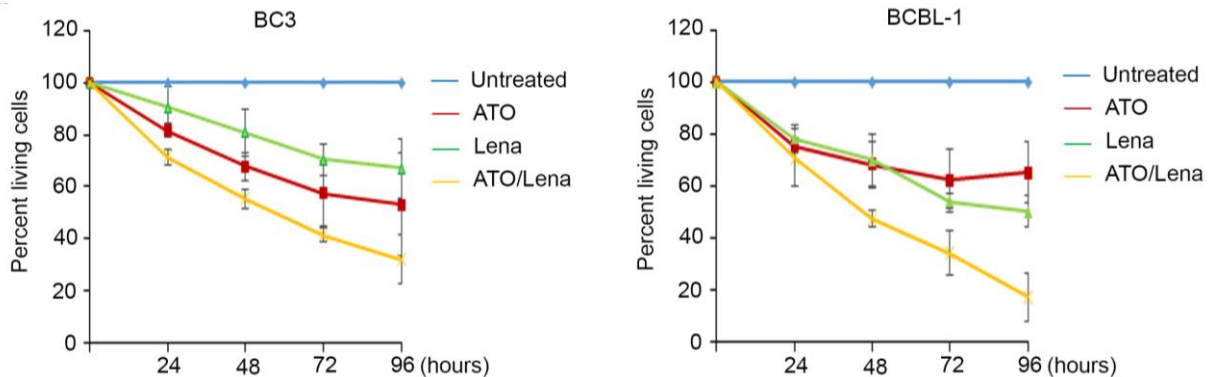


Figure 20. ATO/Lena inhibit cell proliferation in ascites-derived PEL cells. Cell proliferation of ascites-derived BC-3 (left) or BCBL-1 cells (right) following *ex vivo* treatment with ATO and/or Lena for 24, 48, 72, and 96 h. Results are presented as percent of control, plotted as mean \pm SD, and represent an average of three independent experiments.

To investigate the potential mechanisms underlying the growth inhibitory effect of ATO/Lena combination on PEL cells, immunoblot analysis and immunofluorescent assays were implemented to assess the expression of KSHV latent proteins, key players in PEL

oncogenesis. Interestingly, 48 h post treatment, the combination of ATO/Lena decreased the expression levels of LANA-1 and LANA-2 latent proteins in both BC-3 and BCBL-1 ascites-derived cells (Figure 11). Single agents, however, had no significant effect on LANA-1 or LANA-2 protein levels.

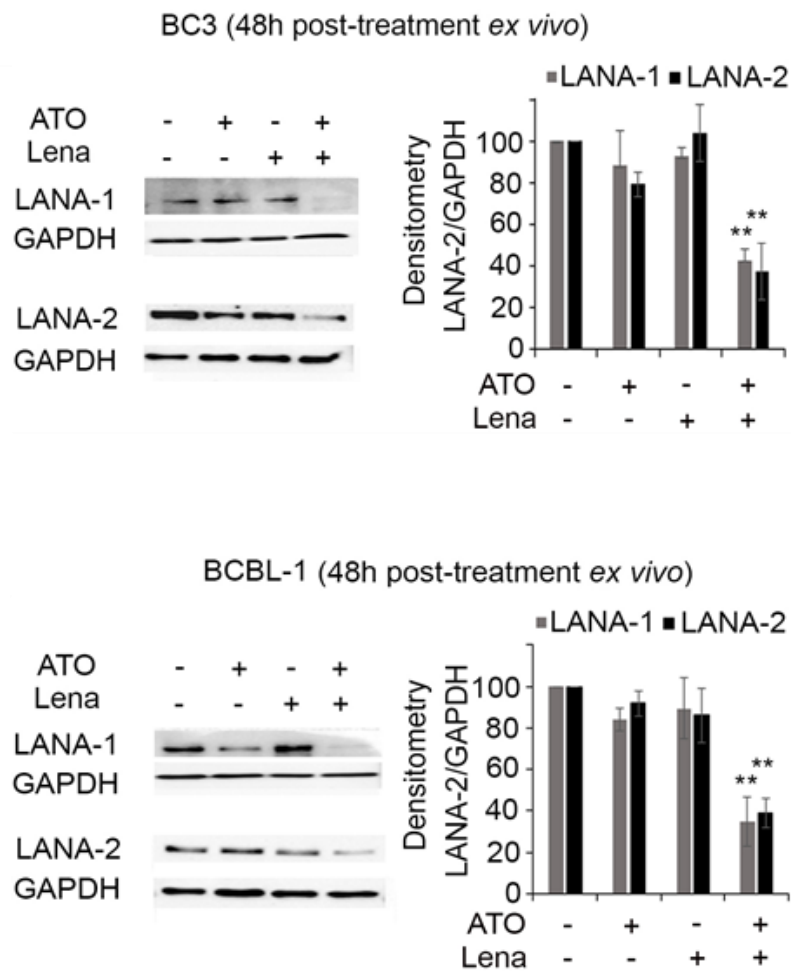


Figure 21. ATO/Lena decreases Latent gene expression in ascites-mediated PEL cells. Immunoblot analysis of KSHV latent proteins LANA-1 and LANA-2 following 48 h *ex vivo* treatment with ATO and /or Lena in ascites-derived BC-3 (left) or BCBL-1(right)

cells. Histograms represent densitometry analysis of an average of 3 independent experiments. (**) indicates $p < 0.01$.

In immunoflorescent assay, nuclear speckles of LANA-1 were hardly detected following treatment with ATO/Lena in both PEL derived cells. (Figure 12).

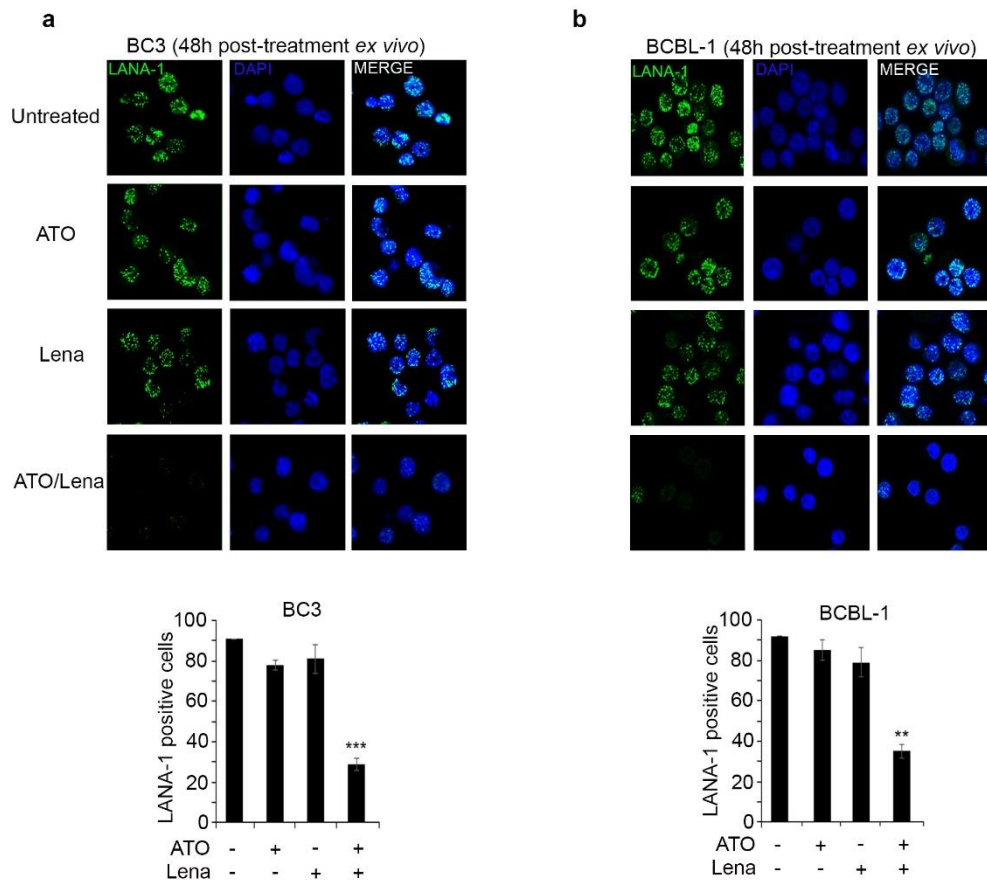


Figure 22 . a,b) Confocal microscopy analysis of LANA-1 nuclear expression in ascites-derived BC-3 (a) and BCBL-1 (b).LANA-1 was stained with rat anti-LANA-1 antibody (green). Nuclei were stained with Hoechst (blue). Histograms represent the average percentage of LANA-1 positive cells from three independent experiments. (**) indicates $p < 0.01$; and (***) indicates $p < 0.001$.

Similarly, while single agents failed to result in a significant effect, ATO/Lena combination significantly downregulated transcript levels of KSHV latent v-FLIP and v-Cyclin in BC-3 ascites derived cells ($p < 0.01$) (Figure 13). Conversely, in BCBL-1 ascites derived cells, single agent treatment resulted in a significant yet moderate reduction in v-FLIP and v-Cyclin transcription ($p < 0.05$ and 0.01 , respectively). However, this reduction was more profound following treatment with ATO/Lena ($p < 0.01$) (Figure 2c). Cell growth inhibition and decreased latent protein expression, drivers of oncogenesis and PEL cells' survival, may translate the decreased peritoneal effusion and enhanced survival.

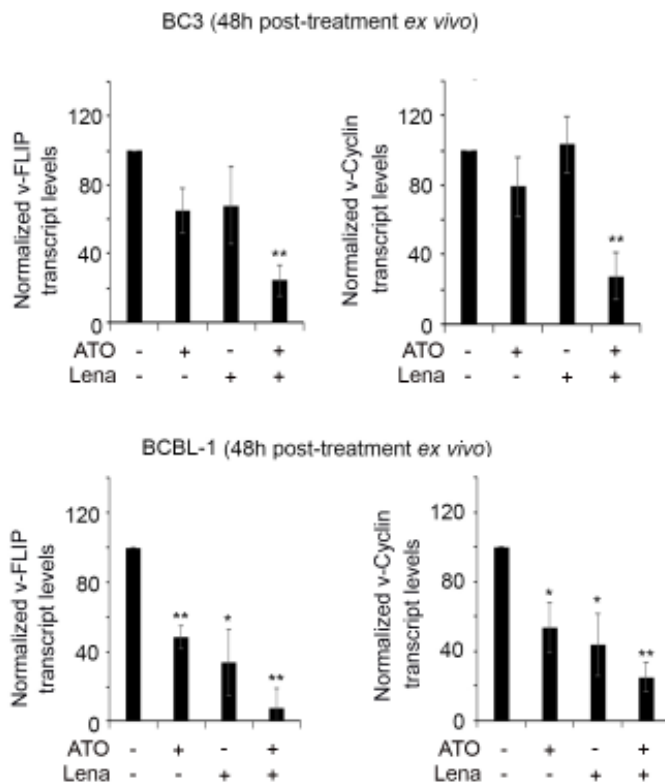


Figure 23. Real- time quantitative PCR analysis of KSHV latent v-FLIP and v-Cyclin in ascites-derived BC-3 and BCBL-1 cells. Results are presented as percent of control, plotted as mean \pm SD, and represent an average of three independent experiments. (**) indicates $p < 0.01$

4. ATO/Lena reduces Tumor Burden via Inhibition of NF κ B and Autocrine growth-promoting Cytokines in Ex vivo Ascites-Derived PEL Cells

v-FLIP had been established as a key player in the activation of NF- κ B, a constitutively activated pathway critical for PEL progression and cell survival^{107, 240}. In line with the downregulated v-FLIP expression, we showed that, at 48 h post treatment, ATO/Lena decreased the phosphorylation of I κ B α protein in both BC-3 and BCBL-1 ascites derived cells (Figure 14). Phosphorylation of I κ B α is essential for the activation of canonical NF- κ B pathway.



Figure 24. ATO/Lena decreases I κ B α phosphorylation in ascites-mediated PEL cells. Immunoblot analysis of decreased I κ B α phosphorylation in BC-3 and BCBL-1 ascites derived cells 48 h following treatment with ATO/Lena

I κ B α phosphorylation is essential for activation of canonical NF- κ B pathway²⁴¹. In consistent with the decrease in I κ B α phosphorylation, we observed a reduced nuclear translocation of p65, a mandatory step for the activation of NF- κ B pathway and downstream genes, in both BC-3 and BCBL-1 ascites-derived cells (Figure 15). In contrast, single agents failed to decrease I κ B α phosphorylation and exhibited no significant effect on p65 nuclear translocation (Figure 15).

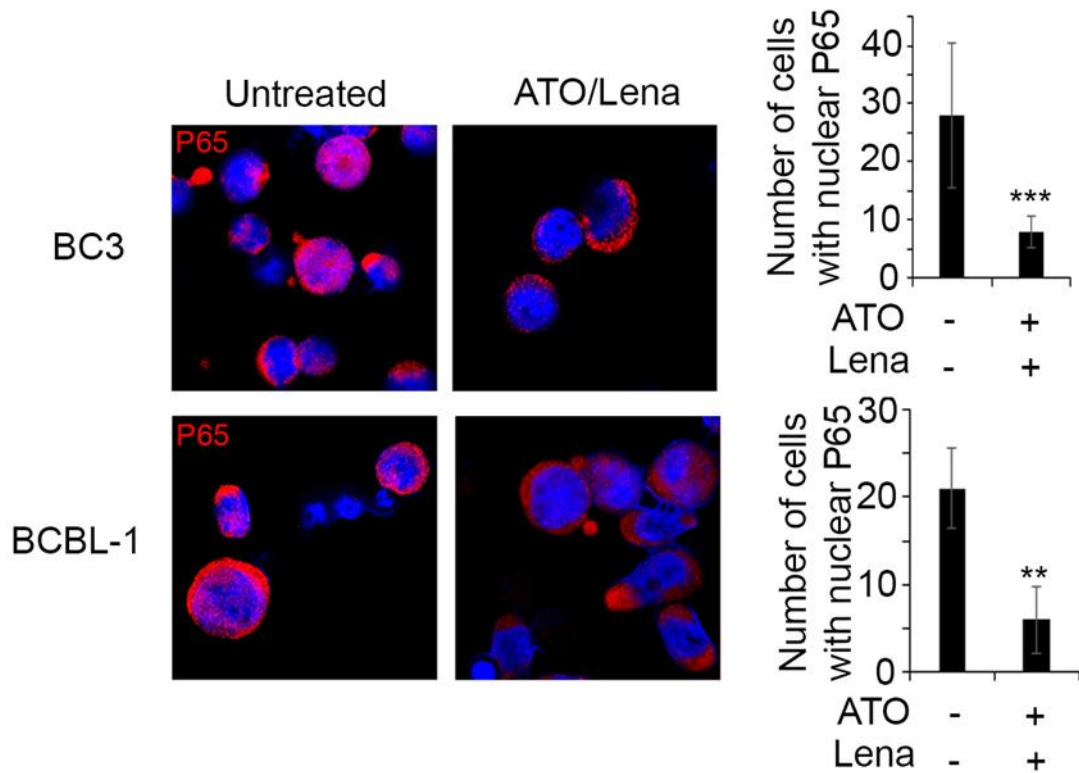


Figure 25. Confocal microscopy analysis of P65 translocation in BC-3 and BCBL-1 ascites derived cells 48 h post treatment with ATO/Lena. p65 was stained with anti-p65 antibody (red) and nuclei were stained by Hoechst stain (blue). Images represent z-sections. Histograms represented number of cells with nuclear p65 translocation.

Among various downstream target genes, NF- κ B transactivates the transcription of multiple cytokines such as IL-6 and IL-10. Of note, these cytokines are known as essential growth factors that promote PEL cell proliferation and survival¹⁷⁵⁻¹⁷⁷. Decreased NF- κ B activation by ATO/Lena prompted us to investigate the transcript levels of IL-6 and IL-10 in ATO and/or Lena treated cells. In both BC-3 and BCBL-1 ascites mediated cells, single agent ATO exhibited no significant effect on cellular IL-6 transcription, while Lena significantly decreased IL-6 transcripts in BC-3 ($p < 0.01$) and BCBL-1 cells ($p < 0.05$) to less than 50% compared to untreated cells (Figure 16). However, single agents ATO or Lena did not affect cellular IL-10 transcription. Interestingly, in BC-3 ascites derived cells, ATO/Lena combination significantly reduced IL-6 transcription to around 27% ($p < 0.01$) and completely diminished IL-10 expression ($p < 0.001$) (Figure 16).

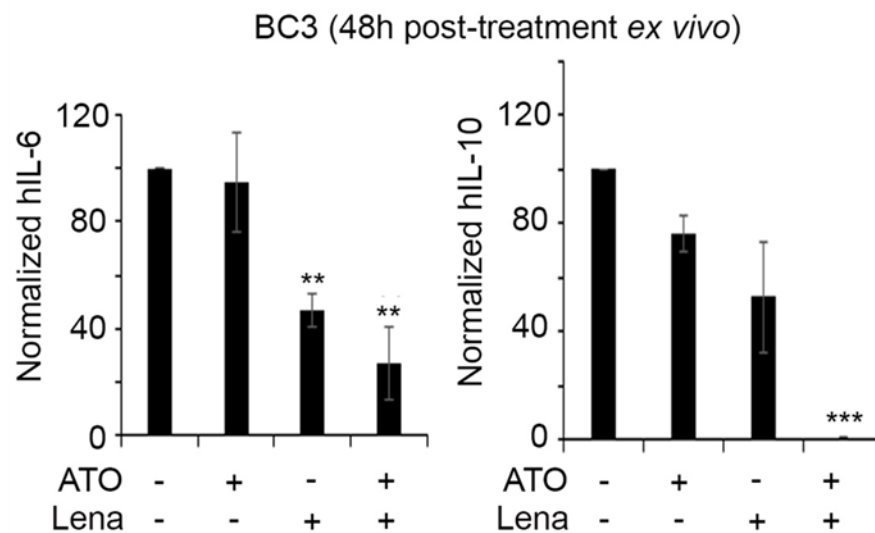


Figure 26 . Real-time quantitative PCR analysis of human IL-6 and IL-10 in BC-3 ascites derived cells 48 h post treatment with ATO and/ or Lena. Results are presented as percent

of control, plotted as mean \pm SD, and represent an average of three independent experiments. (**) indicates $p < 0.01$, (***) indicates $p < 0.001$.

Similarly, ATO/Lena decreased IL-6 transcript levels to 18% ($p < 0.01$) and IL-10 transcript levels to 31% ($p < 0.05$) in BCBL-1 ascites-derived cells 48h post treatment (Figure 17).

Altogether, these data may explain the anti-proliferative effect of ATO/Lena, where decreased cell growth might be attributed to decreased NF- κ B, resulting in successive reduction in transcription of autocrine target cytokines critical for PEL cell survival.

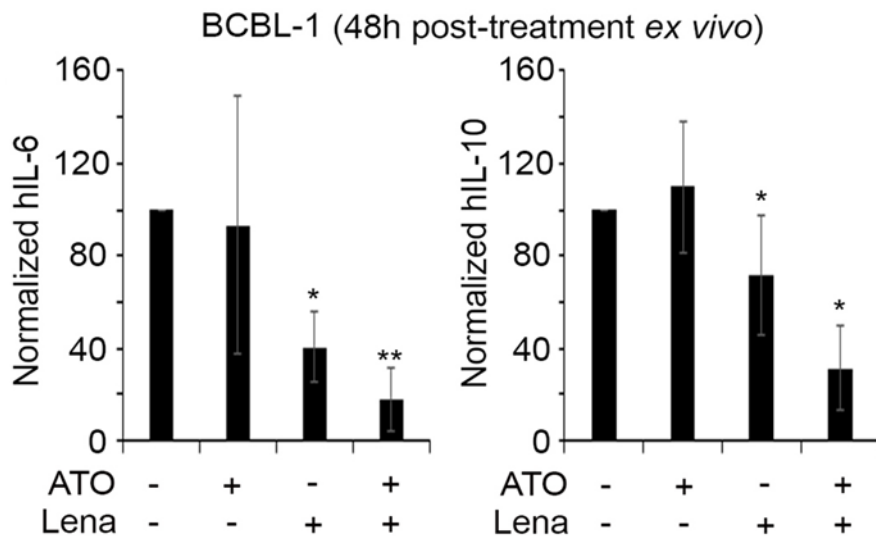


Figure 27. Real-time quantitative PCR analysis of human IL-6 and IL-10 in BC-3 and BCBL-1 ascites derived cells 48 h post treatment with ATO and/ or Lena. Results are presented as percent of control, plotted as mean \pm SD, and represent an average of three independent experiments. (*) indicates $p < 0.05$, (**) indicates $p < 0.01$.

5. *ATO/Lena Induces KSHV Lytic Gene Expression in Ex vivo Ascites-Derived PEL Cells*

Prior studies demonstrated that the constitutive activation of NF- κ B in PEL subverts KSHV lytic reactivation and contribute to maintaining latency via inhibition of viral lytic gene expression^{144, 146}. Paradoxically, KSHV lytic reactivation is often associated with decreased latent gene transcription and apoptosis¹⁷³. Thus, we investigated the expression profile of known KSHV lytic viral genes following 24 and 48 h treatment with ATO/Lena. Interestingly, ATO/Lena induced a significant induction in transcription of early lytic genes (RTA and ORFK8) at 24 h and late lytic gene (K8.1) at 48 h following *ex vivo* treatment of ascites-derived PEL cells (Figure 18). RTA is a major early lytic gene that is sufficient for switch into KSHV viral lytic gene transcription by activation of transcription of most viral proteins¹⁵⁸. In BC3 ascites-derived cells, Lena alone had no significant effect on lytic gene expression, while ATO single agent induced a moderate significant increase in RTA transcript levels at 24 h following treatment ($p < 0.05$) (Figure 18).

Surprisingly, the ATO/Lena combination induced a highly significant increase in RTA transcript levels ($p = 0.01263$). Likewise, ATO/Lena also increased the transcription of early lytic gene ORFK8 ($p = 0.0177$) after 24 h of treatment. However, single agents ATO and Lena had no significant effect on ORFK8 transcription (Figure 18). Similarly, in BCBL-1 derived ascites, the combination of ATO/Lena resulted in a significantly increased levels of RTA ($p < 0.05$) and ORFK8 ($p < 0.01$) gene transcripts (Figure 18).

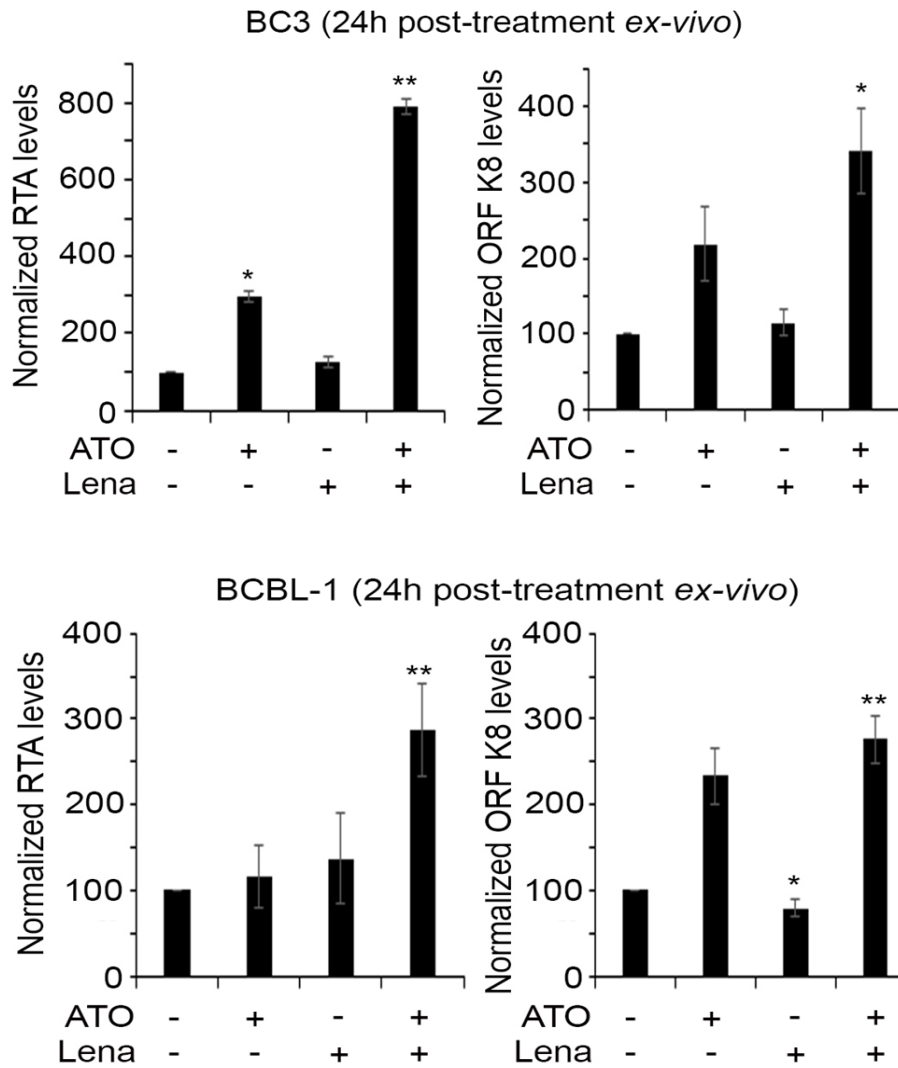


Figure 28. Real-time quantitative PCR analysis of RTA and ORFK8 expression in BC-3 and BCBL-1 ascites derived cells 48 h post treatment with ATO and/ or Lena. Results are presented as percent of control, plotted as mean \pm SD, and represent an average of three independent experiments. (*) indicates $p < 0.05$, (**) indicates $p < 0.01$.

KSHV lytic reactivation follows a sequential pattern of gene expression whereby immediate and early genes are transcribed first followed by late structural genes^{157, 159}. Thus, we investigated the late lytic gene K8.1 transcript levels at 48h post *ex vivo*

treatment of ascites-derived PEL cells. Our results revealed a significant induction of K8.1 transcription upon treatment with the combination of ATO/Lena, in both BC-3 ($p < 0.01$) and BCBL-1 ascites-derived cells ($p < 0.05$) (Figure 19).

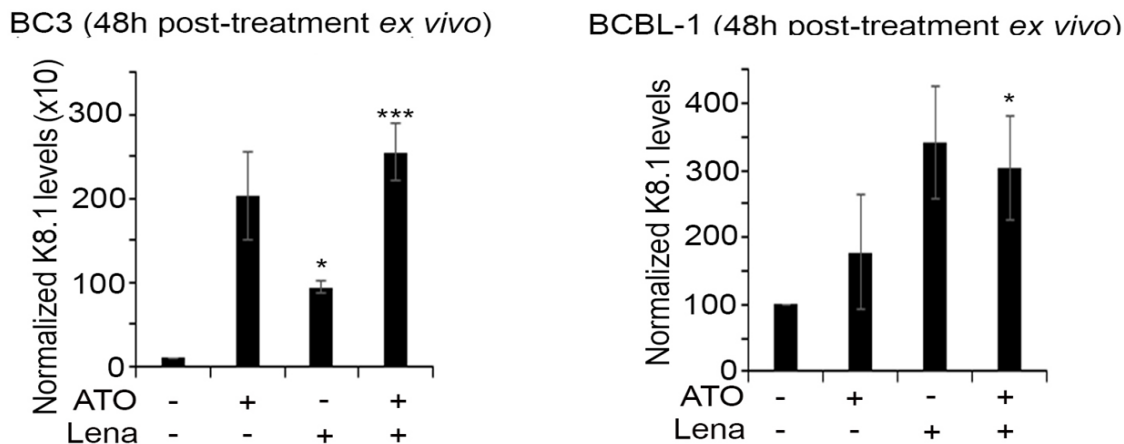


Figure 29. Real-time quantitative PCR analysis of K8.1 expression in BC-3 and BCBL-1 ascites derived cells 48 h post treatment with ATO and/ or Lena. Results are presented as percent of control, plotted as mean \pm SD, and represent an average of three independent experiments. (*) indicates $p < 0.05$. (***) indicates $p < 0.001$.

6. ATO/Lena Induces Apoptosis in ex vivo Ascites-Derived PEL Cells

In prior studies, inhibition of the constitutively activated NF- κ B resulted in apoptosis on PEL cells *in vitro* and prolonged survival of PEL mice *in vivo*^{240, 242}. Herein, ATO/Lena inhibited the activation of NF- κ B and resulted in suppressed cell survival and proliferation. Therefore, we assessed the effect of ATO/Lena on apoptosis in ascites-derived BC-3 and BCBL-1 cells 48 h post treatment. In both cell types, ATO/Lena combination resulted in an eminent cleavage of procaspase-3, a key mediator of apoptosis,

paralleled with increased levels of cleaved caspase-3 protein (Figure 20). In accordance with these results, 48 h *ex vivo* treatment with ATO/Lena also induced the cleavage of PARP-1, a downstream target of caspase-3, in both BC3 and BCBL-1 ascitic cells (Figure 20).

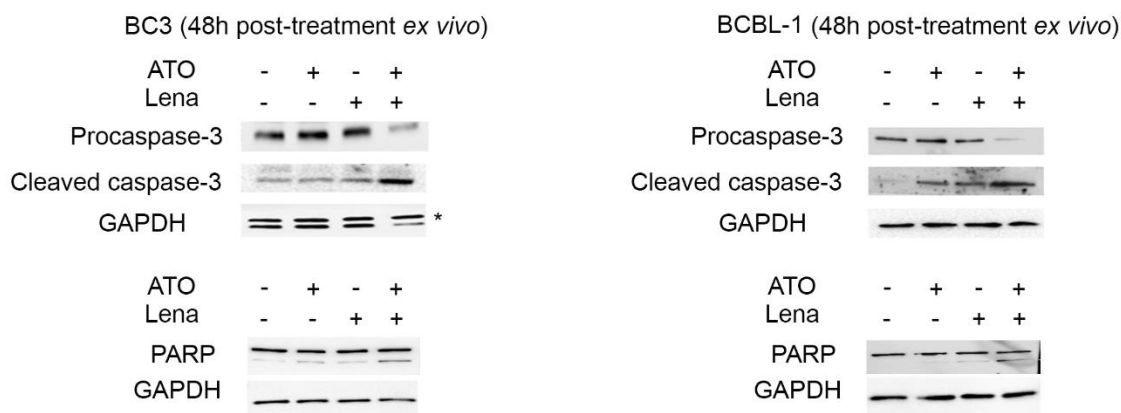


Figure 30. Immunoblot analysis procaspase-3, cleaved caspase-3, and and PARP expression in BC-3 and BCBL-1 ascites derived cells 48 h post treatment with ATO/Lena.

In addition, cell death was also detected by DAPI staining of ATO/Lena treated BC3 and BCBL-1 ascites derived cells (Figure 21). This staining allows for the evaluation of chromatin condensation, a hallmark of apoptosis. For both ascites-derived BC-3 and BCBL-1, cells treated with the combination therapy presented a nucleus with condensed nucleic material and were smaller in size with irregularly shaped cytoplasm, characteristics of apoptotic cells (Figure 21). Collectively, these data strongly suggest that the combination of ATO/Lena induces apoptosis of PEL cells.

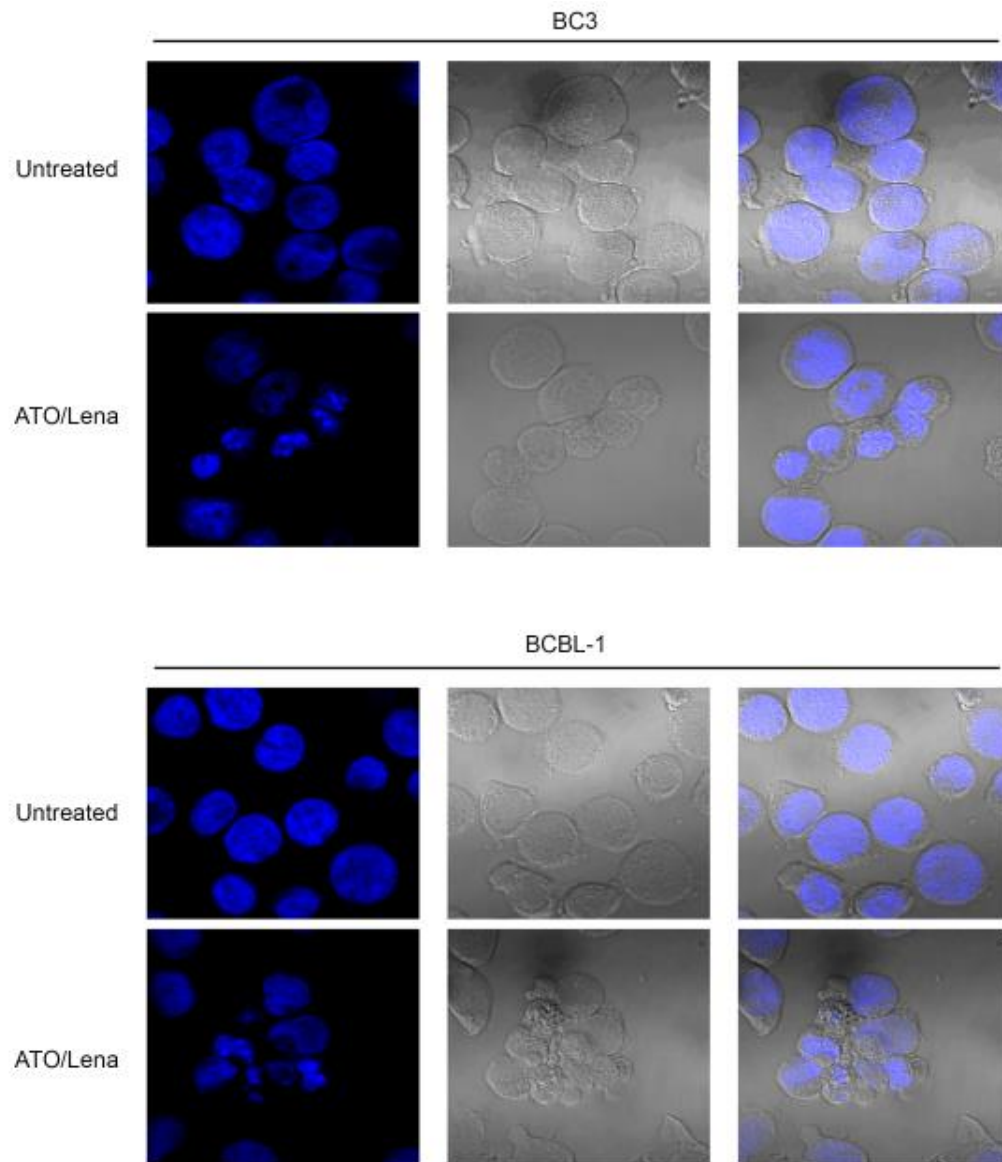


Figure 31. Confocal microscopy analysis of ascites-derived BC3 or BCBL-1 cells stained with Diamidine-2'-phenylindole dihydrochloride (Dapi) following 48h treatment with ATO/Lena.

7. *ATO/Lena suppresses VEGF-mediated Endothelial Cells Tube Formation*

Upon sacrifice of BC-3 inoculated PEL mice treated for one week of ATO and/or Lena, we came across an observation of decreased peritoneal vascularization following treatment of BC3 inoculated mice with ATO/Lena combination (Figure 22).

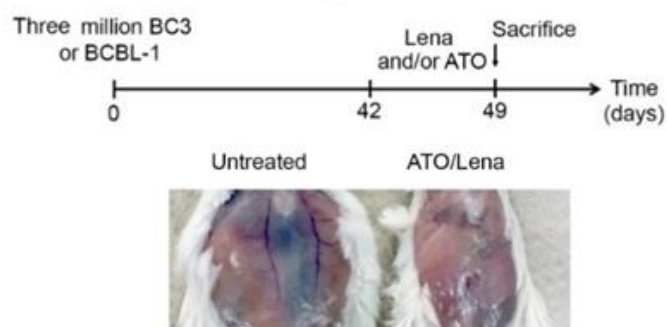


Figure 32. Mice peritoneum vascularization before and after one-week treatment of BC-3 PEL mice with ATO/Lena.

The anti-angiogenic properties of Lena were previously reported by multiple studies investigating hematological tumors²²³. More importantly, PEL cells were shown to secrete VEGF into lymphomatous ascites *in vivo* to promote VEGF-mediated angiogenesis and PEL development^{178, 243}. Ascites-derived BC-3 and BCBL-1 cells were previously shown to secrete higher VEGF levels than their respective cells lines.

Based on our *in vivo* findings, we investigated the effect of ATO/Lena on VEGF-induced angiogenesis. HAEC cells were grown on Matrigel were incubated with cell-free supernatant of treated or untreated ascites-derived PEL (BC-3 or BCBL-1) for 48 hr

(Figure 23). When cultured alone, HAEC exhibited a normal fibroblast phenotype and failed to develop structured tube network. In contrast, added supernatants from untreated ascites-derived PEL cells (BC-3 or BCBL-1), resulted in formation of capillary-tube like structures with multi-centric junctions (Figure 23). This phenotype was VEGF dependent, the addition of bevacizumab to supernatants from untreated BC3 or BCBL-1 cells inhibits capillary tube formation by HAEC (Figure 23).

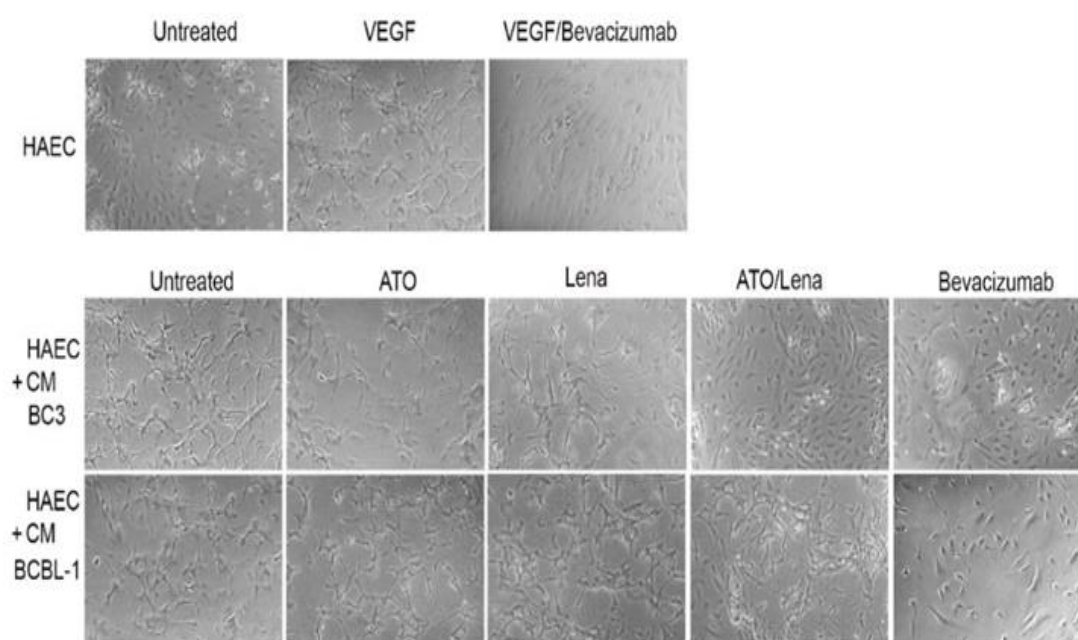


Figure 33. Light microscopy images of capillary-like tube formations in HAEC cells. HAEC cells were incubation with supernatants from ATO and/ or Lena treated BC-3 or BCBL-1 ascites cells for 48 h. Images were taken with 5x microscope scale.

Supernatants from single agents, ATO or Lena, did not display any significant effect on tubal formation capacity of cells. Conversely, supernatant from ATO/Lena treated BC-3 PEL mice ascites resulted in significant reduction of the capillary-like tube formation capacity to 20% compared to that from untreated cells (Figure 23 and 24).

Quantification of capillary tube formation depended on counting nodes (defined intersection of three or more branches) (Figure 24).

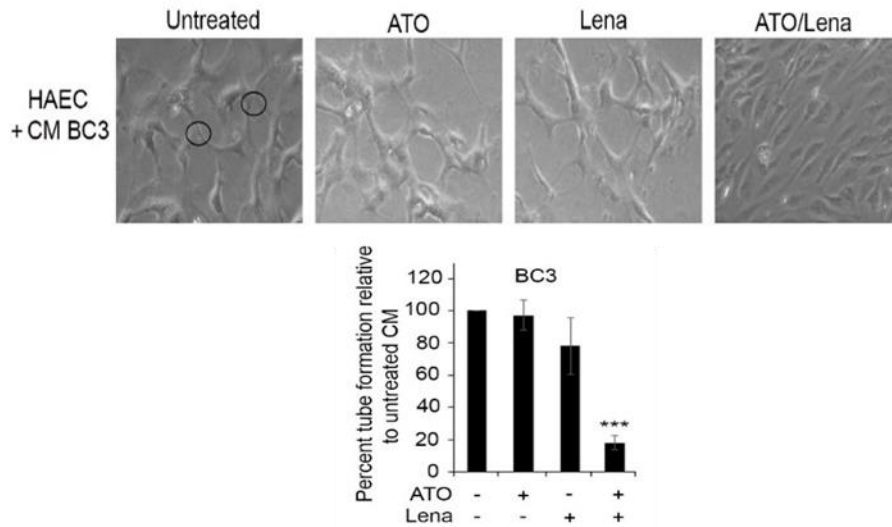


Figure 34. The capillary-tube formation analysis method used. Nodes with three or more branches were counted and compared. A minimum of 5 images were counted per condition. Histogram represents the percentage of tube formation relative to untreated BC-3 ascites PEL cells. Data represent an average of 3 independent experiments

Surprisingly, supernatant from ATO/Lena treated BCBL-1 PEL mice ascites did not reduce the tube formation capacity compared to untreated cells (Figure 23). This might be due to the overwhelming amount of VEGF secreted by BCBL-1 ascites¹⁷⁸. These data suggest that decreased VEGF-dependent angiogenesis may be one of the potential mechanisms that contribute to ATL/Lena elimination of ascites-derived BC-3 but not BCBL-1 cells.

8. ATO/Lena reduces Organ Infiltration *in vivo*

To further investigate the anti-tumor effect of ATO/Lena *in vivo* and the potential mechanism of action contributing to mice survival, PEL mice (inoculated with BC3 or BCBL-1 cells) were left to develop malignant effusion for around 6 weeks before initiating a one week with the ATO/Lena combination (Timeline explained in Figure 25). We first assessed the effect of this therapeutic combination on organ infiltration. Compared to untreated mice, ATO/Lena treated mice presented with decreased infiltration of malignant cells specifically in the lungs and livers of both BC-3 and BCBL-1 murine models (Figure 25).

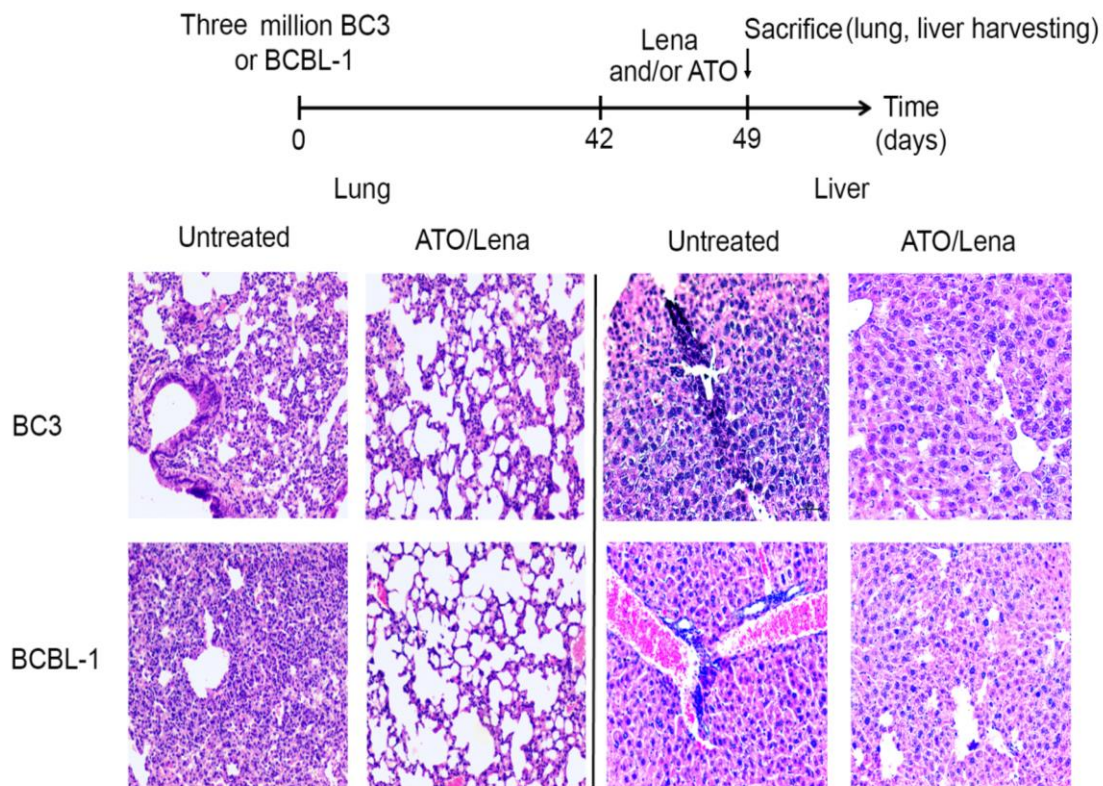


Figure 35. ATO/Lena decreased organ infiltration in PEL mice. Experimental design of *in vivo* experiment: mice injected with BC-3 or BCBL-1 were allowed to develop ascites for 6 weeks, treated with ATO and/or Lena for one week, and then sacrificed. Histopathology sections of lung and spleens from ATO/Lena treated or untreated BC-3 and BCBL-1 PEL mice.

9. ATO/Lena decreases KSHV Latent Protein and cellular Cytokine Expression

The molecular mechanism of action of ATO/Lena was investigated *in vivo*.

Consistent with *ex vivo* data, treatment with ATO/Lena decreased the expression of KSHV latent proteins LANA-1 and LANA-2 in both BC-3 and BCBL-1 PEL mice. We questioned whether this decrease was attributed to a decrease in the percentage of PEL cells being eliminated by ATO/Lena. Thus, CD45 staining of ascites derived from ATO/Lena treated BC-3 and BCBL-1 was carried. CD45 is a marker of human leukocytes and is commonly used in *in vivo* studies to monitor infiltration or engraftment of malignant cells. For ascites derived from BC3 treated PEL mice, CD45 staining exhibited no significant variation in the percentage of CD45 positivity, indicative of PEL cell number, when compared to untreated mice (Figure 26).

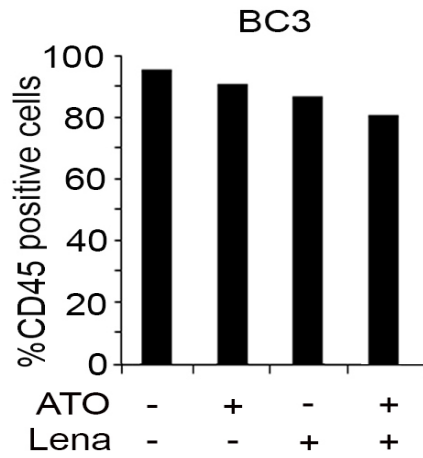


Figure 36. Immunophenotype analysis of CD45 expression in peritoneal ascites of BC3 PEL mice. percentage of CD45 positive cells in ascites cells derived from BC3 mice treated with ATO and/or Lena for one week.

Therefore, the observed decrease in LANA-1 and LANA-2 protein expression post treatment with ATO/Lena was not due to lower number of PEL cells, but is rather a direct effect of the combination on latent KSHV protein expression (Figure 27).

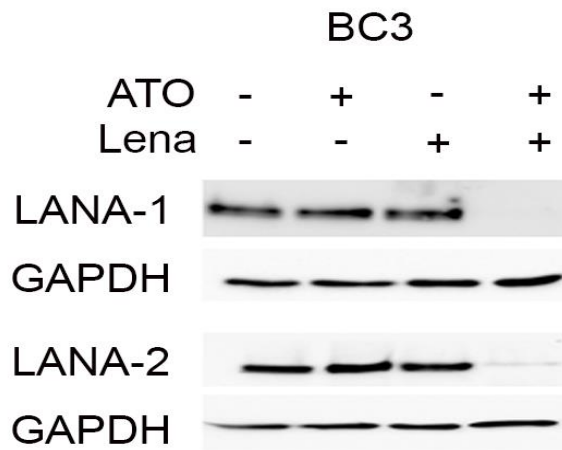


Figure 37. ATO/Lena decreased latent protein expression in BC-3 PEL mice. Immunoblot analysis of the expression of LANA-1 of LANA-2 KSHV latent proteins in ascites derived from BC-3 PEL mice treated with ATO and/ or Lena for one week.

In contrast, CD45 staining of ascites from BCBL-1 treated mice revealed that ATO/Lena affects the number of PEL cells where a significant 50% reduction in CD45 positivity was reported in ATO/Lena treated mice. (Figure 28).

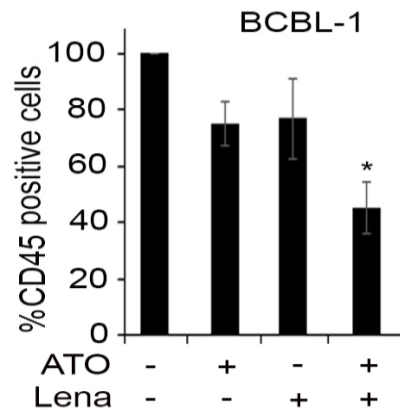


Figure 38. Immunophenotype analysis of CD45 expression in peritoneal ascites of BCBL-1 PEL mice. percentage of CD45 positive cells in ascites derived from BCBL-1 mice treated with ATO and/or Lena for one week. (*) denotes ($p < 0.05$).

We thus sorted CD45 positive BCBL-1 cells before assessing the effect of the combination on viral protein expression in BCBL-1 ascites-derived cells, and we demonstrated that the ATO/Lena combination also decreased LANA-1 and LANA-2 protein expression in these cells (Figure 29).

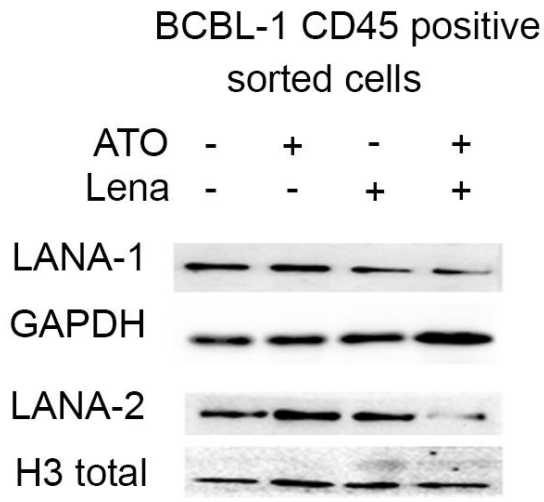


Figure 39. ATO/Lena decreased latent protein expression in BCBL-1 PEL mice. Immunoblot analysis of the expression of LANA-1 of LANA-2 KSHV latent proteins in ascites derived from BC-3 PEL mice treated with ATO and/ or Lena for one week.

We also investigated the effect of ATO/Lena on gene transcription of cellular cytokines, IL-6 and IL-10, in the lungs of treated PEL mice (Figure 30). In the BC-3 PEL model, the decrease in cytokine transcription by ATO/Lena was significant for IL-6 where transcript levels were decreased to 25% ($p < 0.05$) (Figure 30).

In BCBL-1 PEL mice decreased cytokine transcription was significant for both IL-6 and IL-10 which declined to 25% ($p < 0.05$) and 45% ($p < 0.05$), respectively (Figure 30). Collectively, these data support and emphasize that the *ex vivo* dissected mechanism of action might be involved in the anti-tumor activity of ATO/Lena combination *in vivo*.

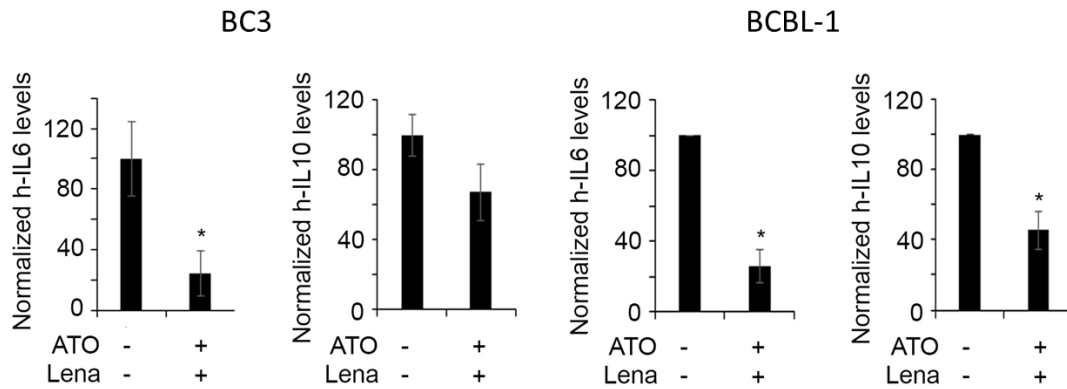


Figure 40. Real-time quantitative PCR analysis of cytokine expression in PEL treated mice. Human IL-6 and IL-10 expression in lung tissues derived from BC3 or BCBL-1 PEL mice treated with ATO/Lena for one week. Results are presented as percent of control, plotted as mean \pm SD, and represent an average at least 3 mice. (*) indicates $p < 0.05$.

B. ATL Part

1. Unlike Tax, HBZ lacks transformative capacity in a *Drosophila* model

To investigate the *in vivo* effects of HBZ, *hbz* transgenic fly model was established using the same approach implemented in our previously generated tax transgenic model³³⁰. Using the GMR-GAL4 promoter, the expression HBZ or Tax was directed to differentiated photoreceptor cells, posterior to the morphogenetic furrow³⁸³. As a result, gene expression was exclusively induced in the fly's eyes. Thus, to compare the transformation capacity of HBZ and Tax, we examined the ommatidial structures in transgenic eyes using SEM. Eye phenotypes were analyzed and scored according to extent of ommatidial loss or degree of disruption of mechano-sensory bristle such as misplacement, alignment, or duplication^{330, 384}. In accordance with our previously published data³³⁰, all *tax* transgenic flies (Tax Tg) displayed a rough eye phenotype, a suggestive of cellular transformation (Figure 42). On contrary, in *hbz*

transgenic flies (HBZ Tg) only 32% of flies, 12 out of 37 eyes, exhibited minimal alterations in the normal ommatidial morphology compared to control flies. The rest of the flies, however, did not display any ommatidial difference when compared with control ones (Figure 42).

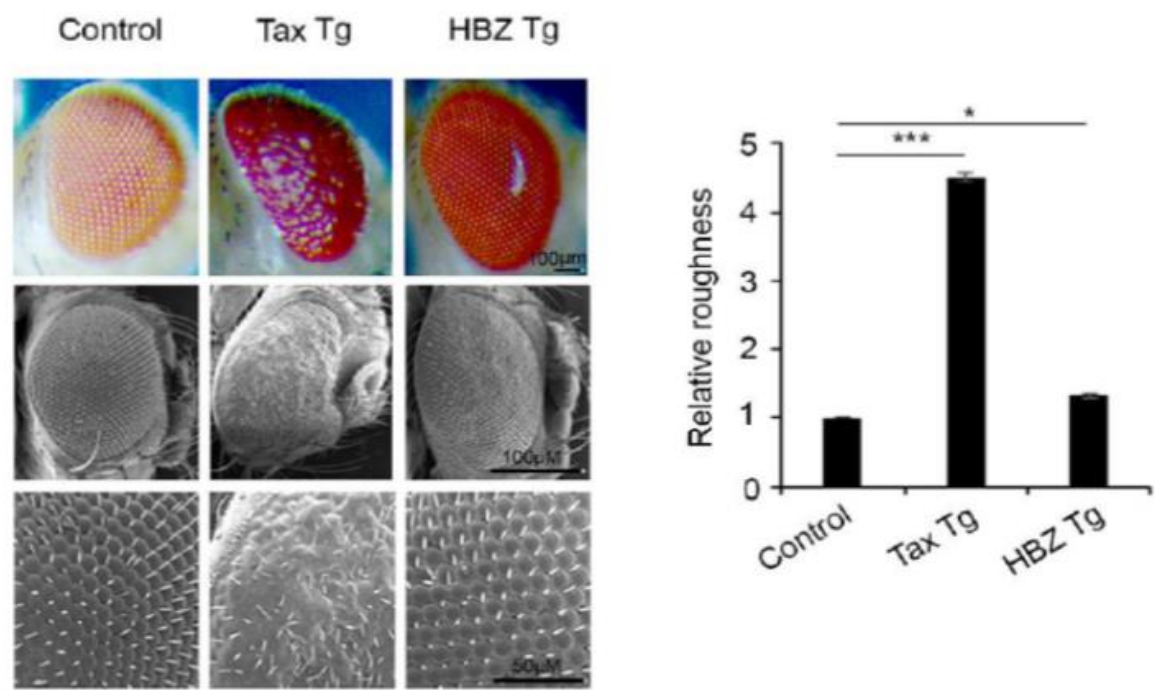


Figure 41. Tax but not HBZ induce eye roughness in transgenic flies. Representative images from light microscope (100µm scale bar) and scanning electron microscope (50µm and 100µm scale bar) of adult fly eyes pertaining to control (GMR-GAL4>*w1118*), *tax* transgenic (Tax Tg: GMR-Gal4>UAS-Tax) or *hbz* transgenic (HBZ Tg: GMR-Gal4>UAS-HBZ) flies. Histograms represent relative roughness, calculated according to a previously established scoring system. Results are reported as average of n=37 fly eye from three independent crosses. Data represent mean ± standard error of the mean, $p < 0.05$ (*), $p < 0.001$ (***)

Using quantitative RT-PCR and immunoblot, we confirmed the expression of Tax and HBZ in respective transgenic flies (Figure 43).

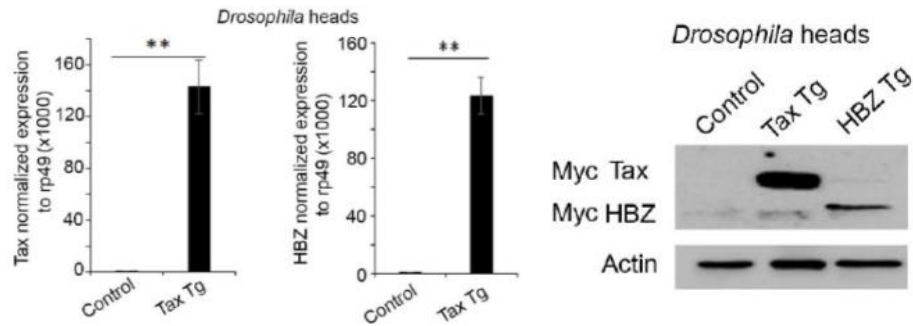


Figure 42. RTq-PCR and Immunoblot analysis of expression of Tax and HBZ in *tax* transgenic (Tax Tg) and *hbz* transgenic (HBZ Tg) fly heads. For RTq-PCR gene expression was normalized to drosophila internal control RP-49. For immunoblot analysis, anti-myc tag antibody (the tag in *tax* and *hbz* transgenics) was used. Expression of Tax and HBZ was under the control of GMR-GAL4, an eye-specific promoter. Results were obtained from three independent crosses. Data represent mean \pm standard error of the mean, $p < 0.01$ (**).

Since HBZ resulted in no phenotypic changes in ommatidial structures of HBZ Tg model, we conducted a functional assay to confirm that the HBZ protein expressed was functional. Indeed, higher transcript levels of JunD, an HBZ downstream gene, was observed in HBZ-Tg flies, as compared to Tax Tg or control flies thereby confirming the activity of HBZ (Figure 44).

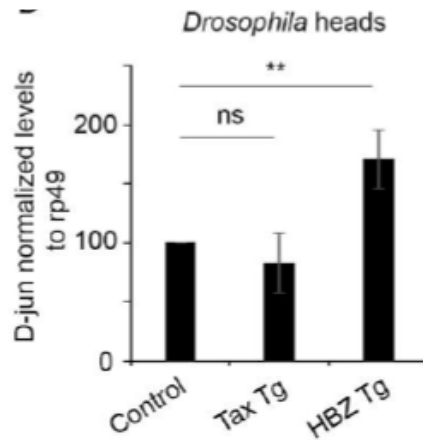


Figure 43. Real-time quantitative PCR analysis of Jun D expression in *hbz* transgenic fly heads. Expression of Jun D was normalized to Rp-49. The expression of Tax and HBZ was under the control of GMR-GAL4, an eye-specific promoter. Results are reported as average of three independent experiments. Data represent mean \pm standard error of the mean, $p < 0.01$ (**). ns: non significant.

Given that ATL is a blood malignancy associated with lymphocytosis, we sought to assess the effect of HBZ on the flies' hematopoietic system. Using the UAS-Gal4 system, the expression of Tax or HBZ was directed to hemocytes using a hemocytes-specific promoter referred to as HML Δ -Gal4. Expression of Tax or HBZ in hemocytes was first confirmed via quantitative RT-qPCR and Western Blot (Figure 45).

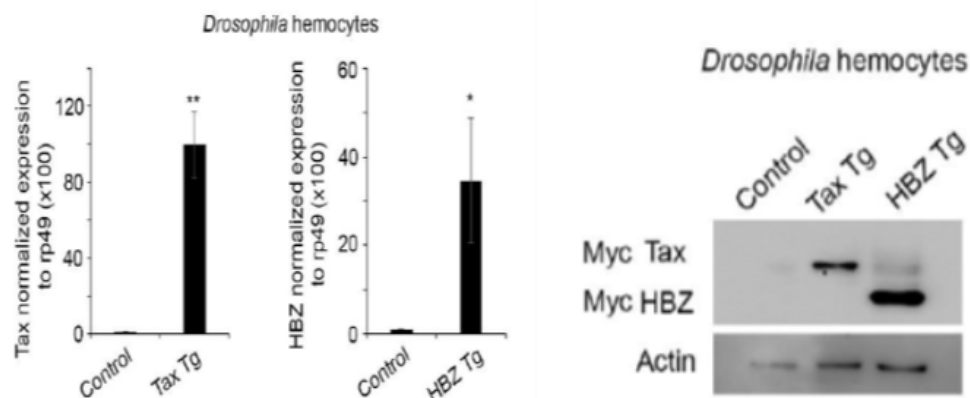


Figure 44. Real time quantitative PCR analysis and immunoblot analysis of Tax or HBZ in circulating hemocytes from control, Tax Tg, or HBZ Tg flies. Expression of Tax and HBZ was induced under the control of HML Δ -Gal4, a hemocyte-specific promoter. For real time quantitative PCR, expression was normalized to RP-49. For immunoblot, the expression of myc-tag (Tag for Tax or HBZ) was assessed. For each experiment a minimum of thirty third-instar larvae were bled and hemocytes were collected. Results are reported from average of three independent crosses. Data represent mean \pm standard error of the mean, $p < 0.05$ (*), $p < 0.01$ (**).

In consistent with our previous findings, Tax-Tg flies exhibited a significantly increased hemocytes count in third instar larvae to around 15,000 cells compared to 5000 cells in control flies (Figure 46). In contrast, HBZ expression in HBZ Tg flies resulted in a modest increase in circulating hemocytes from 5000 cells in control to almost 7000 in around 16% of larvae (5 out of 30 larvae) (Figure 46). Collectively, these data provide a conclusive evidence that, unlike the potent oncogenic Tax, HBZ protein exhibits a minimal oncogenic potential.

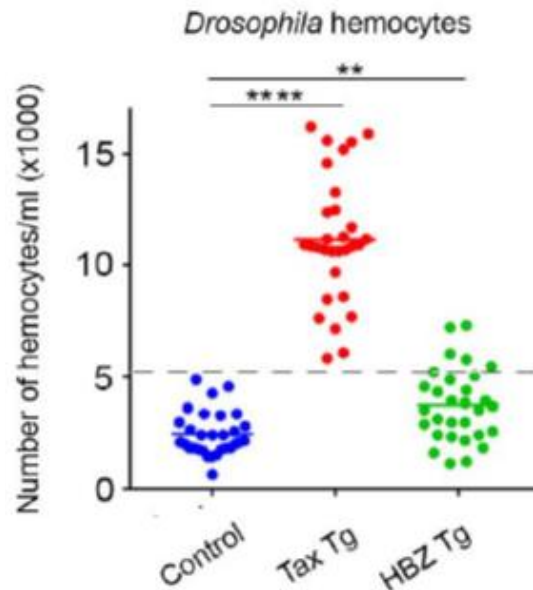


Figure 45. Tax increases the number of circulating hemocytes to a higher extent than HBZ in transgenic flies. Circulating hemocyte count in control (HML Δ -Gal4>*w1118*), Tax Tg (HML Δ -Gal4>UAS-Tax), or HBZ Tg (HML Δ -Gal4>UAS-HBZ) third instar larvae. N=30 larvae were bled and counted from three independent crosses. Data represent mean \pm standard error of the mean. P<0.01 (**) and p< 0.0001 (****).

2. Tax and HBZ activated key subunits of polycomb PRC2 complex resulting in H3K27me3 accumulation.

Polycomb PRC2 complex is deregulated and overexpressed in ATL at almost half of the genes. Indeed, prior research elucidated that Tax enhanced PRC2 activity by binding and increasing EZH2 expression resulting in increased H3K27me3 accumulation²⁹⁰. Yet, the putative relation between HBZ and PRC2 complex remains ambiguous. Given the high degree of homology in Polycomb complex between *Drosophila* and humans, we took advantage of our transgenic models to characterize and compare epigenetic modulations mediated by Tax and HBZ *in vivo*. Consistent with previously described findings in human lymphocytes²⁹⁰, expression of Tax in flies was associated with increased levels of E(z) and

Suz12, homologs of human EZH2 and Suz12 respectively (Figure 47). This increase was accompanied by elevated levels of H3K27me3, a repressive mark downstream E(z), and decreased expression of H3K4me3, a transcription activation mark (Figure 47).

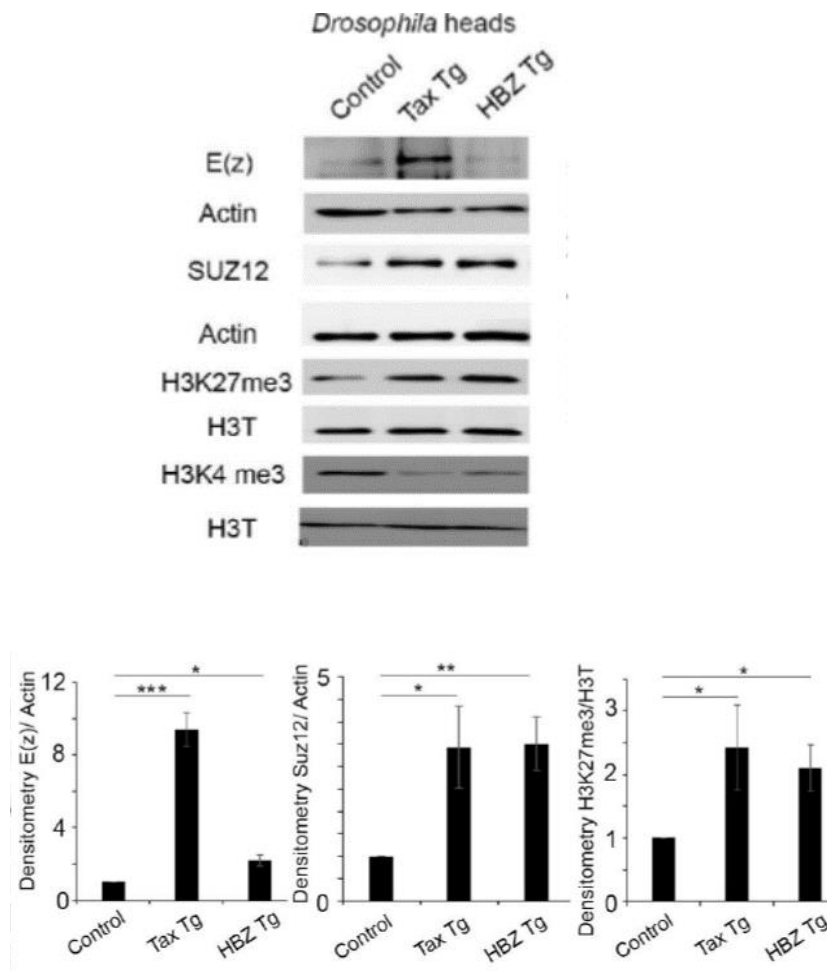


Figure 46. Immunoblot analysis of the expression of E(z), SUZ12, H3K27me3, and H3K4me3 in fly heads from control , Tax-Tg and HBZ Tg flies. Expression of Tax and HBZ in flies was induced under the GMR-Gal4, an eye-specific promoter. Histograms represent the densitometry analysis on three independent experiments from three independent crosses. $p < 0.05$ (*), $p < 0.01$ (**) and $p < 0.0001$ (****).

In contrast to *tax* transgenic flies, *hbz* transgenic flies exhibited no changes in the expression of E(z). However, SUZ12 protein levels were elevated when compared to control flies. This increase in SUZ12 was very similar to that induced by Tax and was accompanied with increased expression of H3K27me3 paralleled with decreased levels of H3K4me3 (Figure 47). Collectively, these data suggest that both Tax and HBZ induce the accumulation of repressive epigenetic histone mark, H3K27me3, through regulation of different PRC2 complex subunits.

3. *Tax-mediated transformation partially depends on PRC2 activity but highly requires activation of NF- κ B*

Altered PRC2 activity and excessive accumulation of H3K27me3 repressive mark are key players in progression of multiple cancers^{250, 290}. Despite the accumulation of H3K27me3 in both *tax* and *hbz* transgenic flies, cellular transformation (rough eye phenotype) was only reported in *tax* flies. To dissect the role of activated PRC2 complex in Tax-mediated transformation, we made use of the UAS-RNAi system and GMR-GAL4 driver to knock down the expression of E(z) and SUZ12 in *tax* flies specifically in the eyes. mcherry RNAi, a scrambled RNAi, was used as control. Silenced expression of E(z) and SUZ12 was confirmed using quantitative RT-PCR (Figure 48). The expression of Tax in knockdown flies was validated by western blot (Figure 48).

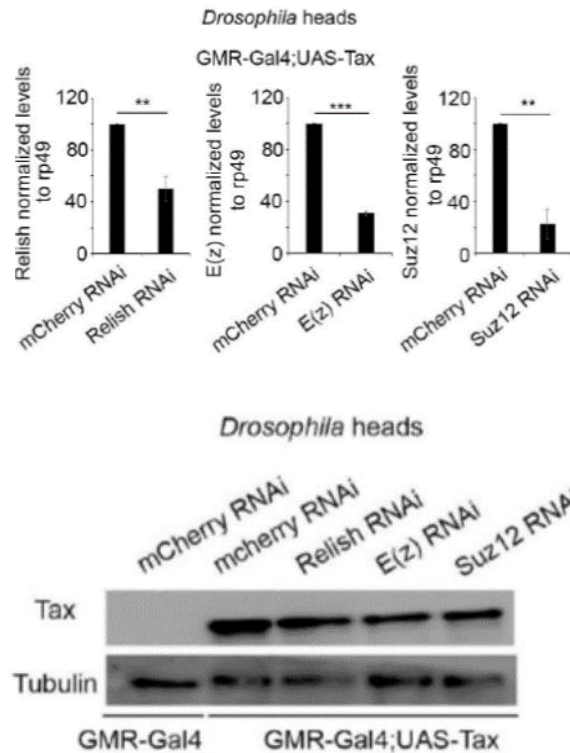


Figure 47. RTq-PCR analysis of the expression of Relish, E(z), and SUZ12 in heads of Tax Tg crossed with Relish-RNAi, E(z) RNAi, and Sua12 RNAi respectively. Gene expression was targeted to the ommatidial via GMR-Gal4. Results are from three independent crosses and expression is reported relative to RP49 *Drosophila* housekeeping gene. $p < 0.05$ (*), $p < 0.01$ (**), and $p < 0.0001$ (****). mCherry RNAi is a scrambled RNAi that targets a non-specific sequence. Immunoblot analysis of the expression of Tax in heads of control (GMR-Gal4) or Tax Tg flies (GMR-Gal4; UAS-Tax) with knocked down expression for E(z), SUZ12, and Relish.

Surprisingly, knocking down E(z) or SUZ12 expression in *tax* flies, partially rescued the rough eye phenotype induced by Tax (Figure 49). We then investigated the effect of silencing PRC2 components on hemocyte count in *tax* flies using the hemolectin driver (HMLΔ-Gal4) which drives Tax and RNAi expression to circulating hemocytes. Interestingly, silencing E(z) and SUZ12 in *tax* flies resulted in a partial, yet significant, decrease in Tax-elevated hemocyte count from 10,000 cells in larvae from mcherry RNAi

tax flies to 6000 cells in larvae from E(z)- RNAi or SUZ12-RNAi *tax* flies (Figure 50). These data strongly suggest that PRC2 components may contribute to Tax-imposed transformation and elevated hemocyte counts but are not the sole players driving Tax's effect *in vivo*.

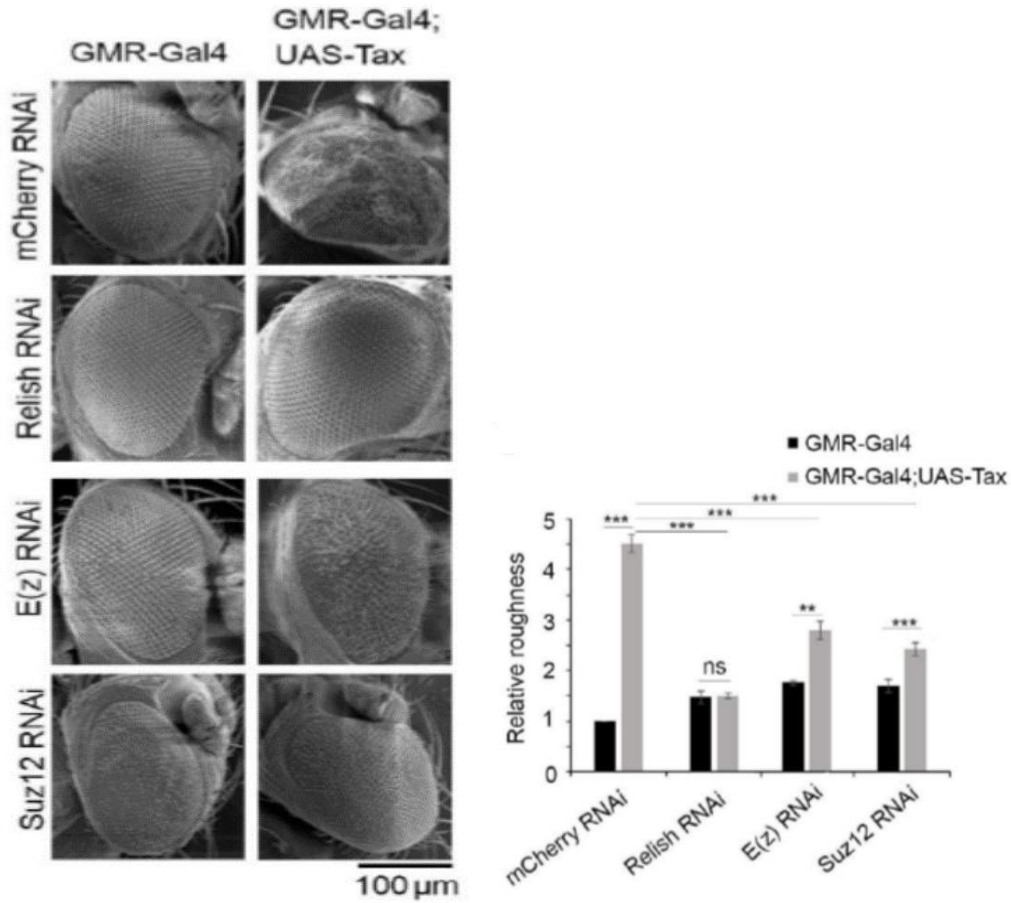


Figure 48. Scanning electron microscopy images of adult fly eyes of control (GMR-Gal4) or *tax* transgenic flies (GMR-Gal4; UAS-Tax) crossed with Relish-RNAi, E(z) RNAi, and Sua12 RNAi respectively. Histogram represents relative roughness using a previously established scoring system. Data reported was generated from three independent crosses. $p < 0.01$ (**) and $p < 0.001$ (***).

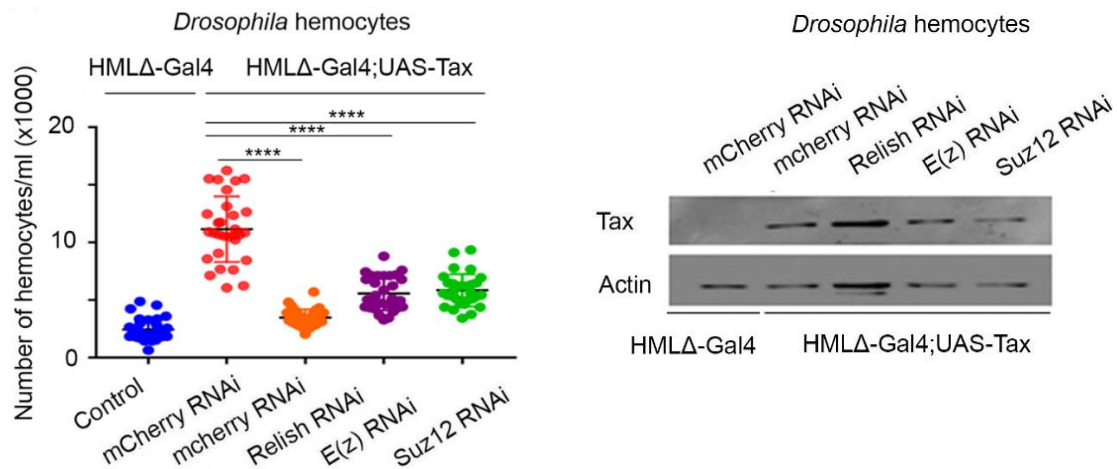


Figure 49. Hemocyte count in *Tax* flies following knockdown of Relish or PRC2 components. Relish, E(z), or SUZ12 subunits were silenced by RNAi in *tax* flies expressing *Tax* in hemocytes. Hemocytes from third instar larvae of control (HMLΔ-Gal4>mCherry RNAi), *Tax* (HMLΔ-Gal4; UAS-*Tax*>mCherry RNAi), (HMLΔ-Gal4;UAS *Tax*>Relish RNAi), (HMLΔ-Gal4;UAS-*Tax*>E(z) RNAi) and (HMLΔ-Gal4;UAS-*Tax*>Suz12 RNAi) were counted and compared. (n=30 Larvae were bled from three independent crosses). Data represented as mean ± standard error of mean. p<0.0001 (****). Representative immunoblot of *Tax* carried to confirm the expression of *Tax* in Larval hemocytes.

NF-κB was previously depicted as the major driver pathway for ATL oncogenesis and was shown to be constitutively activated by *Tax*³⁷⁷. Therefore, we investigated the transcription level of Relish³⁸⁵, the NF-κB transcription factor in *Drosophila*, and Dipterucin, downstream effector transcriptional target of relish in *tax* transgenic flies³⁸⁶. In line with prior findings, *Tax* expression significantly increased the transcription of both relish and Dipterucin in *tax* flies (Figure 51). Moreover, Relish protein levels were also elevated (Figure 51).

To affirm the importance of NF-κB activation in *Tax*-mediated transformation, Relish expression was knocked down in flies expressing *tax* under GMR-GAL4

ommatidial driver. In line with our previously reported data³³⁰, silencing relish completely abrogated and rescued the eye roughness phenotype imposed by Tax strongly suggesting that of NF- κ B activation is critical for the transformative capacity of Tax (Figure 49). Moreover, knocking down Relish in *tax* flies completely reversed the increased hemocyte count back to normal levels (Figure 50) implying that constitutive activation of NF- κ B is indispensable for Tax-mediated transformation and increased blood count *in vivo*.

In contrary, the lack of transformation phenotype in *hbz* flies was accompanied by unchanged levels of Relish and Diptericin compared to control flies (Figure 51) implicating that HBZ failed to activate NF- κ B and induce transformation *in vivo*.

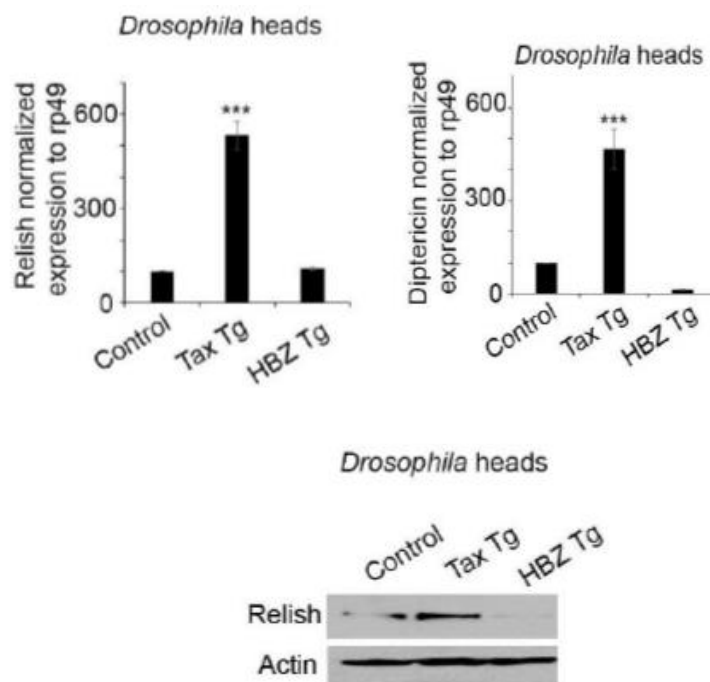


Figure 50. RTq-PCR expression of Relish and Diptericin in fly heads from control, Tax Tg, or HBZ Tg flies. Expression is reported relative to RP49 *Drosophila* housekeeping gene. Immunoblot analysis of Relish expression in fly heads from control, Tax Tg, or HBZ Tg flies. Expression of Tax and HBZ is induced under GMR-GAL4 promoter. Data is

represented as average of three independent crosses. $p < 0.05$ (*), $p < 0.01$ (**) and $p < 0.0001$ (****).

PRC2 complex activity has been previously reported to modulate the expression and activity of NF- κ B pathway^{289, 290}. Indeed, EZH2 contributed to NF- κ B activation where pharmacological inhibition of EZH2 previously inhibited NF- κ B activity in ATL cells²⁹⁰. Conversely, inhibition of IKK- β in ATL cell lines also decreased transcription of EZH2 suggesting a putative link between PRC2 complex and NF- κ B in ATL²⁹⁰. We hypothesized that this plausible crosstalk between the two complexes PRC2 and NF- κ B may explain the partial or complete rescue observed upon PRC2 or NF- κ B knock down in *tax* flies. To this end, Relish RNAi, E(z) RNAi, or Suz12 RNAi were crossed with *tax* transgenics expressing Tax under the GMR-Gal4 promoter. We assessed the transcription levels of NF- κ B components (Relish and Diptericin) or PRC2 components (E(z) and Suz12) in the resultant fly lines with mCherry RNAi used as scrambled control (Figure 52).

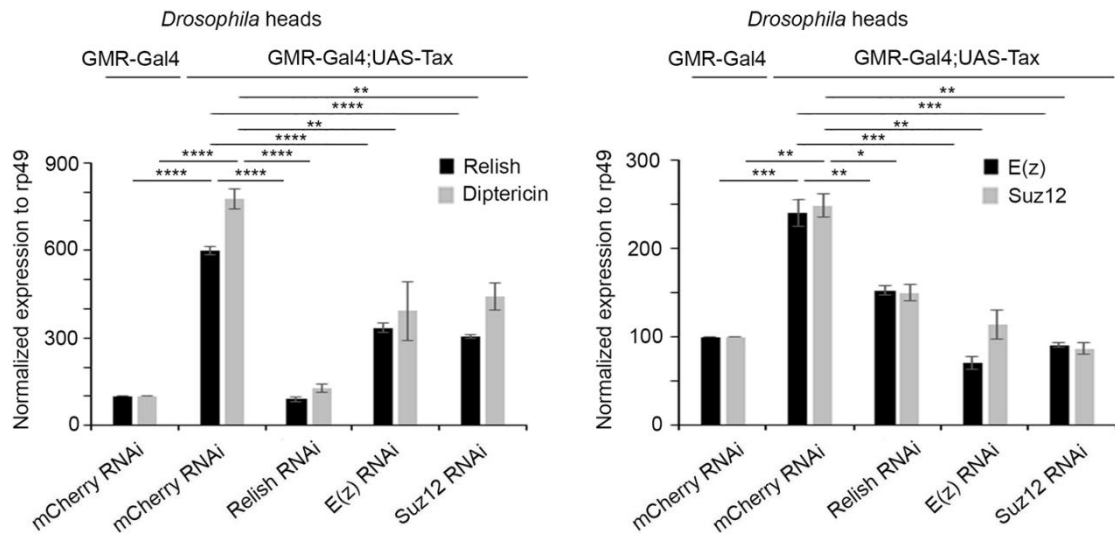


Figure 51. RTq-PCR analysis of the expression of NF- κ B or PRC2 components in fly heads from control or Tax Tg flies with knocked down Relish, E(z), or SUZ12. Control (GMR-Gal4> mCherry RNAi), Tax control RNAi (GMR-Gal4;UAS-Tax>mCherry RNAi), Tax/Relish RNAi (GMR-Gal4;UAS-Tax>Relish RNAi), Tax/E(z) RNAi (GMR-Gal4;UAS-Tax>E(z) RNAi) and Tax/Suz12 RNAi (GMR-Gal4;UAS-Tax>Suz12 RNAi) adult fly heads were used. Data reported are from three independent crosses and expression is reported relative to RP49 *Drosophila* housekeeping gene. $p < 0.01$ (**), $p < 0.001$ (***), and $p < 0.0001$ (****).

Consistent with our previous data, Tax/mCherry RNAi flies exhibited significantly increased transcript levels of relish, Dipteracin as well as E(z) and Suz12 compared to control mCherry RNAi lines (Figure 52). Interestingly, silencing Relish in Tax/Relish RNAi flies completely abrogated NF- κ B activation. Indeed, Relish RNAi reversed the increased transcription of Relish and Dipteracin to levels similar to control flies (Figure 52). More importantly, Relish RNAi significantly downregulated transcript levels of E(z) and Suz12 in Tax flies. This decrease in PRC2 components transcription was accompanied by decreased expression of H3k27me3 in Tax/Relish RNAi flies (Figure 53). In contrast, Tax/ E(z) RNAi and Tax/ Suz12 RNAi flies, with knocked-down expression of E(z) or

Suz12 respectively, only exhibited a partial reversal in Tax-induced NF- κ B activation (Figure 52).

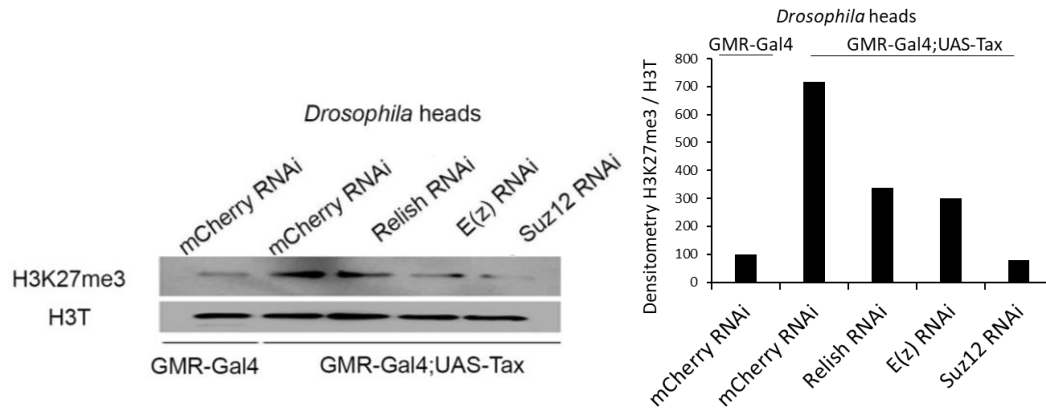


Figure 52. Representative immunoblot of the expression of H3k27me3. H3k27me3 expression was assessed in control (GMR-Gal4> mCherry RNAi), Tax control RNAi (GMR-Gal4;UAS-Tax>mCherry RNAi), Tax/Relish RNAi (GMR-Gal4;UAS-Tax>Relish RNAi), Tax/E(z) RNAi (GMR-Gal4;UAS-Tax>E(z) RNAi) and Tax/Suz12 RNAi (GMR-Gal4;UAS-Tax>Suz12 RNAi) transgenic adult flies heads using western blot and probing against H3K27me3 antibody.

Collectively, these data strongly correlate the transformative potential of Tax with both NF- κ B and PRC2 activation and suggests that PRC2 activation is implicated in both Tax-mediated proliferation and NF- κ B activation. Additionally, Tax-induced constitutive activation of NF- κ B also increased PRC2 activity, thereby we report a potential activation loop between both pathways that drives Tax- induced transformation *in vivo*.

4. *HBZ expression in tax transgenic flies attenuates PRC2 and NF- κ B activation and rescues Tax-mediated transformation*

HBZ has been previously reported to counteract Tax-mediated transactivation and multiple Tax functions³⁵². To investigate the interplay between Tax and HBZ *in vivo* and

the effect of HBZ on Tax-mediated transformation, we generated double transgenic flies co-expressing both HBZ and Tax (referred to as Tax/HBZ Tg flies). We first confirmed the expression of both Tax and HBZ in generated flies by western blot (Figure 54).

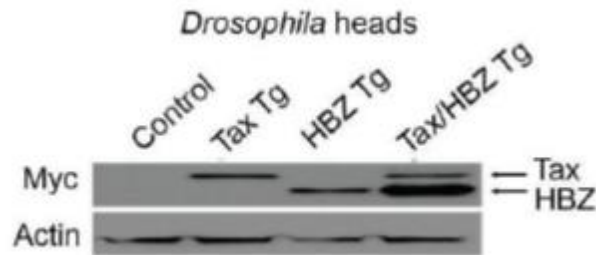


Figure 53. Immunoblot analysis of the expression of Tax and HBZ in fly heads of control, Tax Tg, HBZ Tg, or Tax/HBZ Tg fly heads. Expression of myc tag (the tag for Tax and/or HBZ was assessed). Expression of target genes was under control of GMR-Gal4 promoter.

We then investigated the effect of Tax and HBZ co-expression on Tax-mediated transformation. Surprisingly, co-expression of both proteins resulted in absence of eye roughness phenotype, similar to control flies. This suggests that co-expressing HBZ totally abrogated or reversed Tax-induced roughness phenotype (Figure 55).

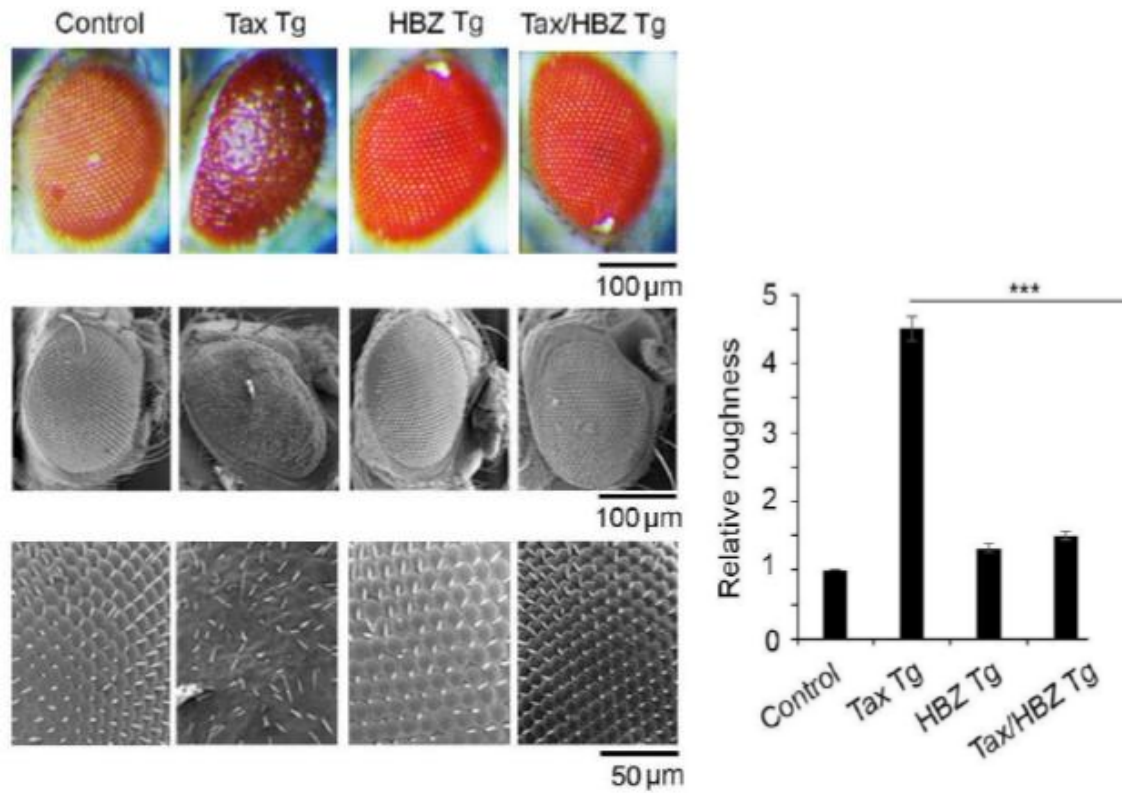


Figure 54. HBZ co-expression in Tax Tg flies rescues Tax-mediated eye roughness. Representative images from light microscope (100µm scale bar) and scanning electron microscope (50µm and 100µm scale bar) of adult fly eyes pertaining to control (GMR-GAL4>*w1118*), Tax transgenic (Tax tg: GMR-Gal4>UAS-Tax), HBZ transgenic (HBZ Tg: GMR-Gal4>UAS-HBZ), or Tax/HBZ transgenic flies (GMR-GAL4>UAS-Tax-HBZ). Histograms represent relative roughness, calculated according to a previously established scoring system. Results are reported as average of n=37 fly eye from three independent crosses. p<0.05 (*), p<0.001 (***)

To confirm this result, the effect of HBZ expression on circulating hemocyte count from double *tax/hbz* transgenic mice was evaluated. Indeed, while tax results in increased numbers of circulating hemocytes, the co-expression of Tax and HBZ resulted in hemocyte counts similar those of control or *hbz* transgenic flies (Figure 56). These results were in line with the lack of transformation observed in *tax/hbz* double transgenic flies.

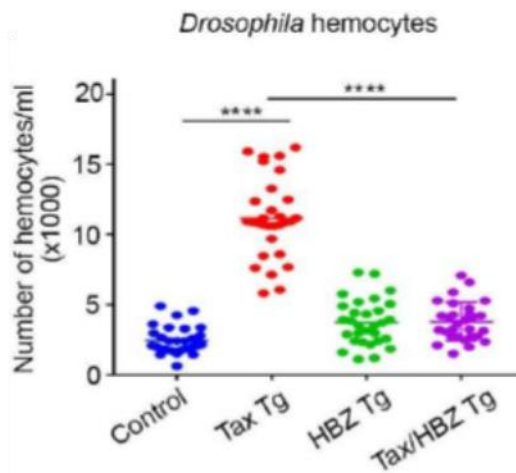


Figure 55. HBZ prevent Tax-mediated increase in hemocyte count in Tax Tg flies. Circulating hemocyte count in control (HML Δ -Gal4>*w1118*), Tax Tg (HML Δ -Gal4>UAS-Tax), HBZ Tg (HML Δ -Gal4>UAS-HBZ), or Tax/HBZ transgenic (HML Δ -Gal4>UAS-Tax:HBZ) third instar larvae. N=30 larvae were bled and counted, from three independent crosses. Data represent mean \pm standard error of the mean. P<0.01 (**) and p< 0.0001 (****).

To dissect the mechanism pertaining to the loss of ommatidial phenotype in Tax/HBZ flies, we assessed the functional activity of NF- κ B, major driver of Tax-mediate transformation³³² in these flies. Interestingly, Relish and Diptericin transcripts were significantly decreased in *tax/hbz* flies as compared to *tax* transgenics (Figure 57).

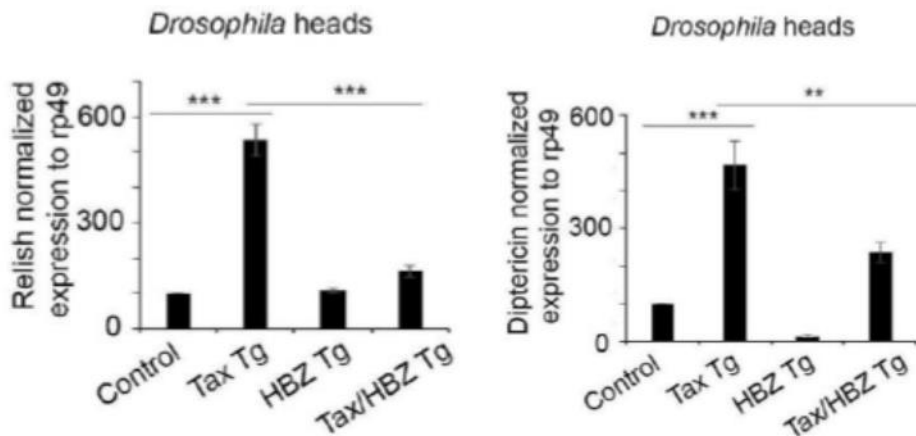


Figure 56. Real time quantitative PCR analysis of the expression of Relish and Diptericin in control, Tax Tg, HBZ Tg, and Tax/HBZ Tg fly heads. Expression of Tax and HBZ was induced under GMR/Gal4 promoter. Expression was normalized over rp-49. Data presented is average of 3 independent experiments. Data represent mean \pm standard error of the mean, $P < 0.01$ (**) and $p < 0.0001$ (****).

The activity of PRC2 complex subunits was then investigated in the Tax/HBZ transgenic model. Compared to Tax Tg flies, Tax/HBZ transgenic flies exhibited decreased levels of E(z), SUZ12, and H3K27me3 proteins (Figure 58). Altogether, these data revealed that HBZ expression significantly abrogates Tax-induced NF- κ B activation, PRC2 activation, as well as *in vivo* transformation seen in Tax Tg flies.

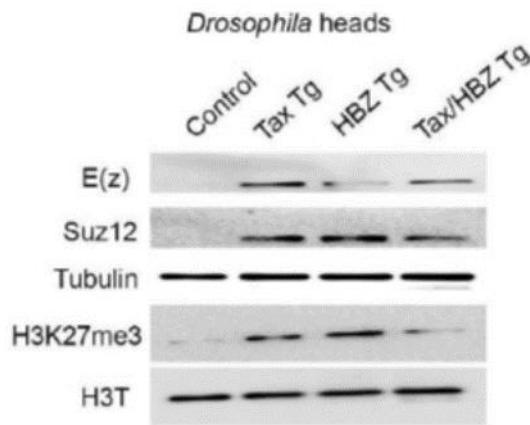


Figure 57. Expression of PRC2 components in control, Tax Tg, HBZ Tg, and Tax/HBZ Tg flies. Representative western blot analysis of the expression of E(z), Suz12, and H3k27me3 in fly heads of control, Tax Tg, HBX Tg, and Tax/HBZ Tg transgenic flies. Gene expression was induced under the GMR-GAL4 promoter.

5. *HBZ overexpression attenuates Tax-mediated senescence in double transgenic flies in vivo*

Zhi et al. previously demonstrated that HBZ may alleviate Tax-mediated senescence secondary to constitutive activation of NF- κ B in Hela cells *in vitro*³⁸⁷. In line with these data, Tax expression in larvae of *tax* transgenic flies resulted in induction of senescence observed as increased SA- β -gal activity in larval eye disks (Figure 59). Interestingly, senescence was completely abolished by the co-expression of HBZ in larvae from *tax/hbz* double transgenic flies (Figure 59).

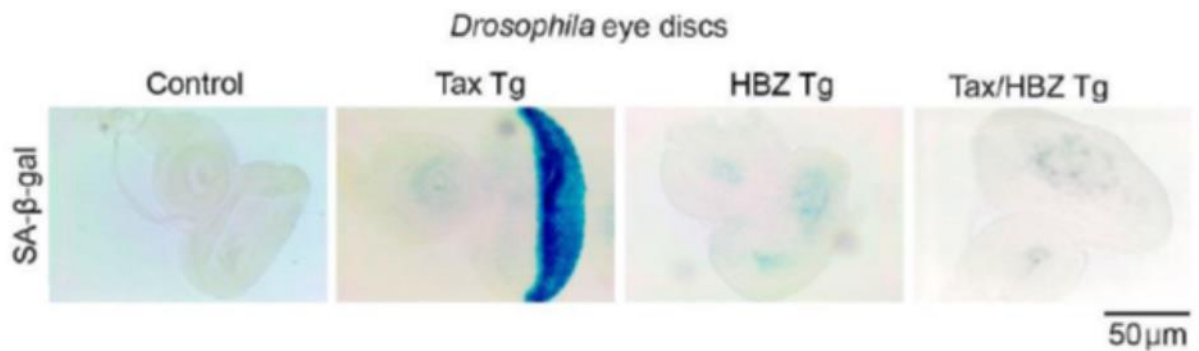


Figure 58. SA-β-gal expression eye imaginal discs of third instar larvae of control (GMR-GAL4>*w¹¹¹⁸*), Tax Tg (GMR-Gal4>UAS-Tax), HBZ Tg (GMR-Gal4>UAS-HBZ) or Tax/HBZ Tg (GMR-Gal4;UAS-Tax>UAS-HBZ).

To further validate this finding, the transcript levels of Dacapo, a *Drosophila* p21/p27 homologue and a cyclin dependent kinase inhibitor used as marker of cell cycle arrest³⁸⁸, were assessed. Indeed, Tax expression in *tax* flies resulted in a strikingly significant induction of Dacapo transcription where Dacapo transcript levels increased to 1200% compared to control flies (Figure 60). Importantly, concurrent expression of HBZ and Tax in double transgenic flies resulted in reversal of Dacapo transcription where Tax/HBZ Tg exhibited levels of Dacapo slightly different that the control (Figure 60). These data suggest that HBZ impedes Tax-induced senescence caused by excessive activation of NF-κB by Tax.

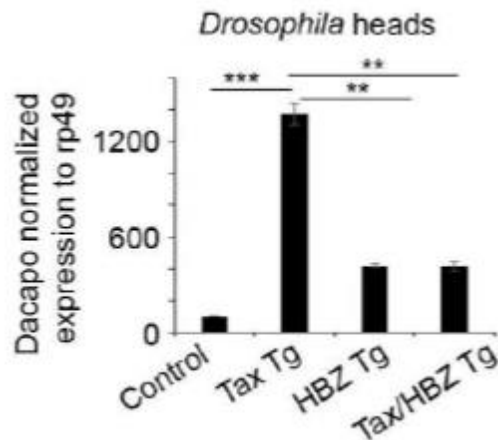


Figure 59. Real time quantitative PCR analysis of the expression of Dacapo in fly heads from control, Tax Tg, HBZ Tg, or Tax/HBZ Tg flies. Expression was induced under the GMR-GAL4 promoter. Results are from three independent crosses and expression is reported relative to RP49 *Drosophila* housekeeping gene. Data represent mean \pm standard error of the mean, $p < 0.01$ (**) and $p < 0.0001$ (****).

The opposing roles of HBZ and Tax on senescence were confirmed in *Drosophila* hematopoietic system. The expression of Tax and HBZ was first confirmed in hemocytes using RTq-PCR (Figure 61).

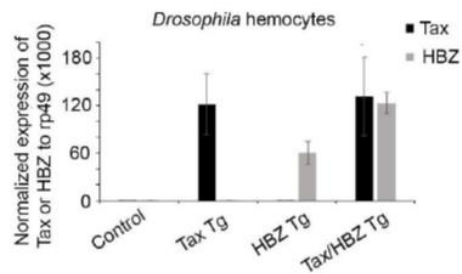


Figure 60. Real time quantitative PCR analysis of the expression of Tax and HBZ in circulating hemocytes. Control (HMLΔ-Gal4>*w1118*), Tax Tg (HMLΔ-Gal4>UAS-Tax), HBZ Tg (HMLΔ-Gal4>UAS-HBZ), or Tax/HBZ transgenic (HMLΔ-Gal4>UAS-Tax:HBZ) third instar larvae were used. Expression of Tax and HBZ was induced under the control of HMLΔ-Gal4, a hemocyte-specific promoter. N=30 larvae were used.

Hemocytes from Tax Tg flies exhibited a markedly increased SA- β -gal activity when compared to hemocytes from control flies (Figure 62). HBZ alone resulted in insignificant SA- β -gal activity. Interestingly, concurrent expression of Tax and HBZ in double transgenic flies totally abrogated the increased SA- β -gal activity seen in Tax Tg flies (Figure 62). Altogether, these results strongly suggest that HBZ counteracts Tax-induced senescence both *in vitro* and *in vivo*.

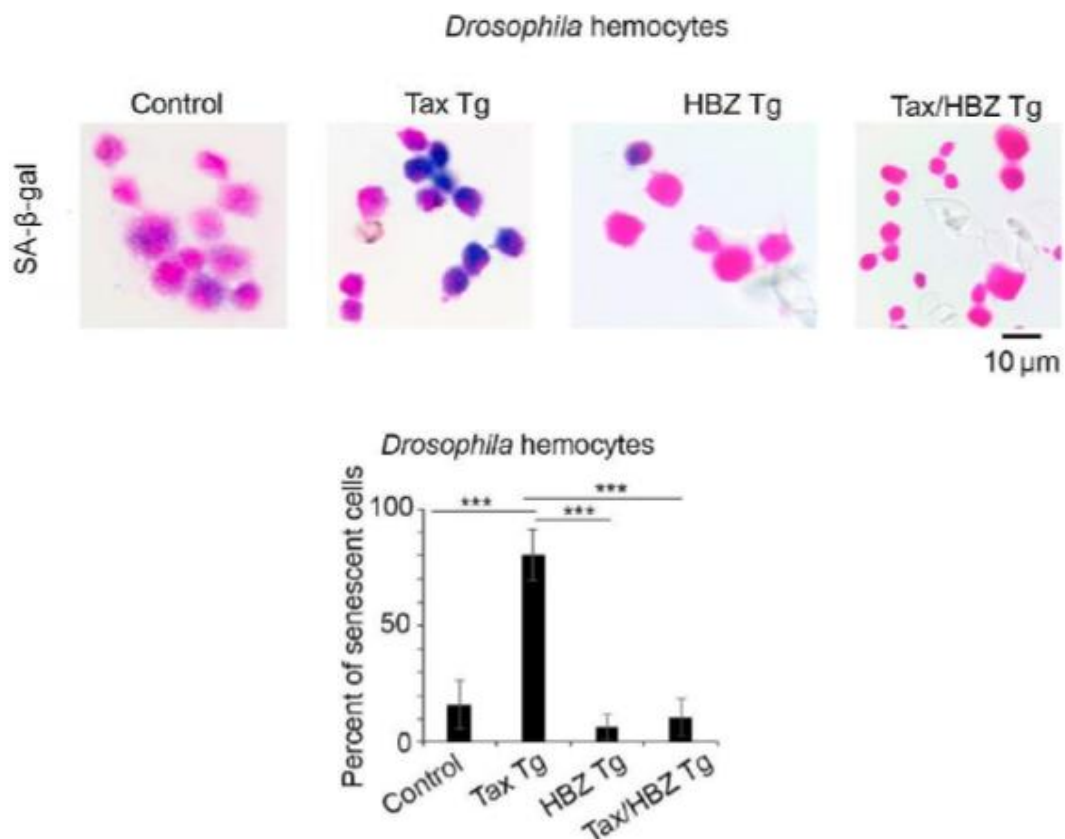


Figure 61. SA- β -gal activity in circulating hemocytes derived from control (HML Δ -Gal4>*w1118*), Tax Tg (HML Δ -Gal4>UAS-Tax), HBZ Tg (HML Δ -Gal4>UAS-HBZ), or Tax/HBZ transgenic (HML Δ -Gal4>UAS-Tax:HBZ) third instar larvae. A total of 100 cells were counted and results are reported from three independent crosses. Histogram represents the percentage of senescent cells compared to control. Data represent mean \pm standard error of the mean. $p > 0.001$ (***)

We then investigated the potential role of PRC2 complex in HBZ-mediated suppression of Tax-induced NF- κ B activation and senescence. Briefly, Tax-mediated senescence was assessed in Tax Tg flies with knocked down expression of Relish, E(z), or Suz12 (defective for NF- κ B or PRC2 complex respectively) with Tax/mCherry RNAi serving as control. Interestingly, inhibition of Relish expression in Tax/Relish RNAi flies resulted in total abrogation of SA- β -gal activity in circulating hemocytes from third instar larvae when compared to Tax/mCherry RNAi (Figure 63) suggesting that inhibition of Tax-mediated activation of NF- κ B result in disappearance of Tax-mediated senescence phenotype. More importantly, silencing PRC2 subunits E(z) or Suz12 resulted in a significant, yet partial, rescue of Tax mediated senescence compared to Tax/mCherry flies (Figure 63). Collectively, these results elucidate that PRC2 subunits, E(z) and Suz12, are involved, at least partially, in Tax-induced NF- κ B activation and subsequent senescence, and further suggest a link between NF- κ B and PRC2 pathways in modulating Tax-mediated transformation.

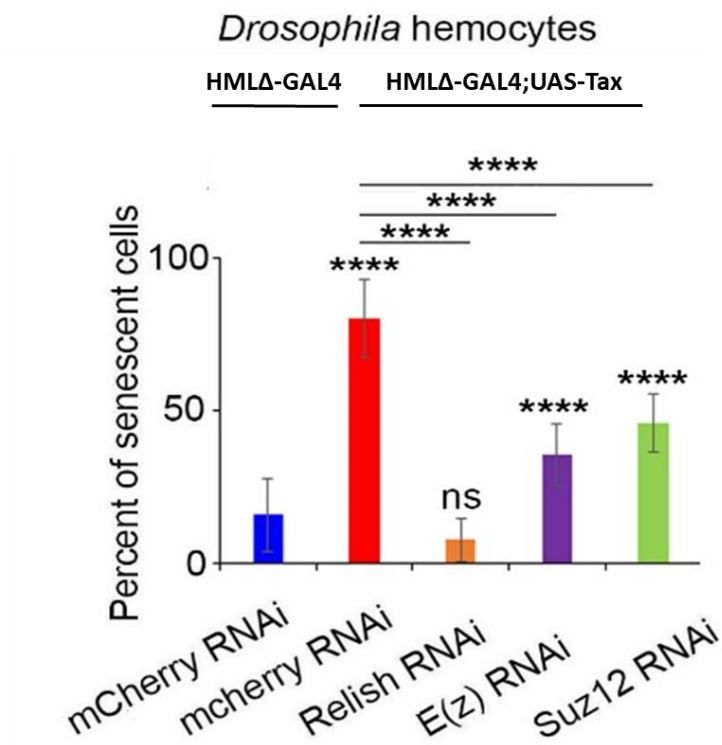


Figure 62. SA- β -gal expression in circulating hemocytes from flies with silenced Relish, E(z), and Suz12 expression. Histogram representing SA- β -gal expression in circulating hemocytes from larvae of control mCherry RNAi (HML Δ -Gal4> mCherry RNAi), control Tax/mCherry RNAi (HML Δ -Gal4;UAS-Tax>mCherry RNAi), Tax/Relish RNAi (HML Δ -Gal4;UAS Tax>Relish RNAi), Tax/E(z) RNAi (HML Δ -Gal4;UAS-Tax>E(z) RNAi) and Tax/Suz12 RNAi (HML Δ -Gal4;UAS-Tax>Suz12 RNAi) as indicated. Results are derived from three independent crosses as percentage of control. (ns= not significant), $p < 0.0001$ (****).

6. *HBZ inhibits Tax-induced PRC2 complex activation in mammalian cells*

To confirm results generated in *Drosophila* models, HBZ, as HBZ-myc tagged plasmid, was overexpressed in HEK293T mammalian cells at increasing concentration in presence of Tax. In accordance with previous findings²⁹⁰, Tax overexpression resulted in increased levels of EZH2 and SUZ12 and subsequent increase in global H3K27me3 levels (Figure 64).

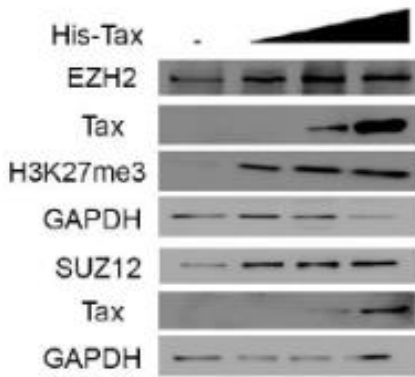


Figure 63. representative immunoblot analysis of the expression of EZH2, SUZ12, H3K27me3, Tax, and HBZ in HEK293T cells transfected for 48 h with increasing concentrations of His-Tax plasmid.

The gradual increase in HBZ expression was first validated by immunoblotting using myc tag (Figure 65). Nevertheless, Co-expression of Tax and HBZ in HEK293T dramatically decreased global H3K27me3 levels compared to cells expressing Tax alone (Figure 66). Decreased global H3k27me3 levels, upon co-expression of Tax and HBZ, coincided with significant decrease in EZH2 and SUZ12 expression levels compared to levels observed upon expression of Tax alone (Figure 65). These data are consistent with findings from Tax/HBZ Tg transgenic flies and strongly suggest that HBZ may inhibit Tax-mediated PRC2 activation.

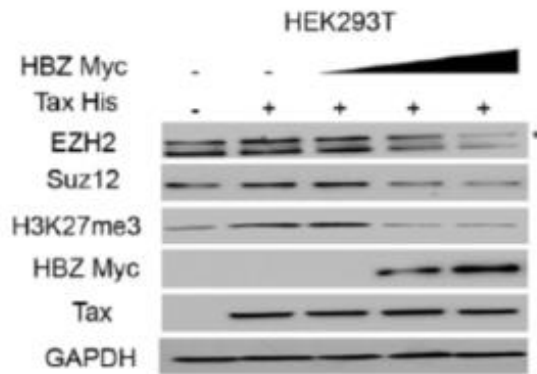


Figure 64. Immunoblot analysis of the expression of EZH2, Suz12, H3K27me3, Tax, and HBZ in HEK293T cells transfected for 48 h with increasing concentrations of HBZ in presence of exogenous Tax.

Since ATL is a CD4⁺ malignancy, we validated the above results in human CD4⁺ T cells, Jurkat cells. In brief, Jurkat cells were transfected with an empty vector, His-Tax, Myc-HBZ, or His-Tax/Myc-HBZ vectors together. The effect of Tax or HBZ on the expression of PRC2 core components, EZH2 and SUZ12, and their downstream H3K27me3 was then assessed. In line with our data in *Drosophila* and HEK293T-transfected cells, Tax expression alone upregulated both EZH2 and SUZ12 protein levels as well as the level of downstream H3K27me3 (Figure. 66). HBZ expression alone increased SUZ12 and H3K27me3 protein levels but failed to upregulate EZH2 protein levels (Figure. 66). In contrast, the co-expression of Tax and HBZ downregulated the protein levels of both PRC2 components EZH2 and SUZ12. Importantly, global protein levels of H3K27me3 were decreased in cells co-expressing Tax and HBZ compared to cells expressing either viral proteins alone (Figure 66) thereby confirming our previous *in vivo Drosophila* data in a more relevant system, CD4⁺ T cell system.

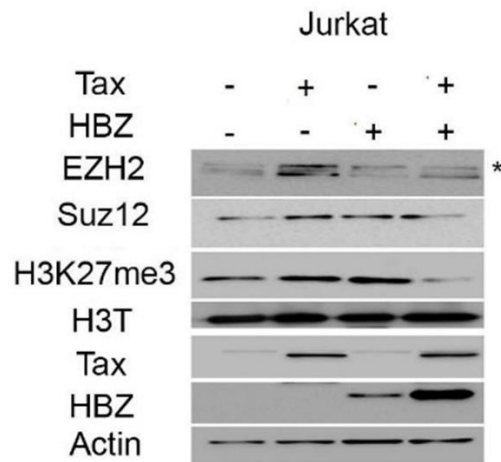


Figure 65. Immunoblot analysis of the expression of EZH2, Suz12, H3K27me3, Tax, and HBZ in Jurkat cells transfected with empty vector, His-Tax, Myc-HBZ, or His-Tax/Myc-HBZ vectors together.

Given these results, we hypothesized that HBZ may potentially affect the enrichment levels of H3K27me3 at promoters of genes dependent on Tax. To test this hypothesis, a chip-qPCR assay was conducted to compare the enrichment levels of H3k27me3 in HEK293T cells expressing empty vector, His-Tax, myc-HBZ, or His-Tax plus myc-HBZ (Figure 67). As reported above, Transfection with Tax resulted in a significant increase in H3K27me3 accumulation specifically at the promoter of target genes such as HEG1, CDKN1a, and NDRG2 as compared to empty-vector transfected cells (Figure 67). Thus, these were considered as Tax-dependent genes. As predicted, transfection with HBZ alone resulted in no significant accumulation of H3K27me3 on the promoter of Tax-dependent genes (Figure 67). Interestingly, in cells co-transfected with

Tax and HBZ, HBZ decreased H3K27me3 accumulation at the promoter Tax-dependent genes compared to cells transfected solely with Tax. In accordance with the Chip RT-qPCR data of H3K27me3 enrichment, transcript levels of Tax-dependent CDKN1A and NDRG2 genes were significantly lower in Tax- transfected cells compared to control (empty vector) transfected cells (Figure 68). Importantly, transcript levels were restored to normal values upon co-expression of both Tax and HBZ (Figure 68). To address the specificity of our results, the enrichment of H3K27me3 was assessed at the promoter region of BIM gene, an HBZ controlled gene. Interestingly, a selective and specific enrichment of H3K27me3 was observed at the promoter of BIM in HBZ-transfected cells (Figure 67). Surprisingly, increased enrichment at BIM promoter was not affected upon co-expression of Tax and HBZ. In line with these results, transcript levels of BIM were significantly lower in HBZ and Tax/HBZ transfected cells compared to control (empty vector) transfected cells (figure 68). Collectively, these data elucidate the specificity of our results in terms of Tax-dependent and HBZ-dependent genes and strongly suggest that HBZ may affect the recruitment of PRC2 complex to the promoter regions of Tax-dependent genes to affect gene expression.

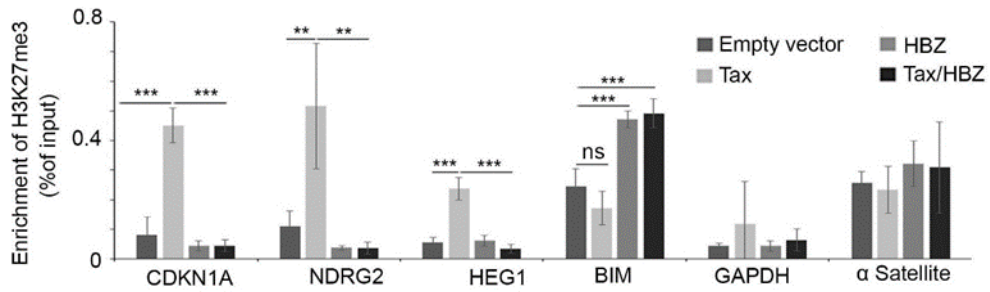


Figure 66. ChIP- qPCR analysis of H3K27me3 enrichment at target genes in empty vector, His-Tax, Myc-HBZ, or Tax/HBZ transfected HEK293T cells for 48 h. GAPDH and α Satellite were used as negative and positive controls respectively. Following chromatin immunoprecipitation of fixed and sheared DNA with H3K27me3 antibody, immunoprecipitated complexes were quantified using real time quantitative PCR. Results of each condition were normalized to its own input and expressed as %DNA input. Data represent average of three experiments. $p < 0.01$ (**), and $p < 0.001$ (***).

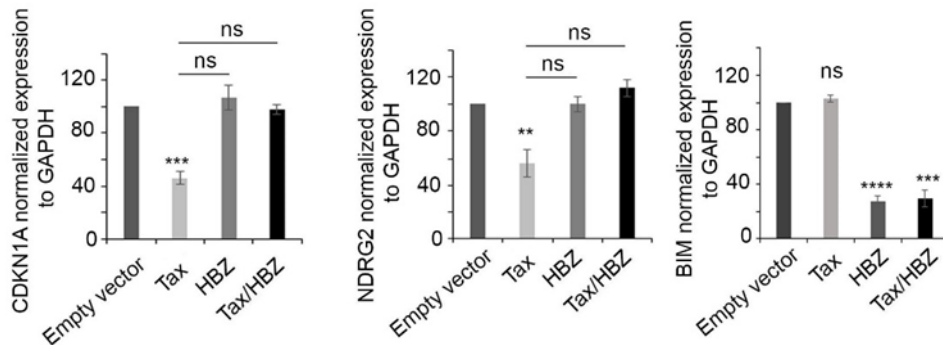


Figure 67. Real time quantitative PCR analysis of CDKN1A, NDRG2, and BIM expression in cells transfected with Tax and/or HBZ. HEK293T cells were transfected with empty, His-Tax, Myc-HBZ, or His Tax/Myc-HBZ for 48 hours. Results reported are average of three independent experiments. Data represent mean \pm standard error of the mean. $p < 0.01$ (**), $p < 0.001$ (***), and $p < 0.0001$ (****).

To dissect the mechanism by which HBZ affects the PRC2 activity, we made use of ATL-derived MT1 cells, known to express HBZ with undetectable Tax expression. knocking down HBZ in MT-1 cells resulted in a significant increase in EZH2 and

H3K27me3 levels (Figure 69). Surprisingly, Suz12 levels remained unchanged (Figure 69). Successful silencing of HBZ was confirmed by RT-PCR (Figure 69).

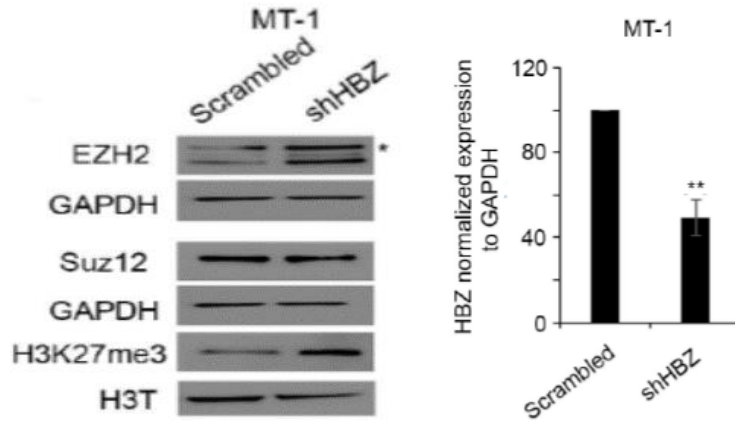


Figure 68. Representative immunoblot of the expression of EZH2, SUZ12, and H3K27me3 in ATL-derived MT-1 cells transduced with scrambled or shHBZ vector. Real time q-PCR analysis of the silenced expression of HBZ in MT-1 cells following transduction with shHBZ. Experiments were conducted for three times. Data represent mean \pm standard error of the mean. $p < 0.01$ (**).

Tax was previously reported to bind both PRC2 core components, EZH2 and SUZ-12 in ATL derived cells²⁹⁰. Conversely, whether HBZ binds PRC2 subunits is still unknown. Both Tax and HBZ, when expressed alone, resulted in increased H3K27me3 while their concomitant expression unexpectedly abolished the increased H3k27me3 levels. Thus, we postulated that HBZ might compete with Tax for bidding EZH2 and activating repressive marks. Consistent with previous data by Fujikawa et al.,²⁹⁰ immunoprecipitation assay confirmed the interaction between Tax with EZH2 (Figure 70). More importantly, co-transfection with Tax and HBZ abrogated this interaction (Figure

70), strongly suggesting a potential competition between Tax and HBZ for binding EZH2 protein.

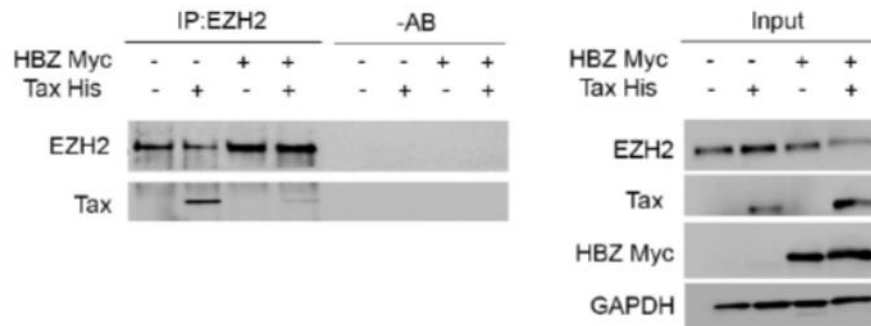


Figure 69. Representative Immunoprecipitation blot revealing the interaction between Tax and EZH2 in Tax and/or HBZ transfected HEK293T cells.

7. *HBZ protein interacts with PRC2 core components*

To validate whether HBZ competes with Tax for binding EZH2 and increasing H3K27me3 accumulation, we assessed the relationship between HBZ and PRC2 core subunits as well as the effect of HBZ on PRC2 expression in human cells. Consistent with data obtained in HBZ Tg flies, HBZ-transfected 293T cells exhibited increased levels of SUZ12 and H3K27me3 when compared to control cells (Empty vector transfected-cells) (Figure 71). In contrast, EZH2 levels were not affected by HBZ expression.



Figure 70. Representative immunoblots of the expression of EZH2, SUZ12, H3K27me3, and HBZ in HEK293T cells transfected for 48 h with increasing concentrations of HBZ. Experiments were conducted for minimum of three times.

Using immunoprecipitation assay, we demonstrated a novel interaction between viral protein HBZ and endogenous SUZ12 and EZH2 in HBZ-transfected cells (Figure 72). To our knowledge, this finding has not been reported before.

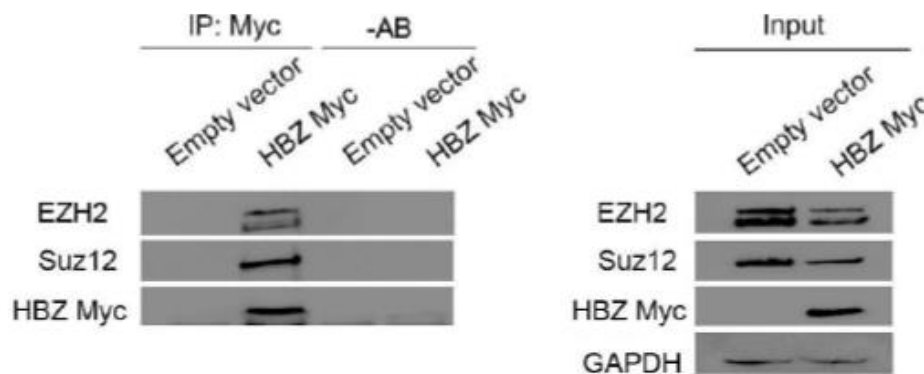


Figure 71. Representative immunoblot of the immunoprecipitation assay for the interaction between EZH2 AND SUZ12 with HBZ in Myc-HBZ-transfected 293T following 48 h of transfection. Immunoprecipitation was repeated for three independent experiments.

These data were also verified using proximity ligation assay, Duolink®. Indeed, endogenous EZH2 and SUZ12 interacted with endogenous HBZ in MT-1 cells as well as with exogenous HBZ in Hela transfected with HBZ (Figure 73).

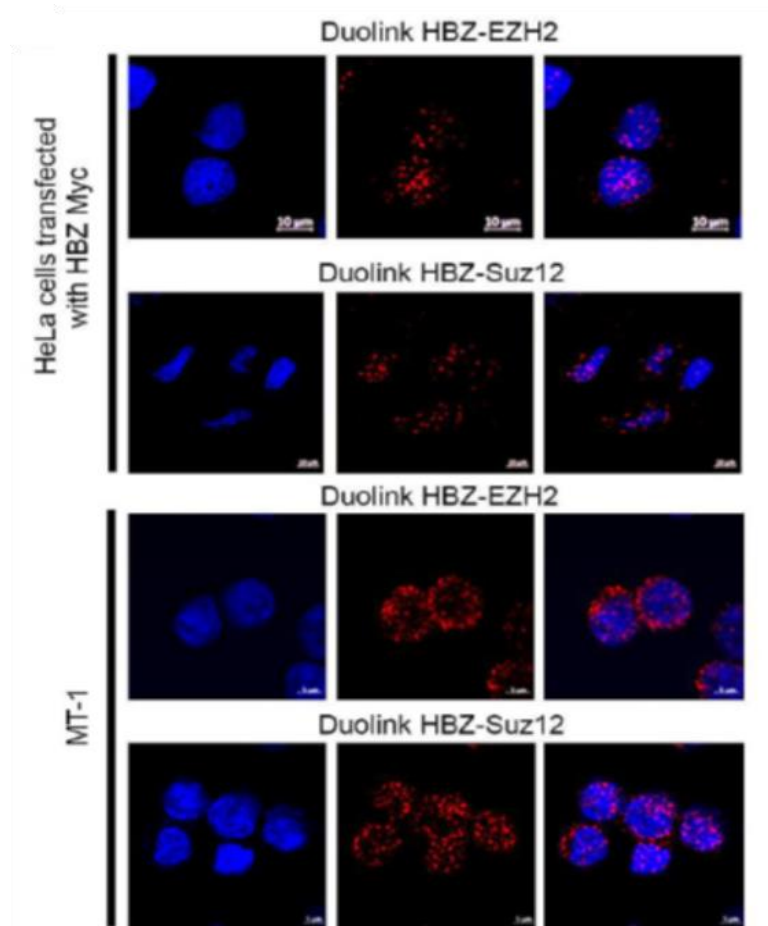


Figure 72. Representative confocal microscopy images of interactions between endogenous EZH2 or SUZ12 with HBZ using Duolink® proximity ligation assay in HBZ-transfected HeLa cells or ATL-derived MT-1 cells with endogenous HBZ. Nuclei were stained with Hoechst (blue). Scale bar :5µm

However, we observed that the pattern of co-localization or binding of HBZ was different for EZH2 and SUZ12. Indeed, we reported that HBZ partially co-localized with endogenous EZH2 in discrete nuclear foci (Figure 74). On the other hand, HBZ and SUZ12 col-localized all over the nucleus in small speckle-like structures (Figure 74). Collectively, these results not only validate our findings in HBZ Tg flies, but also reveal an unreported interaction between HBZ and key PRC2 subunits, EZH2 and SUZ12, in both

ATL cells and human cell systems. Binding of HBZ to PRC2 core subunits may help explain how HBZ increases H3K27me3 levels and how it modulates H3K27me3 recruitment at the promoter of Tax-mediated genes.

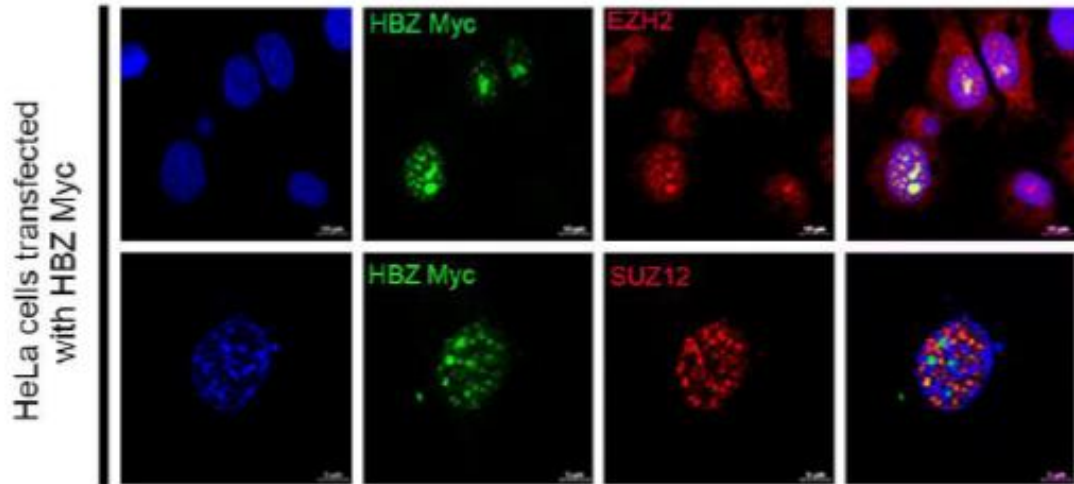


Figure 73. Representative confocal microscopy images of the co-localization of HBZ and EZH2 or SUZ12 in Hela cells transfected with Myc-HBZ vector. Cells were stained with anti-Myc-tag antibody for HBZ expression (green color), anti-EZH2 (red color), and anti-Suz12 (red color). Nuclei were stained with Hoescht die (blue). Images were taken as Z-Stacks with 10µm scale bar.

CHAPTER V

DISCUSSION

PEL remains a challenging lymphoma with an extremely dismal prognosis^{3, 20, 35}. Significance barriers including lack of large-scale longitudinal clinical trials, high rate of relapse, and rapid emergence of chemoresistance have contributed towards poor clinical outcomes associated with current PEL therapy^{2, 18, 20}. Chemotherapy has long been the mainstay regimen for treating PEL¹⁸. Yet, an optimal regimen is still lacking and current chemotherapies such as CHOP presented an unsatisfactorily short overall survival rate of one year in 40% of treated patients^{3, 18}. Preclinical studies provide insights of potential targeted option for PEL. Among these, the combination of ATO and IFN exhibited promising *in vivo* results by decreasing lymphoma progression and enhancing survival of PEL mice²¹⁷. Yet, the combination failed to exhibit a curative potential *in vivo*²¹⁷. Additionally, the anti-proliferative effects of Lena on PEL cells *in vitro* have been recently reported^{225, 226}. In clinical settings, Lena as a single therapy have resulted in complete long lasting remission in an elderly PEL patient²²⁸. Currently, a combination of Lena and chemotherapy with rituximab is in clinical trials (NCT02911142). Altogether, these factors directed our investigation towards a potential combination therapy with two agents that hold individual clinical promise.

ATO have been extensively studied in various hematological neoplasia^{201, 244}. Combined with other agents, ATO exhibits a promising cytotoxic effect. For instance, ATO, combined with retinoic acid, is approved as an upfront regimen for treatment of acute promyelocytic leukemia^{200, 208, 209}. In acute myeloid leukemia, ATO/retinoic acid combination reduced leukemic blasts in patients and resulted in selective apoptosis of acute myeloid leukemia cells harboring nucleophomin-1 mutation^{203, 213}. In addition, ATO synergized with IFN α to induce apoptosis of ATL cells, eliminated leukemia initiating cells leading to cure in murine ATL model, and resulted in high remission rate in chronic ATL patients^{202, 210-212}. ATO/IFN α also inhibited cell proliferation, inflicted apoptosis, and decreased KSHV latent transcripts in ascites-derived PEL cells and PEL cell lines^{216, 217}. More importantly, in a murine PEL model, ATO/ IFN α decreased peritoneal ascites, a pathological feature that complicates the treatment of PEL, and enhanced the survival of mice²¹⁷. Studies on multiple myeloma have previously investigated ATO in combination with Lena^{214, 215}. ATO and Lena were shown to have independent anti-myeloma effects²¹⁴. Nevertheless, ATO rendered the myeloma cells sensitive to Lena therapy via induction of cereblon expression, target for Lena, or downregulation of cdc25c resulting in cell death²¹⁵. In a recent study, supra-pharmacological dose of Lena (50 mg/kg/day) decreased ascites formation in PEL mice *in vivo* and promoted apoptosis of PEL cell lines²²⁵. Paradoxically, our results demonstrated that *ex vivo* treatment of BC-3 or BCBL-1 ascites-derived PEL cells with Lena as single agent resulted in moderate inhibition of cell growth and failed to decrease peritoneal volume of PEL mice *in vivo* (Figures 9 and 10). This might be due to the fact that Lena concentration utilized in our *in vivo* experiments was 10-fold lower. Nevertheless, Lena as a single agent succeeded to enhance the survival of BC-3 PEL mice

and cured 25% of BCBL-1 PEL mice (Figure 7). Moreover, compared to ATO that resulted in a higher survival in BC-3 PEL mice, Lena yielded a better survival outcome on BCBL-1 PEL mice. However, both drugs, as single agents, failed to exhibit a significant effect on peritoneal ascites volume (Figure 8). Surprisingly, the combination of both drugs successfully impeded ascites expansion (Figures 8 and 9), reduced organ infiltration (Figure 25), increased survival (Figure 7), and more importantly resulted in a cure in 25% and 75% of BC3 and BCBL-1 injected PEL mice respectively (Figure 7).

KSHV latency is paramount for the development and maintenance of KSHV-associated malignancies^{38, 130}. It is a key driver of oncogenesis that substantially impedes the elimination of tumor cells by promoting cell growth and survival^{38, 57, 98}. In PEL ascites and cell lines, KSHV persists in its latent state via the expression of oncogenic latent proteins⁵⁷. ATO/Lena downregulated the expression of KSHV latent proteins LANA-1 and LANA-2 in both lymphomatous ascites derived cells and *in vivo* (Figures 11, 27 and 29). It also decreased the transcription of other latent proteins, v-FLIP and v-Cyclin (Figure 13). v-FLIP is an oncogenic latent protein critical for the proliferation and survival of PEL¹⁰⁷. Indeed, silencing v-FLIP was associated with apoptosis in PEL cells¹⁰⁷. In addition, v-FLIP exhibits transformative and oncogenic potential whereby its expression in rat cells increased cell proliferation and transformation¹³⁸. Further investigation is required to determine the detailed mechanism by which ATO/Lena downregulated KSHV latency. A potential mechanism might be through induction of accumulation of reactive oxygen species (ROS) in treated cells^{245, 246}. Increased ROS levels were associated with decreased viral latency, lytic reactivation, and cell death in PEL cells²⁴⁵. Moreover, both ATO and

Lena, when used alone, were shown to increase oxidative stress and ROS accumulation. Indeed, in multiple myeloma, Lena prevented decomposition of hydrogen peroxide leading to increased oxidative stress and apoptosis²⁴⁷. Similarly, accumulation of ROS is one of the established mechanisms through which ATO induce cytotoxicity in target cells²⁴⁶.

Constitutive activation of NF- κ B pathway is critical for KSHV oncogenesis^{142, 240}. It is involved in cellular transformation, resistance to cell death, and survival of PEL cells²⁴². Prior studies have investigated NF- κ B as a rational target for therapy^{142, 240}. Indeed, inhibition of NF- κ B delayed tumor growth and enhanced disease-free survival in PEL mice²⁴⁰. In PEL cells, v-FLIP appears to be a major activator of NF- κ B where silencing v-FLIP suppressed NF- κ B activation and led to apoptosis of PEL cells *in vitro* and *in vivo*¹⁰⁷. In accordance with these studies, we have demonstrated that ATO/Lena-mediated decrease in v-FLIP expression was accompanied by the inhibition of the NF- κ B pathway (Figure 14 and 15). PEL cells produce high levels of cytokines that contribute to their proliferation¹⁷⁷. Among these are cellular IL-6 and IL-10 which are established as autocrine growth factors that promote proliferation of PEL cells^{175, 177, 248}. Interestingly, v-FLIP was recently shown to activate IL-6 promoter via activation of NF- κ B¹⁷⁶. In addition, IL-6 and IL-10 are downstream target genes of NF- κ B²⁴¹. In a recent retrospective study, both cytokines were identified as prognostic factors that affect clinical response and development of PEL³¹. In line with these data, inhibition of NF- κ B by ATO/Lena was accompanied by reduction in IL-6 and IL-10 transcripts *ex vivo* and *in vivo* (Figures 16, 17 and 30). Decreased KSHV latency in addition to reduction of paramount autocrine growth

factors may together explain the profound inhibition of cell growth inflicted by the ATO/Lena treatment.

Inhibition of viral lytic gene expression is a cardinal mechanism through which KSHV maintains latency in PEL^{97, 120}. Latent oncogenic proteins inhibit viral lytic state and maintain oncogenesis¹²⁰. To this end, LANA-1, the major regulator of KSHV latency, was shown to suppress lytic gene expression either through binding to gene promoters resulting in transcriptional inhibition or via epigenetic silencing of the viral genome^{38, 120}. Furthermore, v-FLIP suppress the promoter activity of RTA, major lytic switch protein, which results in repression of viral lytic reactivation¹⁷⁶. This effect of v-FLIP on lytic reactivation is attributed to v-FLIP-mediated activation of NF-κB pathway and inhibition of AP-1¹⁴⁶. Indeed, silencing v-FLIP was associated with increased lytic gene expression and reactivation¹⁴⁶. More importantly, inhibition of NF-κB was recently correlated with lytic reactivation and cell death in PEL cells^{116, 174}. Indeed, a recently suggested therapeutic approach relied on KSHV reactivation as a potential mechanism for PEL eradication. In consistent with these reports, downregulation of viral latent gene expression and inhibition of NF-κB along with the subsequent reduction in IL-6 and IL-10 was accompanied by increased viral lytic expression in cells treated with ATO/Lena. Indeed, ATO/Lena enhanced the transcription of early, RTA and ORF K8, and late, K8.1, viral lytic genes resulting in apoptosis (Figures 18 and 19).

PEL cells are known to secrete the angiogenesis promoting factor VEGF which was shown to be involved in PEL progression²⁴³. Indeed, targeting VEGF hindered ascites formation and disease progression in PEL mice¹⁷⁵. In PEL mice, the peritoneum showed

extensive vascularization (Figure 22). yet, in mice treated with ATO/Lena, a remarkable reduction in peritoneal vascularization was observed in BC3 PEL mice Figure 22). These data were aligned with reduced tube formation capacity of HAEC cells by supernatant of ascites-derived BC-3 treated with ATO/Lena *ex vivo* (Figure 23 and 24). Basal secretion levels of VEGF are higher in ascites-derived BCBL-1 cells compared to ascites-derived BC3 cells¹⁷⁸. This can explain why supernatant from ATO/Lena treated BCBL-1 cells did not affect tube formation.

Altogether, our study provides strong coherent evidence on the potency of ATO/Lena against PEL *in vivo* and *ex vivo*, which strongly supports the clinical testing of this combination for a better management of PEL.

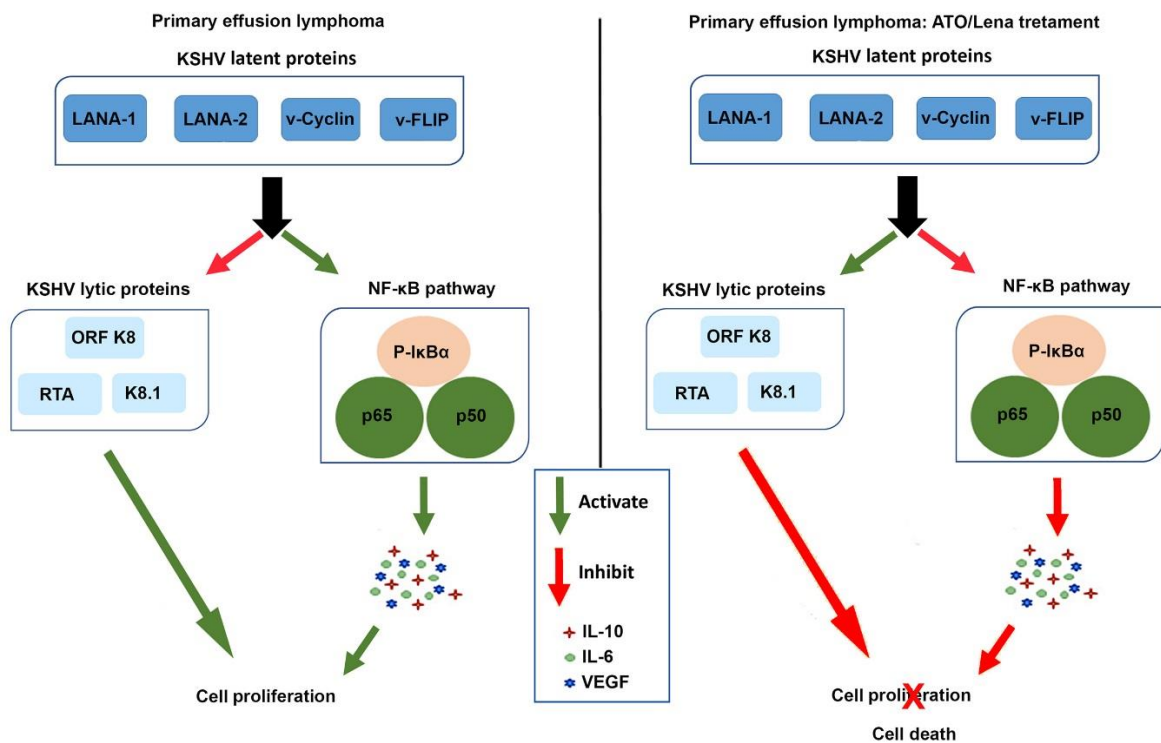


Figure 74. Illustrative model summarizing the suggested mechanism of action of ATO/Lena in primary effusion lymphoma.

Tax is established as a potent oncogene^{321, 327}. HBZ has been shown to counteract Tax functions where the two exhibit differential roles in HTLV-1 infection and ATL development³¹⁶. Yet, how exactly HBZ contributes to oncogenesis and how it modulates Tax functions including transformation are not fully understood. In our study, we generated an *in vivo* *hbz* transgenic *Drosophila* model and elucidated that, on contrary to Tax, HBZ expression failed to induce NF- κ B activation and ommatidial transformation in *hbz* transgenic flies (Figure 42). Thus, HBZ lacked any direct oncogenic potential in flies. In line with previous data, we made use of previously established *tax* transgenic flies³³⁰ and validated that Tax results in activation of both NF- κ B and PRC2 pathways *in vivo*. Despite the lack of transformative capacity, HBZ was found to bind to key PRC2 subunits, EZH2 and SUZ12, resulting in H3K27me3 accumulation (Figure 58, 71 and 72). More importantly, we demonstrated that co-expression of HBZ in *tax* transgenic flies abrogated Tax-mediated NF- κ B activation and its resultant senescence (Figures 57, 59, and 62), and reversed the ommatidial transformation phenotype induced by Tax (Figure 55). HBZ co-expression with Tax was also found to abolish PRC2 activation and decrease H3K27me3 recruitment to the promoters of Tax-dependent genes. Importantly, we delineate a novel potential competition mechanism between HBZ and Tax on epigenetic marks.

Both Tax and HBZ are involved in HTLV-1 pathogenesis and ATL development³¹⁶. The oncogenic roles of Tax are established and extensively supported by

an array of *in vitro* and *in vivo* studies. Indeed, Tax expression resulted in transformation and immortalization of various cells; including rat fibroblasts, T-lymphocytes, and PBMC³²⁵⁻³²⁷. Tax increased cell proliferation and activated multiple cellular survival pathways³¹⁸. Despite being undetected in primary ATL cells, Tax is indispensable for ATL cell's survival³²³. Recently, sporadic bursts of Tax expression were discovered in ATL-derived cells and were found to be critical for the survival of the whole population of cells³²⁴. On the contrary, overexpression of HBZ in T lymphocytes only triggered a moderate increase in cell proliferation yet HBZ was not deemed essential for immortalization of cells *in vitro* or *in vivo*^{366, 381}. While ATL cells are addicted to the continuous expression of Tax for their survival³²³, loss of HBZ only reduced proliferation and did not inflict cell death *in vitro*. However, HBZ is constantly expressed by all ATL cells suggesting a prominent role for HBZ in ATL development or phenotype. The oncogenic potential of Tax was mainly delineated *in vivo* where Tax expression resulted in leukemia with ATL-like characteristics in transgenic mice with profound NF-κB activation. Conversely, the *in vivo* oncogenic potential of HBZ was reported in two transgenic murine models. In the first model, mice exhibited a systemic inflammatory disease with late onset of lymphoma in small percentage of mice³⁷¹. In the second model, *hbz* under the Granzyme promoter led to a delayed lymphoproliferative disease in 60% of mice³⁸⁰. In a humanized model, absence of functional HBZ did not affect development of lymphoproliferative disease by HTLV-1 and no survival benefit was reported compared to control mice strongly suggesting that alone HBZ comprise weak oncogenic potential and is not essential for early tumor development³⁸¹. Moreover, HBZ Tg mice models failed to present with NF-κB activation, a characteristic critical feature of ATL³⁷¹. HTLV-1 is

known to naturally infect primates. Thus, ideally, mice models present a more relevant system than Fly models to assess the biology of HTLV-1. Unfortunately, these model comprise a major hurdle represented by the long latency period required for development of ATL. Indeed, this long latency have exceeded 18 months in some *tax* transgenic and *hbz* transgenic models and may be due to the cumulative acquisition of multiple cellular mutations. Unfortunately, this long period makes it impossible to differentiate whether the obtained phenotype or pathophysiology results from the expression of viral oncoprotein, Tax or HBZ, or is due to the accumulated mutations.

In this regard, the use of *Drosophila* models is associated with multiple advantages. Indeed, rapid generation time, high progeny yield, as well as availability of fast genetic screens makes *Drosophila* a popular model in biology research. In addition, the availability of wide array of mutants, RNAi fly lines, and a collection of driver systems, that direct the selective expression of genes into specific sites such as eyes or hemocytes, are readily available. More importantly, prominent signaling pathways and chromatin complexes are highly conserved between humans and flies. These include NF- κ B pathway³⁸⁵, PRC2 complex³⁸⁹, and several pathways implicated in regulating the differentiation of hematopoietic cells^{389, 390}. Our previously established *tax* transgenic *Drosophila* model exhibited a rough eye phenotype, indicative of cell transformation, elevated hemocytes count, in addition to activated NF- κ B pathway³³⁰. Herein, we show that unlike Tax, HBZ failed to inflict cellular transformation and rather resulted in minimal elevation of hemocytes count in the *hbz* transgenic fly model (Figures 42 and 46). Surprisingly, HBZ upregulated the expression of PRC2 core component SUZ12 and resulted in PRC2

complex activation. More importantly, the co-expression of HBZ and Tax in Tax/HBZ Tg flies reversed eye roughness and abrogated increased hemocytes count observed in *tax* transgenics elucidating a potential antagonistic role for HBZ in mitigating Tax-induced transformation *in vivo* (Figure 55).

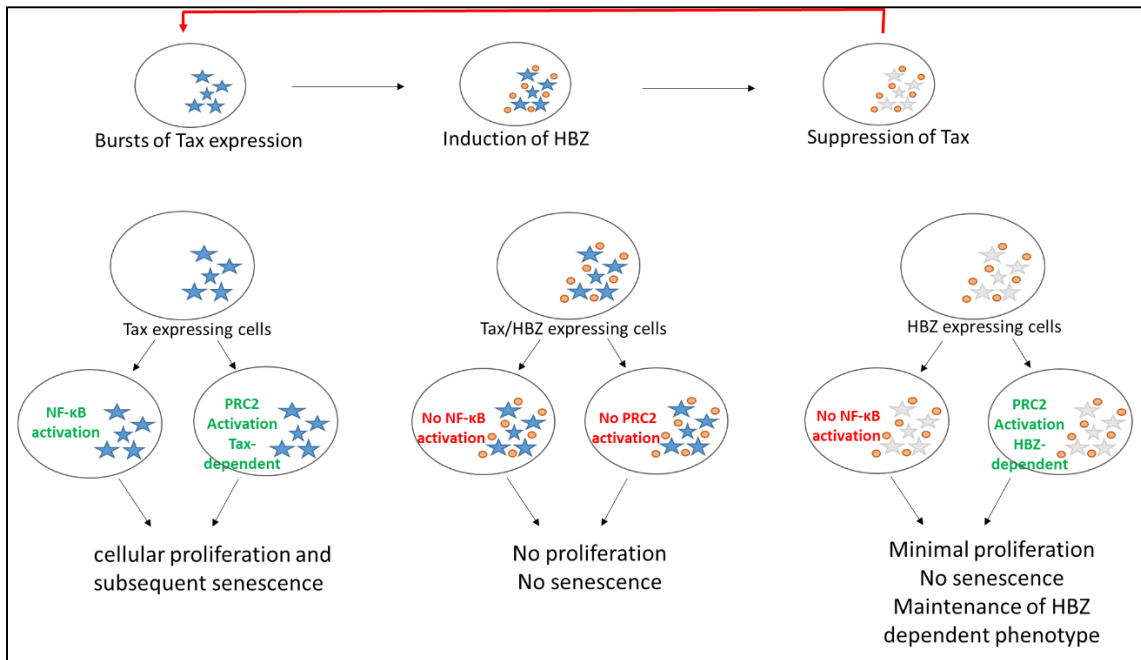


Figure 75. Proposed model for the interplay between Tax and HBZ for modulating NF-κB and PRC2.

In addition to its role as oncogene, Tax is a powerful immunogenic protein³³². Downregulation of Tax expression in ATL cells is momentous for escaping the immune system which allows maintenance of latency and development of ATL^{321, 387}. Tax is also an essential activator for NF-κB pathway^{377, 391, 392}. In Tax Tg flies, relish and Dipteracin expressions were increased indicating an activation of NF-κB, similar to that seen in ATL

cell lines and patients^{332,377}. The constitutive and persistent activation of NF- κ B results in induction of Tax-induced senescence as a protective mechanism for the cells³⁷⁶. Briefly, once activated canonical NF- κ B subunit P65 degrades p21/p27 checkpoint resulting in cell cycle arrest and senescence³⁷⁶. In consistence with these previously reported findings, we showed that Tax expression in *tax* transgenics led to *in vivo* senescence in larvae eye imaginal disks and circulating hemocytes (Figures 59 and 62). On the other hand, HBZ is known to inhibit the canonical NF- κ B pathway via degradation of p65³²⁰. In line with this data, we showed that *hbz* flies exhibited no increase in the expression relish and in its downstream gene Dipteracin, coinciding with lack of eye roughness phenotype (Figures 42 and 51). Interestingly, we showed that HBZ overexpression in *tax* flies abolished Tax-mediated NF- κ B activation *in vivo* (Figure 57). These data were in line with a prior study that established that in Hela cells transfected with Tax, HBZ downregulated NF- κ B activation and alleviated Tax-induced senescence allowing continuous cell growth and persistent latent infection³⁷⁶. In our study, we validated these results *in vivo* whereby HBZ expression in *tax* flies relieved senescence and decreased the expression of Dacapo (p21/p27 homolog) (Figure 59, 60, and 62). We postulate that the differences in the transformative capacity of Tax and HBZ may be attributed, at least in part, to the antagonistic/differential roles in NF- κ B modulation. To this end, HBZ alone failed to induce cellular transformation but played a key role in alleviating the detrimental effects of Tax, which allowed for maintenance of latent infection, cell growth, and succeeding transformation.

Accumulating evidence point towards the critical involvement of epigenetic alterations in ATL development²⁹⁰. Indeed, primary ATL cells present an altered PRC2

activity with increased levels of EZH2 and H3k27me3 repressive marks²⁸⁸. Recently, ATL cells were shown to harbor an ATL-specific epigenetic landscape with hyper-activation of PRC2 and global accumulation of H3k27 at almost half of the genes²⁹⁰. More importantly, Tax expression in PBMC was linked to the increased activation of PRC2 by upregulating transcription of EZH2 and SUZ12 leading to accumulation of H3k27me3 in a manner strikingly similar to ATL cells. Tax was also shown to physically interact with EZH2 and SUZ12²⁹⁰. In accordance with these results, we reported a significantly elevated expression of EZH2, SUZ12 and H3K27me3 in both cells and flies expressing Tax (Figure 47 and 64). Importantly, we observed that Tax binds to EZH2 and SUZ12 and enhanced the recruitment of H3K27me3 to the promoter of Tax-dependent genes deregulated in ATL cells (Figure 67 and 70). These include tumor suppresser genes such as NDRG2 and CDKN1A which present a decreased expression in ATL (Figure 67 and 68).

In contrary to the knockdown of Relish which results in total alleviation of Tax-imposed eye roughness, knocking down EZH2 or SUZ12 expression in tax flies only led to partial rescue of phenotype (Figure 49). Moreover, despite increasing PRC2 activity and H3K27me3 accumulation (Figure 47 and 67), HBZ expression failed to induce ommatidial transformation *in vivo* strongly suggesting that despite being important, PRC2 complex is not sufficient to induce cellular transformation. Interestingly, increased H3K27me3 accumulation secondary to HBZ expression is consistent with previously reported accumulation of H3K27me3 at the promoter of HBZ target genes such as the pro-apoptotic gene BIM³⁷⁰. Consequently, this implies that similar to Tax, HBZ may alter epigenetic pathways in HTLV-1 infected cells. Further dwelling into the mechanism by which HBZ alters PRC2 activity, we showed that HBZ co-localized and interacted with EZH2 and

SUZ12 in both mammalian cells and flies (Figures 72, 73, and 74). Consistent with reported data, HBZ didn't alter EZH2 transcription (Figure 47).

Surprisingly, upon co-expression with Tax, HBZ abrogated Tax-induced PRC2 activation in both Tax-HBZ expressing cells and *tax/hbz* transgenic flies (Figure 58 and 64). It also inhibited the recruitment of H3K27me3 to Tax-dependent genes (Figure 67). More importantly, we reported that HBZ abolished the interaction between EZH2 and Tax implying that HBZ might compete with Tax for binding EZH2 leading to decreased accumulation of H3K27me3 (Figure 70). Silencing HBZ in ATL derived MT-1 cells, with sporadic bursts of Tax expression, resulted in elevated expression of EZH2 with increased H3K27me3 accumulation (Figure 69). Given the opposite effects of HBZ on PRC2 activity, we hypothesized that HBZ, when expressed alone in the absence of Tax, activates PRC2 activity possibly through direct interaction with both EZH2 and Suz12 and upregulation of Suz12 expression. In contrast, upon co-expression with Tax, HBZ abrogates Tax-induced PRC2 activation possibly due to the inhibitory effect exerted by HBZ on Tax-mediated NF- κ B activation resulting in inhibition of Tax-mediated upregulation of EZH2 and abolishment of Tax-EZH2 binding. We postulate that HBZ may antagonize Tax via a novel mechanism of competition for binding with PRC2 epigenetic core subunits. Interestingly, knocking down HBZ in ATL-derived MT-1 cells with undetected sporadic bursts of Tax expression increased EZH2 and H3K27me3 levels and PRC2 activity. Yet, whether the two viral proteins bind to the same or distinct EZH2 domains should be further investigated. Finally, we have showed that both NF- κ B and PRC2 activation both contribute to Tax-mediated transformation. Thus, the rescue of Tax-

induced effects in Tax/HBZ transfected cells may be attributed to inhibition of NF- κ B and PRC2 activation.

Collectively, we have shown that both Tax and HBZ are key players in HTLV-1 persistence and transformation (proposed model summarized in Figure 75). Tax alone results in PRC2 activation, constitutive hyper-activation of NF- κ B, increased proliferation, immune system stimulation, and senescence. HBZ plays key roles via antagonizing deleterious Tax effects, specifically activation of NF- κ B and senescence, thus allows for persistence of latent HTLV-1 infection critical for cell transformation. In addition, we demonstrated that HBZ can maintain PRC2 activation in the absence of Tax. In ATL cells, transient expression of Tax in the form of sporadic bursts was reported. This expression is paramount for maintenance of NF- κ B activation, genetic instability, and continuous accumulation of sporadic mutations all of which eventually lead to ATL development in small population of HTLV-1 infected patients. Altogether, we established a paramount and robust *in vivo* tool that allowed for investigation of the antagonistic role of HBZ on Tax-imposed transformation, signaling, and epigenetic alteration. This *hbz* transgenic model may allow for further investigation of future HBZ functions *in vivo*.

CHAPTER VI

GENERAL CONCLUSION

Hematological malignancies arise from the uncontrolled proliferation of hematopoietic and lymphoid tissue. In our study, we tackled two virally induced hematological malignancies, PEL and ATL, secondary to infections with KSHV and HTLV-1 respectively. PEL and ATL are both associated with dismal prognosis mainly due to profound chemoresistance and relapse.

In PEL, current treatment regimens rely on an aggressive lymphoma chemotherapy combination. Yet these regimens present an unsatisfactorily short overall survival rate of one year in only 40% of treated patients. In the first part of our study, we investigated the anti-tumor potential of ATO/Lena, and demonstrated that this combination exhibited promising curative potential *in vivo*. Importantly, ATO/Lena decreased organ infiltration and inhibited accumulation of lymphomatous peritoneal ascites, a pathological feature that complicates treatment in PEL. Treatment of *ex vivo* ascites-derived cells showed that ATO/Lena inhibited cell proliferation and decreased the expression of latent KSHV proteins established as drivers of KSHV-mediated oncogenesis such as LANA-1 and v-FLIP. Further dwelling into the mechanism of action unveiled that the combination inhibited NF- κ B activation and decreased the expression of critical cytokines that function as growth factors for PEL proliferation. Importantly, ATO/Lena resulted in lytic reactivation and induced cell death. Reactivation was recently suggested as a promising

approach for targeting PEL cells. Altogether, our study presented a promising therapeutic combination for PEL management and our data warrant for further clinical investigations.

In the second part of the work, we investigated the roles of key pathways in ATL, PRC2 and NF- κ B, in the context of Tax and/or HBZ. We established an *hbz* transgenic fly model and demonstrated that while Tax induced a rough eye phenotype, HBZ failed to exhibit a transformative phenotype *in vivo*. In *tax* transgenic model, we showed that both pathways NF- κ B (to higher extent) and PRC2 contribute to Tax-mediated transformation, increased hemocytes count, and senescence. Interestingly, our data suggest that these pathways are connected whereby silencing Relish inhibited E(z) and SUZ12 expression in *tax* flies. Importantly, we reported a novel interaction between HBZ and PRC2 core subunits, EZH2 and SUZ12. Alone HBZ increased SUZ12 expression and resulted in accumulation of H3K27me3 and subsequent PRC2 activation. Remarkably, our study elucidated a potential role for HBZ in attenuating Tax-mediated transformation through inhibition of PRC2 and NF- κ B activation in the presence of Tax. The exact mechanism should be further investigated but it might be possibly through competitive binding of both viral proteins with PRC2 components. This counteracting function of HBZ might be crucial for survival of ATL cells as it prevents the over-activation of NF- κ B and the resultant senescence induced by Tax.

Future perspectives should focus on further dissection of the mechanism of interplay between Tax and HBZ in modulating cellular pathway. Whether Tax and HBZ bind the same domains in PRC2 components should be also investigated. Moreover, we know that Tax binds EZH2 and results in activation of PRC2. However, the exact mechanism by which HBZ activates PRC2 complex is still unknown. In ATL cells, Tax is

often undetected where sporadic bursts of Tax ensure continuous activation of NF- κ B, PRC2, and excessive proliferation. Our data indicates that HBZ may lack direct transformative potential *in vivo*. Future studies should focus on understanding how HBZ contribute to the survival of ATL cells following malignant transformation.

Overall, our work proposed a promising therapeutic approach for PEL and offered a better molecular understanding on viral transformation in ATL.

REFERENCES

1. Katano, H., Pathological Features of Kaposi's Sarcoma-Associated Herpesvirus Infection. In *Human Herpesviruses*, Kawaguchi, Y.; Mori, Y.; Kimura, H., Eds. Springer Singapore: Singapore, 2018; pp 357-376.
2. Shimada, K.; Hayakawa, F.; Kiyoi, H., Biology and management of primary effusion lymphoma. *Blood* **2018**, *132* (18), 1879-1888.
3. Arora, N.; Gupta, A.; Sadeghi, N., Primary effusion lymphoma: current concepts and management. *Curr Opin Pulm Med* **2017**, *23* (4), 365-370.
4. Boulanger, E.; Afonso, P. V.; Yahiaoui, Y.; Adle-Biassette, H.; Gabarre, J.; Agbalika, F., Human Herpesvirus-8 (HHV-8)-Associated Primary Effusion Lymphoma in two Renal Transplant Recipients Receiving Rapamycin. *American Journal of Transplantation* **2008**, *8* (3), 707-710.
5. Gupta, A.; Sen, S.; Marley, E.; Chen, W.; Naina, H. V., Management and Outcomes of HIV-Associated Primary Effusion Lymphoma: A Single Center Experience. *Clin Lymphoma Myeloma Leuk* **2016**, *16* Suppl, S175-80.
6. Simonelli, C.; Spina, M.; Cinelli, R.; Talamini, R.; Tedeschi, R.; Gloghini, A.; Vaccher, E.; Carbone, A.; Tirelli, U., Clinical features and outcome of primary effusion lymphoma in HIV-infected patients: a single-institution study. *J Clin Oncol* **2003**, *21* (21), 3948-54.
7. Knowles, D. M.; Inghirami, G.; Ubriaco, A.; Dalla-Favera, R., Molecular genetic analysis of three AIDS-associated neoplasms of uncertain lineage demonstrates their B-cell derivation and the possible pathogenetic role of the Epstein-Barr virus. *Blood* **1989**, *73* (3), 792-9.
8. Nador, R. G.; Cesarman, E.; Chadburn, A.; Dawson, D. B.; Ansari, M. Q.; Sald, J.; Knowles, D. M., Primary effusion lymphoma: a distinct clinicopathologic entity associated with the Kaposi's sarcoma-associated herpes virus. *Blood* **1996**, *88* (2), 645-56.
9. Chen, Y. B.; Rahemtullah, A.; Hochberg, E., Primary effusion lymphoma. *Oncologist* **2007**, *12* (5), 569-76.
10. Cesarman, E.; Chang, Y.; Moore, P. S.; Said, J. W.; Knowles, D. M., Kaposi's Sarcoma-Associated Herpesvirus-Like DNA Sequences in AIDS-Related Body-Cavity-Based Lymphomas. *New England Journal of Medicine* **1995**, *332* (18), 1186-1191.
11. Swerdlow, S. H., WHO classification of tumours of haematopoietic and lymphoid tissues. *WHO classification of tumours* **2008**, *22008*, 439.
12. Minhas, V.; Wood, C., Epidemiology and transmission of Kaposi's sarcoma-associated herpesvirus. *Viruses* **2014**, *6* (11), 4178-94.
13. Christenson, E. S.; Teply, B.; Agrawal, V.; Illei, P.; Gurakar, A.; Kanakry, J. A., Human Herpesvirus 8-Related Primary Effusion Lymphoma After Liver Transplantation. *Am J Transplant* **2015**, *15* (10), 2762-6.
14. Hsieh, P. Y.; Huang, S. I.; Li, D. K.; Mao, T. L.; Sheu, J. C.; Chen, C. H., Primary effusion lymphoma involving both pleural and abdominal cavities in a patient with hepatitis B virus-related liver cirrhosis. *J Formos Med Assoc* **2007**, *106* (6), 504-8.
15. Boulanger, E.; Hermine, O.; Ferman, J.-P.; Radford-Weiss, I.; Brousse, N.; Meignin, V.; Gessain, A., Human herpesvirus 8 (HHV-8)-associated peritoneal primary effusion lymphoma (PEL) in two HIV-negative elderly patients. *American Journal of Hematology* **2004**, *76* (1), 88-91.
16. Castillo, J. J.; Shum, H.; Lahijani, M.; Winer, E. S.; Butera, J. N., Prognosis in primary effusion lymphoma is associated with the number of body cavities involved. *Leuk Lymphoma* **2012**, *53* (12), 2378-82.
17. El-Fattah, M. A., Clinical characteristics and survival outcome of primary effusion lymphoma: A review of 105 patients. *Hematol Oncol* **2017**, *35* (4), 878-883.

18. Dukers, N. H.; Rezza, G., Human herpesvirus 8 epidemiology: what we do and do not know. *Aids* **2003**, *17* (12), 1717-30.
19. Bhutani, M.; Polizzotto, M. N.; Uldrick, T. S.; Yarchoan, R., Kaposi sarcoma-associated herpesvirus-associated malignancies: epidemiology, pathogenesis, and advances in treatment. *Semin Oncol* **2015**, *42* (2), 223-46.
20. Yuan, L.; Cook, J. R.; Elsheikh, T. M., Primary effusion lymphoma in human immune deficiency (HIV)-negative non-organ transplant immunocompetent patients. *Diagn Cytopathol* **2020**, *48* (4), 380-385.
21. Narkhede, M.; Arora, S.; Ujjani, C., Primary effusion lymphoma: current perspectives. *Oncotargets Ther* **2018**, *11*, 3747-3754.
22. Brimo, F.; Popradi, G.; Michel, R. P.; Auger, M., Primary effusion lymphoma involving three body cavities. *Cytojournal* **2009**, *6*, 21.
23. Patel, S.; Xiao, P., Primary effusion lymphoma. *Arch Pathol Lab Med* **2013**, *137* (8), 1152-4.
24. Chadburn, A.; Hyjek, E.; Mathew, S.; Cesarman, E.; Said, J.; Knowles, D. M., KSHV-Positive Solid Lymphomas Represent an Extra-Cavitary Variant of Primary Effusion Lymphoma. *The American Journal of Surgical Pathology* **2004**, *28* (11), 1401-1416.
25. Foster, W. R.; Bischin, A.; Dorer, R.; Aboulafia, D. M., Human Herpesvirus Type 8-associated Large B-cell Lymphoma: A Nonserous Extracavitary Variant of Primary Effusion Lymphoma in an HIV-infected Man: A Case Report and Review of the Literature. *Clin Lymphoma Myeloma Leuk* **2016**, *16* (6), 311-21.
26. Shah, N. N.; Harrison, N.; Stonecypher, M.; Frank, D.; Amorosa, V.; Svoboda, J., Extracavitary primary effusion lymphoma initially presenting with hemophagocytic lymphohistocytosis. *Clinical Lymphoma, Myeloma & Leukemia* **2014**, *14* (5), e157-60.
27. Pan, Z. G.; Zhang, Q. Y.; Lu, Z. B.; Quinto, T.; Rozenvald, I. B.; Liu, L. T.; Wilson, D.; Reddy, V.; Huang, Q.; Wang, H. Y.; Ren, Y. S., Extracavitary KSHV-associated large B-Cell lymphoma: a distinct entity or a subtype of primary effusion lymphoma? Study of 9 cases and review of an additional 43 cases. *Am J Surg Pathol* **2012**, *36* (8), 1129-40.
28. Kim, Y.; Leventaki, V.; Bhajee, F.; Jackson, C. C.; Medeiros, L. J.; Vega, F., Extracavitary/solid variant of primary effusion lymphoma. *Ann Diagn Pathol* **2012**, *16* (6), 441-6.
29. Kaplan, L. D., Human herpesvirus-8: Kaposi sarcoma, multicentric Castleman disease, and primary effusion lymphoma. *Hematology Am Soc Hematol Educ Program* **2013**, *2013*, 103-8.
30. Boulanger, E.; Gérard, L.; Gabarre, J.; Molina, J. M.; Rapp, C.; Abino, J. F.; Cadranel, J.; Chevret, S.; Oksenhendler, E., Prognostic factors and outcome of human herpesvirus 8-associated primary effusion lymphoma in patients with AIDS. *J Clin Oncol* **2005**, *23* (19), 4372-80.
31. Lurain, K.; Polizzotto, M. N.; Aleman, K.; Bhutani, M.; Wyvill, K. M.; Goncalves, P. H.; Ramaswami, R.; Marshall, V. A.; Miley, W.; Steinberg, S. M.; Little, R. F.; Wilson, W.; Filie, A. C.; Pittaluga, S.; Jaffe, E. S.; Whitby, D.; Yarchoan, R.; Uldrick, T. S., Viral, immunologic, and clinical features of primary effusion lymphoma. *Blood* **2019**, *133* (16), 1753-1761.
32. Guillet, S.; Gérard, L.; Meignin, V.; Agbalika, F.; Cuccini, W.; Denis, B.; Katlama, C.; Galicier, L.; Oksenhendler, E., Classic and extracavitary primary effusion lymphoma in 51 HIV-infected patients from a single institution. *Am J Hematol* **2016**, *91* (2), 233-7.
33. Brimo, F.; Michel, R. P.; Khetani, K.; Auger, M., Primary effusion lymphoma: a series of 4 cases and review of the literature with emphasis on cytomorphologic and immunocytochemical differential diagnosis. *Cancer* **2007**, *111* (4), 224-33.
34. Dittmer, D. P.; Damania, B., Kaposi sarcoma-associated herpesvirus: immunobiology, oncogenesis, and therapy. *J Clin Invest* **2016**, *126* (9), 3165-75.
35. Kim, Y.; Park, C. J.; Roh, J.; Huh, J., Current concepts in primary effusion lymphoma and other effusion-based lymphomas. *Korean J Pathol* **2014**, *48* (2), 81-90.

36. Hsi, E. D.; Foreman, K. E.; Duggan, J.; Alkan, S.; Kauffman, C. A.; Aronow, H. D.; Nickoloff, B. J., Molecular and pathologic characterization of an AIDS-related body cavity-based lymphoma, including ultrastructural demonstration of human herpesvirus-8: a case report. *Am J Surg Pathol* **1998**, *22* (4), 493-9.
37. Wakely, P. E., Jr.; Menezes, G.; Nuovo, G. J., Primary effusion lymphoma: cytopathologic diagnosis using in situ molecular genetic analysis for human herpesvirus 8. *Mod Pathol* **2002**, *15* (9), 944-50.
38. Uppal, T.; Banerjee, S.; Sun, Z.; Verma, S. C.; Robertson, E. S., KSHV LANA--the master regulator of KSHV latency. *Viruses* **2014**, *6* (12), 4961-98.
39. Patel, R. M.; Goldblum, J. R.; Hsi, E. D., Immunohistochemical detection of human herpes virus-8 latent nuclear antigen-1 is useful in the diagnosis of Kaposi sarcoma. *Mod Pathol* **2004**, *17* (4), 456-60.
40. Matolcsy, A.; Nádor, R. G.; Cesarman, E.; Knowles, D. M., Immunoglobulin VH gene mutational analysis suggests that primary effusion lymphomas derive from different stages of B cell maturation. *Am J Pathol* **1998**, *153* (5), 1609-14.
41. Carbone, A.; Ghoghini, A.; Larocca, L. M.; Capello, D.; Pierconti, F.; Canzonieri, V.; Tirelli, U.; Dalla-Favera, R.; Gaidano, G., Expression profile of MUM1/IRF4, BCL-6, and CD138/syndecan-1 defines novel histogenetic subsets of human immunodeficiency virus-related lymphomas. *Blood* **2001**, *97* (3), 744-51.
42. Klein, U.; Ghoghini, A.; Gaidano, G.; Chadburn, A.; Cesarman, E.; Dalla-Favera, R.; Carbone, A., Gene expression profile analysis of AIDS-related primary effusion lymphoma (PEL) suggests a plasmablastic derivation and identifies PEL-specific transcripts. *Blood* **2003**, *101* (10), 4115-21.
43. Chang, Y.; Cesarman, E.; Pessin, M.; Lee, F.; Culpepper, J.; Knowles, D.; Moore, P., Identification of herpesvirus-like DNA sequences in AIDS-associated Kaposi's sarcoma. *Science* **1994**, *266* (5192), 1865-1869.
44. Lange, P.; Damania, B., Kaposi Sarcoma-Associated Herpesvirus (KSHV). *Trends Microbiol* **2020**, *28* (3), 236-237.
45. <2018_Book_HumanHerpesviruses.pdf>.
46. Fields, B. N.; Knipe, D. M.; Howley, P. M., *Fields virology*. Wolters Kluwer Health/Lippincott Williams & Wilkins: Philadelphia, 2013.
47. Sehrawat, S.; Kumar, D.; Rouse, B. T., Herpesviruses: Harmonious Pathogens but Relevant Cofactors in Other Diseases? *Front Cell Infect Microbiol* **2018**, *8*, 177.
48. Mesri, E. A.; Cesarman, E.; Arvanitakis, L.; Rafii, S.; Moore, M. A.; Posnett, D. N.; Knowles, D. M.; Asch, A. S., Human herpesvirus-8/Kaposi's sarcoma-associated herpesvirus is a new transmissible virus that infects B cells. *J Exp Med* **1996**, *183* (5), 2385-90.
49. Fukumoto, H.; Kanno, T.; Hasegawa, H.; Katano, H., Pathology of Kaposi's Sarcoma-Associated Herpesvirus Infection. *Front Microbiol* **2011**, *2*, 175.
50. Staskus, K. A.; Zhong, W.; Gebhard, K.; Herndier, B.; Wang, H.; Renne, R.; Beneke, J.; Pudney, J.; Anderson, D. J.; Ganem, D.; Haase, A. T., Kaposi's sarcoma-associated herpesvirus gene expression in endothelial (spindle) tumor cells. *J Virol* **1997**, *71* (1), 715-9.
51. Beral, V.; Peterman Ta Fau - Berkelman, R. L.; Berkelman RI Fau - Jaffe, H. W.; Jaffe, H. W., Kaposi's sarcoma among persons with AIDS: a sexually transmitted infection? (0140-6736 (Print)).
52. Giraldo G Fau - Beth, E.; Beth E Fau - Haguenu, F.; Haguenu, F., Herpes-type virus particles in tissue culture of Kaposi's sarcoma from different geographic regions. (0027-8874 (Print)).

53. Russo, J. J.; Bohenzky, R. A.; Chien, M. C.; Chen, J.; Yan, M.; Maddalena, D.; Parry, J. P.; Peruzzi, D.; Edelman, I. S.; Chang, Y.; Moore, P. S., Nucleotide sequence of the Kaposi sarcoma-associated herpesvirus (HHV8). *Proc Natl Acad Sci U S A* **1996**, *93* (25), 14862-7.
54. Neipel, F.; Albrecht Jc Fau - Fleckenstein, B.; Fleckenstein, B., Cell-homologous genes in the Kaposi's sarcoma-associated rhadinovirus human herpesvirus 8: determinants of its pathogenicity? (0022-538X (Print)).
55. Goncalves, P. H.; Ziegelbauer, J.; Uldrick, T. S.; Yarchoan, R., Kaposi sarcoma herpesvirus-associated cancers and related diseases. *Curr Opin HIV AIDS* **2017**, *12* (1), 47-56.
56. Soulier, J.; Grollet, L.; Oksenhendler, E.; Cacoub, P.; Cazals-Hatem, D.; Babinet, P.; d'Agay, M. F.; Clauvel, J. P.; Raphael, M.; Degos, L.; et al., Kaposi's sarcoma-associated herpesvirus-like DNA sequences in multicentric Castlemans disease. *Blood* **1995**, *86* (4), 1276-80.
57. Dupin, N.; Fisher C Fau - Kellam, P.; Kellam P Fau - Ariad, S.; Ariad S Fau - Tulliez, M.; Tulliez M Fau - Franck, N.; Franck N Fau - van Marck, E.; van Marck E Fau - Salmon, D.; Salmon D Fau - Gorin, I.; Gorin I Fau - Escande, J. P.; Escande Jp Fau - Weiss, R. A.; Weiss Ra Fau - Alitalo, K.; Alitalo K Fau - Boshoff, C.; Boshoff, C., Distribution of human herpesvirus-8 latently infected cells in Kaposi's sarcoma, multicentric Castleman's disease, and primary effusion lymphoma. (0027-8424 (Print)).
58. Uldrick, T. S.; Wang V Fau - O'Mahony, D.; O'Mahony D Fau - Aleman, K.; Aleman K Fau - Wyvill, K. M.; Wyvill Km Fau - Marshall, V.; Marshall V Fau - Steinberg, S. M.; Steinberg Sm Fau - Pittaluga, S.; Pittaluga S Fau - Maric, I.; Maric I Fau - Whitby, D.; Whitby D Fau - Tosato, G.; Tosato G Fau - Little, R. F.; Little Rf Fau - Yarchoan, R.; Yarchoan, R., An interleukin-6-related systemic inflammatory syndrome in patients co-infected with Kaposi sarcoma-associated herpesvirus and HIV but without Multicentric Castleman disease. (1537-6591 (Electronic)).
59. Whitby, D.; Luppi, M.; Barozzi, P.; Boshoff, C.; Weiss, R. A.; Torelli, G., Human herpesvirus 8 seroprevalence in blood donors and lymphoma patients from different regions of Italy. *J Natl Cancer Inst* **1998**, *90* (5), 395-7.
60. Gambús, G.; Bourbouliia, D.; Esteve, A.; Lahoz, R.; Rodriguez, C.; Bolao, F.; Sirera, G.; Muga, R.; del Romero, J.; Boshoff, C.; Whitby, D.; Casabona, J., Prevalence and distribution of HHV-8 in different subpopulations, with and without HIV infection, in Spain. *Aids* **2001**, *15* (9), 1167-74.
61. Gao, S. J.; Kingsley, L.; Li, M.; Zheng, W.; Parravicini, C.; Ziegler, J.; Newton, R.; Rinaldo, C. R.; Saah, A.; Phair, J.; Detels, R.; Chang, Y.; Moore, P. S., KSHV antibodies among Americans, Italians and Ugandans with and without Kaposi's sarcoma. *Nat Med* **1996**, *2* (8), 925-8.
62. Baillargeon, J.; Leach, C. T.; Deng, J. H.; Gao, S. J.; Jenson, H. B., High prevalence of human herpesvirus 8 (HHV-8) infection in south Texas children. *J Med Virol* **2002**, *67* (4), 542-8.
63. Casper, C.; Wald, A.; Pauk, J.; Tabet, S. R.; Corey, L.; Celum, C. L., Correlates of prevalent and incident Kaposi's sarcoma-associated herpesvirus infection in men who have sex with men. *J Infect Dis* **2002**, *185* (7), 990-3.
64. Wang, X.; He, B.; Zhang, Z.; Liu, T.; Wang, H.; Li, X.; Zhang, Q.; Lan, K.; Lu, X.; Wen, H., Human herpesvirus-8 in northwestern China: epidemiology and characterization among blood donors. *Virol J* **2010**, *7*, 62.
65. Wakeham, K.; Webb, E. L.; Sebina, I.; Muhangi, L.; Miley, W.; Johnson, W. T.; Ndibazza, J.; Elliott, A. M.; Whitby, D.; Newton, R., Parasite infection is associated with Kaposi's sarcoma associated herpesvirus (KSHV) in Ugandan women. *Infect Agent Cancer* **2011**, *6* (1), 15.
66. Mesri, E. A.; Cesarman, E.; Boshoff, C., Kaposi's sarcoma and its associated herpesvirus. *Nat Rev Cancer* **2010**, *10* (10), 707-19.
67. Cesarman, E.; Damania, B.; Krown, S. E.; Martin, J.; Bower, M.; Whitby, D., Kaposi sarcoma. *Nat Rev Dis Primers* **2019**, *5* (1), 9.

68. Martin, J. N.; Ganem, D. E.; Osmond, D. H.; Page-Shafer, K. A.; Macrae, D.; Kedes, D. H., Sexual transmission and the natural history of human herpesvirus 8 infection. *N Engl J Med* **1998**, *338* (14), 948-54.
69. Casper, C.; Krantz, E.; Selke, S.; Kuntz, S. R.; Wang, J.; Huang, M. L.; Pauk, J. S.; Corey, L.; Wald, A., Frequent and asymptomatic oropharyngeal shedding of human herpesvirus 8 among immunocompetent men. *J Infect Dis* **2007**, *195* (1), 30-6.
70. Renne, R.; Lagunoff, M.; Zhong, W.; Ganem, D., The size and conformation of Kaposi's sarcoma-associated herpesvirus (human herpesvirus 8) DNA in infected cells and virions. *J Virol* **1996**, *70* (11), 8151-4.
71. Orenstein, J. M.; Alkan, S.; Blauvelt, A.; Jeang, K. T.; Weinstein, M. D.; Ganem, D.; Herndier, B., Visualization of human herpesvirus type 8 in Kaposi's sarcoma by light and transmission electron microscopy. *Aids* **1997**, *11* (5), F35-45.
72. Dourmishev, L. A.; Dourmishev, A. L.; Palmeri, D.; Schwartz, R. A.; Lukac, D. M., Molecular genetics of Kaposi's sarcoma-associated herpesvirus (human herpesvirus-8) epidemiology and pathogenesis. *Microbiol Mol Biol Rev* **2003**, *67* (2), 175-212, table of contents.
73. Mettenleiter, T. C.; Klupp Bg Fau - Granzow, H.; Granzow, H., Herpesvirus assembly: an update. (1872-7492 (Electronic)).
74. Yan, L.; Majerciak, V.; Zheng, Z. M.; Lan, K., Towards Better Understanding of KSHV Life Cycle: from Transcription and Posttranscriptional Regulations to Pathogenesis. *Virol Sin* **2019**, *34* (2), 135-161.
75. Ganem, D., KSHV and Kaposi's sarcoma: the end of the beginning? *Cell* **1997**, *91* (2), 157-60.
76. Bechtel, J. T.; Winant, R. C.; Ganem, D., Host and Viral Proteins in the Virion of Kaposi's Sarcoma-Associated Herpesvirus. *Journal of Virology* **2005**, *79* (8), 4952.
77. Nealon, K.; Newcomb, W. W.; Pray, T. R.; Craik, C. S.; Brown, J. C.; Kedes, D. H., Lytic replication of Kaposi's sarcoma-associated herpesvirus results in the formation of multiple capsid species: isolation and molecular characterization of A, B, and C capsids from a gammaherpesvirus. *J Virol* **2001**, *75* (6), 2866-78.
78. Full, F.; Jungnickl, D.; Reuter, N.; Bogner, E.; Brulois, K.; Scholz, B.; Stürzl, M.; Myoung, J.; Jung, J. U.; Stamminger, T.; Ensser, A., Kaposi's sarcoma associated herpesvirus tegument protein ORF75 is essential for viral lytic replication and plays a critical role in the antagonization of ND10-instituted intrinsic immunity. (1553-7374 (Electronic)).
79. Sathish, N.; Wang X Fau - Yuan, Y.; Yuan, Y., Tegument Proteins of Kaposi's Sarcoma-Associated Herpesvirus and Related Gamma-Herpesviruses. (1664-302X (Electronic)).
80. Baghian, A.; Luftig, M.; Black, J. B.; Meng, Y. X.; Pau, C. P.; Voss, T.; Pellett, P. E.; Kousoulas, K. G., Glycoprotein B of human herpesvirus 8 is a component of the virion in a cleaved form composed of amino- and carboxyl-terminal fragments. *Virology* **2000**, *269* (1), 18-25.
81. Wang, F. Z.; Akula, S. M.; Pramod, N. P.; Zeng, L.; Chandran, B., Human herpesvirus 8 envelope glycoprotein K8.1A interaction with the target cells involves heparan sulfate. *J Virol* **2001**, *75* (16), 7517-27.
82. Naranatt, P. P.; Akula, S. M.; Chandran, B., Characterization of gamma2-human herpesvirus-8 glycoproteins gH and gL. *Arch Virol* **2002**, *147* (7), 1349-70.
83. Akula, S. M.; Pramod, N. P.; Wang, F. Z.; Chandran, B., Human herpesvirus 8 envelope-associated glycoprotein B interacts with heparan sulfate-like moieties. *Virology* **2001**, *284* (2), 235-49.
84. Choi, J.; Means Re Fau - Damania, B.; Damania B Fau - Jung, J. U.; Jung, J. U., Molecular piracy of Kaposi's sarcoma associated herpesvirus. (1359-6101 (Print)).
85. Moore, P. S.; Chang, Y., Antiviral activity of tumor-suppressor pathways: clues from molecular piracy by KSHV. (0168-9525 (Print)).

86. Avitabile, E.; Forghieri C Fau - Campadelli-Fiume, G.; Campadelli-Fiume, G., Cross talk among the glycoproteins involved in herpes simplex virus entry and fusion: the interaction between gB and gH/gL does not necessarily require gD. (1098-5514 (Electronic)).
87. Pertel, P. E., Human herpesvirus 8 glycoprotein B (gB), gH, and gL can mediate cell fusion. (0022-538X (Print)).
88. Hahn, A. S.; Kaufmann Jk Fau - Wies, E.; Wies E Fau - Naschberger, E.; Naschberger E Fau - Panteleev-Ivlev, J.; Panteleev-Ivlev J Fau - Schmidt, K.; Schmidt K Fau - Holzer, A.; Holzer A Fau - Schmidt, M.; Schmidt M Fau - Chen, J.; Chen J Fau - König, S.; König S Fau - Ensser, A.; Ensser A Fau - Myoung, J.; Myoung J Fau - Brockmeyer, N. H.; Brockmeyer Nh Fau - Stürzl, M.; Stürzl M Fau - Fleckenstein, B.; Fleckenstein B Fau - Neipel, F.; Neipel, F., The ephrin receptor tyrosine kinase A2 is a cellular receptor for Kaposi's sarcoma-associated herpesvirus. (1546-170X (Electronic)).
89. Hensler, H. R.; Tomaszewski, M. J.; Rappocciolo, G.; Rinaldo, C. R.; Jenkins, F. J., Human herpesvirus 8 glycoprotein B binds the entry receptor DC-SIGN. (1872-7492 (Electronic)).
90. Kaleeba, J. A.; Berger, E. A., Kaposi's sarcoma-associated herpesvirus fusion-entry receptor: cystine transporter xCT. *Science* **2006**, *311* (5769), 1921-4.
91. Dutta, D.; Chakraborty S Fau - Bandyopadhyay, C.; Bandyopadhyay C Fau - Valiya Veettil, M.; Valiya Veettil M Fau - Ansari, M. A.; Ansari Ma Fau - Singh, V. V.; Singh Vv Fau - Chandran, B.; Chandran, B., EphrinA2 regulates clathrin mediated KSHV endocytosis in fibroblast cells by coordinating integrin-associated signaling and c-Cbl directed polyubiquitination. (1553-7374 (Electronic)).
92. DeCotiis, J. L.; Lukac, D. M., KSHV and the Role of Notch Receptor Dysregulation in Disease Progression. *Pathogens* **2017**, *6* (2).
93. Raghu, H.; Sharma-Walia N Fau - Veettil, M. V.; Veettil Mv Fau - Sadagopan, S.; Sadagopan S Fau - Caballero, A.; Caballero A Fau - Sivakumar, R.; Sivakumar R Fau - Varga, L.; Varga L Fau - Bottero, V.; Bottero V Fau - Chandran, B.; Chandran, B., Lipid rafts of primary endothelial cells are essential for Kaposi's sarcoma-associated herpesvirus/human herpesvirus 8-induced phosphatidylinositol 3-kinase and RhoA-GTPases critical for microtubule dynamics and nuclear delivery of viral DNA but dispensable for binding and entry. (0022-538X (Print)).
94. Chakraborty, S.; Veettil Mv Fau - Bottero, V.; Bottero V Fau - Chandran, B.; Chandran, B., Kaposi's sarcoma-associated herpesvirus interacts with EphrinA2 receptor to amplify signaling essential for productive infection. (1091-6490 (Electronic)).
95. Naranatt, P. P.; Akula Sm Fau - Zien, C. A.; Zien Ca Fau - Krishnan, H. H.; Krishnan Hh Fau - Chandran, B.; Chandran, B., Kaposi's sarcoma-associated herpesvirus induces the phosphatidylinositol 3-kinase-PKC-zeta-MEK-ERK signaling pathway in target cells early during infection: implications for infectivity. (0022-538X (Print)).
96. Sharma-Walia, N.; Naranatt Pp Fau - Krishnan, H. H.; Krishnan Hh Fau - Zeng, L.; Zeng L Fau - Chandran, B.; Chandran, B., Kaposi's sarcoma-associated herpesvirus/human herpesvirus 8 envelope glycoprotein gB induces the integrin-dependent focal adhesion kinase-Src-phosphatidylinositol 3-kinase-rho GTPase signal pathways and cytoskeletal rearrangements. (0022-538X (Print)).
97. Veettil, M. V.; Sharma-Walia N Fau - Sadagopan, S.; Sadagopan S Fau - Raghu, H.; Raghu H Fau - Sivakumar, R.; Sivakumar R Fau - Naranatt, P. P.; Naranatt Pp Fau - Chandran, B.; Chandran, B., RhoA-GTPase facilitates entry of Kaposi's sarcoma-associated herpesvirus into adherent target cells in a Src-dependent manner. (0022-538X (Print)).
98. Ballestas, M. E.; Chatis Pa Fau - Kaye, K. M.; Kaye, K. M., Efficient persistence of extrachromosomal KSHV DNA mediated by latency-associated nuclear antigen. (0036-8075 (Print)).

99. Ye, F.; Lei X Fau - Gao, S.-J.; Gao, S. J., Mechanisms of Kaposi's Sarcoma-Associated Herpesvirus Latency and Reactivation. LID - 193860 [pii]. (1687-8639 (Print)).
100. Faure, A.; Hayes, M.; Sugden, B., How Kaposi's sarcoma-associated herpesvirus stably transforms peripheral B cells towards lymphomagenesis. *Proc Natl Acad Sci U S A* **2019**, *116* (33), 16519-16528.
101. Dollery, S. J., Towards Understanding KSHV Fusion and Entry. *Viruses* **2019**, *11* (11).
102. Toth, Z.; Brulois, K.; Lee, H. R.; Izumiya, Y.; Tepper, C.; Kung, H. J.; Jung, J. U., Biphasic euchromatin-to-heterochromatin transition on the KSHV genome following de novo infection. *PLoS Pathog* **2013**, *9* (12), e1003813.
103. Uppal, T.; Jha, H. C.; Verma, S. C.; Robertson, E. S., Chromatinization of the KSHV Genome During the KSHV Life Cycle. *Cancers (Basel)* **2015**, *7* (1), 112-42.
104. Wen, K. W.; Damania, B., Kaposi sarcoma-associated herpesvirus (KSHV): molecular biology and oncogenesis. *Cancer Lett* **2010**, *289* (2), 140-50.
105. Schulz, T. F.; Cesarman, E., Kaposi Sarcoma-associated Herpesvirus: mechanisms of oncogenesis. *Curr Opin Virol* **2015**, *14*, 116-28.
106. Pearce, M.; Matsumura, S.; Wilson, A. C., Transcripts encoding K12, v-FLIP, v-cyclin, and the microRNA cluster of Kaposi's sarcoma-associated herpesvirus originate from a common promoter. *Journal of virology* **2005**, *79* (22), 14457-14464.
107. Kedes, D. H.; Lagunoff, M.; Renne, R.; Ganem, D., Identification of the gene encoding the major latency-associated nuclear antigen of the Kaposi's sarcoma-associated herpesvirus. *J Clin Invest* **1997**, *100* (10), 2606-10.
108. Guasparri, I.; Keller, S. A.; Cesarman, E., KSHV vFLIP is essential for the survival of infected lymphoma cells. *J Exp Med* **2004**, *199* (7), 993-1003.
109. Sun, Q.; Zachariah, S.; Chaudhary, P. M., The human herpes virus 8-encoded viral FLICE-inhibitory protein induces cellular transformation via NF-kappaB activation. *J Biol Chem* **2003**, *278* (52), 52437-45.
110. Godden-Kent, D.; Talbot, S. J.; Boshoff, C.; Chang, Y.; Moore, P.; Weiss, R. A.; Mittnacht, S., The cyclin encoded by Kaposi's sarcoma-associated herpesvirus stimulates cdk6 to phosphorylate the retinoblastoma protein and histone H1. *J Virol* **1997**, *71* (6), 4193-8.
111. Sadler, R.; Wu, L.; Forghani, B.; Renne, R.; Zhong, W.; Herndier, B.; Ganem, D., A complex translational program generates multiple novel proteins from the latently expressed kaposin (K12) locus of Kaposi's sarcoma-associated herpesvirus. *J Virol* **1999**, *73* (7), 5722-30.
112. Cai, X.; Lu, S.; Zhang, Z.; Gonzalez, C. M.; Damania, B.; Cullen, B. R., Kaposi's sarcoma-associated herpesvirus expresses an array of viral microRNAs in latently infected cells. *Proc Natl Acad Sci U S A* **2005**, *102* (15), 5570-5.
113. Wies, E.; Mori, Y.; Hahn, A.; Kremmer, E.; Stürzl, M.; Fleckenstein, B.; Neipel, F., The viral interferon-regulatory factor-3 is required for the survival of KSHV-infected primary effusion lymphoma cells. *Blood* **2008**, *111* (1), 320-7.
114. Sin, S. H.; Dittmer, D. P., Viral latency locus augments B-cell response in vivo to induce chronic marginal zone enlargement, plasma cell hyperplasia, and lymphoma. *Blood* **2013**, *121* (15), 2952-63.
115. Broussard, G.; Damania, B., KSHV: Immune Modulation and Immunotherapy. *Front Immunol* **2019**, *10*, 3084.
116. Davis, D. A.; Rinderknecht, A. S.; Zoetewij, J. P.; Aoki, Y.; Read-Connole, E. L.; Tosato, G.; Blauvelt, A.; Yarchoan, R., Hypoxia induces lytic replication of Kaposi sarcoma-associated herpesvirus. *Blood* **2001**, *97* (10), 3244-50.
117. Li, X.; Feng, J.; Sun, R., Oxidative stress induces reactivation of Kaposi's sarcoma-associated herpesvirus and death of primary effusion lymphoma cells. *J Virol* **2011**, *85* (2), 715-24.

118. Fejér, G.; Medveczky, M. M.; Horvath, E.; Lane, B.; Chang, Y.; Medveczky, P. G., The latency-associated nuclear antigen of Kaposi's sarcoma-associated herpesvirus interacts preferentially with the terminal repeats of the genome in vivo and this complex is sufficient for episomal DNA replication. *J Gen Virol* **2003**, *84* (Pt 6), 1451-1462.
119. Hu, J.; Renne, R., Characterization of the minimal replicator of Kaposi's sarcoma-associated herpesvirus latent origin. *J Virol* **2005**, *79* (4), 2637-42.
120. Si, H.; Verma, S. C.; Lampson, M. A.; Cai, Q.; Robertson, E. S., Kaposi's sarcoma-associated herpesvirus-encoded LANA can interact with the nuclear mitotic apparatus protein to regulate genome maintenance and segregation. *J Virol* **2008**, *82* (13), 6734-46.
121. Lan, K.; Kuppers, D. A.; Verma, S. C.; Robertson, E. S., Kaposi's sarcoma-associated herpesvirus-encoded latency-associated nuclear antigen inhibits lytic replication by targeting Rta: a potential mechanism for virus-mediated control of latency. *J Virol* **2004**, *78* (12), 6585-94.
122. Shamay, M.; Krithivas, A.; Zhang, J.; Hayward, S. D., Recruitment of the de novo DNA methyltransferase Dnmt3a by Kaposi's sarcoma-associated herpesvirus LANA. *Proc Natl Acad Sci U S A* **2006**, *103* (39), 14554-9.
123. Lan, K.; Kuppers, D. A.; Robertson, E. S., Kaposi's sarcoma-associated herpesvirus reactivation is regulated by interaction of latency-associated nuclear antigen with recombination signal sequence-binding protein Jkappa, the major downstream effector of the Notch signaling pathway. *J Virol* **2005**, *79* (6), 3468-78.
124. Jin, Y.; He, Z.; Liang, D.; Zhang, Q.; Zhang, H.; Deng, Q.; Robertson, E. S.; Lan, K., Carboxyl-terminal amino acids 1052 to 1082 of the latency-associated nuclear antigen (LANA) interact with RBP-J κ and are responsible for LANA-mediated RTA repression. *J Virol* **2012**, *86* (9), 4956-69.
125. Li, Q.; Zhou, F.; Ye, F.; Gao, S. J., Genetic disruption of KSHV major latent nuclear antigen LANA enhances viral lytic transcriptional program. *Virology* **2008**, *379* (2), 234-44.
126. Cai, Q. L.; Knight, J. S.; Verma, S. C.; Zald, P.; Robertson, E. S., EC5S ubiquitin complex is recruited by KSHV latent antigen LANA for degradation of the VHL and p53 tumor suppressors. *PLoS Pathog* **2006**, *2* (10), e116.
127. Radkov, S. A.; Kellam, P.; Boshoff, C., The latent nuclear antigen of Kaposi sarcoma-associated herpesvirus targets the retinoblastoma-E2F pathway and with the oncogene Hras transforms primary rat cells. *Nat Med* **2000**, *6* (10), 1121-7.
128. Friberg, J., Jr.; Kong, W.; Hottiger, M. O.; Nabel, G. J., p53 inhibition by the LANA protein of KSHV protects against cell death. *Nature* **1999**, *402* (6764), 889-94.
129. Cai, Q.; Xiao, B.; Si, H.; Cervini, A.; Gao, J.; Lu, J.; Upadhyay, S. K.; Verma, S. C.; Robertson, E. S., Kaposi's sarcoma herpesvirus upregulates Aurora A expression to promote p53 phosphorylation and ubiquitylation. *PLoS Pathog* **2012**, *8* (3), e1002566.
130. Wei, F.; Gan, J.; Wang, C.; Zhu, C.; Cai, Q., Cell Cycle Regulatory Functions of the KSHV Oncoprotein LANA. *Front Microbiol* **2016**, *7*, 334.
131. Fakhari, F. D.; Jeong, J. H.; Kanan, Y.; Dittmer, D. P., The latency-associated nuclear antigen of Kaposi sarcoma-associated herpesvirus induces B cell hyperplasia and lymphoma. *J Clin Invest* **2006**, *116* (3), 735-42.
132. Lu, F.; Tsai, K.; Chen, H. S.; Wikramasinghe, P.; Davuluri, R. V.; Showe, L.; Domsic, J.; Marmorstein, R.; Lieberman, P. M., Identification of host-chromosome binding sites and candidate gene targets for Kaposi's sarcoma-associated herpesvirus LANA. *J Virol* **2012**, *86* (10), 5752-62.
133. Liu, J.; Martin, H.; Shamay, M.; Woodard, C.; Tang, Q. Q.; Hayward, S. D., Kaposi's sarcoma-associated herpesvirus LANA protein downregulates nuclear glycogen synthase kinase 3 activity and consequently blocks differentiation. *J Virol* **2007**, *81* (9), 4722-31.

134. Liu, J.; Martin, H. J.; Liao, G.; Hayward, S. D., The Kaposi's sarcoma-associated herpesvirus LANA protein stabilizes and activates c-Myc. *J Virol* **2007**, *81* (19), 10451-9.
135. Rivas, C.; Thlick, A. E.; Parravicini, C.; Moore, P. S.; Chang, Y., Kaposi's sarcoma-associated herpesvirus LANA2 is a B-cell-specific latent viral protein that inhibits p53. *J Virol* **2001**, *75* (1), 429-38.
136. Muñoz-Fontela, C.; Marcos-Villar, L.; Hernandez, F.; Gallego, P.; Rodriguez, E.; Arroyo, J.; Gao, S. J.; Avila, J.; Rivas, C., Induction of paclitaxel resistance by the Kaposi's sarcoma-associated herpesvirus latent protein LANA2. *J Virol* **2008**, *82* (3), 1518-25.
137. Laura, M. V.; de la Cruz-Herrera, C. F.; Ferreirós, A.; Baz-Martínez, M.; Lang, V.; Vidal, A.; Muñoz-Fontela, C.; Rodríguez, M. S.; Collado, M.; Rivas, C., KSHV latent protein LANA2 inhibits sumo2 modification of p53. *Cell Cycle* **2015**, *14* (2), 277-82.
138. Manzano, M.; Günther, T.; Ju, H.; Nicholas, J.; Bartom, E. T.; Grundhoff, A.; Gottwein, E., Kaposi's Sarcoma-Associated Herpesvirus Drives a Super-Enhancer-Mediated Survival Gene Expression Program in Primary Effusion Lymphoma. *mBio* **2020**, *11* (4).
139. Thome, M.; Schneider, P.; Hofmann, K.; Fickenscher, H.; Meinel, E.; Neipel, F.; Mattmann, C.; Burns, K.; Bodmer, J. L.; Schröter, M.; Scaffidi, C.; Krammer, P. H.; Peter, M. E.; Tschoop, J., Viral FLICE-inhibitory proteins (FLIPs) prevent apoptosis induced by death receptors. *Nature* **1997**, *386* (6624), 517-21.
140. Field, N.; Low, W.; Daniels, M.; Howell, S.; Daviet, L.; Boshoff, C.; Collins, M., KSHV vFLIP binds to IKK-gamma to activate IKK. *J Cell Sci* **2003**, *116* (Pt 18), 3721-8.
141. Liu, L.; Eby, M. T.; Rathore, N.; Sinha, S. K.; Kumar, A.; Chaudhary, P. M., The human herpes virus 8-encoded viral FLICE inhibitory protein physically associates with and persistently activates the I κ B kinase complex. *J Biol Chem* **2002**, *277* (16), 13745-51.
142. Chaudhary, P. M.; Jasmin, A.; Eby, M. T.; Hood, L., Modulation of the NF-kappa B pathway by virally encoded death effector domains-containing proteins. *Oncogene* **1999**, *18* (42), 5738-46.
143. Hussain, A. R.; Ahmed, S. O.; Ahmed, M.; Khan, O. S.; Al Abdulmohsen, S.; Plataniias, L. C.; Al-Kuraya, K. S.; Uddin, S., Cross-talk between NF κ B and the PI3-kinase/AKT pathway can be targeted in primary effusion lymphoma (PEL) cell lines for efficient apoptosis. *PLoS One* **2012**, *7* (6), e39945.
144. An, J.; Sun, Y.; Fisher, M.; Rettig, M. B., Antitumor effects of bortezomib (PS-341) on primary effusion lymphomas. *Leukemia* **2004**, *18* (10), 1699-704.
145. Brown, H. J.; Song, M. J.; Deng, H.; Wu, T. T.; Cheng, G.; Sun, R., NF-kappaB inhibits gammaherpesvirus lytic replication. *J Virol* **2003**, *77* (15), 8532-40.
146. Grossmann, C.; Ganem, D., Effects of NFkappaB activation on KSHV latency and lytic reactivation are complex and context-dependent. *Virology* **2008**, *375* (1), 94-102.
147. Ye, F. C.; Zhou, F. C.; Xie, J. P.; Kang, T.; Greene, W.; Kuhne, K.; Lei, X. F.; Li, Q. H.; Gao, S. J., Kaposi's sarcoma-associated herpesvirus latent gene vFLIP inhibits viral lytic replication through NF-kappaB-mediated suppression of the AP-1 pathway: a novel mechanism of virus control of latency. *J Virol* **2008**, *82* (9), 4235-49.
148. Ballon, G.; Chen, K.; Perez, R.; Tam, W.; Cesarman, E., Kaposi sarcoma herpesvirus (KSHV) vFLIP oncoprotein induces B cell transdifferentiation and tumorigenesis in mice. *J Clin Invest* **2011**, *121* (3), 1141-53.
149. Van Dross, R.; Yao, S.; Asad, S.; Westlake, G.; Mays, D. J.; Barquero, L.; Duell, S.; Pietenpol, J. A.; Browning, P. J., Constitutively active K-cyclin/cdk6 kinase in Kaposi sarcoma-associated herpesvirus-infected cells. *J Natl Cancer Inst* **2005**, *97* (9), 656-66.
150. Swanton, C.; Mann, D. J.; Fleckenstein, B.; Neipel, F.; Peters, G.; Jones, N., Herpes viral cyclin/Cdk6 complexes evade inhibition by CDK inhibitor proteins. *Nature* **1997**, *390* (6656), 184-7.

151. Sarek, G.; Järviluoma, A.; Moore, H. M.; Tojkander, S.; Vartia, S.; Biberfeld, P.; Laiho, M.; Ojala, P. M., Nucleophosmin phosphorylation by v-cyclin-CDK6 controls KSHV latency. *PLoS Pathog* **2010**, *6* (3), e1000818.
152. Jones, T.; Ramos da Silva, S.; Bedolla, R.; Ye, F.; Zhou, F.; Gao, S. J., Viral cyclin promotes KSHV-induced cellular transformation and tumorigenesis by overriding contact inhibition. *Cell Cycle* **2014**, *13* (5), 845-58.
153. Zhi, H.; Zahoor, M. A.; Shudofsky, A. M.; Giam, C. Z., KSHV vCyclin counters the senescence/G1 arrest response triggered by NF- κ B hyperactivation. *Oncogene* **2015**, *34* (4), 496-505.
154. Aneja, K. K.; Yuan, Y., Reactivation and Lytic Replication of Kaposi's Sarcoma-Associated Herpesvirus: An Update. *Front Microbiol* **2017**, *8*, 613.
155. Carroll, K. D.; Khadim, F.; Spadavecchia, S.; Palmeri, D.; Lukac, D. M., Direct interactions of Kaposi's sarcoma-associated herpesvirus/human herpesvirus 8 ORF50/Rta protein with the cellular protein octamer-1 and DNA are critical for specifying transactivation of a delayed-early promoter and stimulating viral reactivation. *J Virol* **2007**, *81* (16), 8451-67.
156. Jenner, R. G.; Albà, M. M.; Boshoff, C.; Kellam, P., Kaposi's sarcoma-associated herpesvirus latent and lytic gene expression as revealed by DNA arrays. *J Virol* **2001**, *75* (2), 891-902.
157. Saveliev, A.; Zhu, F.; Yuan, Y., Transcription mapping and expression patterns of genes in the major immediate-early region of Kaposi's sarcoma-associated herpesvirus. *Virology* **2002**, *299* (2), 301-14.
158. Sun, R.; Lin, S. F.; Staskus, K.; Gradoville, L.; Grogan, E.; Haase, A.; Miller, G., Kinetics of Kaposi's sarcoma-associated herpesvirus gene expression. *J Virol* **1999**, *73* (3), 2232-42.
159. Gradoville, L.; Gerlach, J.; Grogan, E.; Shedd, D.; Nikiforow, S.; Metroka, C.; Miller, G., Kaposi's sarcoma-associated herpesvirus open reading frame 50/Rta protein activates the entire viral lytic cycle in the HH-B2 primary effusion lymphoma cell line. *J Virol* **2000**, *74* (13), 6207-12.
160. Zhu, F. X.; Cusano, T.; Yuan, Y., Identification of the immediate-early transcripts of Kaposi's sarcoma-associated herpesvirus. *J Virol* **1999**, *73* (7), 5556-67.
161. Davis, Z. H.; Verschuere, E.; Jang, G. M.; Kleffman, K.; Johnson, J. R.; Park, J.; Von Dollen, J.; Maher, M. C.; Johnson, T.; Newton, W.; Jäger, S.; Shales, M.; Horner, J.; Hernandez, R. D.; Krogan, N. J.; Glaunsinger, B. A., Global mapping of herpesvirus-host protein complexes reveals a transcription strategy for late genes. *Mol Cell* **2015**, *57* (2), 349-60.
162. Mettenleiter, T. C., Herpesvirus assembly and egress. *J Virol* **2002**, *76* (4), 1537-47.
163. Skepper, J. N.; Whiteley, A.; Browne, H.; Minson, A., Herpes simplex virus nucleocapsids mature to progeny virions by an envelopment --> deenvelopment --> reenvelopment pathway. *J Virol* **2001**, *75* (12), 5697-702.
164. Lukac, D. M.; Renne, R.; Kirshner, J. R.; Ganem, D., Reactivation of Kaposi's sarcoma-associated herpesvirus infection from latency by expression of the ORF 50 transactivator, a homolog of the EBV R protein. *Virology* **1998**, *252* (2), 304-12.
165. West, J. T.; Wood, C., The role of Kaposi's sarcoma-associated herpesvirus/human herpesvirus-8 regulator of transcription activation (RTA) in control of gene expression. *Oncogene* **2003**, *22* (33), 5150-63.
166. Purushothaman, P.; Thakker, S.; Verma, S. C., Transcriptome analysis of Kaposi's sarcoma-associated herpesvirus during de novo primary infection of human B and endothelial cells. *J Virol* **2015**, *89* (6), 3093-111.
167. Lukac, D. M.; Kirshner, J. R.; Ganem, D., Transcriptional activation by the product of open reading frame 50 of Kaposi's sarcoma-associated herpesvirus is required for lytic viral reactivation in B cells. *J Virol* **1999**, *73* (11), 9348-61.

168. Byun, H.; Gwack, Y.; Hwang, S.; Choe, J., Kaposi's sarcoma-associated herpesvirus open reading frame (ORF) 50 transactivates K8 and ORF57 promoters via heterogeneous response elements. *Mol Cells* **2002**, *14* (2), 185-91.
169. Chen, J.; Ye, F.; Xie, J.; Kuhne, K.; Gao, S. J., Genome-wide identification of binding sites for Kaposi's sarcoma-associated herpesvirus lytic switch protein, RTA. *Virology* **2009**, *386* (2), 290-302.
170. Deng, H.; Young, A.; Sun, R., Auto-activation of the rta gene of human herpesvirus-8/Kaposi's sarcoma-associated herpesvirus. *J Gen Virol* **2000**, *81* (Pt 12), 3043-3048.
171. Zhao, Q.; Liang, D.; Sun, R.; Jia, B.; Xia, T.; Xiao, H.; Lan, K., Kaposi's sarcoma-associated herpesvirus-encoded replication and transcription activator impairs innate immunity via ubiquitin-mediated degradation of myeloid differentiation factor 88. *J Virol* **2015**, *89* (1), 415-27.
172. Lan, K.; Kuppers, D. A.; Verma, S. C.; Sharma, N.; Murakami, M.; Robertson, E. S., Induction of Kaposi's sarcoma-associated herpesvirus latency-associated nuclear antigen by the lytic transactivator RTA: a novel mechanism for establishment of latency. *J Virol* **2005**, *79* (12), 7453-65.
173. Chmura, J. C.; Herold, K.; Ruffin, A.; Atuobi, T.; Fabiyi, Y.; Mitchell, A. E.; Choi, Y. B.; Ehrlich, E. S., The Itch ubiquitin ligase is required for KSHV RTA induced vFLIP degradation. *Virology* **2017**, *501*, 119-126.
174. Zhou, F.; Shimoda, M.; Olney, L.; Lyu, Y.; Tran, K.; Jiang, G.; Nakano, K.; Davis, R. R.; Tepper, C. G.; Maverakis, E.; Campbell, M.; Li, Y.; Dandekar, S.; Izumiya, Y., Oncolytic Reactivation of KSHV as a Therapeutic Approach for Primary Effusion Lymphoma. *Mol Cancer Ther* **2017**, *16* (11), 2627-2638.
175. Reid, E. G., Bortezomib-induced Epstein-Barr virus and Kaposi sarcoma herpesvirus lytic gene expression: oncolytic strategies. *Curr Opin Oncol* **2011**, *23* (5), 482-7.
176. Goto, H.; Kudo, E.; Kariya, R.; Taura, M.; Katano, H.; Okada, S., Targeting VEGF and interleukin-6 for controlling malignant effusion of primary effusion lymphoma. *J Cancer Res Clin Oncol* **2015**, *141* (3), 465-74.
177. An, J.; Sun, Y.; Sun, R.; Rettig, M. B., Kaposi's sarcoma-associated herpesvirus encoded vFLIP induces cellular IL-6 expression: the role of the NF-kappaB and JNK/AP1 pathways. *Oncogene* **2003**, *22* (22), 3371-85.
178. Jones, K. D.; Aoki, Y.; Chang, Y.; Moore, P. S.; Yarchoan, R.; Tosato, G., Involvement of interleukin-10 (IL-10) and viral IL-6 in the spontaneous growth of Kaposi's sarcoma herpesvirus-associated infected primary effusion lymphoma cells. *Blood* **1999**, *94* (8), 2871-9.
179. Haddad, L.; El Hajj, H.; Abou-Merhi, R.; Kfoury, Y.; Mahieux, R.; El-Sabban, M.; Bazarbachi, A., KSHV-transformed primary effusion lymphoma cells induce a VEGF-dependent angiogenesis and establish functional gap junctions with endothelial cells. *Leukemia* **2008**, *22* (4), 826-34.
180. Okada, S.; Goto, H.; Yotsumoto, M., Current status of treatment for primary effusion lymphoma. *Intractable Rare Dis Res* **2014**, *3* (3), 65-74.
181. Little, R. F.; Pittaluga, S.; Grant, N.; Steinberg, S. M.; Kavlick, M. F.; Mitsuya, H.; Franchini, G.; Gutierrez, M.; Raffeld, M.; Jaffe, E. S.; Shearer, G.; Yarchoan, R.; Wilson, W. H., Highly effective treatment of acquired immunodeficiency syndrome-related lymphoma with dose-adjusted EPOCH: impact of antiretroviral therapy suspension and tumor biology. *Blood* **2003**, *101* (12), 4653-9.
182. El-Ayass, W.; Yu, E. M.; Karcher, D. S.; Aragon-Ching, J. B., Complete response to EPOCH in a patient with HIV and extracavitary primary effusion lymphoma involving the colon: a case report and review of literature. *Clin Lymphoma Myeloma Leuk* **2012**, *12* (2), 144-7.
183. Boulanger, E.; Daniel, M. T.; Agbalika, F.; Oksenhendler, E., Combined chemotherapy including high-dose methotrexate in KSHV/HHV8-associated primary effusion lymphoma. *Am J Hematol* **2003**, *73* (3), 143-8.

184. Terasaki, Y.; Okumura, H.; Saito, K.; Sato, Y.; Yoshino, T.; Ichinohasama, R.; Ishida, Y., HHV-8/KSHV-negative and CD20-positive primary effusion lymphoma successfully treated by pleural drainage followed by chemotherapy containing rituximab. *Intern Med* **2008**, *47* (24), 2175-8.
185. Suzuki, K.; Ino, K.; Sugawara, Y.; Mizutani, M.; Sekine, T.; Katayama, N., [Prolonged survival in a patient with human herpesvirus-8-negative primary effusion lymphoma after combination chemotherapy with rituximab]. *Gan To Kagaku Ryoho* **2008**, *35* (4), 691-4.
186. Oksenhendler, E.; Clauvel, J. P.; Jouveshomme, S.; Davi, F.; Mansour, G., Complete remission of a primary effusion lymphoma with antiretroviral therapy. *Am J Hematol* **1998**, *57* (3), 266.
187. Williamson, S. J.; Nicol, S. M.; Stürzl, M.; Sabbah, S.; Hislop, A. D., Azidothymidine Sensitizes Primary Effusion Lymphoma Cells to Kaposi Sarcoma-Associated Herpesvirus-Specific CD4+ T Cell Control and Inhibits vIRF3 Function. *PLoS Pathog* **2016**, *12* (11), e1006042.
188. Kariya, R.; Taura, M.; Suzu, S.; Kai, H.; Katano, H.; Okada, S., HIV protease inhibitor Lopinavir induces apoptosis of primary effusion lymphoma cells via suppression of NF- κ B pathway. *Cancer Lett* **2014**, *342* (1), 52-9.
189. Cassoni, A.; Ali, U.; Cave, J.; Edwards, S. G.; Ramsay, A.; Miller, R. F.; Lee, S. M., Remission after radiotherapy for a patient with chemotherapy-refractory HIV-associated primary effusion lymphoma. *J Clin Oncol* **2008**, *26* (32), 5297-9.
190. Won, J. H.; Han, S. H.; Bae, S. B.; Kim, C. K.; Lee, N. S.; Lee, K. T.; Park, S. K.; Hong, D. S.; Lee, D. W.; Park, H. S., Successful eradication of relapsed primary effusion lymphoma with high-dose chemotherapy and autologous stem cell transplantation in a patient seronegative for human immunodeficiency virus. *Int J Hematol* **2006**, *83* (4), 328-30.
191. Bryant, A.; Milliken, S., Successful reduced-intensity conditioning allogeneic HSCT for HIV-related primary effusion lymphoma. *Biol Blood Marrow Transplant* **2008**, *14* (5), 601-2.
192. Luppi, M.; Trovato, R.; Barozzi, P.; Vallisa, D.; Rossi, G.; Re, A.; Ravazzini, L.; Potenza, L.; Riva, G.; Morselli, M.; Longo, G.; Cavanna, L.; Roncaglia, R.; Torelli, G., Treatment of herpesvirus associated primary effusion lymphoma with intracavity cidofovir. *Leukemia* **2005**, *19* (3), 473-6.
193. Marquet, J.; Velazquez-Kennedy, K.; López, S.; Benito, A.; Blanchard, M. J.; Garcia-Vela, J. A., Case report of a primary effusion lymphoma successfully treated with oral valganciclovir after failing chemotherapy. *Hematol Oncol* **2018**, *36* (1), 316-319.
194. Ashizawa, A.; Higashi, C.; Masuda, K.; Ohga, R.; Taira, T.; Fujimuro, M., The Ubiquitin System and Kaposi's Sarcoma-Associated Herpesvirus. *Front Microbiol* **2012**, *3*, 66.
195. Matta, H.; Chaudhary, P. M., The proteasome inhibitor bortezomib (PS-341) inhibits growth and induces apoptosis in primary effusion lymphoma cells. *Cancer Biol Ther* **2005**, *4* (1), 77-82.
196. Greene, W.; Zhang, W.; He, M.; Witt, C.; Ye, F.; Gao, S. J., The ubiquitin/proteasome system mediates entry and endosomal trafficking of Kaposi's sarcoma-associated herpesvirus in endothelial cells. *PLoS Pathog* **2012**, *8* (5), e1002703.
197. Raedler, L., Velcade (Bortezomib) Receives 2 New FDA Indications: For Retreatment of Patients with Multiple Myeloma and for First-Line Treatment of Patients with Mantle-Cell Lymphoma. *Am Health Drug Benefits* **2015**, *8* (Spec Feature), 135-40.
198. Siddiqi, T.; Joyce, R. M., A case of HIV-negative primary effusion lymphoma treated with bortezomib, pegylated liposomal doxorubicin, and rituximab. *Clin Lymphoma Myeloma* **2008**, *8* (5), 300-4.
199. Sin, S. H.; Roy, D.; Wang, L.; Staudt, M. R.; Fakhari, F. D.; Patel, D. D.; Henry, D.; Harrington, W. J., Jr.; Damania, B. A.; Dittmer, D. P., Rapamycin is efficacious against primary effusion lymphoma (PEL) cell lines in vivo by inhibiting autocrine signaling. *Blood* **2007**, *109* (5), 2165-73.

200. Klass, C. M.; Offermann, M. K., Targeting human herpesvirus-8 for treatment of Kaposi's sarcoma and primary effusion lymphoma. *Curr Opin Oncol* **2005**, *17* (5), 447-55.
201. Kedes, D. H.; Ganem, D., Sensitivity of Kaposi's sarcoma-associated herpesvirus replication to antiviral drugs. Implications for potential therapy. *J Clin Invest* **1997**, *99* (9), 2082-6.
202. Saji, C.; Higashi, C.; Niinaka, Y.; Yamada, K.; Noguchi, K.; Fujimuro, M., Proteasome inhibitors induce apoptosis and reduce viral replication in primary effusion lymphoma cells. *Biochem Biophys Res Commun* **2011**, *415* (4), 573-8.
203. Bhatt, S.; Ashlock, B. M.; Toomey, N. L.; Diaz, L. A.; Mesri, E. A.; Lossos, I. S.; Ramos, J. C., Efficacious proteasome/HDAC inhibitor combination therapy for primary effusion lymphoma. *J Clin Invest* **2013**, *123* (6), 2616-28.
204. Goto, H.; Kariya, R.; Shimamoto, M.; Kudo, E.; Taura, M.; Katano, H.; Okada, S., Antitumor effect of berberine against primary effusion lymphoma via inhibition of NF- κ B pathway. *Cancer Sci* **2012**, *103* (4), 775-81.
205. El Hajj, H.; Ali, J.; Ghantous, A.; Hodroj, D.; Daher, A.; Zibara, K.; Journo, C.; Otrock, Z.; Zaatari, G.; Mahieux, R.; El Sabban, M.; Bazarbachi, A.; Abou Merhi, R., Combination of arsenic and interferon-alpha inhibits expression of KSHV latent transcripts and synergistically improves survival of mice with primary effusion lymphomas. *PLoS One* **2013**, *8* (11), e79474.
206. Abou-Merhi, R.; Khoriaty, R.; Arnoult, D.; El Hajj, H.; Dbouk, H.; Munier, S.; El-Sabban, M. E.; Hermine, O.; Gessain, A.; de The, H.; Mahieux, R.; Bazarbachi, A., PS-341 or a combination of arsenic trioxide and interferon-alpha inhibit growth and induce caspase-dependent apoptosis in KSHV/HHV-8-infected primary effusion lymphoma cells. *Leukemia* **2007**, *21* (8), 1792-801.
207. Mediani, L.; Gibellini, F.; Bertacchini, J.; Frasson, C.; Bosco, R.; Accordi, B.; Basso, G.; Bonora, M.; Calabrò, M. L.; Mattiolo, A.; Sgarbi, G.; Baracca, A.; Pinton, P.; Riva, G.; Rampazzo, E.; Petrizza, L.; Prodi, L.; Milani, D.; Luppi, M.; Potenza, L.; De Pol, A.; Cocco, L.; Capitani, S.; Marmiroli, S., Reversal of the glycolytic phenotype of primary effusion lymphoma cells by combined targeting of cellular metabolism and PI3K/Akt/ mTOR signaling. *Oncotarget* **2016**, *7* (5), 5521-37.
208. Mohanty, S.; Kumar, A.; Das, P.; Sahu, S. K.; Choudhuri, T., Multi-targeted therapy of everolimus in Kaposi's sarcoma associated herpes virus infected primary effusion lymphoma. *Apoptosis* **2017**, *22* (9), 1098-1115.
209. Bonsignore, L.; Passelli, K.; Pelzer, C.; Perroud, M.; Konrad, A.; Thurau, M.; Stürzl, M.; Dai, L.; Trillo-Tinoco, J.; Del Valle, L.; Qin, Z.; Thome, M., A role for MALT1 activity in Kaposi's sarcoma-associated herpes virus latency and growth of primary effusion lymphoma. *Leukemia* **2017**, *31* (3), 614-624.
210. Dai, L.; Trillo-Tinoco, J.; Cao, Y.; Bonstaff, K.; Doyle, L.; Del Valle, L.; Whitby, D.; Parsons, C.; Reiss, K.; Zabaleta, J.; Qin, Z., Targeting HGF/c-MET induces cell cycle arrest, DNA damage, and apoptosis for primary effusion lymphoma. *Blood* **2015**, *126* (26), 2821-31.
211. Granato, M.; Gilardini Montani, M. S.; Romeo, M. A.; Santarelli, R.; Gonnella, R.; D'Orazi, G.; Faggioni, A.; Cirone, M., Metformin triggers apoptosis in PEL cells and alters bortezomib-induced Unfolded Protein Response increasing its cytotoxicity and inhibiting KSHV lytic cycle activation. *Cell Signal* **2017**, *40*, 239-247.
212. Davis, D. A.; Mishra, S.; Anagho, H. A.; Aisabor, A. I.; Shrestha, P.; Wang, V.; Takamatsu, Y.; Maeda, K.; Mitsuya, H.; Zeldis, J. B.; Yarchoan, R., Restoration of immune surface molecules in Kaposi sarcoma-associated herpes virus infected cells by lenalidomide and pomalidomide. *Oncotarget* **2017**, *8* (31), 50342-50358.
213. Gopalakrishnan, R.; Matta, H.; Tolani, B.; Triche, T., Jr.; Chaudhary, P. M., Immunomodulatory drugs target IKZF1-IRF4-MYC axis in primary effusion lymphoma in a

- cereblon-dependent manner and display synergistic cytotoxicity with BRD4 inhibitors. *Oncogene* **2016**, *35* (14), 1797-810.
214. Alimoghaddam, K., A review of arsenic trioxide and acute promyelocytic leukemia. *Int J Hematol Oncol Stem Cell Res* **2014**, *8* (3), 44-54.
215. Takahashi, S., Combination therapy with arsenic trioxide for hematological malignancies. *Anticancer Agents Med Chem* **2010**, *10* (6), 504-10.
216. Bazarbachi, A.; El-Sabban, M. E.; Nasr, R.; Quignon, F.; Awaraji, C.; Kersual, J.; Dianoux, L.; Zermati, Y.; Haidar, J. H.; Hermine, O.; de Thé, H., Arsenic trioxide and interferon-alpha synergize to induce cell cycle arrest and apoptosis in human T-cell lymphotropic virus type I-transformed cells. *Blood* **1999**, *93* (1), 278-83.
217. Martelli, M. P.; Gionfriddo, I.; Mezzasoma, F.; Milano, F.; Pierangeli, S.; Mulas, F.; Pacini, R.; Tabarrini, A.; Pettrossi, V.; Rossi, R.; Vetro, C.; Brunetti, L.; Sportoletti, P.; Tiacci, E.; Di Raimondo, F.; Falini, B., Arsenic trioxide and all-trans retinoic acid target NPM1 mutant oncoprotein levels and induce apoptosis in NPM1-mutated AML cells. *Blood* **2015**, *125* (22), 3455-65.
218. Rojewski, M. T.; Baldus, C.; Knauf, W.; Thiel, E.; Schrezenmeier, H., Dual effects of arsenic trioxide (As₂O₃) on non-acute promyelocytic leukaemia myeloid cell lines: induction of apoptosis and inhibition of proliferation. *Br J Haematol* **2002**, *116* (3), 555-63.
219. Zhang, T. D.; Chen, G. Q.; Wang, Z. G.; Wang, Z. Y.; Chen, S. J.; Chen, Z., Arsenic trioxide, a therapeutic agent for APL. *Oncogene* **2001**, *20* (49), 7146-53.
220. Marçais, A.; Cook, L.; Witkover, A.; Asnafi, V.; Avettand-Fenoel, V.; Delarue, R.; Cheminant, M.; Sibon, D.; Frenzel, L.; de Thé, H.; Bangham, C. R. M.; Bazarbachi, A.; Hermine, O.; Suarez, F., Arsenic trioxide (As₂O₃) as a maintenance therapy for adult T cell leukemia/lymphoma. *Retrovirology* **2020**, *17* (1), 5.
221. Ghavamzadeh, A.; Alimoghaddam, K.; Rostami, S.; Ghaffari, S. H.; Jahani, M.; Irvani, M.; Mousavi, S. A.; Bahar, B.; Jalili, M., Phase II study of single-agent arsenic trioxide for the front-line therapy of acute promyelocytic leukemia. *J Clin Oncol* **2011**, *29* (20), 2753-7.
222. Powell, B. L.; Moser, B.; Stock, W.; Gallagher, R. E.; Willman, C. L.; Stone, R. M.; Rowe, J. M.; Coutre, S.; Feusner, J. H.; Gregory, J.; Couban, S.; Appelbaum, F. R.; Tallman, M. S.; Larson, R. A., Arsenic trioxide improves event-free and overall survival for adults with acute promyelocytic leukemia: North American Leukemia Intergroup Study C9710. *Blood* **2010**, *116* (19), 3751-7.
223. Ghavamzadeh, A.; Alimoghaddam, K.; Ghaffari, S. H.; Rostami, S.; Jahani, M.; Hosseini, R.; Mossavi, A.; Baybordi, E.; Khodabadeh, A.; Irvani, M.; Bahar, B.; Mortazavi, Y.; Totonchi, M.; Aghdami, N., Treatment of acute promyelocytic leukemia with arsenic trioxide without ATRA and/or chemotherapy. *Ann Oncol* **2006**, *17* (1), 131-4.
224. El Hajj, H.; Dassouki, Z.; Berthier, C.; Raffoux, E.; Ades, L.; Legrand, O.; Hleihel, R.; Sahin, U.; Tawil, N.; Salameh, A.; Zibara, K.; Darwiche, N.; Mohty, M.; Dombret, H.; Fenaux, P.; de Thé, H.; Bazarbachi, A., Retinoic acid and arsenic trioxide trigger degradation of mutated NPM1, resulting in apoptosis of AML cells. *Blood* **2015**, *125* (22), 3447-54.
225. El Hajj, H.; El-Sabban, M.; Hasegawa, H.; Zaatari, G.; Ablain, J.; Saab, S. T.; Janin, A.; Mahfouz, R.; Nasr, R.; Kfoury, Y.; Nicot, C.; Hermine, O.; Hall, W.; de Thé, H.; Bazarbachi, A., Therapy-induced selective loss of leukemia-initiating activity in murine adult T cell leukemia. *The Journal of experimental medicine* **2010**, *207* (13), 2785-2792.
226. El-Sabban, M. E.; Nasr, R.; Dbaibo, G.; Hermine, O.; Abboushi, N.; Quignon, F.; Ameisen, J. C.; Bex, F.; de Thé, H.; Bazarbachi, A., Arsenic-interferon-alpha-triggered apoptosis in HTLV-I transformed cells is associated with tax down-regulation and reversal of NF-kappa B activation. *Blood* **2000**, *96* (8), 2849-55.

227. Kchour, G.; Tarhini, M.; Kooshyar, M. M.; El Hajj, H.; Wattel, E.; Mahmoudi, M.; Hatoum, H.; Rahimi, H.; Maleki, M.; Rafatpanah, H.; Rezaee, S. A.; Yazdi, M. T.; Shirdel, A.; de Thé, H.; Hermine, O.; Farid, R.; Bazarbachi, A., Phase 2 study of the efficacy and safety of the combination of arsenic trioxide, interferon alpha, and zidovudine in newly diagnosed chronic adult T-cell leukemia/lymphoma (ATL). *Blood* **2009**, *113* (26), 6528-32.
228. H. Wang, X. C., E. Eksioglu, J. Zhou, N. Fortenbery, J. Djeu, A. List and S. Wei, Lenalidomide and Arsenic Trioxide Have Independent Non-Interfering Effects When Used in Combination on Myeloma Cell Lines in Vitro. *Journal of Cancer Therapy* **2013**, vol 4 (No. 3, 2013), 787-796.
229. Jian, Y.; Gao, W.; Geng, C.; Zhou, H.; Leng, Y.; Li, Y.; Chen, W., Arsenic trioxide potentiates sensitivity of multiple myeloma cells to lenalidomide by upregulating cereblon expression levels. *Oncol Lett* **2017**, *14* (3), 3243-3248.
230. Hernandez-Ilizaliturri, F. J.; Bato0, S. A., The emerging role of lenalidomide in the management of lymphoid malignancies. *Ther Adv Hematol* **2011**, *2* (1), 45-53.
231. Kotla, V.; Goel, S.; Nischal, S.; Heuck, C.; Vivek, K.; Das, B.; Verma, A., Mechanism of action of lenalidomide in hematological malignancies. *J Hematol Oncol* **2009**, *2*, 36.
232. Raedler, L. A., Revlimid (Lenalidomide) Now FDA Approved as First-Line Therapy for Patients with Multiple Myeloma. *Am Health Drug Benefits* **2016**, *9* (Spec Feature), 140-3.
233. Dimopoulos, M.; Spencer, A.; Attal, M.; Prince, H. M.; Harousseau, J. L.; Dmoszynska, A.; San Miguel, J.; Hellmann, A.; Facon, T.; Foà, R.; Corso, A.; Masliak, Z.; Olesnyckyj, M.; Yu, Z.; Patin, J.; Zeldis, J. B.; Knight, R. D., Lenalidomide plus dexamethasone for relapsed or refractory multiple myeloma. *N Engl J Med* **2007**, *357* (21), 2123-32.
234. Shortt, J.; Hsu, A. K.; Johnstone, R. W., Thalidomide-analogue biology: immunological, molecular and epigenetic targets in cancer therapy. *Oncogene* **2013**, *32* (36), 4191-202.
235. Buesche, G.; Dieck, S.; Giagounidis, A.; Bock, O.; Wilkens, L.; Schlegelberger, B.; Knight, R.; Bennett, J.; Aul, C.; Kreipe, H. H., Anti-Angiogenic In Vivo Effect of Lenalidomide (CC-5013) in Myelodysplastic Syndrome with del(5q) Chromosome Abnormality and Its Relation to the Course of Disease. *Blood* **2005**, *106* (11), 372-372.
236. Flowers, C. R.; Leonard, J. P.; Fowler, N. H., Lenalidomide in follicular lymphoma. *Blood* **2020**, *135* (24), 2133-2136.
237. Patil, A.; Manzano, M.; Gottwein, E., CK1alpha and IRF4 are essential and independent effectors of immunomodulatory drugs in primary effusion lymphoma. *Blood* **2018**, *132* (6), 577-586.
238. Antar, A.; El Hajj, H.; Jabbour, M.; Khalifeh, I.; El-Merhi, F.; Mahfouz, R.; Bazarbachi, A., Primary effusion lymphoma in an elderly patient effectively treated by lenalidomide: case report and review of literature. *Blood Cancer J* **2014**, *4*, e190.
239. Durer, C.; Babiker, H. M., Adult T Cell Leukemia. In *StatPearls*, StatPearls Publishing
- Copyright © 2020, StatPearls Publishing LLC.: Treasure Island (FL), 2020.
240. Watanabe, T., Adult T-cell leukemia: molecular basis for clonal expansion and transformation of HTLV-1-infected T cells. *Blood* **2017**, *129* (9), 1071-1081.
241. Takatsuki, K.; Uchiyama, T.; Sagawa, K.; Yodoi, J., [Surface markers of malignant lymphoid cells in the classification of lymphoproliferative disorders, with special reference to adult T-cell leukemia (author's transl)]. *Rinsho Ketsueki* **1976**, *17* (4), 416-21.
242. Poiesz, B. J.; Ruscetti, F. W.; Reitz, M. S.; Kalyanaraman, V. S.; Gallo, R. C., Isolation of a new type C retrovirus (HTLV) in primary uncultured cells of a patient with Sézary T-cell leukaemia. *Nature* **1981**, *294* (5838), 268-71.
243. Gonçalves, D. U.; Proietti, F. A.; Ribas, J. G.; Araújo, M. G.; Pinheiro, S. R.; Guedes, A. C.; Carneiro-Proietti, A. B., Epidemiology, treatment, and prevention of human T-cell leukemia virus type 1-associated diseases. *Clin Microbiol Rev* **2010**, *23* (3), 577-89.

244. Afonso, P. V.; Cassar, O.; Gessain, A., Molecular epidemiology, genetic variability and evolution of HTLV-1 with special emphasis on African genotypes. *Retrovirology* **2019**, *16* (1), 39.
245. Gessain, A., [Human retrovirus HTLV-1: descriptive and molecular epidemiology, origin, evolution, diagnosis and associated diseases]. *Bull Soc Pathol Exot* **2011**, *104* (3), 167-80.
246. Bangham, C. R. M., Human T Cell Leukemia Virus Type 1: Persistence and Pathogenesis. *Annu Rev Immunol* **2018**, *36*, 43-71.
247. Chihara, D.; Ito, H.; Katanoda, K.; Shibata, A.; Matsuda, T.; Tajima, K.; Sobue, T.; Matsuo, K., Increase in incidence of adult T-cell leukemia/lymphoma in non-endemic areas of Japan and the United States. *Cancer Sci* **2012**, *103* (10), 1857-60.
248. Malpica, L.; Pimentel, A.; Reis, I. M.; Gotuzzo, E.; Lekakis, L.; Komanduri, K.; Harrington, T.; Barber, G. N.; Ramos, J. C., Epidemiology, clinical features, and outcome of HTLV-1-related ATLL in an area of prevalence in the United States. *Blood Adv* **2018**, *2* (6), 607-620.
249. Uchiyama, T.; Hattori, T.; Wano, Y.; Tsudo, M.; Takatsuki, K.; Uchino, H., Cell surface phenotype and in vitro function of adult T-cell leukemia cells. *Diagn Immunol* **1983**, *1* (3), 150-4.
250. Waldmann, T. A.; Greene, W. C.; Sarin, P. S.; Saxinger, C.; Blayney, D. W.; Blattner, W. A.; Goldman, C. K.; Bongiovanni, K.; Sharrow, S.; Depper, J. M.; et al., Functional and phenotypic comparison of human T cell leukemia/lymphoma virus positive adult T cell leukemia with human T cell leukemia/lymphoma virus negative Sézary leukemia, and their distinction using anti-Tac. Monoclonal antibody identifying the human receptor for T cell growth factor. *J Clin Invest* **1984**, *73* (6), 1711-8.
251. Tian, Y.; Kobayashi, S.; Ohno, N.; Isobe, M.; Tsuda, M.; Zaike, Y.; Watanabe, N.; Tani, K.; Tojo, A.; Uchimar, K., Leukemic T cells are specifically enriched in a unique CD3(dim) CD7(low) subpopulation of CD4(+) T cells in acute-type adult T-cell leukemia. *Cancer Sci* **2011**, *102* (3), 569-77.
252. Shimoyama, M., Diagnostic criteria and classification of clinical subtypes of adult T-cell leukaemia-lymphoma. A report from the Lymphoma Study Group (1984-87). *Br J Haematol* **1991**, *79* (3), 428-37.
253. El Hajj, H.; Tsukasaki, K.; Cheminant, M.; Bazarbachi, A.; Watanabe, T.; Hermine, O., Novel Treatments of Adult T Cell Leukemia Lymphoma. *Front Microbiol* **2020**, *11*, 1062.
254. Pombo De Oliveira, M. S.; Loureiro, P.; Bittencourt, A.; Chiatton, C.; Borducchi, D.; De Carvalho, S. M.; Barbosa, H. S.; Rios, M.; Sill, A.; Cleghorn, F.; Blattner, W., Geographic diversity of adult t-cell leukemia/lymphoma in Brazil. The Brazilian ATLL Study Group. *Int J Cancer* **1999**, *83* (3), 291-8.
255. Katsuya, H.; Ishitsuka, K.; Utsunomiya, A.; Hanada, S.; Eto, T.; Moriuchi, Y.; Saburi, Y.; Miyahara, M.; Sueoka, E.; Uike, N.; Yoshida, S.; Yamashita, K.; Tsukasaki, K.; Suzushima, H.; Ohno, Y.; Matsuoka, H.; Jo, T.; Amano, M.; Hino, R.; Shimokawa, M.; Kawai, K.; Suzumiya, J.; Tamura, K., Treatment and survival among 1594 patients with ATL. *Blood* **2015**, *126* (24), 2570-7.
256. Tamura, K.; Nagamine, N.; Araki, Y.; Seita, M.; Okayama, A.; Kawano, K.; Tachibana, N.; Tsuda, K.; Kuroki, Y.; Narita, H.; et al., Clinical analysis of 33 patients with adult T-cell leukemia (ATL)-diagnostic criteria and significance of high- and low-risk ATL. *Int J Cancer* **1986**, *37* (3), 335-41.
257. Graham, R. L.; Burch, M.; Krause, J. R., Adult T-cell leukemia/lymphoma. *Proc (Bayl Univ Med Cent)* **2014**, *27* (3), 235-8.
258. Kiyokawa, T.; Yamaguchi, K.; Takeya, M.; Takahashi, K.; Watanabe, T.; Matsumoto, T.; Lee, S. Y.; Takatsuki, K., Hypercalcemia and osteoclast proliferation in adult T-cell leukemia. *Cancer* **1987**, *59* (6), 1187-91.

259. Blayney, D. W.; Jaffe, E. S.; Blattner, W. A.; Cossman, J.; Robert-Guroff, M.; Longo, D. L.; Bunn, P. A., Jr.; Gallo, R. C., The human T-cell leukemia/lymphoma virus associated with American adult T-cell leukemia/lymphoma. *Blood* **1983**, *62* (2), 401-5.
260. Bunn, P. A., Jr.; Schechter, G. P.; Jaffe, E.; Blayney, D.; Young, R. C.; Matthews, M. J.; Blattner, W.; Broder, S.; Robert-Guroff, M.; Gallo, R. C., Clinical course of retrovirus-associated adult T-cell lymphoma in the United States. *N Engl J Med* **1983**, *309* (5), 257-64.
261. Ueda, N.; Iwata, K.; Tokuoka, H.; Akagi, T.; Ito, J.; Mizushima, M., Adult T-cell leukemia with generalized cytomegalic inclusion disease and pneumocystis carinii pneumonia. *Acta Pathol Jpn* **1979**, *29* (2), 221-32.
262. Yamaguchi, K.; Nishimura, H.; Kohrogi, H.; Jono, M.; Miyamoto, Y.; Takatsuki, K., A proposal for smoldering adult T-cell leukemia: a clinicopathologic study of five cases. *Blood* **1983**, *62* (4), 758-66.
263. Bazarbachi, A.; Suarez, F.; Fields, P.; Hermine, O., How I treat adult T-cell leukemia/lymphoma. *Blood* **2011**, *118* (7), 1736-45.
264. Cook, L. B.; Fuji, S.; Hermine, O.; Bazarbachi, A.; Ramos, J. C.; Ratner, L.; Horwitz, S.; Fields, P.; Tanase, A.; Bumbea, H.; Cwynarski, K.; Taylor, G.; Waldmann, T. A.; Bittencourt, A.; Marcais, A.; Suarez, F.; Sibon, D.; Phillips, A.; Lunning, M.; Farid, R.; Imaizumi, Y.; Choi, I.; Ishida, T.; Ishitsuka, K.; Fukushima, T.; Uchimar, K.; Takaori-Kondo, A.; Tokura, Y.; Utsunomiya, A.; Matsuoka, M.; Tsukasaki, K.; Watanabe, T., Revised Adult T-Cell Leukemia-Lymphoma International Consensus Meeting Report. *J Clin Oncol* **2019**, *37* (8), 677-687.
265. Bazarbachi, A.; Ghez, D.; Lepelletier, Y.; Nasr, R.; de Thé, H.; El-Sabban, M. E.; Hermine, O., New therapeutic approaches for adult T-cell leukaemia. *Lancet Oncol* **2004**, *5* (11), 664-72.
266. Katsuya, H.; Ishitsuka, K., Treatment advances and prognosis for patients with adult T-cell leukemia-lymphoma. *J Clin Exp Hematop* **2017**, *57* (3), 87-97.
267. Gill, P. S.; Harrington, W., Jr.; Kaplan, M. H.; Ribeiro, R. C.; Bennett, J. M.; Liebman, H. A.; Bernstein-Singer, M.; Espina, B. M.; Cabral, L.; Allen, S.; et al., Treatment of adult T-cell leukemia-lymphoma with a combination of interferon alfa and zidovudine. *N Engl J Med* **1995**, *332* (26), 1744-8.
268. Hermine, O.; Bouscary, D.; Gessain, A.; Turlure, P.; Leblond, V.; Franck, N.; Buzyn-Veil, A.; Rio, B.; Macintyre, E.; Dreyfus, F.; et al., Brief report: treatment of adult T-cell leukemia-lymphoma with zidovudine and interferon alfa. *N Engl J Med* **1995**, *332* (26), 1749-51.
269. Bazarbachi, A.; Hermine, O., Treatment with a combination of zidovudine and alpha-interferon in naive and pretreated adult T-cell leukemia/lymphoma patients. *J Acquir Immune Defic Syndr Hum Retrovirol* **1996**, *13 Suppl 1*, S186-90.
270. Kchour, G.; Rezaee, R.; Farid, R.; Ghantous, A.; Rafatpanah, H.; Tarhini, M.; Kooshyar, M. M.; El Hajj, H.; Berry, F.; Mortada, M.; Nasser, R.; Shirdel, A.; Dassouki, Z.; Ezzedine, M.; Rahimi, H.; Ghavamzadeh, A.; de Thé, H.; Hermine, O.; Mahmoudi, M.; Bazarbachi, A., The combination of arsenic, interferon-alpha, and zidovudine restores an "immunocompetent-like" cytokine expression profile in patients with adult T-cell leukemia lymphoma. *Retrovirology* **2013**, *10*, 91.
271. Bazarbachi, A.; Plumelle, Y.; Carlos Ramos, J.; Tortevoe, P.; Otrrock, Z.; Taylor, G.; Gessain, A.; Harrington, W.; Panelatti, G.; Hermine, O., Meta-analysis on the use of zidovudine and interferon-alfa in adult T-cell leukemia/lymphoma showing improved survival in the leukemic subtypes. *J Clin Oncol* **2010**, *28* (27), 4177-83.
272. Ratner, L.; Harrington, W.; Feng, X.; Grant, C.; Jacobson, S.; Noy, A.; Sparano, J.; Lee, J.; Ambinder, R.; Campbell, N.; Lairmore, M., Human T cell leukemia virus reactivation with progression of adult T-cell leukemia-lymphoma. *PLoS One* **2009**, *4* (2), e4420.

273. White, J. D.; Wharfe, G.; Stewart, D. M.; Maher, V. E.; Eicher, D.; Herring, B.; Derby, M.; Jackson-Booth, P. G.; Marshall, M.; Lucy, D.; Jain, A.; Cranston, B.; Hanchard, B.; Lee, C. C.; Top, L. E.; Fleisher, T. A.; Nelson, D. L.; Waldmann, T. A., The combination of zidovudine and interferon alpha-2B in the treatment of adult T-cell leukemia/lymphoma. *Leuk Lymphoma* **2001**, *40* (3-4), 287-94.
274. Hermine, O.; Allard, I.; Lévy, V.; Arnulf, B.; Gessain, A.; Bazarbachi, A., A prospective phase II clinical trial with the use of zidovudine and interferon-alpha in the acute and lymphoma forms of adult T-cell leukemia/lymphoma. *Hematol J* **2002**, *3* (6), 276-82.
275. Hodson, A.; Crichton, S.; Montoto, S.; Mir, N.; Matutes, E.; Cwynarski, K.; Kumaran, T.; Ardeshta, K. M.; Pagliuca, A.; Taylor, G. P.; Fields, P. A., Use of zidovudine and interferon alfa with chemotherapy improves survival in both acute and lymphoma subtypes of adult T-cell leukemia/lymphoma. *J Clin Oncol* **2011**, *29* (35), 4696-701.
276. Iqbal, M.; Reljic, T.; Klocksieben, F.; Sher, T.; Ayala, E.; Murthy, H.; Bazarbachi, A.; Kumar, A.; Kharfan-Dabaja, M. A., Efficacy of Allogeneic Hematopoietic Cell Transplantation in Human T Cell Lymphotropic Virus Type 1-Associated Adult T Cell Leukemia/Lymphoma: Results of a Systematic Review/Meta-Analysis. *Biol Blood Marrow Transplant* **2019**, *25* (8), 1695-1700.
277. Bazarbachi, A.; Cwynarski, K.; Boumendil, A.; Finel, H.; Fields, P.; Raj, K.; Nagler, A.; Mohty, M.; Sureda, A.; Dreger, P.; Hermine, O., Outcome of patients with HTLV-1-associated adult T-cell leukemia/lymphoma after SCT: a retrospective study by the EBMT LWP. *Bone Marrow Transplant* **2014**, *49* (10), 1266-8.
278. Dasanu, C. A., Newer developments in adult T-cell leukemia/lymphoma therapeutics. *Expert Opin Pharmacother* **2011**, *12* (11), 1709-17.
279. Ishii, T.; Ishida, T.; Utsunomiya, A.; Inagaki, A.; Yano, H.; Komatsu, H.; Iida, S.; Imada, K.; Uchiyama, T.; Akinaga, S.; Shitara, K.; Ueda, R., Defucosylated humanized anti-CCR4 monoclonal antibody KW-0761 as a novel immunotherapeutic agent for adult T-cell leukemia/lymphoma. *Clin Cancer Res* **2010**, *16* (5), 1520-31.
280. Sasaki, D.; Imaizumi, Y.; Hasegawa, H.; Osaka, A.; Tsukasaki, K.; Choi, Y. L.; Mano, H.; Marquez, V. E.; Hayashi, T.; Yanagihara, K.; Moriwaki, Y.; Miyazaki, Y.; Kamihira, S.; Yamada, Y., Overexpression of Enhancer of zeste homolog 2 with trimethylation of lysine 27 on histone H3 in adult T-cell leukemia/lymphoma as a target for epigenetic therapy. *Haematologica* **2011**, *96* (5), 712-9.
281. Fujikawa, D.; Nakagawa, S.; Hori, M.; Kurokawa, N.; Soejima, A.; Nakano, K.; Yamochi, T.; Nakashima, M.; Kobayashi, S.; Tanaka, Y.; Iwanaga, M.; Utsunomiya, A.; Uchimarui, K.; Yamagishi, M.; Watanabe, T., Polycomb-dependent epigenetic landscape in adult T-cell leukemia. *Blood* **2016**, *127* (14), 1790-802.
282. Kerppola, T. K., Polycomb group complexes--many combinations, many functions. *Trends Cell Biol* **2009**, *19* (12), 692-704.
283. Yamagishi, M.; Hori, M.; Fujikawa, D.; Ohsugi, T.; Honma, D.; Adachi, N.; Katano, H.; Hishima, T.; Kobayashi, S.; Nakano, K.; Nakashima, M.; Iwanaga, M.; Utsunomiya, A.; Tanaka, Y.; Okada, S.; Tsukasaki, K.; Tobinai, K.; Araki, K.; Watanabe, T.; Uchimarui, K., Targeting Excessive EZH1 and EZH2 Activities for Abnormal Histone Methylation and Transcription Network in Malignant Lymphomas. *Cell Rep* **2019**, *29* (8), 2321-2337.e7.
284. Haberland, M.; Montgomery, R. L.; Olson, E. N., The many roles of histone deacetylases in development and physiology: implications for disease and therapy. *Nat Rev Genet* **2009**, *10* (1), 32-42.
285. Zhang, Q.; Wang, S.; Chen, J.; Yu, Z., Histone Deacetylases (HDACs) Guided Novel Therapies for T-cell lymphomas. *Int J Med Sci* **2019**, *16* (3), 424-442.

286. Zimmerman, B.; Sargeant, A.; Landes, K.; Fernandez, S. A.; Chen, C. S.; Lairmore, M. D., Efficacy of novel histone deacetylase inhibitor, AR42, in a mouse model of, human T-lymphotropic virus type 1 adult T cell lymphoma. *Leuk Res* **2011**, *35* (11), 1491-7.
287. Yasunaga, J. I., Strategies of Human T-Cell Leukemia Virus Type 1 for Persistent Infection: Implications for Leukemogenesis of Adult T-Cell Leukemia-Lymphoma. *Front Microbiol* **2020**, *11*, 979.
288. Bai, X. T.; Nicot, C., Overview on HTLV-1 p12, p8, p30, p13: accomplices in persistent infection and viral pathogenesis. *Front Microbiol* **2012**, *3*, 400.
289. Matsuoka, M.; Jeang, K. T., Human T-cell leukaemia virus type 1 (HTLV-1) infectivity and cellular transformation. *Nat Rev Cancer* **2007**, *7* (4), 270-80.
290. Matsuoka, M.; Jeang, K. T., Human T-cell leukemia virus type 1 (HTLV-1) and leukemic transformation: viral infectivity, Tax, HBZ and therapy. *Oncogene* **2011**, *30* (12), 1379-89.
291. Giam, C. Z.; Semmes, O. J., HTLV-1 Infection and Adult T-Cell Leukemia/Lymphoma-A Tale of Two Proteins: Tax and HBZ. *Viruses* **2016**, *8* (6).
292. Ma, G.; Yasunaga, J.; Matsuoka, M., Multifaceted functions and roles of HBZ in HTLV-1 pathogenesis. *Retrovirology* **2016**, *13*, 16.
293. Wattel, E.; Vartanian, J. P.; Pannetier, C.; Wain-Hobson, S., Clonal expansion of human T-cell leukemia virus type I-infected cells in asymptomatic and symptomatic carriers without malignancy. *J Virol* **1995**, *69* (5), 2863-8.
294. Curren, R.; Van Duyne, R.; Jaworski, E.; Guendel, I.; Sampey, G.; Das, R.; Narayanan, A.; Kashanchi, F., HTLV tax: a fascinating multifunctional co-regulator of viral and cellular pathways. *Front Microbiol* **2012**, *3*, 406.
295. Shirinian, M.; Kfoury, Y.; Dassouki, Z.; El-Hajj, H.; Bazarbachi, A., Tax-1 and Tax-2 similarities and differences: focus on post-translational modifications and NF- κ B activation. *Front Microbiol* **2013**, *4*, 231.
296. Fochi, S.; Ciminale, V.; Trabetti, E.; Bertazzoni, U.; D'Agostino, D. M.; Zipeto, D.; Romanelli, M. G., NF- κ B and MicroRNA Deregulation Mediated by HTLV-1 Tax and HBZ. *Pathogens* **2019**, *8* (4).
297. Mohanty, S.; Harhaj, E. W., Mechanisms of Oncogenesis by HTLV-1 Tax. *Pathogens* **2020**, *9* (7).
298. Kfoury, Y.; Setterblad, N.; El-Sabban, M.; Zamborlini, A.; Dassouki, Z.; El Hajj, H.; Hermine, O.; Pique, C.; de Thé, H.; Saïb, A.; Bazarbachi, A., Tax ubiquitylation and SUMOylation control the dynamic shuttling of Tax and NEMO between Ubc9 nuclear bodies and the centrosome. *Retrovirology* **2011**, *8* (Suppl 1), A146.
299. Hleihel, R.; Khoshnood, B.; Dacklin, I.; Omran, H.; Mouawad, C.; Dassouki, Z.; El-Sabban, M.; Shirinian, M.; Grabbe, C.; Bazarbachi, A., The HTLV-1 oncoprotein Tax is modified by the ubiquitin related modifier 1 (Urm1). *Retrovirology* **2018**, *15* (1), 33.
300. Nasr, R.; Chiari, E.; El-Sabban, M.; Mahieux, R.; Kfoury, Y.; Abdulhay, M.; Yazbeck, V.; Hermine, O.; de Thé, H.; Pique, C.; Bazarbachi, A., Tax ubiquitylation and sumoylation control critical cytoplasmic and nuclear steps of NF-kappaB activation. *Blood* **2006**, *107* (10), 4021-9.
301. Bazarbachi, A.; Abou Merhi, R.; Gessain, A.; Talhouk, R.; El-Khoury, H.; Nasr, R.; Gout, O.; Sulahian, R.; Homaidan, F.; de Thé, H.; Hermine, O.; El-Sabban, M. E., Human T-cell lymphotropic virus type I-infected cells extravasate through the endothelial barrier by a local angiogenesis-like mechanism. *Cancer Res* **2004**, *64* (6), 2039-46.
302. El-Sabban, M. E.; Merhi, R. A.; Haidar, H. A.; Arnulf, B.; Khoury, H.; Basbous, J.; Nijmeh, J.; de Thé, H.; Hermine, O.; Bazarbachi, A., Human T-cell lymphotropic virus type 1-transformed cells induce angiogenesis and establish functional gap junctions with endothelial cells. *Blood* **2002**, *99* (9), 3383-9.

303. Dassouki, Z.; Sahin, U.; El Hajj, H.; Jollivet, F.; Kfoury, Y.; Lallemand-Breitenbach, V.; Hermine, O.; de Thé, H.; Bazarbachi, A., ATL response to arsenic/interferon therapy is triggered by SUMO/PML/RNF4-dependent Tax degradation. *Blood* **2015**, *125* (3), 474-82.
304. Mahgoub, M.; Yasunaga, J. I.; Iwami, S.; Nakaoka, S.; Koizumi, Y.; Shimura, K.; Matsuoka, M., Sporadic on/off switching of HTLV-1 Tax expression is crucial to maintain the whole population of virus-induced leukemic cells. *Proc Natl Acad Sci U S A* **2018**, *115* (6), E1269-e1278.
305. Tanaka, A.; Takahashi, C.; Yamaoka, S.; Nosaka, T.; Maki, M.; Hatanaka, M., Oncogenic transformation by the tax gene of human T-cell leukemia virus type I in vitro. *Proc Natl Acad Sci U S A* **1990**, *87* (3), 1071-5.
306. Robek, M. D.; Ratner, L., Immortalization of CD4(+) and CD8(+) T lymphocytes by human T-cell leukemia virus type 1 Tax mutants expressed in a functional molecular clone. *J Virol* **1999**, *73* (6), 4856-65.
307. Akagi, T.; Ono, H.; Shimotohno, K., Characterization of T cells immortalized by Tax1 of human T-cell leukemia virus type 1. *Blood* **1995**, *86* (11), 4243-9.
308. Moodad, S.; Akkouche, A.; Hleihel, R.; Darwiche, N.; El-Sabban, M.; Bazarbachi, A.; El Hajj, H., Mouse Models That Enhanced Our Understanding of Adult T Cell Leukemia. *Front Microbiol* **2018**, *9*, 558.
309. Hasegawa, H.; Sawa, H.; Lewis, M. J.; Orba, Y.; Sheehy, N.; Yamamoto, Y.; Ichinohe, T.; Tsunetsugu-Yokota, Y.; Katano, H.; Takahashi, H.; Matsuda, J.; Sata, T.; Kurata, T.; Nagashima, K.; Hall, W. W., Thymus-derived leukemia-lymphoma in mice transgenic for the Tax gene of human T-lymphotropic virus type I. *Nat Med* **2006**, *12* (4), 466-72.
310. Shirinian, M.; Kambris, Z.; Hamadeh, L.; Grabbe, C.; Journo, C.; Mahieux, R.; Bazarbachi, A., A Transgenic Drosophila melanogaster Model To Study Human T-Lymphotropic Virus Oncoprotein Tax-1-Driven Transformation In Vivo. *J Virol* **2015**, *89* (15), 8092-5.
311. Harhaj, E. W.; Giam, C. Z., NF- κ B signaling mechanisms in HTLV-1-induced adult T-cell leukemia/lymphoma. *Febs j* **2018**, *285* (18), 3324-3336.
312. Fochi, S.; Mutascio, S.; Bertazzoni, U.; Zipeto, D.; Romanelli, M. G., HTLV Deregulation of the NF- κ B Pathway: An Update on Tax and Antisense Proteins Role. *Front Microbiol* **2018**, *9*, 285.
313. Park, M. H.; Hong, J. T., Roles of NF- κ B in Cancer and Inflammatory Diseases and Their Therapeutic Approaches. *Cells* **2016**, *5* (2).
314. Qu, Z.; Xiao, G., Human T-cell lymphotropic virus: a model of NF- κ B-associated tumorigenesis. *Viruses* **2011**, *3* (6), 714-49.
315. Jeong, S. J.; Radonovich, M.; Brady, J. N.; Pise-Masison, C. A., HTLV-I Tax induces a novel interaction between p65/RelA and p53 that results in inhibition of p53 transcriptional activity. *Blood* **2004**, *104* (5), 1490-7.
316. Pise-Masison, C. A.; Mahieux, R.; Jiang, H.; Ashcroft, M.; Radonovich, M.; Duvall, J.; Guillermin, C.; Brady, J. N., Inactivation of p53 by human T-cell lymphotropic virus type 1 Tax requires activation of the NF-kappaB pathway and is dependent on p53 phosphorylation. *Mol Cell Biol* **2000**, *20* (10), 3377-86.
317. Ariumi, Y.; Kaida, A.; Lin, J. Y.; Hirota, M.; Masui, O.; Yamaoka, S.; Taya, Y.; Shimotohno, K., HTLV-1 tax oncoprotein represses the p53-mediated trans-activation function through coactivator CBP sequestration. *Oncogene* **2000**, *19* (12), 1491-9.
318. Suzuki, T.; Uchida-Toita, M.; Yoshida, M., Tax protein of HTLV-1 inhibits CBP/p300-mediated transcription by interfering with recruitment of CBP/p300 onto DNA element of E-box or p53 binding site. *Oncogene* **1999**, *18* (28), 4137-43.
319. Tawara, M.; Hogerzeil, S. J.; Yamada, Y.; Takasaki, Y.; Soda, H.; Hasegawa, H.; Murata, K.; Ikeda, S.; Imaizumi, Y.; Sugahara, K.; Tsuruda, K.; Tsukasaki, K.; Tomonaga, M.; Hirakata,

- Y.; Kamihira, S., Impact of p53 aberration on the progression of Adult T-cell Leukemia/Lymphoma. *Cancer Lett* **2006**, *234* (2), 249-55.
320. Kawakami, A.; Nakashima, T.; Sakai, H.; Urayama, S.; Yamasaki, S.; Hida, A.; Tsuboi, M.; Nakamura, H.; Ida, H.; Migita, K.; Kawabe, Y.; Eguchi, K., Inhibition of caspase cascade by HTLV-I tax through induction of NF-kappaB nuclear translocation. *Blood* **1999**, *94* (11), 3847-54.
321. Deveraux, Q. L.; Leo, E.; Stennicke, H. R.; Welsh, K.; Salvesen, G. S.; Reed, J. C., Cleavage of human inhibitor of apoptosis protein XIAP results in fragments with distinct specificities for caspases. *Embo j* **1999**, *18* (19), 5242-51.
322. Zhang, M.; Mathews Griner, L. A.; Ju, W.; Duveau, D. Y.; Guha, R.; Petrus, M. N.; Wen, B.; Maeda, M.; Shinn, P.; Ferrer, M.; Conlon, K. D.; Bamford, R. N.; O'Shea, J. J.; Thomas, C. J.; Waldmann, T. A., Selective targeting of JAK/STAT signaling is potentiated by Bcl-xL blockade in IL-2-dependent adult T-cell leukemia. *Proc Natl Acad Sci U S A* **2015**, *112* (40), 12480-5.
323. Vajente, N.; Trevisan, R.; Saggioro, D., HTLV-1 Tax protein cooperates with Ras in protecting cells from apoptosis. *Apoptosis* **2009**, *14* (2), 153-63.
324. Horiuchi, S.; Yamamoto, N.; Dewan, M. Z.; Takahashi, Y.; Yamashita, A.; Yoshida, T.; Nowell, M. A.; Richards, P. J.; Jones, S. A.; Yamamoto, N., Human T-cell leukemia virus type-I Tax induces expression of interleukin-6 receptor (IL-6R): Shedding of soluble IL-6R and activation of STAT3 signaling. *Int J Cancer* **2006**, *119* (4), 823-30.
325. Leung, K.; Nabel, G. J., HTLV-1 transactivator induces interleukin-2 receptor expression through an NF-kappa B-like factor. *Nature* **1988**, *333* (6175), 776-8.
326. Nicot, C., HTLV-I Tax-Mediated Inactivation of Cell Cycle Checkpoints and DNA Repair Pathways Contribute to Cellular Transformation: "A Random Mutagenesis Model". *J Cancer Sci* **2015**, *2* (2).
327. Haller, K.; Wu, Y.; Derow, E.; Schmitt, I.; Jeang, K. T.; Grassmann, R., Physical interaction of human T-cell leukemia virus type 1 Tax with cyclin-dependent kinase 4 stimulates the phosphorylation of retinoblastoma protein. *Mol Cell Biol* **2002**, *22* (10), 3327-38.
328. Lemasson, I.; Thébault, S.; Sardet, C.; Devaux, C.; Mesnard, J. M., Activation of E2F-mediated transcription by human T-cell leukemia virus type I Tax protein in a p16(INK4A)-negative T-cell line. *The Journal of biological chemistry* **1998**, *273* (36), 23598-23604.
329. Chowdhury, I. H.; Farhadi A Fau - Wang, X.-F.; Wang Xf Fau - Robb, M. L.; Robb MI Fau - Birx, D. L.; Birx DI Fau - Kim, J. H.; Kim, J. H., Human T-cell leukemia virus type 1 Tax activates cyclin-dependent kinase inhibitor p21/Waf1/Cip1 expression through a p53-independent mechanism: Inhibition of cdk2. (0020-7136 (Print)).
330. Dayaram, T.; Lemoine Fj Fau - Donehower, L. A.; Donehower La Fau - Marriott, S. J.; Marriott, S. J., Activation of WIP1 phosphatase by HTLV-1 Tax mitigates the cellular response to DNA damage. (1932-6203 (Electronic)).
331. Kibler, K. V.; Jeang, K. T., CREB/ATF-dependent repression of cyclin a by human T-cell leukemia virus type 1 Tax protein. (0022-538X (Print)).
332. Philpott, S. M.; Buehring, G. C., Defective DNA repair in cells with human T-cell leukemia/bovine leukemia viruses: role of tax gene. (0027-8874 (Print)).
333. Kao, S. Y.; Marriott, S. J., Disruption of nucleotide excision repair by the human T-cell leukemia virus type 1 Tax protein. (0022-538X (Print)).
334. Matsuoka, M.; Green, P. L., The HBZ gene, a key player in HTLV-1 pathogenesis. *Retrovirology* **2009**, *6*, 71.
335. Larocca, D.; Chao, L. A.; Seto, M. H.; Brunck, T. K., Human T-cell leukemia virus minus strand transcription in infected T-cells. *Biochem Biophys Res Commun* **1989**, *163* (2), 1006-13.
336. Gaudray, G.; Gachon, F.; Basbous, J.; Biard-Piechaczyk, M.; Devaux, C.; Mesnard, J. M., The complementary strand of the human T-cell leukemia virus type 1 RNA genome encodes a bZIP transcription factor that down-regulates viral transcription. *J Virol* **2002**, *76* (24), 12813-22.

337. Satou, Y.; Yasunaga, J.; Yoshida, M.; Matsuoka, M., HTLV-I basic leucine zipper factor gene mRNA supports proliferation of adult T cell leukemia cells. *Proc Natl Acad Sci U S A* **2006**, *103* (3), 720-5.
338. Yoshida, M.; Satou, Y.; Yasunaga, J.; Fujisawa, J.; Matsuoka, M., Transcriptional control of spliced and unspliced human T-cell leukemia virus type 1 bZIP factor (HBZ) gene. *J Virol* **2008**, *82* (19), 9359-68.
339. Usui, T.; Yanagihara, K.; Tsukasaki, K.; Murata, K.; Hasegawa, H.; Yamada, Y.; Kamihira, S., Characteristic expression of HTLV-1 basic zipper factor (HBZ) transcripts in HTLV-1 provirus-positive cells. *Retrovirology* **2008**, *5*, 34.
340. Hivin, P.; Frédéric, M.; Arpin-André, C.; Basbous, J.; Gay, B.; Thébault, S.; Mesnard, J. M., Nuclear localization of HTLV-I bZIP factor (HBZ) is mediated by three distinct motifs. *J Cell Sci* **2005**, *118* (Pt 7), 1355-62.
341. Zhao, T.; Matsuoka, M., HBZ and its roles in HTLV-1 oncogenesis. *Front Microbiol* **2012**, *3*, 247.
342. Fan, J.; Ma, G.; Nosaka, K.; Tanabe, J.; Satou, Y.; Koito, A.; Wain-Hobson, S.; Vartanian, J. P.; Matsuoka, M., APOBEC3G generates nonsense mutations in human T-cell leukemia virus type 1 proviral genomes in vivo. *J Virol* **2010**, *84* (14), 7278-87.
343. Lemasson, I.; Lewis, M. R.; Polakowski, N.; Hivin, P.; Cavanagh, M. H.; Thébault, S.; Barbeau, B.; Nyborg, J. K.; Mesnard, J. M., Human T-cell leukemia virus type 1 (HTLV-1) bZIP protein interacts with the cellular transcription factor CREB to inhibit HTLV-1 transcription. *J Virol* **2007**, *81* (4), 1543-53.
344. Clerc, I.; Polakowski, N.; André-Arpin, C.; Cook, P.; Barbeau, B.; Mesnard, J. M.; Lemasson, I., An interaction between the human T cell leukemia virus type 1 basic leucine zipper factor (HBZ) and the KIX domain of p300/CBP contributes to the down-regulation of tax-dependent viral transcription by HBZ. *J Biol Chem* **2008**, *283* (35), 23903-13.
345. Hagiya, K.; Yasunaga, J.; Satou, Y.; Ohshima, K.; Matsuoka, M., ATF3, an HTLV-1 bZip factor binding protein, promotes proliferation of adult T-cell leukemia cells. *Retrovirology* **2011**, *8*, 19.
346. Nakayama, T.; Higuchi, T.; Oiso, N.; Kawada, A.; Yoshie, O., Expression and function of FRA2/JUND in cutaneous T-cell lymphomas. *Anticancer Res* **2012**, *32* (4), 1367-73.
347. Thébault, S.; Basbous, J.; Hivin, P.; Devaux, C.; Mesnard, J. M., HBZ interacts with JunD and stimulates its transcriptional activity. *FEBS Lett* **2004**, *562* (1-3), 165-70.
348. Gazon, H.; Lemasson, I.; Polakowski, N.; Césaire, R.; Matsuoka, M.; Barbeau, B.; Mesnard, J. M.; Peloponese, J. M., Jr., Human T-cell leukemia virus type 1 (HTLV-1) bZIP factor requires cellular transcription factor JunD to upregulate HTLV-1 antisense transcription from the 3' long terminal repeat. *J Virol* **2012**, *86* (17), 9070-8.
349. Arnold, J.; Zimmerman, B.; Li, M.; Lairmore, M. D.; Green, P. L., Human T-cell leukemia virus type-1 antisense-encoded gene, Hbz, promotes T-lymphocyte proliferation. *Blood* **2008**, *112* (9), 3788-97.
350. Ma, G.; Yasunaga, J.; Fan, J.; Yanagawa, S.; Matsuoka, M., HTLV-1 bZIP factor dysregulates the Wnt pathways to support proliferation and migration of adult T-cell leukemia cells. *Oncogene* **2013**, *32* (36), 4222-30.
351. Polakowski, N.; Terol, M.; Hoang, K.; Nash, I.; Laverdure, S.; Gazon, H.; Belrose, G.; Mesnard, J. M.; Césaire, R.; Péloponèse, J. M.; Lemasson, I., HBZ stimulates brain-derived neurotrophic factor/TrkB autocrine/paracrine signaling to promote survival of human T-cell leukemia virus type 1-infected T cells. *J Virol* **2014**, *88* (22), 13482-94.
352. Wurm, T.; Wright, D. G.; Polakowski, N.; Mesnard, J. M.; Lemasson, I., The HTLV-1-encoded protein HBZ directly inhibits the acetyl transferase activity of p300/CBP. *Nucleic Acids Res* **2012**, *40* (13), 5910-25.

353. Tanaka-Nakanishi, A.; Yasunaga, J.; Takai, K.; Matsuoka, M., HTLV-1 bZIP factor suppresses apoptosis by attenuating the function of FoxO3a and altering its localization. *Cancer Res* **2014**, *74* (1), 188-200.
354. Satou, Y.; Yasunaga, J.; Zhao, T.; Yoshida, M.; Miyazato, P.; Takai, K.; Shimizu, K.; Ohshima, K.; Green, P. L.; Ohkura, N.; Yamaguchi, T.; Ono, M.; Sakaguchi, S.; Matsuoka, M., HTLV-1 bZIP factor induces T-cell lymphoma and systemic inflammation in vivo. *PLoS Pathog* **2011**, *7* (2), e1001274.
355. Yamamoto-Taguchi, N.; Satou, Y.; Miyazato, P.; Ohshima, K.; Nakagawa, M.; Katagiri, K.; Kinashi, T.; Matsuoka, M., HTLV-1 bZIP factor induces inflammation through labile Foxp3 expression. *PLoS Pathog* **2013**, *9* (9), e1003630.
356. Zhao, T.; Satou, Y.; Sugata, K.; Miyazato, P.; Green, P. L.; Imamura, T.; Matsuoka, M., HTLV-1 bZIP factor enhances TGF- β signaling through p300 coactivator. *Blood* **2011**, *118* (7), 1865-76.
357. Mitagami, Y.; Yasunaga, J.; Kinoshita, H.; Ohshima, K.; Matsuoka, M., Interferon- γ Promotes Inflammation and Development of T-Cell Lymphoma in HTLV-1 bZIP Factor Transgenic Mice. *PLoS Pathog* **2015**, *11* (8), e1005120.
358. Sugata, K.; Satou, Y.; Yasunaga, J.; Hara, H.; Ohshima, K.; Utsunomiya, A.; Mitsuyama, M.; Matsuoka, M., HTLV-1 bZIP factor impairs cell-mediated immunity by suppressing production of Th1 cytokines. *Blood* **2012**, *119* (2), 434-44.
359. Zhi, H.; Yang, L.; Kuo, Y. L.; Ho, Y. K.; Shih, H. M.; Giam, C. Z., NF- κ B hyper-activation by HTLV-1 tax induces cellular senescence, but can be alleviated by the viral anti-sense protein HBZ. *PLoS Pathog* **2011**, *7* (4), e1002025.
360. Zhao, T.; Yasunaga, J.; Satou, Y.; Nakao, M.; Takahashi, M.; Fujii, M.; Matsuoka, M., Human T-cell leukemia virus type 1 bZIP factor selectively suppresses the classical pathway of NF-kappaB. *Blood* **2009**, *113* (12), 2755-64.
361. Panfil, A. R.; Dissinger, N. J.; Howard, C. M.; Murphy, B. M.; Landes, K.; Fernandez, S. A.; Green, P. L., Functional Comparison of HBZ and the Related APH-2 Protein Provides Insight into Human T-Cell Leukemia Virus Type 1 Pathogenesis. *J Virol* **2016**, *90* (7), 3760-72.
362. Esser, A. K.; Rauch, D. A.; Xiang, J.; Harding, J. C.; Kohart, N. A.; Ross, M. H.; Su, X.; Wu, K.; Huey, D.; Xu, Y.; Vij, K.; Green, P. L.; Rosol, T. J.; Niewiesk, S.; Ratner, L.; Weilbaecher, K. N., HTLV-1 viral oncogene HBZ induces osteolytic bone disease in transgenic mice. *Oncotarget* **2017**, *8* (41), 69250-69263.
363. Xiang, J.; Rauch, D. A.; Huey, D. D.; Panfil, A. R.; Cheng, X.; Esser, A. K.; Su, X.; Harding, J. C.; Xu, Y.; Fox, G. C.; Fontana, F.; Kobayashi, T.; Su, J.; Sundaramoorthi, H.; Wong, W. H.; Jia, Y.; Rosol, T. J.; Veis, D. J.; Green, P. L.; Niewiesk, S.; Ratner, L.; Weilbaecher, K. N., HTLV-1 viral oncogene HBZ drives bone destruction in adult T cell leukemia. *JCI Insight* **2019**, *4* (19).
364. Mitobe, Y.; Yasunaga, J.; Furuta, R.; Matsuoka, M., HTLV-1 bZIP Factor RNA and Protein Impart Distinct Functions on T-cell Proliferation and Survival. *Cancer Res* **2015**, *75* (19), 4143-52.
365. Flavahan, W. A.; Gaskell, E.; Bernstein, B. E., Epigenetic plasticity and the hallmarks of cancer. *Science* **2017**, *357* (6348).
366. Esteller, M., Epigenetics in evolution and disease. *The Lancet* **2008**, *372*, S90-S96.
367. Levine, S. S.; Weiss, A.; Erdjument-Bromage, H.; Shao, Z.; Tempst, P.; Kingston, R. E., The core of the polycomb repressive complex is compositionally and functionally conserved in flies and humans. *Mol Cell Biol* **2002**, *22* (17), 6070-8.
368. Bracken, A. P.; Dietrich, N.; Pasini, D.; Hansen, K. H.; Helin, K., Genome-wide mapping of Polycomb target genes unravels their roles in cell fate transitions. *Genes Dev* **2006**, *20* (9), 1123-36.

369. Müller, J.; Verrijzer, P., Biochemical mechanisms of gene regulation by polycomb group protein complexes. *Curr Opin Genet Dev* **2009**, *19* (2), 150-8.
370. Cao, R.; Wang, L.; Wang, H.; Xia, L.; Erdjument-Bromage, H.; Tempst, P.; Jones, R. S.; Zhang, Y., Role of histone H3 lysine 27 methylation in Polycomb-group silencing. *Science* **2002**, *298* (5595), 1039-43.
371. Birve, A.; Sengupta, A. K.; Beuchle, D.; Larsson, J.; Kennison, J. A.; Rasmuson-Lestander, Å.; Müller, J., *Su(z)12*, a novel *Drosophila* Polycomb group gene that is conserved in vertebrates and plants. *Development* **2001**, *128* (17), 3371.
372. Kuzmichev, A.; Nishioka, K.; Erdjument-Bromage, H.; Tempst, P.; Reinberg, D., Histone methyltransferase activity associated with a human multiprotein complex containing the Enhancer of Zeste protein. *Genes Dev* **2002**, *16* (22), 2893-905.
373. Pasini, D.; Bracken, A. P.; Helin, K., Polycomb group proteins in cell cycle progression and cancer. *Cell Cycle* **2004**, *3* (4), 396-400.
374. Pasini, D.; Bracken, A. P.; Jensen, M. R.; Lazzerini Denchi, E.; Helin, K., Suz12 is essential for mouse development and for EZH2 histone methyltransferase activity. *Embo j* **2004**, *23* (20), 4061-71.
375. Cao, Q.; Wang, X.; Zhao, M.; Yang, R.; Malik, R.; Qiao, Y.; Poliakov, A.; Yocum, A. K.; Li, Y.; Chen, W.; Cao, X.; Jiang, X.; Dahiya, A.; Harris, C.; Feng, F. Y.; Kalantry, S.; Qin, Z. S.; Dhanasekaran, S. M.; Chinnaiyan, A. M., The central role of EED in the orchestration of polycomb group complexes. *Nat Commun* **2014**, *5*, 3127.
376. Margueron, R.; Reinberg, D., The Polycomb complex PRC2 and its mark in life. *Nature* **2011**, *469* (7330), 343-9.
377. Völkel, P.; Dupret, B.; Le Bourhis, X.; Angrand, P. O., Diverse involvement of EZH2 in cancer epigenetics. *Am J Transl Res* **2015**, *7* (2), 175-93.
378. Zhou, Z.; Gao, J.; Popovic, R.; Wolniak, K.; Parimi, V.; Winter, J. N.; Licht, J. D.; Chen, Y. H., Strong expression of EZH2 and accumulation of trimethylated H3K27 in diffuse large B-cell lymphoma independent of cell of origin and EZH2 codon 641 mutation. *Leuk Lymphoma* **2015**, *56* (10), 2895-901.
379. Gan, L.; Yang, Y.; Li, Q.; Feng, Y.; Liu, T.; Guo, W., Epigenetic regulation of cancer progression by EZH2: from biological insights to therapeutic potential. *Biomark Res* **2018**, *6*, 10.
380. Nakagawa, M.; Kitabayashi, I., Oncogenic roles of enhancer of zeste homolog 1/2 in hematological malignancies. *Cancer Sci* **2018**, *109* (8), 2342-2348.
381. Yamagishi, M.; Nakano, K.; Miyake, A.; Yamochi, T.; Kagami, Y.; Tsutsumi, A.; Matsuda, Y.; Sato-Otsubo, A.; Muto, S.; Utsunomiya, A.; Yamaguchi, K.; Uchimaru, K.; Ogawa, S.; Watanabe, T., Polycomb-mediated loss of miR-31 activates NIK-dependent NF-κB pathway in adult T cell leukemia and other cancers. *Cancer Cell* **2012**, *21* (1), 121-35.

